



## BONUS BIO-C3

### Biodiversity changes: causes, consequences and management implications

Deliverable No: 3.2		Workpackage number and leader: WP3, P6	
Date:	05/09/2016	Delivery due date: 05/09/2016	32, 2016
Title:	Report on the nature and types of driver interactions including their potential future		
Lead partner for deliverable:	P6, EMI, Jonne Kotta		
Other contributing partners	P1, P2, P9, P12		
Authors	Jonne Kotta; Elin Almroth-Rosell; Helén C. Andersson; Margit Eero; Kari Eilola; Hans Harald Hinrichsen; Holger Jänes; Brian MacKenzie; H.E. Markus Meier; Henn Ojaveer; Merli Pärnoja; Henrik Skov; Burkhard von Dewitz;		
DOI: 10.3289/BIO-C3_D3.2			
Kotta, J., Almroth-Rosell, E., Andersson, H.C., Eero, M., Eilola, K., Hinrichsen, H.H., Jänes, H., MacKenzie, B., Meier, H.E.M., Ojaveer, H., Pärnoja, M., Skov, H., von Dewitz, B. (2016) <i>Report on the nature and types of driver interactions including their potential future</i> . BIO-C3 Deliverable, D3.2.			
Dissemination level (PU=public, CO=confidential)	(PU=public, PP=Restricted,	PU	
Nature of the Deliverable (RE=Report, OT=Other)	RE		

#### Acknowledgements

The research leading to these results is part of the BIO-C3 project and has received funding from BONUS, the joint Baltic Sea research and development programme (Art 185), funded jointly from the European Union's Seventh Programme for research, technological development and demonstration and from national funding institutions.



## **BIO-C3 overview**

The importance of biodiversity for ecosystems on land has long been acknowledged. In contrast, its role for marine ecosystems has gained less research attention. The overarching aim of BIO-C3 is to address biodiversity changes, their causes, consequences and possible management implications for the Baltic Sea. Scientists from 7 European countries and 13 partner institutes are involved. Project coordinator is the GEOMAR Helmholtz Centre for Ocean Research Kiel, Germany, assisted by DTU Aqua, National Institute of Aquatic Resources, Technical University of Denmark.

## **Why is Biodiversity important?**

An estimated 130 animal and plant species go extinct every day. In 1992 the United Nations tried countering this process with the "Biodiversity Convention". It labeled biodiversity as worthy of preservation – at land as well as at sea. Biological variety should not only be preserved for ethical reasons: It also fulfils key ecosystem functions and provides ecosystem services. In the sea this includes healthy fish stocks, clear water without algal blooms but also the absorption of nutrients from agriculture.

## **Biodiversity and BIO-C3**

To assess the role of biodiversity in marine ecosystems, BIO-C3 uses a natural laboratory: the Baltic Sea. The Baltic is perfectly suited since its species composition is very young, with current salt level persisting for only a few thousand years. It is also relatively species poor, and extinctions of residents or invasions of new species is therefore expected to have a more dramatic effect compared to species rich and presumably more stable ecosystems.

Moreover, human impacts on the Baltic ecosystem are larger than in most other sea regions, as this marginal sea is surrounded by densely populated areas. A further BIO-C3 focus is to predict and assess future anthropogenic impacts such as fishing and eutrophication, as well as changes related to global (climate) change using a suite of models.

If talking about biological variety, it is important to consider genetic diversity as well, a largely neglected issue. A central question is whether important organisms such as zooplankton and fish can cope or even adapt on contemporary time scales to changed environmental conditions anticipated under different global change scenarios.

BIO-C3 aims to increase understanding of both temporal changes in biodiversity - on all levels from genetic diversity to ecosystem composition - and of the environmental and anthropogenic pressures driving this change. For this purpose, we are able to exploit numerous long term data sets available from the project partners, including on fish stocks, plankton and benthos organisms as well as abiotic environmental conditions. Data series are extended and expanded through a network of Baltic cruises with the research vessels linked to the consortium, and complemented by extensive experimental, laboratory, and modeling work.

## **From science to management**

The ultimate BIO-C3 goal is to use understanding of what happened in the past to predict what will happen in the future, under different climate projections and management scenarios: essential information for resource managers and politicians to decide on the course of actions to maintain and improve the biodiversity status of the Baltic Sea for future generations.

# Contents

<b>1</b>	<b>Executive Summary</b> .....	<b>4</b>
<b>2</b>	<b>Introduction</b> .....	<b>4</b>
<b>3</b>	<b>Core activity</b> .....	<b>6</b>
	3.1 Baltic inflow events and the prediction of the eastern Baltic cod spawning environment (P1)	6
	3.2 Impact of increased eutrophication on production of forage fish in the 20th century (P2) .....	12
	3.3 Current status of shipping in the Baltic Sea (P6) .....	18
	3.4 Current status of fishing in the Baltic Sea (P6).....	28
	3.5 Current status of non-indigenous species (NIS) in the Baltic Sea (P6) .....	32
	3.6 Interactions between eutrophication and temperature (P9).....	49
	3.7 Relationships between Baltic Sea inflows and physical and biochemical parameters (P12) ..	64
	3.8 Habitat sensitivity to eutrophication of selected pelagic species in the Baltic Sea (P1).....	75
<b>4</b>	<b>References</b> .....	<b>96</b>
<b>5</b>	<b>List of appendices</b> .....	<b>110</b>
	<b>APPENDIX I</b> .....	<b>111</b>
	<b>APPENDIX II</b> .....	<b>124</b>
	<b>APPENDIX III</b> .....	<b>157</b>
	<b>APPENDIX IV</b> .....	<b>174</b>
	<b>APPENDIX V</b> .....	<b>192</b>

# **1 Executive Summary**

The Baltic Sea is a dynamic environment responding to various drivers operating at different temporal and spatial scales. In response to climate change, the Baltic Sea is warming and the frequency of extreme climatic events is increasing (Lima & Wetthey 2012, BACC 2008, Poloczanska et al. 2007). Coastal development, human population growth and globalization intensify stressors associated with human activities, such as nutrient loading, fisheries and proliferation of invasive and bloom-forming species. Such abrupt changes have unforeseen consequences for the biodiversity and the function of food webs and may result in loss of ecological key species, alteration and fragmentation of habitats. To mitigate undesired effects on the Baltic ecosystem, an efficient marine management will depend on the understanding of historical and current drivers, i.e. physical and chemical environmental conditions and human activities that precipitate pressures on the natural environment.

This task examined a set of key interactions of selected natural and anthropogenic drivers in space and time, identified in Task 3.1 as well as WP1 and WP2 (e.g. physico-chemical features vs climate forcing; eutrophication vs oxygen deficiency vs bio-invasions; fisheries vs climate change impacts) by using overlay-mapping and sensitivity analyses. The benthic ecosystem models developed under Task 2.1 were used to investigate interactions between sea temperature and eutrophication for various depth strata in coastal (P9) and offshore areas (P1) of the Baltic Sea. This also included investigation on how the frequency and magnitude of deep-water inflow events determines volume and variance of salinity and temperature under the halocline, deep-water oxygen levels and sediment fluxes of nutrients, using observations and model results from 1850 to present (P1, P2, P6, P9, P12). The resulting synthesis on the nature and magnitude of different driver interactions will feed into all other tasks of this WP3 and WP2/WP4. Moreover, the results presented in this report improve the process-based and mechanistic understanding of environmental change in the Baltic Sea ecosystem, thereby fostering the implementation of the Marine Strategy Framework Directive.

## **2 Introduction**

BIO-C3 aims to significantly advance our knowledge base towards management of the Baltic Sea biodiversity in an ecosystem perspective, considering the meso-scale spatial and regional

heterogeneity of the system, origin of the biota and current/future pressures of drivers impacting the Baltic and its subsystems. This requires knowledge on sensitivity and resilience of marine biodiversity under different environmental scenarios including information on i) species, habitat and functional diversity, ii) the effect of human induced environmental pressures as well as climate on spatial and temporal dynamics of species and habitats and iii) the ecology of bio-invasions and effects of none-indigenous species. Such a significant challenge requires an interdisciplinary approach that analyses biodiversity from functional and dynamic perspectives (see e.g. Tornroos and Bonsdorff 2012), addressing genotypes, species, populations, habitats (including their associated communities) and ecosystems. BIO-C3 explores resilience and resistance of Baltic Sea ecosystems to changes in natural and anthropogenic drivers, considering explicitly their interactions that result in non-linear and non-stationary ecosystem responses as well as associated uncertainties.

As in other marine areas, there is an array of anthropogenic drivers that impact biodiversity. Among the most important ones in the Baltic Sea are climate change/variability, hypoxia/anoxia, eutrophication and fisheries, which all result in spatially heterogeneous cumulative pressures. These pressures affect ecosystem structure and functioning in contrasting (additive, neutralizing or cumulative) patterns. Importantly, all anthropogenic drivers interact with one another (Crain et al. 2008), and change in both mean value and variance. Thus, a key objective of the task 3.2 is to develop scenarios about spatio-temporally varying pressures of human stressors and their interaction considering natural as well as socio-economic drivers to characterize historic, current and future habitats in the Baltic Sea.

Task 3.2 brings together outstanding marine researchers from different universities and institutes around the Baltic Sea area. The aims and goals of the deliverable 3.2 were divided between 5 different project partners (P1, P2, P6, P9, P12) who covered a remarkable amount of topics ranging from abiotic climate forcing's to biological interactions of fauna and flora as well as to economically important topics such as fishing and shipping. Task 3.2 specifically investigated a set of key interactions of selected natural and anthropogenic drivers in space and time, identified in Task 3.1 as well as WP1 and WP2 (e.g. physico-chemical features vs climate forcing; eutrophication vs oxygen deficiency vs bio-invasions; fisheries vs climate change impacts) by using overlay-mapping and sensitivity analyses. The benthic ecosystem models developed under Task 2.1 were used to investigate interactions between sea temperature and eutrophication for various depth strata in coastal (P9) and offshore areas (P1) of the Baltic Sea. This also included investigation on how the frequency and magnitude of deep-water inflow events determines volume and variance of

salinity and temperature under the halocline, deep-water oxygen levels and sediment fluxes of nutrients, using observations and model results from 1850 to present (P1, P2, P6, P9, P12). The resulting synthesis on the nature and magnitude of different driver interactions is being feed into all other tasks of this WP3 and WP2/WP4.

As a result of task 3.2, better management advice that takes into account multitude of human induced pressures to marine ecosystems could be provided to policy makers in charge of the Baltic Sea area. The results presented in this report improve the process-based and mechanistic understanding of environmental change in the Baltic Sea ecosystem, thereby fostering the implementation of the Marine Strategy Framework Directive. Following subsections listed under Core Activity will provide a detailed overview about the work of each project partner and will thus highlight the novelty and importance of the work carried out in Task 3.2.

### **3 Core activity**

#### **3.1 Baltic inflow events and the prediction of the eastern Baltic cod spawning environment (P1)**

*Hans Harald Hinrichsen, GEOMAR*

##### **3.1.1 Abstract/highlights**

The main factor determining the dynamics of suitable water masses for cod reproduction in the eastern Baltic Sea is the advection of highly saline and well-oxygenated water masses from the North Sea. A hydrodynamic model was run to hind-cast the dynamics of highly spatio-temporally resolved hydrographic property fields to be used for the investigation of the cod egg habitat extension. To analyse influences of Baltic inflow events, vertically resolved simulated oxygen concentration data time series of the Bornholm Basin were correlated to vertically resolved salinity data for the western Baltic Sea. The simulations could be performed to establish statistical relationships describing the temporal heterogeneity in the spatial distribution of the Baltic cod spawning environment. Highest correlations occur for the early months of the years between mid-

depth salinity levels in the Arkona Basin and the oxygen-dependent cod spawning environment in the Bornholm Basin. In conjunction with simple parameters that reflect factors affecting recruitment, such as the reproduction volume or the egg survival probability of eastern Baltic cod, this information can probably be used in short-term projections of early life stage mortality and thus could directly feed into assessment procedures. Furthermore, it was obtained that vertically resolved salinity measurements from a routinely operated observational platform located in the centre of the Arkona Basin could be used as predictor for the cod spawning environment in the Bornholm Basin, without any need for cost-intensive survey programmes.

### **3.1.2 Progress and (if applicable) deviations from the original work-plan**

Analyses completed, data time series on the magnitude and frequency of Baltic inflows into the central Baltic Sea are available on request, additional model on the short-term prediction of eastern Baltic cod developed

### **3.1.3 Deviations from the work-plan**

None.

### **3.1.4 Introduction**

The main factor determining the dynamics of suitable water masses for cod reproduction in the eastern Baltic Sea is the advection of highly saline and well-oxygenated water masses from the North Sea and Kattegat area. These water masses enter the central Baltic Sea through the Great Belt and the Øresund. One part of this subtask was to simulate the frequency and magnitude of Baltic inflow events as well as to investigate the possibility of using hydrographic measurements in the western Baltic as a kind of early warning indicator to predict oxygen conditions during spawning time on the presently important eastern Baltic cod spawning ground, the Bornholm Basin. To this end, we present correlation analysis of the influence of saline North Sea and Kattegat water masses at different locations in the western Baltic on the replenishment of the oxygen content in the deep water areas of the Bornholm Basin. Besides providing a time series on the magnitude and frequency of inflow events into the central Baltic, the aim was to estimate the predictive power of data time series of vertical salinity distribution patterns to the west of the Bornholm Basin for potential use in integrated stock assessments. As a second part of the analysis, vertically resolved salinity

measurements obtained from routinely operated observational platforms located at the Darss Sill, the Drogden Sill, and in the centre of the Arkona Basin were used as predictors for the cod spawning environment in the Bornholm Basin.

### 3.1.5 Methods and results

A hydrodynamic model was run to hind-cast the dynamics of highly spatio-temporally resolved hydrographic property fields to be used for the investigation of the cod egg habitat extension. This includes investigations on how the frequency and magnitude of deep water inflows determines the variance of deep-water oxygen levels. To analyse influences of Baltic inflow events, vertically resolved oxygen concentration data time series of the Bornholm Basin were correlated to vertically resolved salinity data for the western Baltic Sea (Fig. 1).

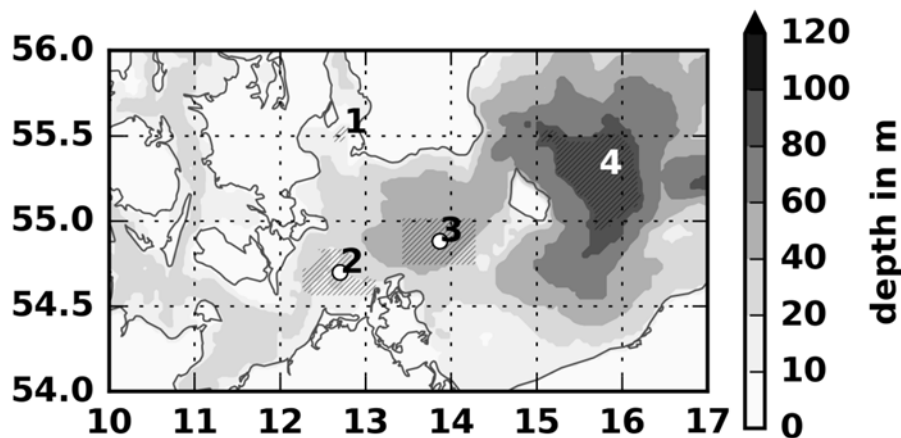


Figure 1. Map of the south-western Baltic Sea. Dots indicate observational platforms and vertically resolved hydrodynamic data (shaded areas) at the Drogden Sill (1), the Darss Sill (2), in the Arkona Basin (3), and in the Bornholm Basin (4).

Monthly averaged profiles were used to study the long-term variability (1971 to 2015) of the eastern Baltic cod spawning environment. Significant relationships of salinity at the Darss and Drogden Sills and those in the Arkona Basin with oxygen below the halocline in the Bornholm Basin were facilitated by use of simple linear regression models. Highest correlation occurs for the early months of the years between the 33 m salinity level in the Arkona Basin and the oxygen-dependent cod spawning environment in the Bornholm Basin (Fig. 2).



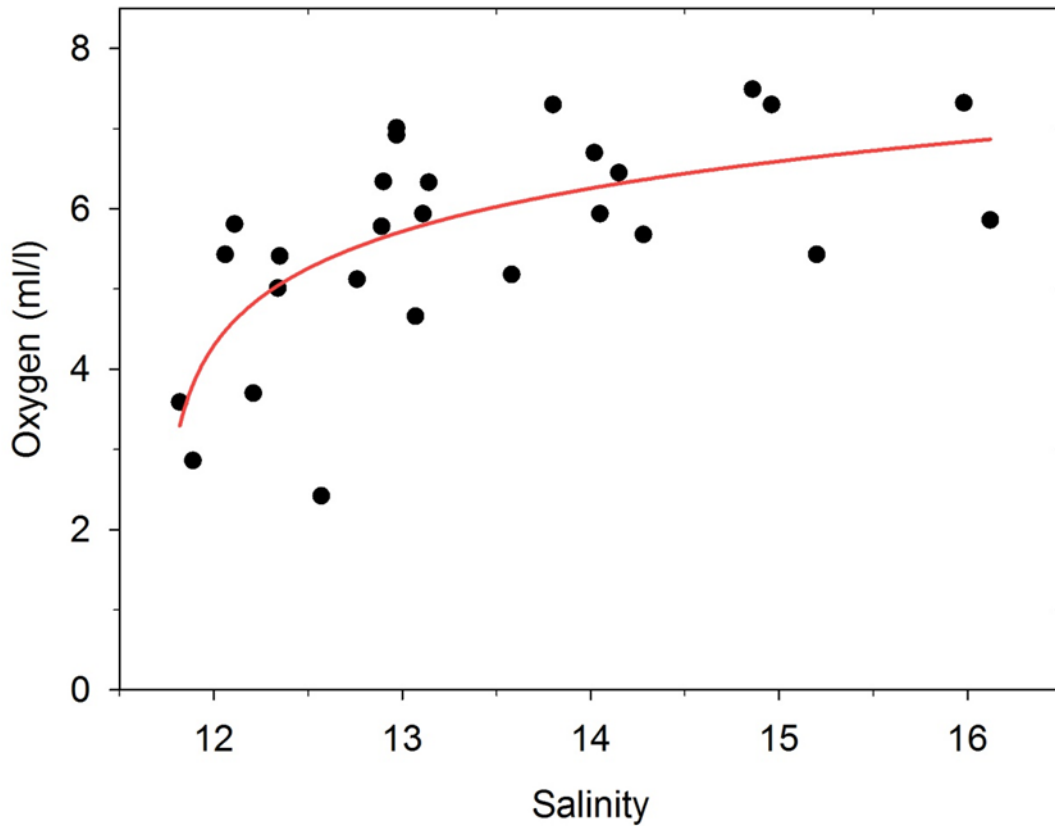


Figure 2. Monthly mean salinity values (November to January) at the 33 m depth level in the Arkona Basin (taken if salinity values exceeded long-term average conditions  $\sim 11.5$  PSU) vs. monthly maximum oxygen concentrations (averages of the depth range from 70 to 95 m) in the Bornholm Basin between November and March. Data obtained from hydrodynamic modelling.

Furthermore, we used the modelled data on oxygen concentration to calculate the potential egg survival probability, which is based on a modelled egg survival function obtained from experimental data. Generally, oxygen-dependent survival was calculated with respect to the above mentioned threshold levels in temperature, salinity and oxygen concentration. Model data time series on the cod spawning habitat characteristics (oxygen-related egg survival probability) were also assembled for different buoyancy levels (1009, 1011, 1013  $\text{kg m}^{-3}$ ). These levels were chosen to represent the buoyancies of eggs of different female age categories: old (large), mid-age (medium size) and young (small) cod.

The analysis of oxygen-related egg survival probability at buoyancy/density levels (1009, 1011, 1013 kg m<sup>-3</sup>) showed significant differences. Survival of eggs of old (large) females, usually floating at highest buoyancy, were almost independent on the 33 m salinity level in the Arkona Basin ( $r=0.30$ ) one to two months before, while the survival probability for eggs spawned by mid-age (medium size,  $r=0.44$ ) and young (small,  $r=0.58$ ) females could be significantly related to this salinity level in the Arkona Basin (Fig. 3).

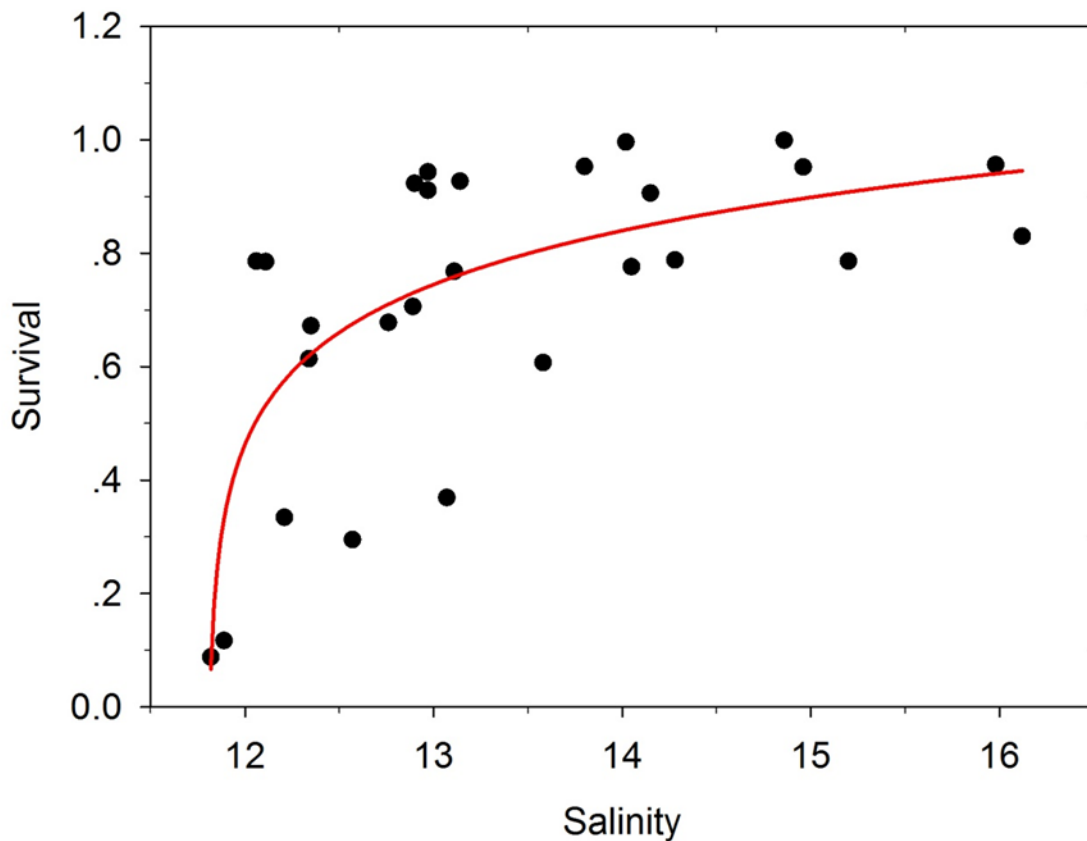


Figure 3. Monthly mean salinity values (November to January) at the 33 m depth level in the Arkona Basin vs. monthly mean maximum oxygen-related eastern Baltic cod egg survival probability at the egg neutral buoyancy level 1013 kg m<sup>-3</sup> in the Bornholm Basin between November and March. Data obtained from hydrodynamic modelling.

Based on the above described correlation analyses, we have classified the magnitude and frequency of saline and oxygen-enriched deep water inflows from the North Sea/Skagerrak area into the Bornholm Basin for the time period 1971–2015 (Fig. 4). In case salinity at 33 m-level in the Arkona

Basin exceeded above average conditions (11.5 PSU), inflows into the Bornholm Basin have been classified from low to strong (Table 1).

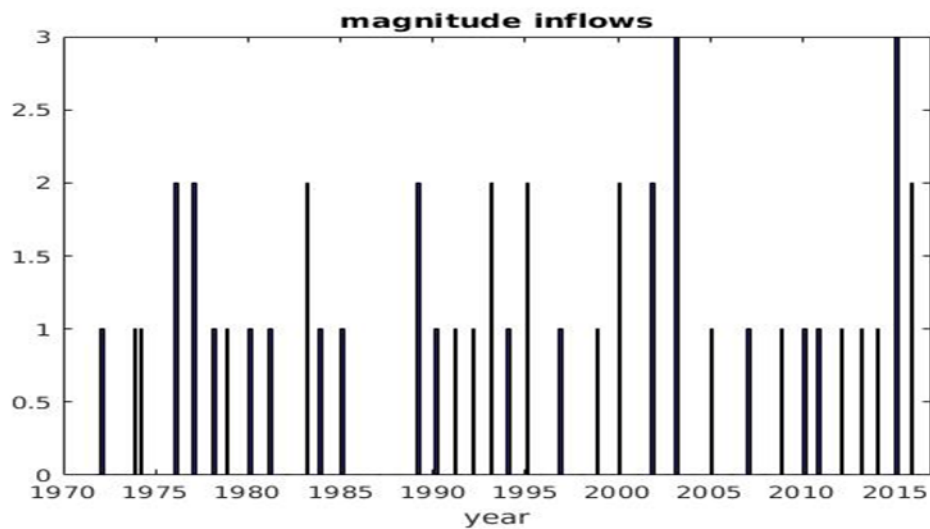


Figure 4. Magnitude and frequency of Baltic inflows into the Bornholm Basin

Table 1. Magnitude and frequency of Baltic inflows into the Bornholm Basin, 0: no, 1: minor, 2: medium, and 3: strong inflow

Salinity at 33 m level in Arkona Basin (PSU)	Magnitude	Number
< 11.5	0	12
11.5 – 13.5	1	23
13.5 – 15.5	2	9
> 15.5	3	2

### 3.1.6 Recommendations

The International Council for the Exploration of the Seas (ICES) is the main fishery advice giving body for the North-Atlantic region, including the Baltic Sea. ICES specifically acknowledged the need to develop and identify ways forward to include environmental and economic considerations in standard fishery advice. We show that future oxygen conditions in the Bornholm Basin, the major spawning ground for eastern Baltic cod, can be predicted based on measurements made in the

western Baltic. For short-term predictions already existing observational platforms can be used. Salinity measurements from platforms located at the Darss Sill, the Drogden Sill, and in the centre of the Arkona Basin are strongly recommended for the performance of short-term predictions of the Eastern Baltic cod spawning environment. This offers a cost-neutral way of improving stock assessment of eastern Baltic cod, proceeding on the way to more integrated advice.

## **3.2 Impact of increased eutrophication on production of forage fish in the 20th century (P2)**

*Margit Eero, DTU Aqua*

### **3.2.1 Abstract/highlights**

Eutrophication is one of the major human drivers of the Baltic Sea and reducing anthropogenic nutrient inputs is a major policy goal for restoring good environmental status of the sea. However, it is unclear to what extent reducing nutrients would also lower fish production and fisheries yields. Empirical examples of changes in nutrient loads and concurrent fish production can provide useful insights to this question. In this study, we investigated to what extent a multi-fold increase in nutrient loads from the 1950s to 1980s enhanced forage fish production in the Baltic Sea. We used monitoring data on fish stock dynamics covering the period of the nutrient increase, combined with nutrient concentrations from a 3-dimensional coupled physical-biogeochemical ocean model. The results suggest that nutrient enrichment enhanced the biomass level of forage fish by up to 50 % in some years and areas due to increased body weight of fish. However, major trends in sprat biomass in past decades have occurred independently of nutrient dynamics, largely driven by climate and top-down control (predation, fishing). Thus, nutrient reduction likely will affect the level of lows and peaks in future biomasses. However, future biomass trajectories may not follow changes in nutrient dynamics, but will probably largely depend on other prevailing ecosystem and climate conditions.

### **3.2.2 Progress and (if applicable) deviations from the work plan**

The results of this study are published in a paper: Eero, M., Andersson, H.C., Almroth-Rosell, E., MacKenzie, B.R. 2016. Has eutrophication promoted forage fish production in the Baltic Sea? *Ambio*, DOI 10.1007/s13280-016-0788-3. (Appendix 1).

### **3.2.3 Deviations from the work-plan**

None.

### **3.2.4 Introduction**

Anthropogenic nutrient enrichment and resulting eutrophication is considered as one of the major human perturbations to marine ecosystems worldwide. Eutrophication is generally associated with negative impacts on the environment, such as toxic algal blooms, degradation of habitats, oxygen deficiency and fish kills (e.g. Kemp et al. 2005, Anderson et al. 2008, Díaz and Rosenberg 2008). Consequently, minimizing human-induced eutrophication is necessary in order to achieve good environmental status of marine ecosystems. The historical, non-impacted status is often used as a basis for defining targets for nutrient reductions (e.g. HELCOM 2007). In this context, it is relevant to consider whether lowering nutrient concentrations to historical in some cases oligotrophic levels would involve trade-offs in terms of potentially reduced fish production and subsequent fisheries yields. Up to a certain level of nutrients, positive effects on fish production can be expected following the principles of an agricultural model, where the amount of production is determined by the food available (Nixon and Buckley 2002). However, the cascading effects of changes in nutrients and primary productivity on fish biomasses are often not apparent in empirical data or are difficult to demonstrate (Micheli 1999).

The Baltic Sea offers a unique opportunity for such investigations due to long time series of observational data on fish production that span over a period of substantial increase in nutrient inputs. In the Baltic Sea, eutrophication first became an issue after World War II, when intensified agriculture with high fertilizer usage, lack of proper wastewater treatment and atmospheric deposition caused a dramatic nutrient-load increase over a few decades from the 1950s to 1980s (Fig. 1). In this study, we assembled observational evidence for changes in recruitment (i.e. production of offspring) and individual growth of major forage fish species in the Baltic Sea, i.e. sprat and herring in the period from the 1950s to 1980s. We combined this information with

nutrient concentrations from a 3-dimensional coupled physical-biogeochemical ocean model and investigated whether positive effects of nutrient enhancement on fish production potentially occurred. The present study provides useful insights to whether reduced fish production can be expected if historical trophic status of the sea is restored, and can contribute to defining good environmental status in a wider ecosystem context.

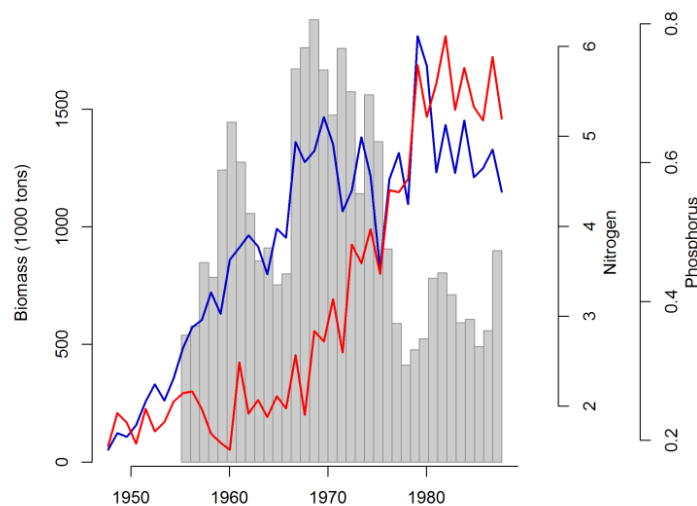


Figure 1. Development of winter nitrogen (blue line) and phosphorus (red line) concentrations ( $\text{mmol m}^{-3}$ ) in the Baltic Sea in comparison with trends in sprat biomass (bars)

### 3.2.5 Methods and Results

Fish biomasses are determined by a combination of recruitment, individual growth and mortality. Nutrients are expected to impact on adult fish biomass mainly via recruitment and growth, while biomasses of forage fish in the Baltic Sea are additionally heavily influenced by mortality due to fishing and predation by cod. In order to minimize the effect of mortality interfering with biomass dynamics, we investigated the potential effect of nutrient increase separately on recruitment and growth.

Recruitment and mean weight of sprat and herring in the Baltic Sea are influenced by a number of environmental and ecological factors, in addition to the potential effect of nutrients. Previous studies focusing on recent decades have related the weight of sprat and herring in the Baltic Sea to temperature, salinity and sprat abundance via intra-specific competition (Cardinale et al. 2002, Möllmann et al. 2005, Casini et al. 2010). Based on this knowledge, we included region-specific

temperature and salinity at 0–50 m depth in spring–summer and sprat abundance as explanatory variables for mean weight of both sprat and herring in all sub-areas, in addition to nitrogen and phosphorus concentrations. Average winter values (December–February) of nitrogen (Nc) and phosphorus (Pc) concentrations in the surface layers (0–9 m) at different sub-areas were extracted from the Swedish Coastal and Ocean Biogeochemical model coupled to the Rossby Centre Ocean circulation model (RCO-SCOBI). The model system is described in Eilola et al. (2009) and Meier et al. (2003) and has been used in various ocean-climate and process studies. Analyses of temporal changes in mean weight were conducted using multiple linear regressions.

Recruitment of forage fish in the Baltic Sea, especially sprat, shows high inter-annual variability. Among the variables investigated, sprat recruitment in a Baltic wide scale has been found to be most correlated with sea surface temperature (SST) in summer that affects the recruitment possibly via impacting on feeding and growth of early life stages (e.g. Margonski et al. 2010). SST has also been found to influence herring recruitment in the central Baltic Sea (Margonski et al. 2010). In a more coastal environment, such as the Gulf of Riga, herring recruitment has been related to the Baltic Sea index (BSI). Also, the size of the parent stock is traditionally considered to affect the amount of offspring. Based on this knowledge, region-specific SST in summer (August), Baltic Sea environmental index (BSE) and spawning stock biomass (SSB) were included as explanatory variables in recruitment (R) models, both for sprat and herring. A standard Ricker stock-recruitment model was applied, incorporating environmental variables.

The nutrient levels estimated from the RCO-SCOBI model show a fivefold increase in nitrogen concentration (Nc) from the 1950 to early 1970s. The concentration of phosphorus (Pc) was relatively stable from the 1950s to 1970s, but increased three to four times from the beginning of the 1970s to the first half of the 1980s (Fig. 1).

The mean body weight of sprat in SW and SE Baltic Sea was approximately 10–15 % higher in the 1970s–1980s compared to the early 1950s. A more pronounced increase in mean weight was recorded in the northern Baltic Proper, where an average sprat was up to 1.7 times heavier in the mid-1980s compared to the early 1960s. A similar increase in mean weight was recorded for herring in the northern Baltic. The positive trends in both sprat and herring body weight in the 1970s–1980s coincided with the pronounced increase in Pc. Accordingly, Pc was found to explain significant amount of variability in mean weight of both sprat and herring in all sub-areas. Nc was significant only for herring in the northern Baltic Sea.

Sprat recruitment models including SSB and SST as explanatory variables explained significant amounts of recruitment variability in all three sub-regions in the Baltic Proper. In the northernmost area, including additionally BSE as an explanatory variable significantly improved the explained variability in recruitment. For herring in the northern Baltic, SST was not found to be significant and the final model therefore only included SSB and BSE as explanatory variables.  $N_c$  and  $P_c$  did not appear significant in any of the recruitment models. Indirectly, the nutrient increase was found to have affected recruitment via mean weight of individual fish that enhanced the biomass, which in turn influenced recruitment.

Changes in body weight of individual fish modify the biomass directly. Additionally, given that a larger SSB produces a higher recruitment, the increase in mean body weight promotes the stock further via enhanced recruitment. Both of these processes were taken into account when simulating sprat biomass dynamics under stable nutrient concentrations from the 1950s. The simulated biomass dynamics in terms of major fluctuations in stock size were similar to the estimates from original stock assessment (Fig. 2). However, the proportional difference between the two time series increased from the 1950s to 1980s and reached up to 50 % (in the 1980s) higher observed sprat biomass in northern Baltic Sea compared to the simulated scenario with no increase in nutrients (Fig. 2). The relative effect of nutrient increase on biomass was lower in SW and SE, up to 30 and 40 %, respectively. In a scale of the entire Baltic Sea, our simulations of sprat dynamics applying constant nutrient concentrations resulted in up to 40 % lower biomass (in the 1980s) compared to the observed level.



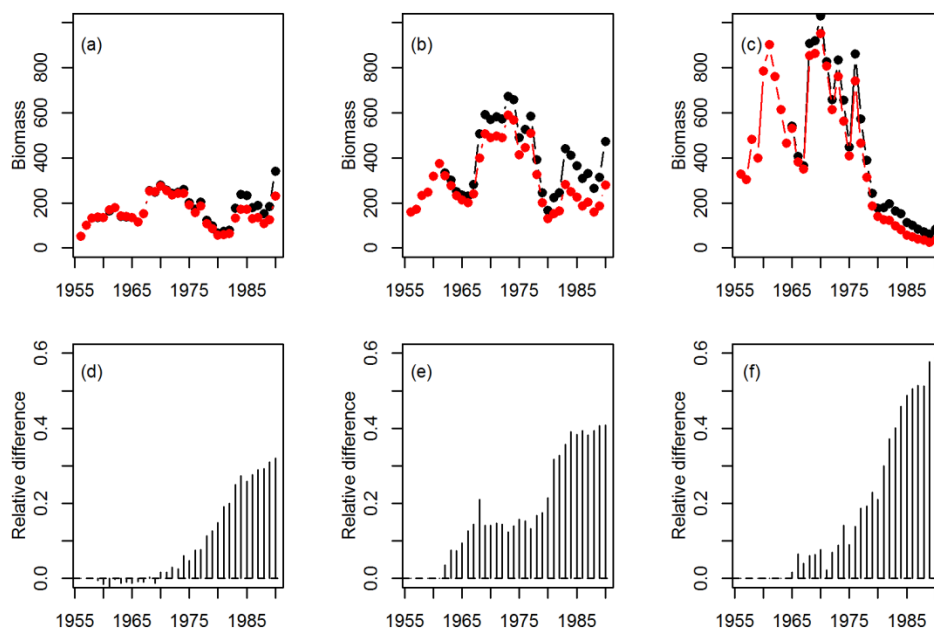


Figure 2. Upper panels: simulated sprat biomass (red line) applying constant nutrient concentrations from the 1950s compared to the observed biomass (black line) as estimated from stock assessment (Eero 2012). Lower panels: proportional difference between the observed and simulated sprat biomass. The results are shown separately for southwestern (a, d), southeastern (b, e) and northern (c, f) areas of the Baltic Proper

### 3.2.6 Recommendations

In summary, although our analyses suggest that the nutrient increase enhanced the level of sprat biomass via mean weight, this effect appears relatively minor compared to the more than fivefold fluctuations in sprat biomass that have occurred over time due to other drivers. In fact, a substantial decline in sprat biomass took place from the late 1960s to 1980s, in contrast to increasing nutrient concentrations (Fig. 1).

Empirical evidence suggests that nutrient increase from the 1950s to 1980s enhanced the level of forage fish biomass (up to 40 % in some years in our analyses) in the Baltic Sea via increased body weight of the fish. Thus, nutrient reduction likely will affect the level of lows and peaks in future biomasses. However, major trends in sprat biomass in past decades have occurred independently of nutrient dynamics, largely driven by climate and top-down control (predation, fishing). This suggests that future biomass trajectories may not follow changes in nutrient dynamics, but will probably largely depend on other prevailing ecosystem and climate conditions. Furthermore, future

nutrient levels and availability for biological production are difficult to predict due to long response times to reduced nutrient loads (e.g. Conley et al. 2009), combined effects of changing climate and nutrient loads (Hägg et al. 2014) and the uncertainty of whether the nutrient loading objectives themselves can be achieved by all Baltic countries.

### **3.3 Current status of shipping in the Baltic Sea (P6)**

*Jonne Kotta, University of Tartu,  
Estonian Marine Institute*

#### **3.3.1 Abstract/highlights**

Shipping has been one of the biggest economic sectors in the Baltic Sea throughout the past centuries. Currently, the most intensive shipping occurs in the central Baltic Sea and the Gulf of Finland. Vessel size and goods volume in ports around the Baltic Sea have increased substantially in recent decades, whereas at the same time as the number of vessels has fallen and the shipping of goods overseas is expected to double by 2050. Intensively used shipping routes can have negative impacts (disturbance, oil spills etc.) on areas of high ecological value. As a potential solution, alternation of shipping routes in ecologically sensitive areas will be considered. This further entails an environmental conflict related to fuel consumptions since rerouting involves an increase in the travel distances, and potentially higher costs and CO<sub>2</sub> emissions (this cost can be partly reduced by using the deep water route which reduces friction). A common Baltic map on areas of high ecological value is being argued to be essential for planning the shipping routes, which can in turn, minimise the impacts caused by shipping accidents and oil spills. Additionally, the contingency plans must take into account the ecologically sensitive areas in targeting the actions and allocation of the technique for rescue operations.

#### **3.3.2 Progress and (if applicable) deviations from the original work plan**

Results from EU FP7 Vectors (<http://www.marine-vectors.eu/>), Baltic Scope (<http://www.balticscope.eu/>) projects, HELCOM and other sources have been reviewed and summarized with an aim to provide current knowledge and data on shipping in Baltic Sea region.

### **3.3.3 Deviations from work plan**

None.

### **3.3.4 Introduction**

In general, shipping is free in marine space taking into account agreed international and national rules. Shipping rules are agreed and set by International Maritime Organization (IMO) and most of the agreed regulations are ratified and integrated into national laws by the states around the Baltic Sea.

International shipping conventions that has the most direct influence to the marine life is the Convention on the International Regulations for Preventing Collisions at Sea (COLREG), 1972; the International Convention for the Safety of Life at Sea (SOLAS), 1974, as amended and the United Nations Convention on the Law of the Sea (UNCLOS).

UNCLOS defines states' rights and responsibilities, both in zones subject to coastal state sovereignty (territorial sea) and jurisdiction (EEZ) and in areas beyond national jurisdiction (the high seas). UNCLOS provides that all states are free to use the high seas with due regard for other states' interests. These freedoms include navigation, fishing, marine scientific research, the laying of undersea cables and pipelines, and the construction of artificial islands. UNCLOS also contains a general obligation for States to protect and preserve the marine environment. According to UNCLOS Article 60 in the EEZ the coastal State shall have the exclusive right to construct and to authorize and regulate the construction of artificial islands, installations, structures and safety zones. Those constructions and the safety zones around them may not be established where interference may be caused to the use of recognized sea lanes essential to international navigation.

Additionally, IMO has highlighted the Baltic Sea as a particularly sensitive marine area within which certain specific measures are to be taken, including traffic management and the stricter application of requirements in respect of discharges and equipment.

Other conventions like the International Convention for the Prevention of Pollution from Ships, 1973, as modified by the Protocol of 1978 relating thereto and by the Protocol of 1997 (MARPOL) or International Convention for the Control and Management of Ships' Ballast Water and Sediments, 2004 are more covering the management issues of shipping as such and have less impact in dividing the marine space between different users and newcomers.

In the EU transport policy, importance is attached to the improved merger of the formerly nationally centred networks into a single EU network and to the external connections of the EU to other nations. Despite of the development of EU single network it is necessary to take into account the needs of country specific solutions and development.

Shipping, as a whole, could be largely divided into two subgroups, small craft and large scale shipping that are having different navigational characteristic and impacts in the marine space. Shipping is directly linked to land – through ports and harbours, different economic activities (industries) taking place on land and socioeconomic aspects (population intensity). The ports are important locations for the forwarding of goods and passengers. For the transport sector to function optimally, the various modes of transport need to cooperate with each other.

### **3.3.5 Methods and Results**

#### **3.3.5.1 Current use of shipping in the Baltic Sea:**

Efficient utilisation of marine space and connecting ports to other infrastructure is one of the main factors in improving Baltic Sea Region's international competitiveness, enabling it to participate in trade between Russia, Asia and Europe. One of the drivers of any country's development around the Baltic Sea is international freight transport.

To give an overview about the use of shipping in the Baltic Sea area shipping intensity analyses were carried out by HELCOM by different ship categories. In general the most intensive shipping takes place in the Danish Straits, Swedish waters passing the island Gotland and heading to the Gulf of Finland (Fig. 1). Figures 2–9 show current average shipping intensities of the Baltic Sea by all different vessel types.

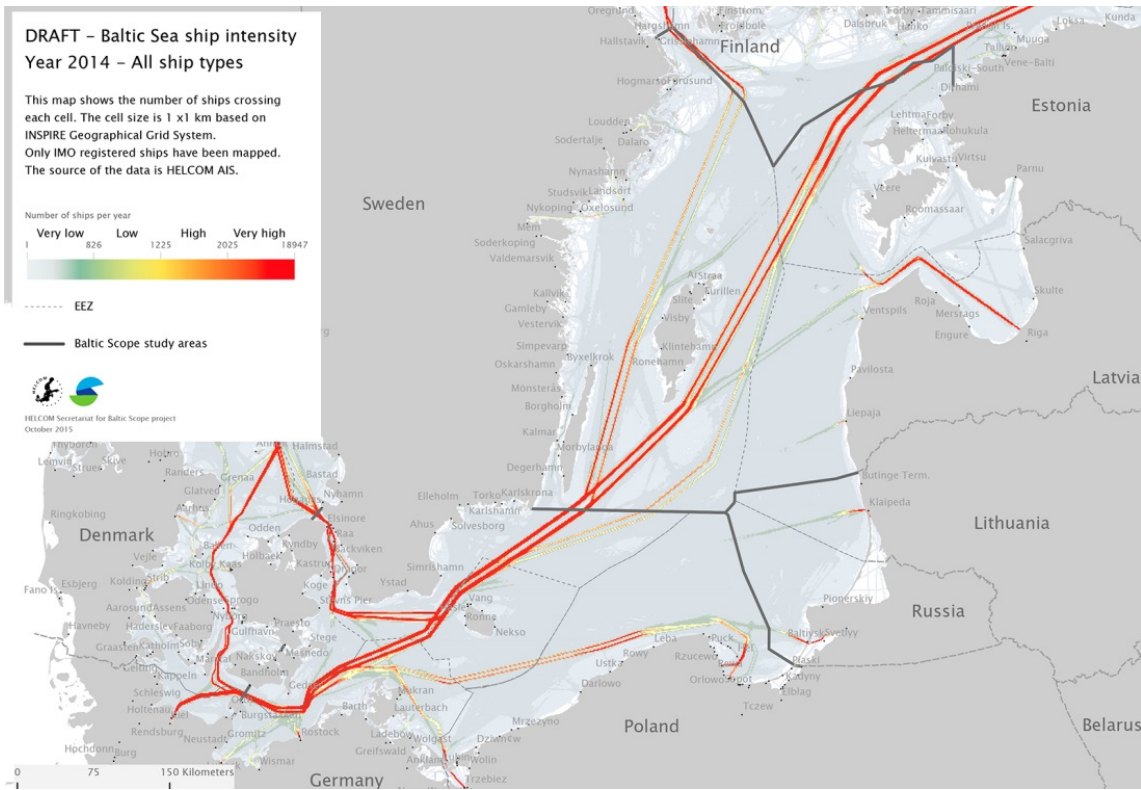


Figure 1. Current use of shipping in the Baltic Sea, all vessel types included (data from the HELCOM Secretariat October 2015).

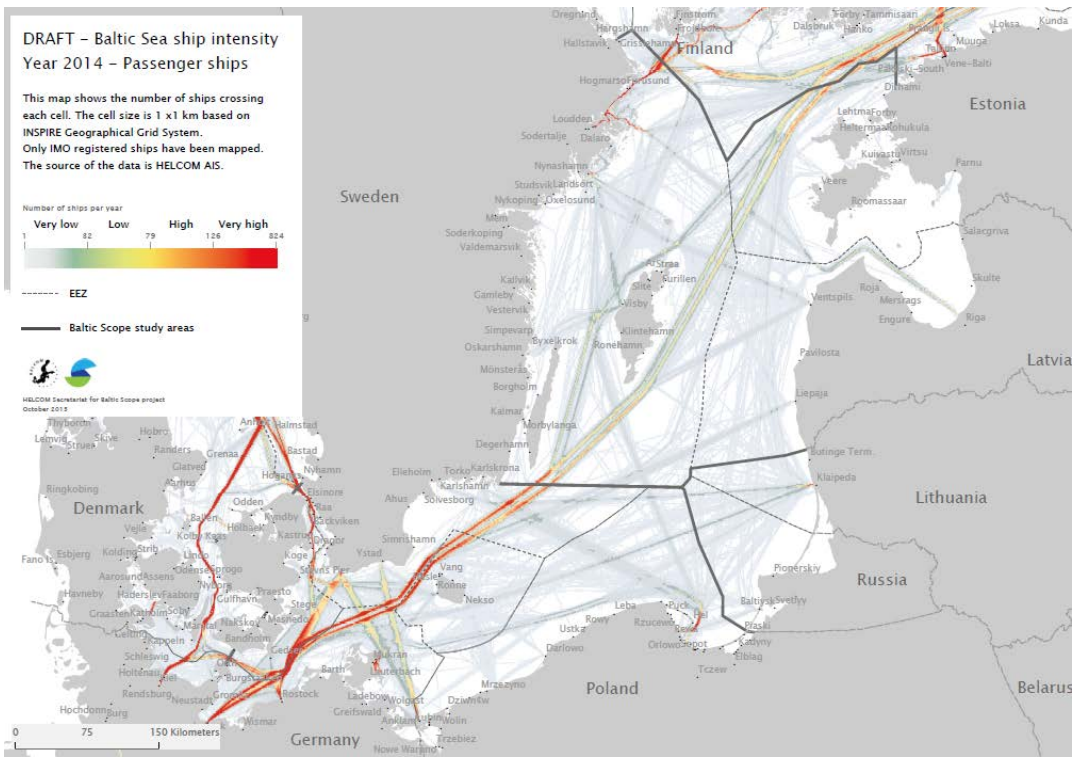


Figure 2. Current use of shipping in the Baltic Sea, passenger ships (data from the HELCOM Secretariat October 2015).

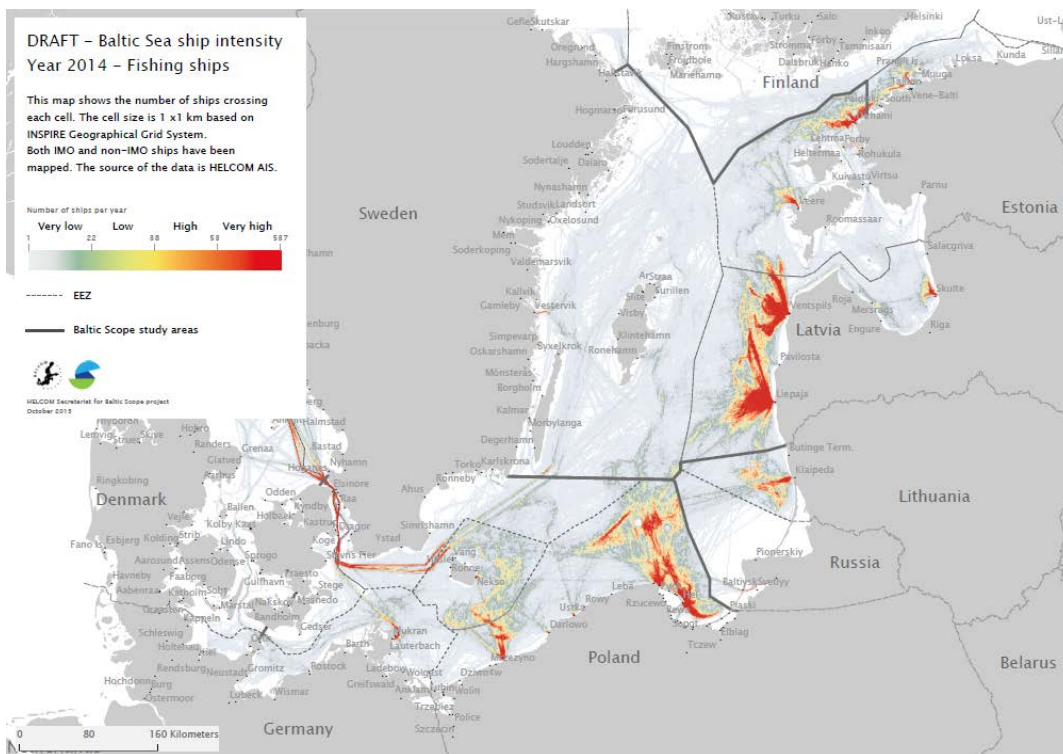


Figure 3. Current use of shipping in the Baltic Sea, fishing ships (data from the HELCOM Secretariat October 2015).

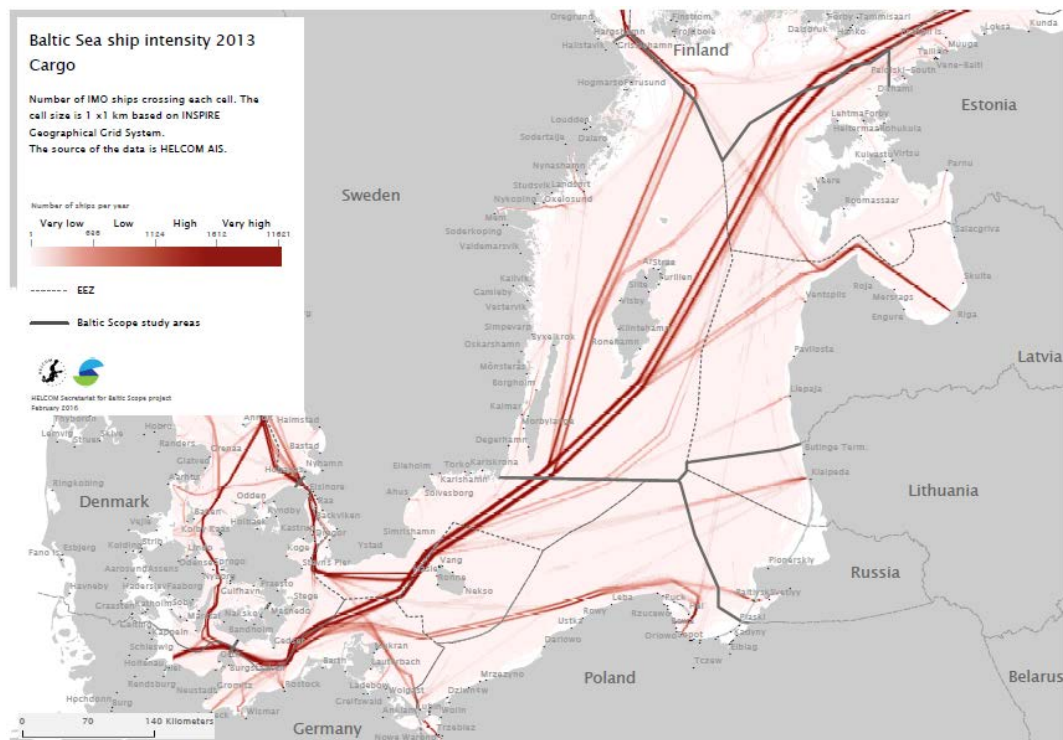


Figure 4. Current use of shipping in the Baltic Sea, cargo ships (data from the HELCOM Secretariat October 2015).

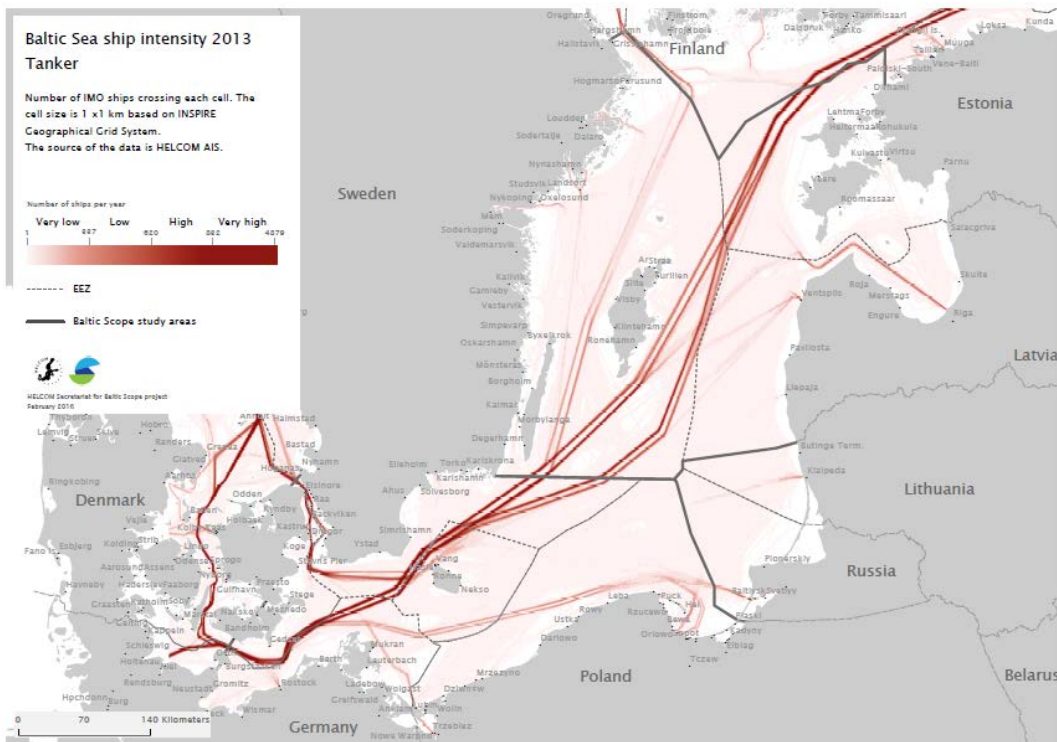


Figure 5. Current use of shipping in the Baltic Sea, tanker ships (data from the HELCOM Secretariat October 2015).

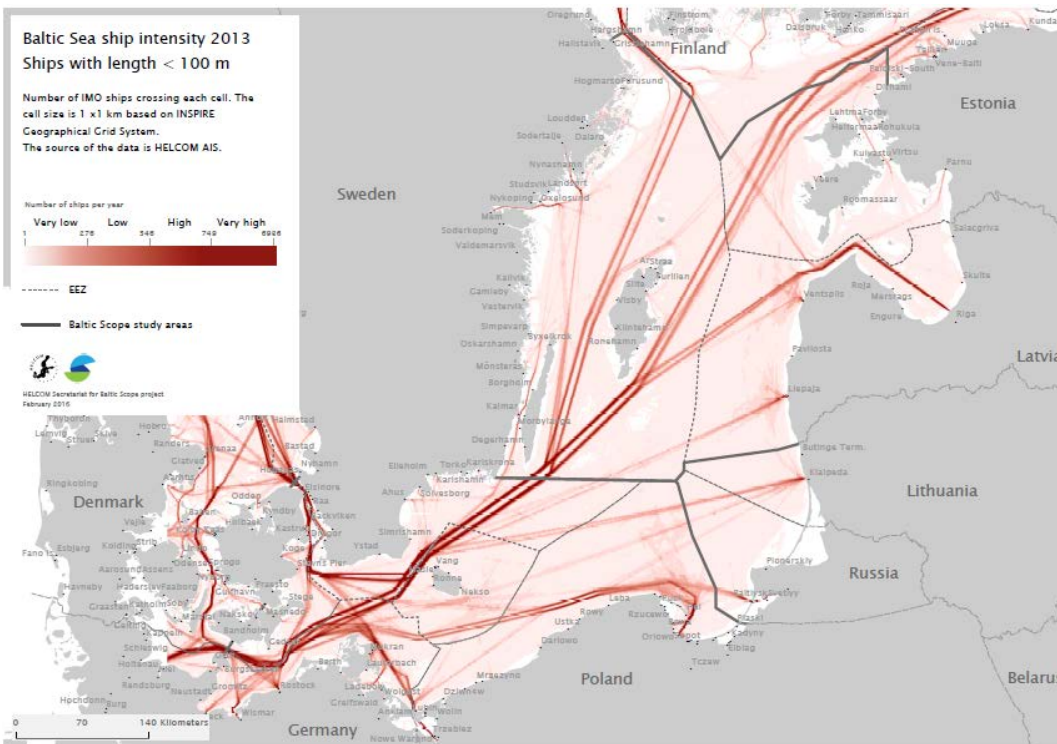


Figure 6. Current use of shipping in the Baltic Sea, ships less than 100 m (data from the HELCOM Secretariat October 2015).

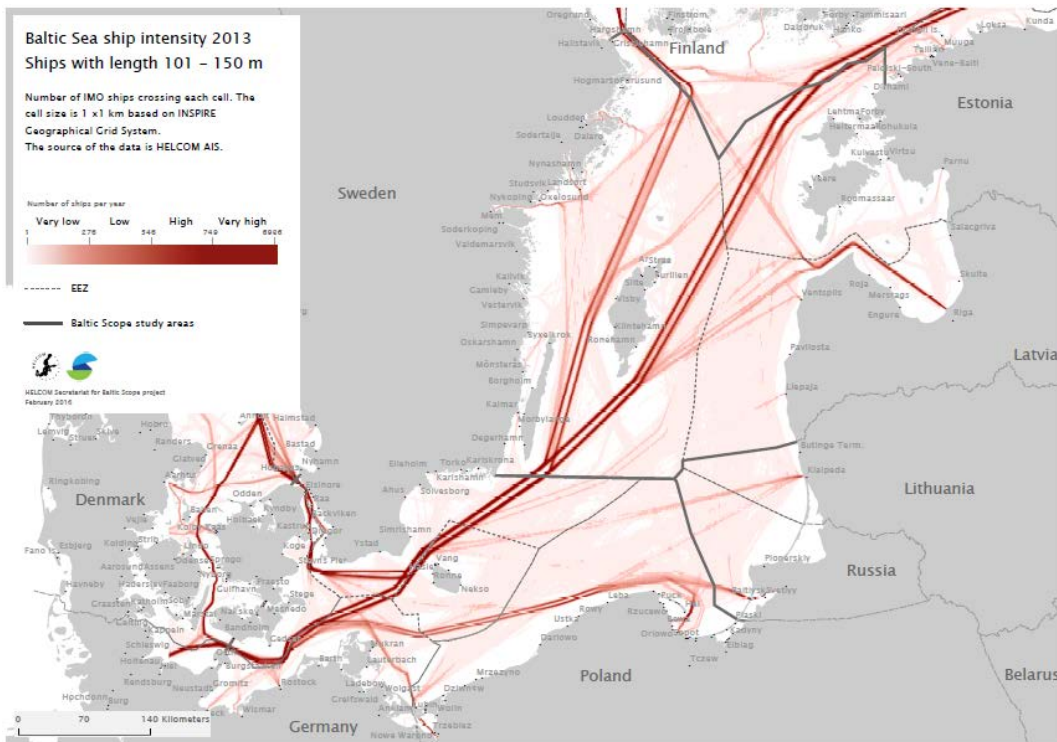


Figure 7. Current use of shipping in the Baltic Sea, ships between 101 and 150 m (data from the HELCOM Secretariat October 2015).

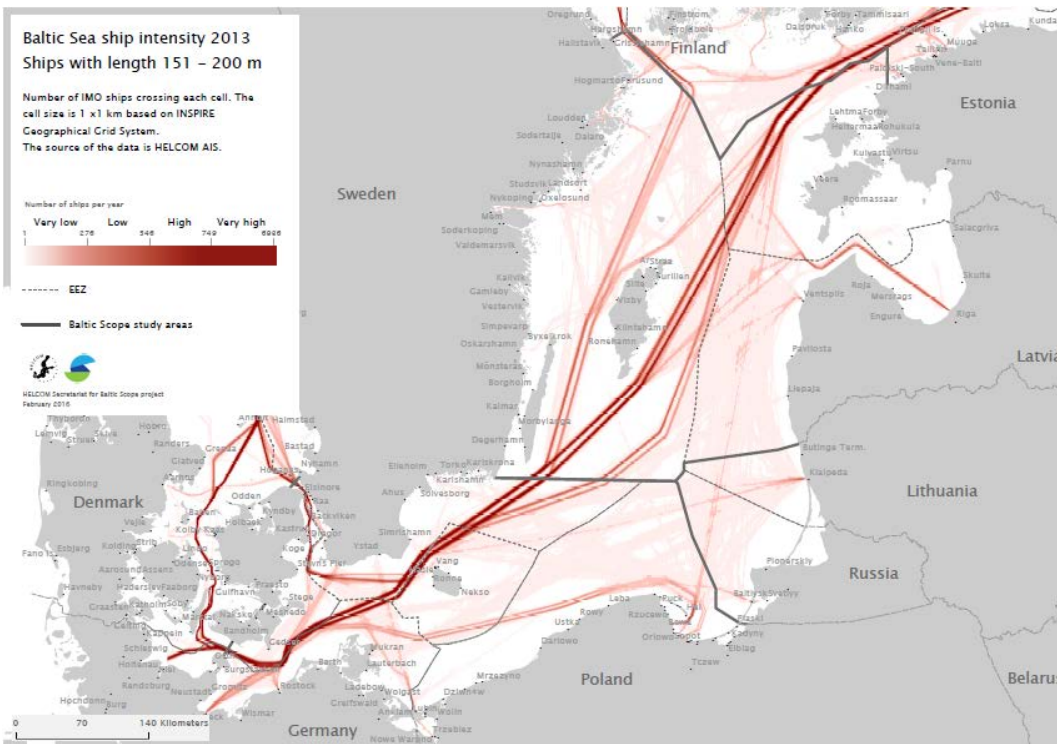




Figure 8. Current use of shipping in the Baltic Sea, ships between 151 and 200 m (data from the HELCOM Secretariat October 2015).

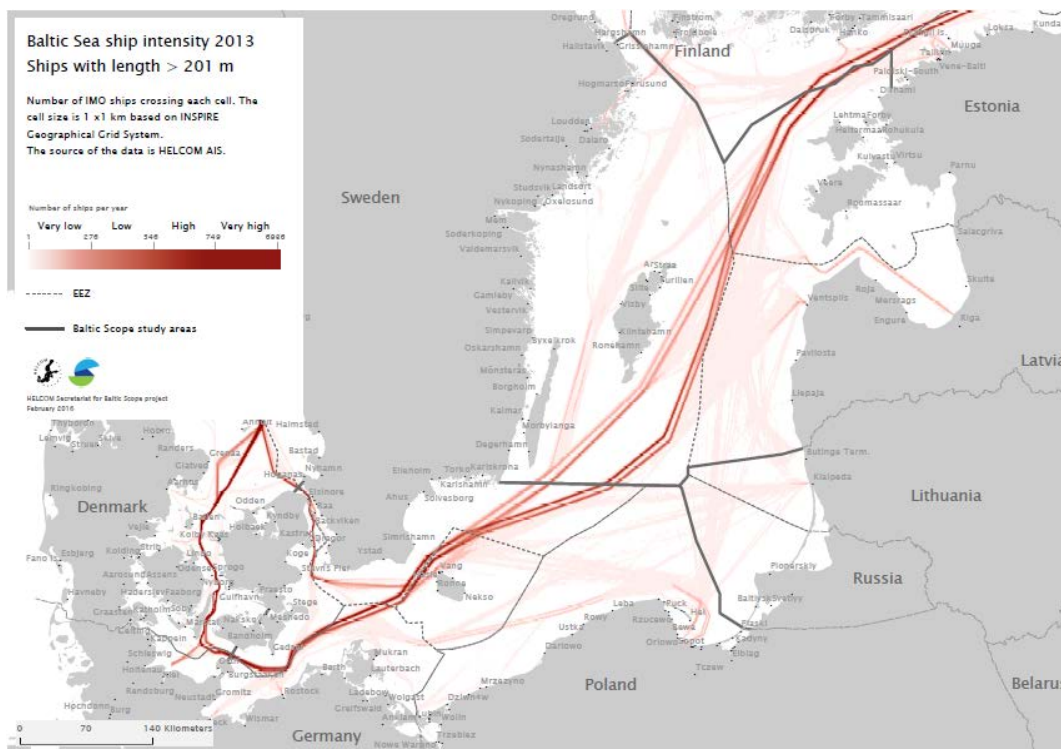


Figure 9. Current use of shipping in the Baltic Sea, ships over 201 m (data from the HELCOM Secretariat October 2015).

### 3.3.5.2 Future developments of shipping in the Baltic Sea

The spatial developments on mainland influence the spatial developments at sea. The trans-European transport network (TEN-T) is a network which comprises roads, railway lines, inland waterways, inland and maritime ports, airports and rail-road terminals throughout the 28 Member States and therefore can be seen as main and strong functional implications to the Baltic Sea area.

The North Sea-Baltic Corridor (Fig. 10) connects the ports of the Eastern shore of the Baltic Sea with the ports of the North Sea. The corridor will connect Finland with Estonia by ferry, provide modern road and rail transport links between the three Baltic States on the one hand and Poland, Germany, the Netherlands and Belgium on the other. Between the Odra River and German, Dutch and Flemish ports, it also includes inland waterways, such as the “Mittelland-Kanal”. The most important project is “Rail Baltic”, a European standard gauge railway between Tallinn, Riga, Kaunas and North-Eastern Poland (EC 2015).

The Scandinavian-Mediterranean Corridor is a crucial north-south axis for the European economy. Crossing the Baltic Sea from Finland to Sweden and passing through Germany, the Alps and Italy, it links the major urban centres and ports of Scandinavia and Northern Germany to continue to the industrialized high production centres of Southern Germany, Austria and Northern Italy further to the Italian ports and Valletta. The most important projects in this corridor are the fixed Fehmarnbelt crossing and Brenner base tunnel, including their access routes. It extends, across the sea, from Southern Italy and Sicily to Malta (EC 2015).

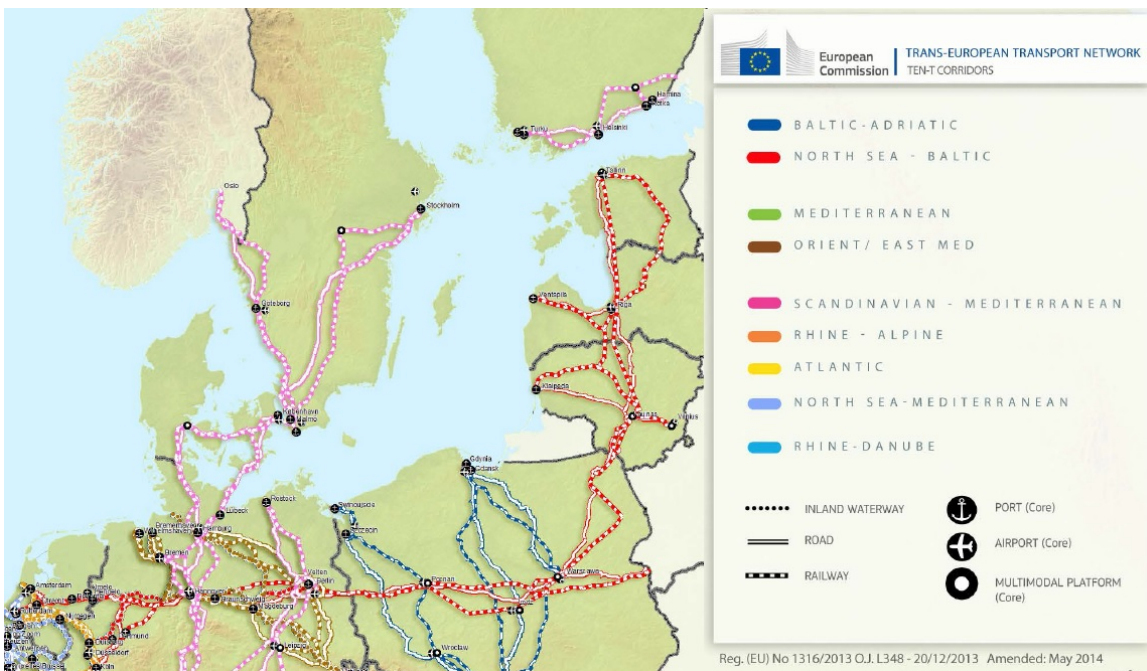


Figure 10. The overall TEN-T corridors (EC 2015).

Vessel size and goods volume in ports around the Baltic Sea have increased substantially in recent decades, whereas at the same time as the number of vessels has fallen. In general, developments within shipping sector mean that the average size of ships is believed to increase with time. But the maximum size is not believed to increase much. This is because the inlets in the Baltic are not deep enough for larger ships. This is unless heavy dredging takes place in Denmark, potentially co-funded by Baltic Sea states.

It is also believed that ship traffic will increase with up to 400 % globally and about 50 % in the Baltic Sea by 2050. The shipping of goods overseas is expected to double by 2050. Moreover, global trade patterns could change by 2050 and long distance shipping may diminish.

The importance of different harbours may change over time. In the winter, northern parts of the Baltic Sea have ice coverage which significantly reduces the spatial options for ship movements. Ice-free routes are few during wintertime and will remain very important although their stretch could be modified. Some countries have expressed political will to increase coastal and inland shipping.

As a result of the Freedom of the Seas ships have no obligation to navigate according to routes. Routes are basically mirrors of the closest path between important harbours and it is important to consider that (a) ships may not follow routes or AIS patterns and (b) the optimal route may differ among different types of ships. However, shipping is also a very flexible sector that can adapt to spatial limitations although at the costs of economic efficiency, environmental performance and potentially safety. With Sea Traffic Management shipping may become much more efficient and possibly this trend can facilitate for future shipping to consider 'soft' regulations such as avoiding environmentally sensitive areas without IMO regulations.

### **3.3.6 Recommendations**

Significant use of maritime services in the Baltic Sea and projected future changes within the sector result in various cross-disciplinary conflicts with environment and fisheries. Specifically, intensively used shipping routes can have negative impacts (disturbance, oil spills etc.) on areas of high ecological value. As a potential solution, alternation of shipping routes in ecologically sensitive areas should be considered. This further entails an environmental conflict related to fuel consumptions since rerouting involves an increase in the travel distances, and potentially higher costs and CO<sub>2</sub> emissions (this cost can be partly reduced by using the deep water route which reduces friction).

A common Baltic map on areas of high ecological value is being argued to be essential for planning the shipping routes, which can in turn, minimize the impacts caused by shipping accidents and oil spills. Additionally, the contingency plans must take into account the ecologically sensitive areas in targeting the actions and allocation of the technique for rescue operations.

Negative impacts of shipping (noise, pollution) to the fisheries (Essential Fish Habitats, spawning and nursery areas) are potentially the main conflicts among these sectors. Relocating shipping routes can be regarded as a solution to minimise the impact of noise and pollution. Other possible measures such as speed limits and passage limitations have been also pointed out.

### **3.4 Current status of fishing in the Baltic Sea (P6)**

*Henn Ojaveer, University of Tartu,  
Estonian Marine Institute*

#### **3.4.1 Abstract/highlights**

The main target species in commercial fishery are cod, herring and sprat. They constitute about 95 % of the total catch. The main fisheries for cod in the Baltic use demersal trawls, gillnets and pelagic trawls. Pelagic trawlers catching a mixture of herring and sprat dominate pelagic fisheries in the Baltic. The proportion of the two species in the catches varies according to area and season. To a minor extent, a predominantly herring fishery is carried out with trap-nets/pound-nets and gill nets in coastal areas as well as with bottom trawls.

South-western Baltic Sea undoubtedly faces the highest fishing pressure, estimated either by the swept area method or number of hours fished. Mostly bottom gears, but also longlines are operating in this region. Fishery by mid-water trawls targeting pelagic fish is more homogeneously spread over the Baltic Sea. Effort in pelagic fishery is relatively high in the north-eastern Baltic (Bothnian Sea, western Gulf of Finland, Gulf of Riga and west of Irbe Strait) compared to most other areas (except perhaps Gulf of Gdansk).

#### **3.4.2 Progress and (if applicable) deviations from the work plan**

Review completed.

#### **3.4.3 Deviations from the work-plan**

None.

#### **3.4.4 Introduction**

The main target species in commercial fishery are cod, herring and sprat. They constitute about 95 % of the total catch. Other target fish species having either local economical importance or ecosystem importance are salmon, plaice, flounder, dab, brill, turbot, pike-perch, pike, perch, vendace, whitefish, turbot, eel and sea-trout.

The main fisheries for cod in the Baltic Sea use demersal trawls, gillnets and pelagic trawls. There was a substantial increase in gillnet fisheries in the 1990s and because of the change in stock age composition in late 1990s and early 2000. Pelagic trawlers catching a mixture of herring and sprat dominate pelagic fisheries in the Baltic Sea. The proportion of the two species in the catches varies according to area and season. To a minor extent, a predominantly herring fishery is carried out with trap-nets/pound-nets and gill nets in coastal areas as well as with bottom trawls.

While feeding in the sea, salmon are caught by long lines (as drift nets have been banned in the Baltic) and during the spawning run they are caught along the coast, mainly in trap nets and fixed gillnets. Where fisheries are allowed in the river mouths, set gill nets and traps nets are used.

The coastal fisheries target a variety of species with a mixture of gears including fixed gears (e.g. gill, pound and trap nets, and weirs) and Danish seines. The main species exploited are herring, salmon, sea trout, flounder, turbot, cod and freshwater and migratory species. In addition, there are demersal trawling activities for herring, cod and flatfishes in some parts of the Baltic, although the trawling is forbidden in the coastal zone in most of the countries. Most of the flatfish fishery is conducted in the western part of the Baltic. Coastal fisheries are conducted along the entire Baltic coastline (ICES 2014).

### **3.4.5 Methods and results**

The information used in this section originates from ICES Special Request Advice on the Baltic Sea Ecoregion (Published 25 August 2015; Version 2, 14 January 2016) as a response to *HELCOM request on pressure from fishing activity (based on VMS/logbook data) in the HELCOM area relating to both seafloor integrity and management of HELCOM MPAs* (ICES 2015a). We have used this information source in evaluation the spatial dimension of various fishing practices as it represents the most up-to-date synthetic information on spatial distribution of fishing in the Baltic Sea.

Fishing abrasion pressure maps were produced for mobile bottom-contacting gears. Separate maps were produced for surface and subsurface abrasion. Maps for midwater trawls and longlines were produced using fishing effort as the number of hours fished, extracted from the submitted VMS data.

‘Swept area’ is generally considered to be an estimate of the area of seabed in contact with the fishing gear and is a function of gear width, vessel speed, and fishing effort. The swept area ratio is

calculated as the swept area divided by the cell area, and the values indicate the number of times the entire grid cell area was swept (note that distribution of effort may not be evenly spread). The swept area ratio is calculated for surface and subsurface abrasion separately. Different gear types interact with the seabed in different ways and thus exert different levels of abrasive pressure, both in terms of the area of substrate affected and the penetration depth. Surface abrasion is defined as the damage to seabed surface features, subsurface abrasion as the penetration and/or disturbance of the substrate below the surface of the seabed

Maps showing fishing effort expressed as number of hours per grid cell have been produced for all requested fisheries individually and combined (mobile bottom-contacting gears, midwater trawls, and longlines).

Based on the reviewed information it can be said that south-western Baltic Sea (incl. Kattegat and Bornholm Sea) undoubtedly face the highest fishing pressure estimated either by the swept area method (Fig. 1) or number of hours fished (Fig. 2). Mostly bottom gears, but also longlines (around and east of Bornholm) are operating in this region.

In difference, fishery by mid-water trawls targeting pelagic fish (herring and sprat) is more homogeneously spread over the Baltic Sea (Fig. 2). Fishing effort seems to be relatively high in the north-eastern Baltic (Bothnian Sea, western Gulf of Finland, Gulf of Riga and west of Irbe Strait) compared to most other areas (except perhaps the Gulf of Gdansk).

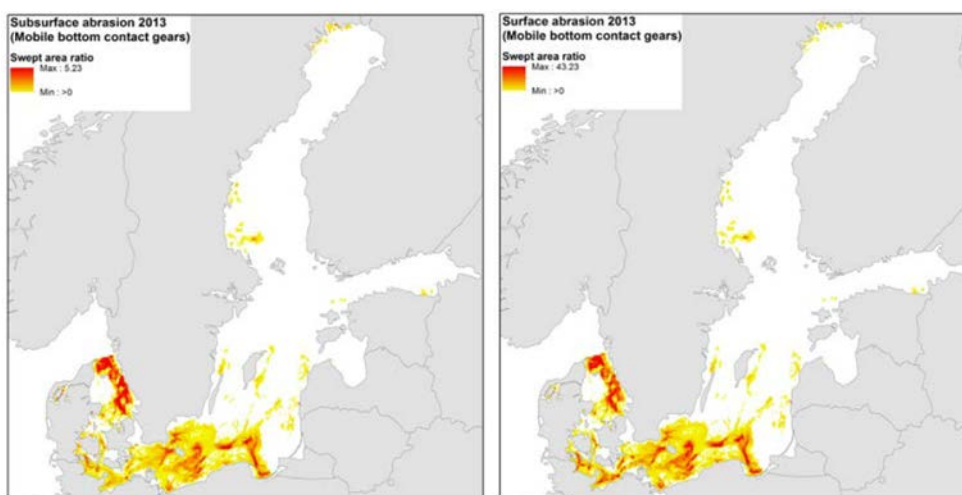


Figure 1. Sub-surface (left) and surface (right) abrasion by mobile bottom-contacting gears in 2013 (ICES 2015a).

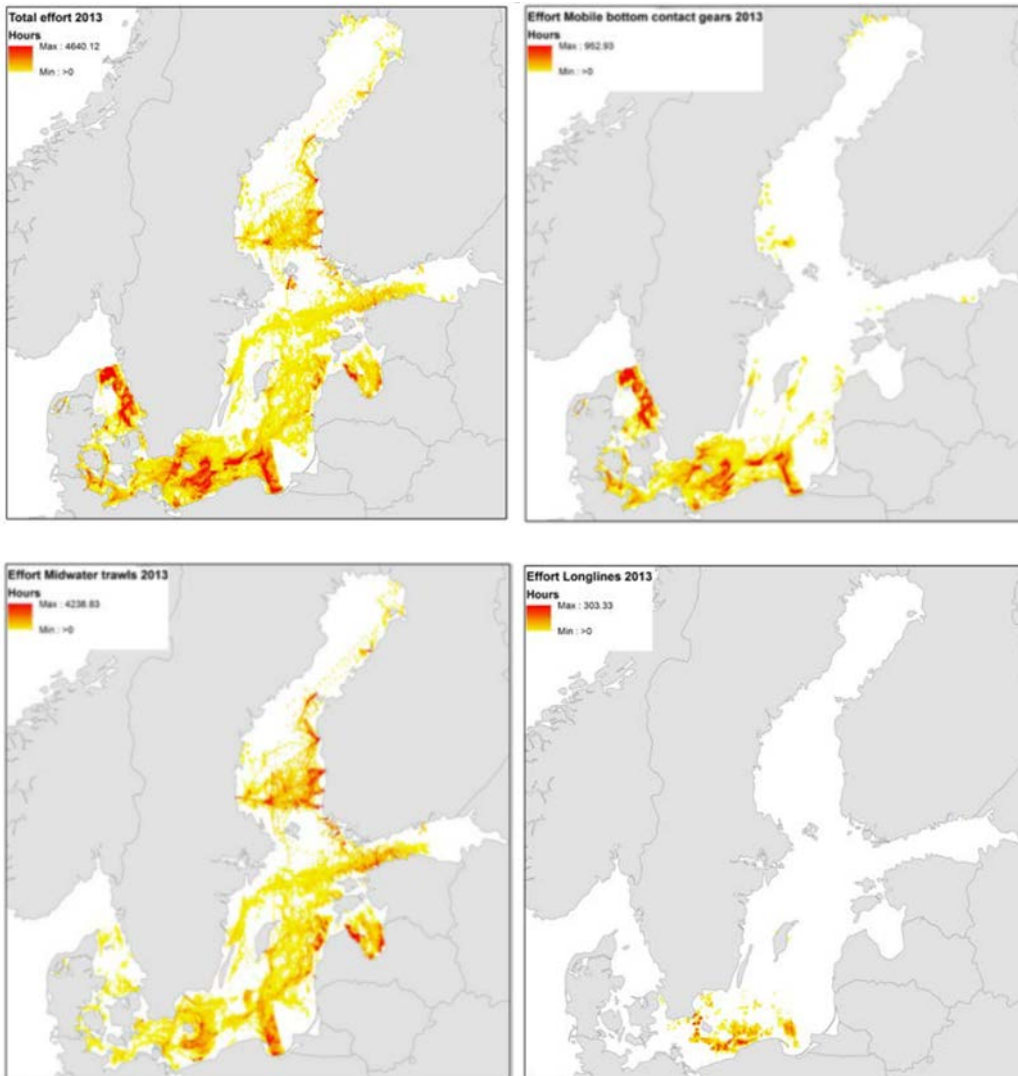


Figure 2. Fishing effort (hours): total (upper left panel), mobile bottom-contacting gears (upper right panel), mid-water trawl (lower left panel) and longlines (lower right panel) in 2013 (ICES 2015a).

### 3.4.6 Recommendations

There were a number of caveats identified relative to the fishing pressure maps produced (ICES 2015a):

- The methods for identifying fishing activity from the VMS data varied between countries; therefore there may be some country-specific biases that ICES cannot evaluate. Additionally, activities other than active towing of gear may have been incorrectly identified as fishing activity.

This would have the effect of overestimating the apparent fishing intensity in ports and in areas used for passage.

- Many countries have substantial fleets of smaller vessels that are not equipped with VMS (<15 m prior to 2012, <12 m thereafter); logbook data is at the spatial resolution of ICES rectangles, but where possible, they have been overlaid with the VMS data for the purpose of analysis.
- The fishing abrasion pressure methodology is based on very broad assumptions in terms of the area affected by abrasion. A single speed and gear width was applied across each gear category in most cases, which can lead to both underestimates and overestimates in actual surface and subsurface abrasion.

These considerations need to be addressed to harmonise the data recording by countries and come up with higher-quality evaluation on spatial distribution of fishing pressure by different fishing practices at the pan-Baltic scale.

### **3.5 Current status of non-indigenous species (NIS) in the Baltic Sea (P6)**

*Henn Ojaveer, University of Tartu,  
Estonian Marine Institute*

#### **3.5.1 Abstract/highlights**

Out of the total of 132 NIS and cryptogenic species (CS) recorded, 59 % are currently established in at least one country surrounding the Baltic Sea. On average, each country currently hosts 27 such species with 15 % of the established species being found in at least 50 % of the countries. Benthic macroinvertebrates dominate; both among those recorded (48 %) and established (59 %) species. Shipping, deliberate stocking and natural spread of NIS previously introduced to the North Sea are the main introduction pathways, with considerable dynamics over time. Amongst the pathways responsible for the currently established species, shipping and natural spread strongly dominate. Substantial uncertainty in the information on introduction pathways (except for deliberate releases) hampers detailed analyses and poses major challenges for management. Spatio-temporal variability in the invasion dynamics reflects both the spatial differences in the main hydrographic conditions of



the Baltic Sea as well as the availability of introduction pathways. We conclude that the Baltic Sea cannot be considered as a uniform waterbody in terms of the established introduced species and at least two major regions with differing hydrographic conditions and introduction pathways can be clearly distinguished.

### **3.5.2 Progress and (if applicable) deviations from the work plan**

Analyses completed and manuscript conditionally accepted to a peer reviewed journal Biological Invasions:

Manuscript: Ojaveer, H., Olenin, S., Narščius, A., Florin, A-B., Ezhova, E., Gollasch, S., Jensen, K.R., Lehtiniemi, M., Minchin, D., Normant-Saremba, M. and Sträke, S. Dynamics of biological invasions and pathways over time: a case study of a temperate coastal sea. (Appendix 2)

### **3.5.3 Deviations from the work-plan**

None.

Page 33 to page 49 were removed because they are under embargo until manuscripts are published.

If there is interest in the data, contact with Henn Ojaveer ([henn.ojaveer@ut.ee](mailto:henn.ojaveer@ut.ee))



































## **3.6 Interactions between eutrophication and temperature (P9)**

*Henrik Skov, DHI*

### **3.6.1 Abstract/highlights**

Spatio-temporal changes in sea surface temperatures and trajectories of temperatures and nitrogen concentrations over the period 1970–2010 have been examined. A long-term increasing trend in sea surface temperature has been recorded with a tendency for intensification after 2001. After 2001, a parallel decreasing trend is seen in winter DIN concentrations in all regions of the Baltic Sea. The

periods before/after 2001 will be used to frame the ecosystem model scenarios for testing the effects of temperature and eutrophication on the benthic productivity in different regions.

### **3.6.2 Progress and (if applicable) deviations from the work plan**

Analyses have been finalized. Results may be integrated with results from 3.1 - time series analyses of nutrient concentrations, which will be published as a scientific paper (either as a stand-alone or combined with other project deliverables from 3.1).

### **3.6.3 Deviations from the work-plan**

Spatio-temporal trends in relations between eutrophication and sea temperature along coastal gradients (littoral-sublittoral) have been examined in the entire southern part of the Baltic Sea, rather than just in two regions as originally planned (the Rügen-Arkona area and the Gulf of Riga). This amendment enables a more comprehensive assessment of temporal changes in the two biodiversity drivers.

### **3.6.4 Introduction**

Baltic trends in sea temperature reflect both climatic oscillations forced by variations in NAO and global warming processes (Siegel et al. 2006). Sea temperature influences biodiversity and bio-productivity in the Baltic Sea e.g. by affecting growth rates or dispersal (due to intolerance to lower or higher temperatures) of primary and secondary producers. The recent increase in sea temperature in the Baltic Sea may have introduced multiple changes in benthic and pelagic biodiversity. The dramatic increase in the stock of sprat *Sprattus sprattus* in the 1980s was likely caused by increases of the prey of sprat larvae (*Acartia spp.* and *Temora longicornis*) due to higher temperatures (Alheit et al. 2005). A northward shift in the winter distribution of 11 waterbird species in the Baltic Sea has been recorded between 1987 and 2010 (Skov et al. 2011).

Eutrophication reflects the anthropogenic nutrient (nitrogen and phosphorus) supply to the sea as a function of population growth and changes in agricultural practices in catchment areas. Together with light and carbon, nutrients act as the primary drivers of phytoplankton production.

The Baltic Sea is currently in a warming phase. SST satellite images from the period 1990–2004 analysed by Siegel (2006) showed a general weak, but positive trend over the period with an increase of 0.8 °C in surface waters, yet with a tendency for a steeper increase and an intensifying

trend after 1999. Summer and autumn temperatures contributed most to the trend. Despite these differences and local variations induced by upwelling, coastal jets and river discharges the trends were shown in all parts of the Baltic Sea, yet stronger in the northern than in the southern parts. In this report, the trend in surface water temperature was assessed based on measured (1970–2010) and modelled (1970–2007) surface temperatures.

The supply of large quantities of nutrients to the coastal regions of the Baltic Sea has caused an increase in phytoplankton growth with cascading positive effects on benthos productivity (Kiørboe et al. 1980, Cederwall and Elmgren 1990, Josefson and Rasmussen 2000). At the same time negative effects have taken place in terms of enlarged areas of hypoxic and anoxic conditions, reduced growth of submerged vegetation (Duarte 1995) and changes towards dominance of microbial food webs over the ‘classic’ planktonic food chain and non-siliceous phytoplankton species over diatoms, and gelatinous zooplankton over crustacean zooplankton (Suikkanen et al. 2013). Since the 1970s the majority of areas in the Baltic Sea have been assessed as areas affected by eutrophication (Andersen et al. 2015), and a number of international management actions and measures have been implemented to prevent further degradation like the HELCOM Baltic Sea Action Plan, the WFD and MSFD.

The spatio-temporal trends in the concentrations of nitrogen and phosphorus were published in the BIO-C3 WP 3.1 report (Oesterwind et al. 2016). They showed that the dynamics of phosphorus correspond to the dynamics of the deep water renewal in the Baltic Proper (Conley et al. 2002), and are at the same level as during the period of excessive nutrient inputs in the 1980’s, whereas nitrogen levels have been reduced to the levels of the 1970s due to improved control of nutrient supply from land-based sources.

The aim of this analysis is to document to what extent the above-mentioned recent changes in temperature and eutrophication in the Baltic Sea have occurred along similar trajectories in space and time to inform the assessment of potential interactions of the two drivers of biodiversity.

### **3.6.5 Methods and results**

In order to resolve spatio-temporal changes in the sea surface temperature in the Baltic Sea measurements and modelled time series were analysed for the eastern and southern parts of the Baltic Sea between 1970 and 2010. Measured temperatures were integrated from 0.1 to 3 m depth, and modelled temperatures from 1 m depth in the summer period (July–September). The measured

data were extracted from the Baltic Nest Institute Data Assimilation System (DAS) database <http://www.balticnest.org/balticnest/thenestsystem/dasdataassimilationsystem.4.74cf9d0413b817d9359ed.html>, and the data were aggregated for coastal and open waters for regions which correspond closely to the standard HELCOM divisions of the Baltic Sea; Gulf of Riga, eastern part of Baltic Proper, Arkona - Bornholm Basins, Kiel Bay - Fehmarn Belt and Kattegat (Fig. 1).

Although many temperature measurements have been made on a large number of monitoring stations in the Baltic Sea over the period, they are patchily distributed in space and time and have to be interpolated in order to describe large-scale seasonal and regional distribution pattern. This can be done by simple linear interpolations, however, the uneven sampling regimes and the long residence time of the surface water and rapidly changing currents make it difficult to statistically characterize distribution patterns. Therefore, hydrodynamic models can provide improved means for calculating temperatures based on the quantification of flow patterns and mixing processes. In order to resolve nutrient concentrations and temperatures at a high spatial resolution we used the dedicated bio-geochemical BIO C3 Baltic Sea model set-up by DHI (Rasmussen 2015) to extract surface temperature, DIN and DIP concentrations for selected stations along depth gradients in the eastern and southern Baltic Sea (Fig. 1). The results for locations with the following depths were selected:

- Irbe Strait: coastal (10 m), open waters (100 m)
- Lithuania: coastal (10 m), open waters (100 m)
- Kaliningrad: coastal (10 m), open waters (100 m)
- Central Polish coast: coastal (10 m), open waters (100 m)
- Arkona and Bornholm Basins: coastal (10 m), open waters (100 m)
- Kiel Bay: coastal (20 m)
- Kattegat: coastal (10 m), open waters 30 m

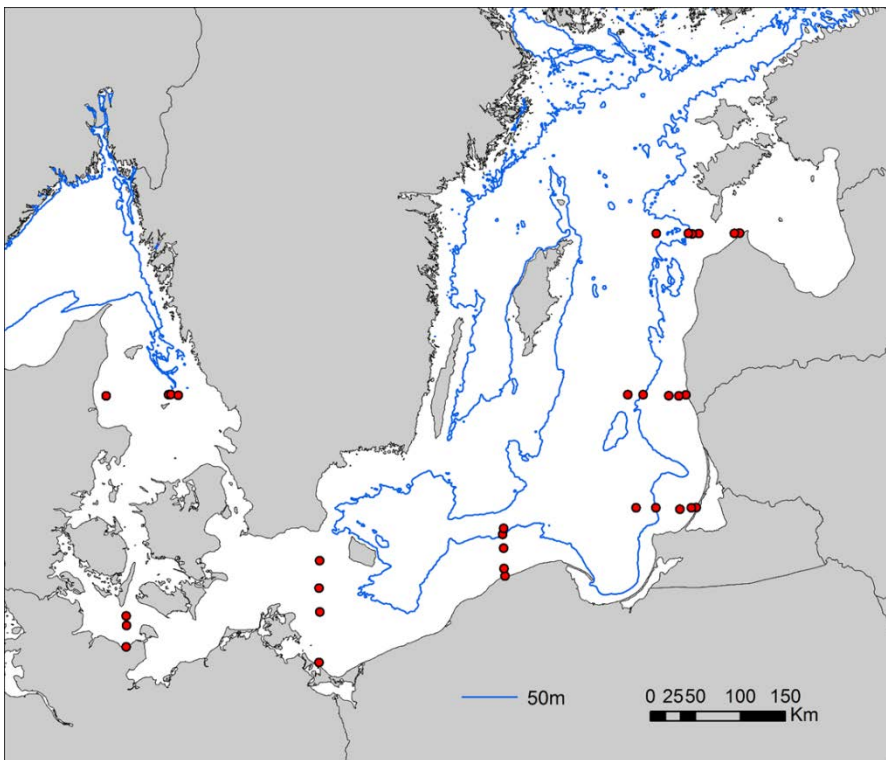
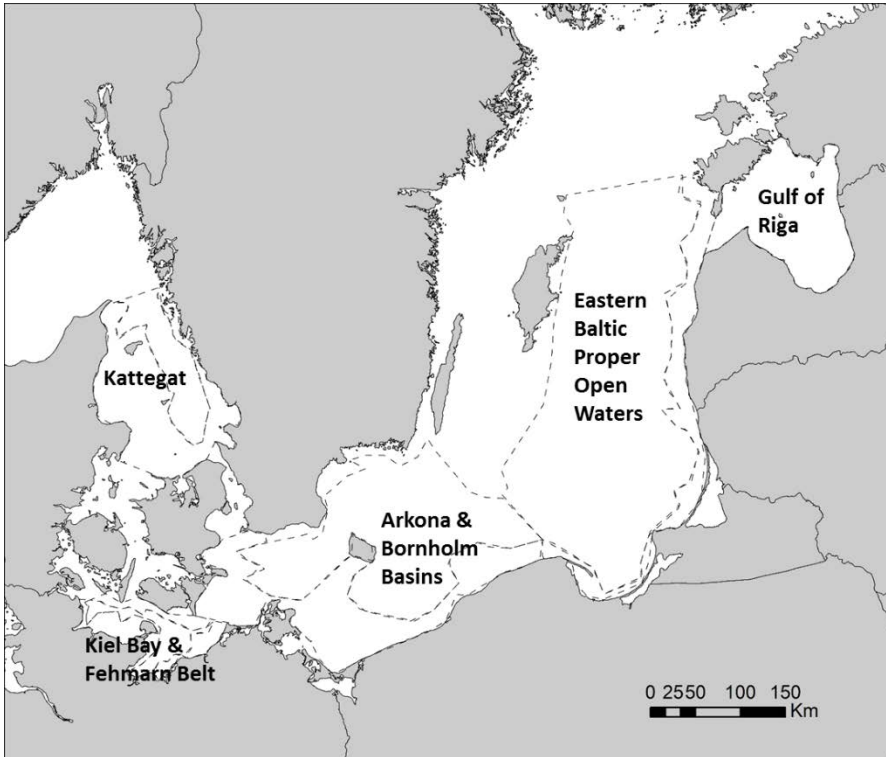
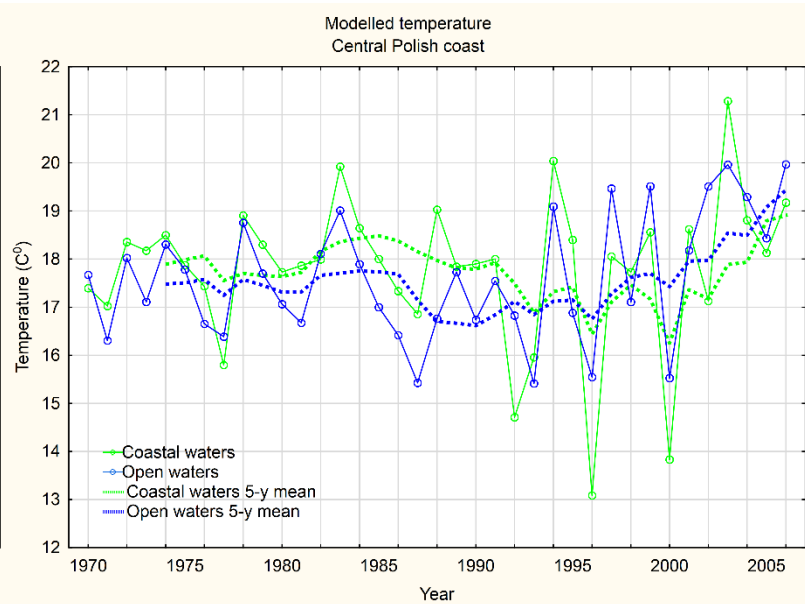
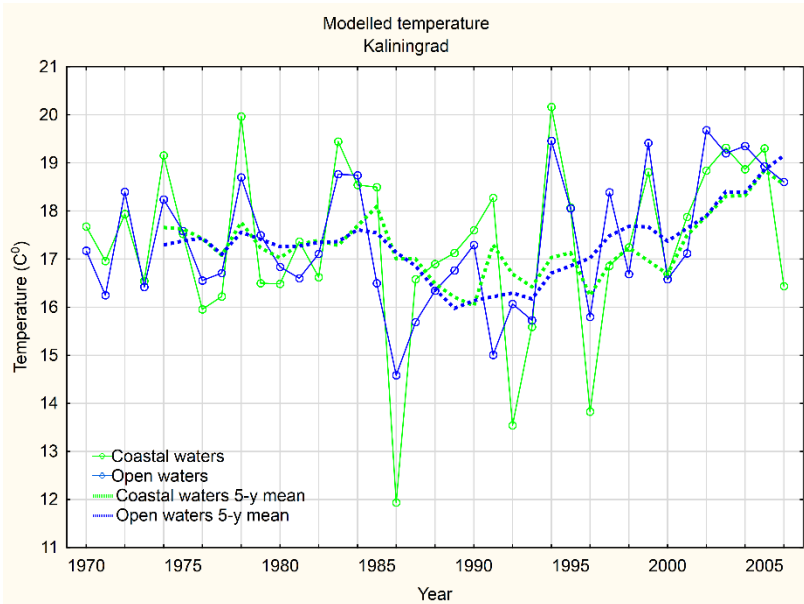
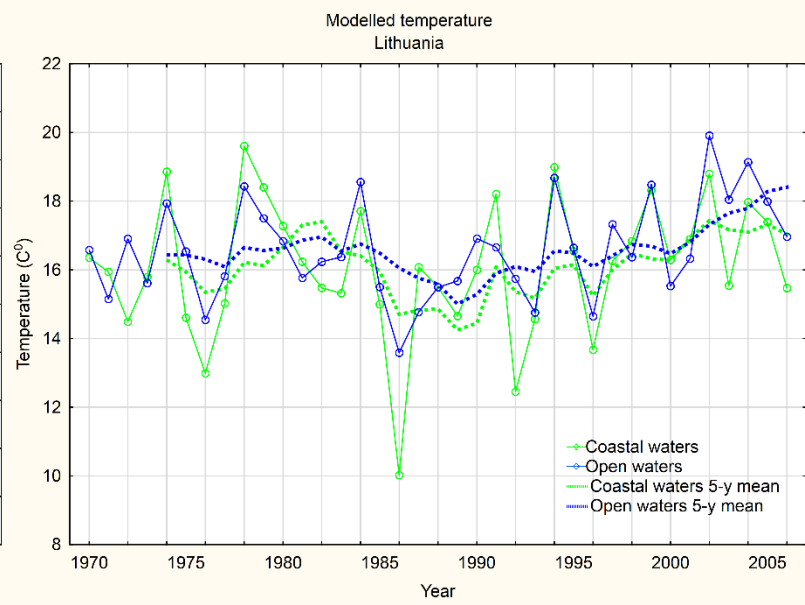
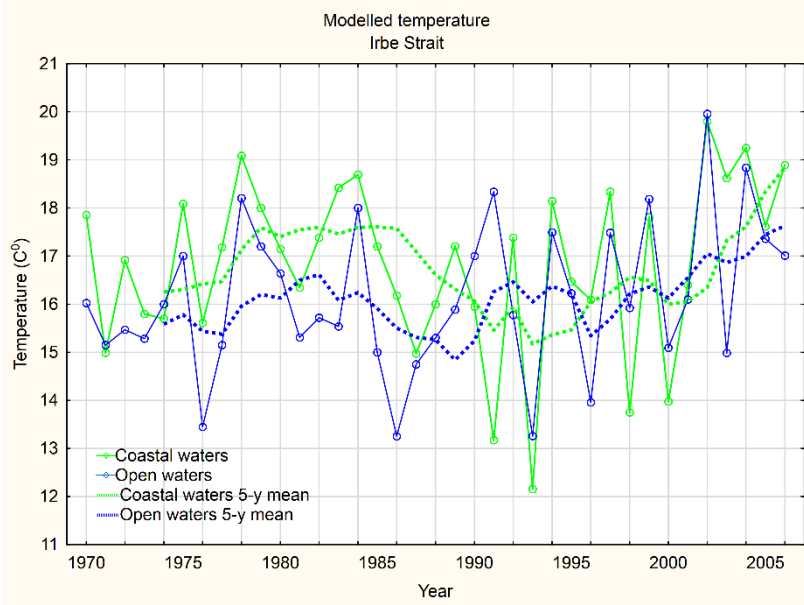


Figure 1. Location of zones used for extraction of temperature measurements from the DAS database, and stations used for extraction of modelled temperature from DHI's Baltic Sea Model.

Temperature: Both measured and modelled sea surface temperatures in coastal and open waters showed similar trends over the period (Fig. 2, Fig. 3). A long-term tendency for increasing temperatures is indicated by the time series in all regions with increases varying between 1–2 °C over the last 20 years. The trend started in the majority of regions around 1996, but was particularly pronounced in all regions after 2001.

DIN: The trends in winter nutrient concentrations published by Oesterwind et al. (2016) documented rather different trends for DIP and DIN. DIP concentrations showed two peaks coinciding with the major inflows in mid 1980s and again in the mid-late 2000s. DIN concentrations, on the other hand, showed an increase in the 1970s, followed by a stabilising period at a high level in the 1980s. After this a long-term decline took place in the majority of regions since late 1980s-early 1990s, which was mimicked in open waters in the southern parts of the Baltic Sea. The declines in DIN concentrations in all coastal areas and in open waters south of Kaliningrad were as strong as 50 %. As the declining trend in winter DIN concentrations share similarity, at least in some regions, with the increasing trend in summer surface temperature a more detailed assessment has been made using trajectory plots of the relationship between the two drivers (Fig. 4).

Temperature – DIN development: The trajectory plots underline that the parallelism between summer surface temperature and winter DIN is coincidental, and is only identified for parts of the studied period. A parallel trend between increasing surface summer temperatures and decreasing winter DIN concentrations is seen in all regions after 2001. This period overlaps with the later part of the period in which nitrogen concentrations dropped markedly in Lithuania and Kaliningrad waters, Central Polish waters, Kiel Bay and Kattegat. Thus, no long-term changes in surface temperatures were apparent in the first part of the period when the decline in DIN concentrations took place between 1990 and 2001.



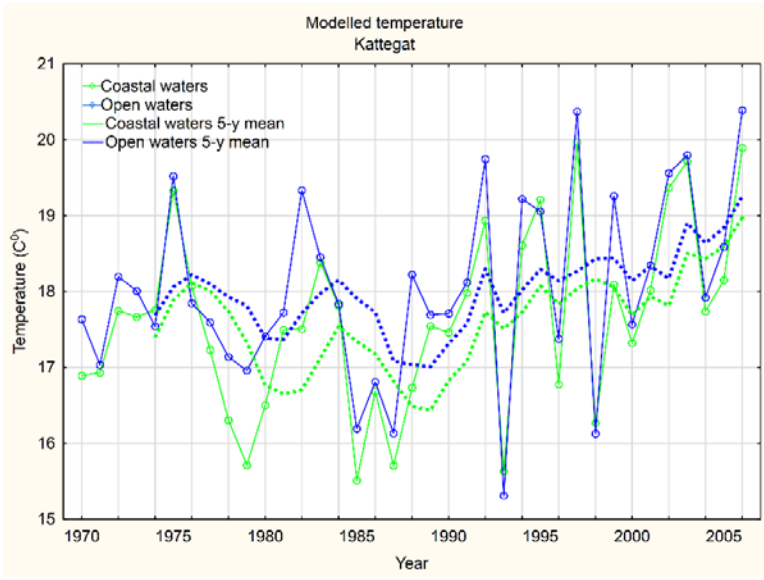
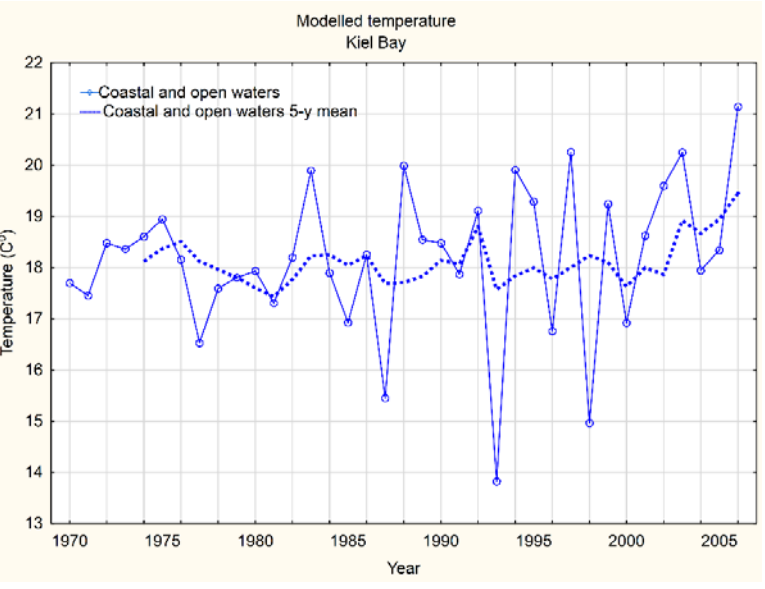
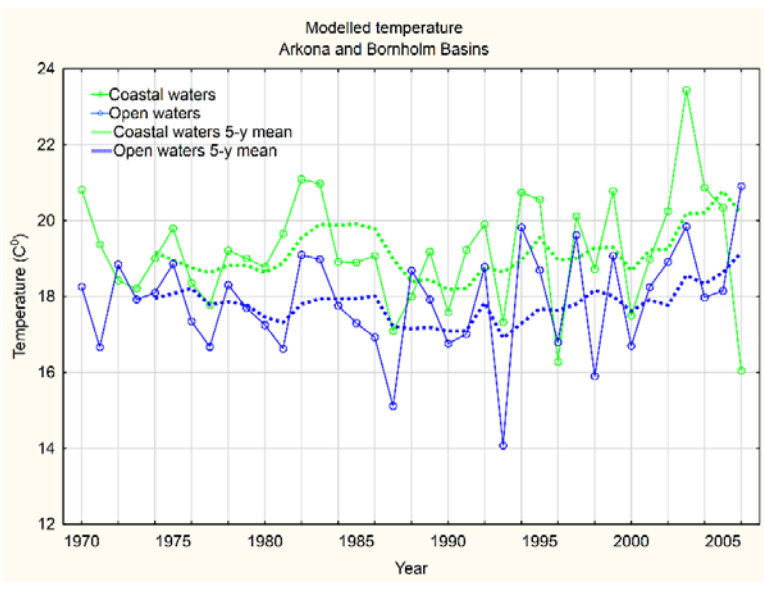
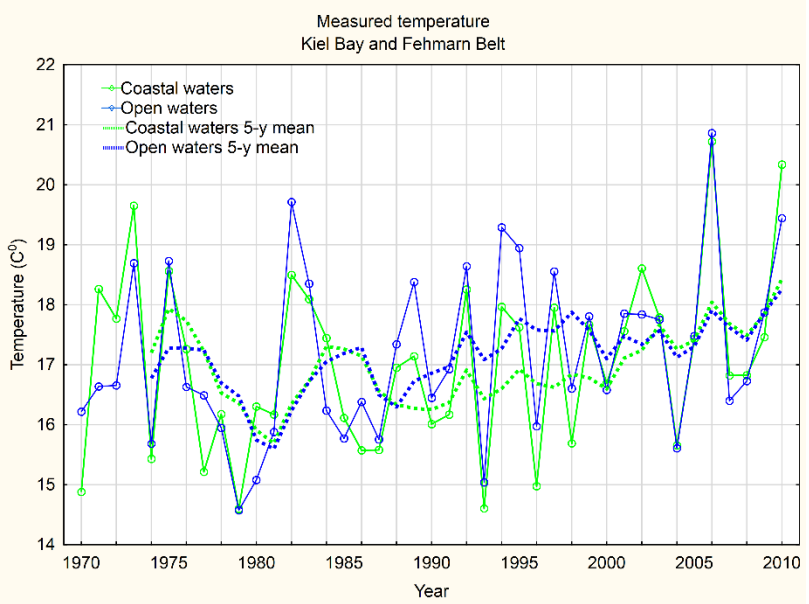
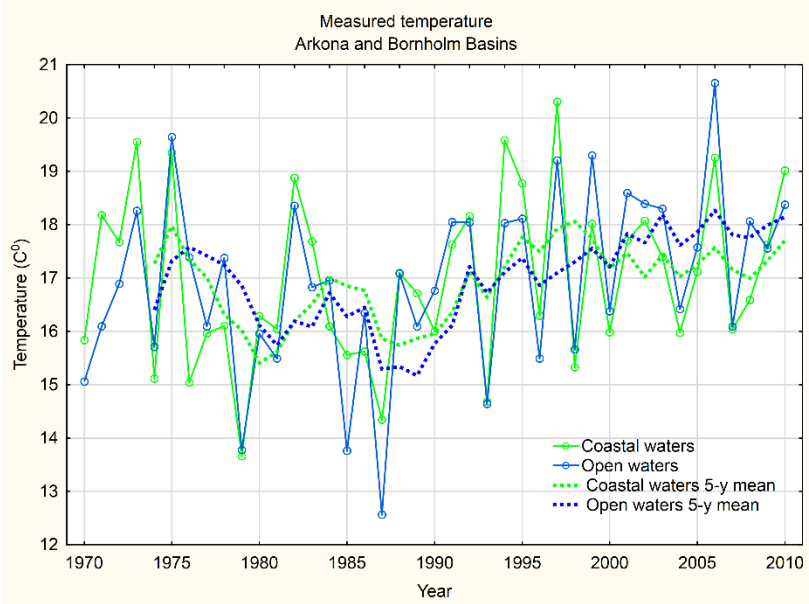
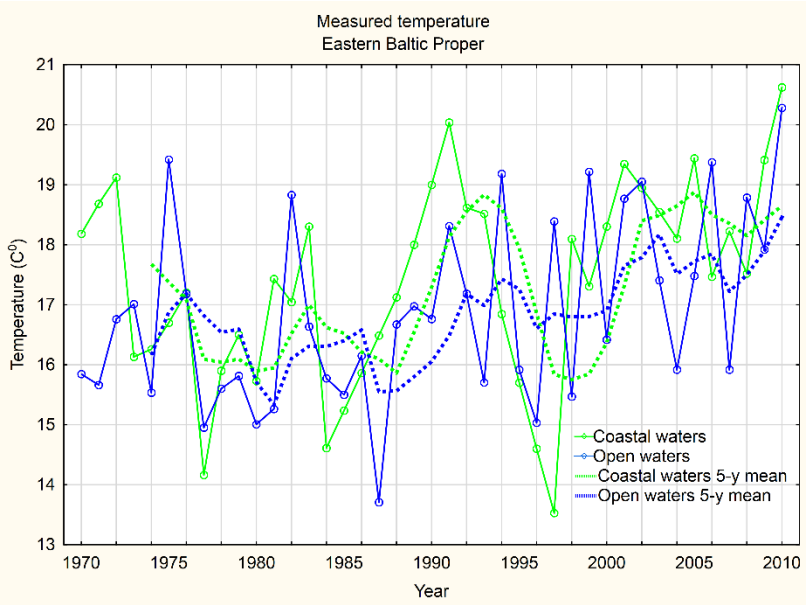
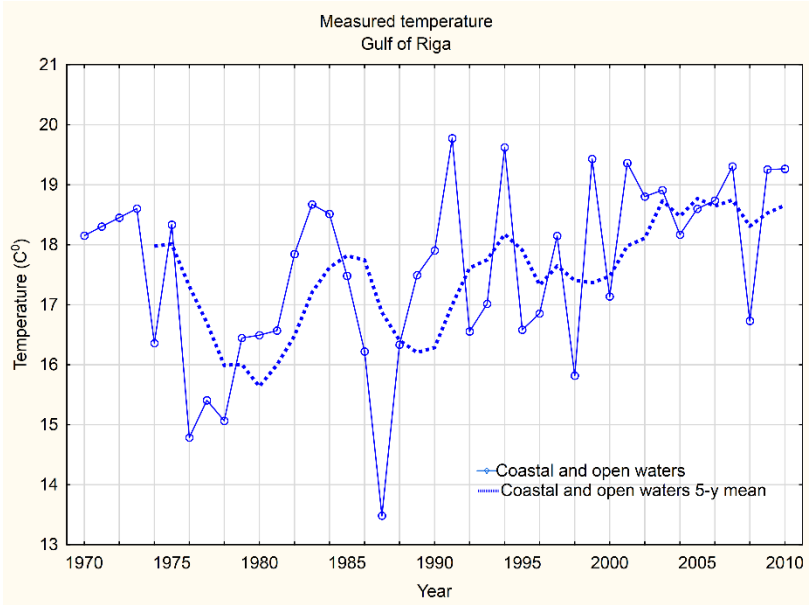


Figure 2. Trends in modelled surface temperatures during the summer months (July–September) 1970–2007. Dotted curves are 5-year moving averages.





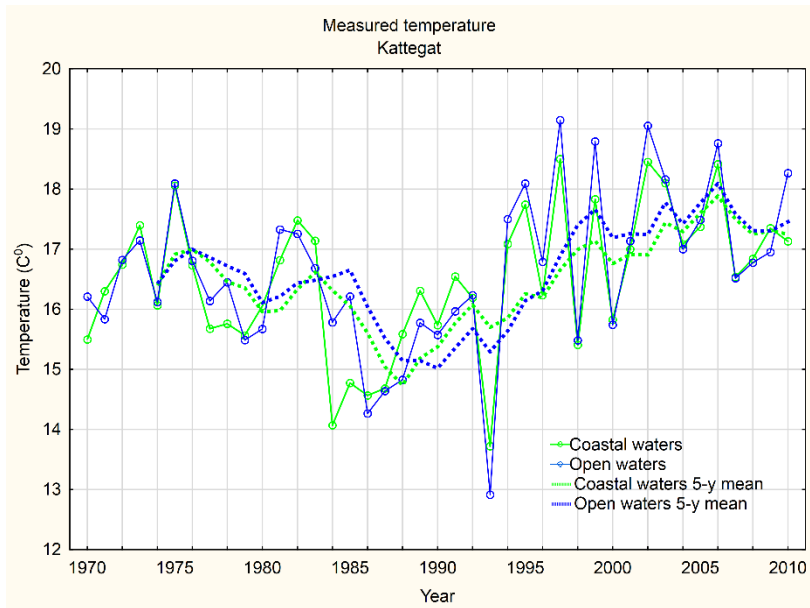
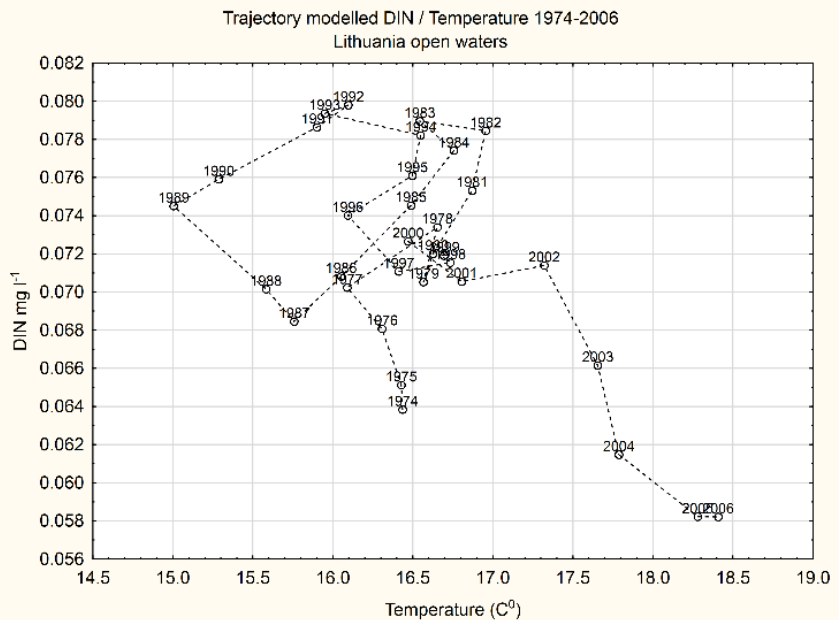
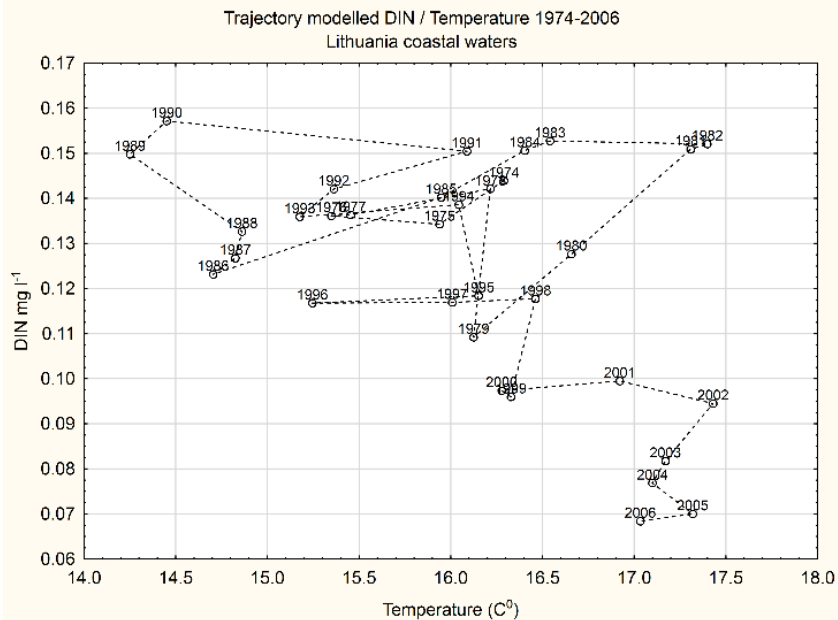
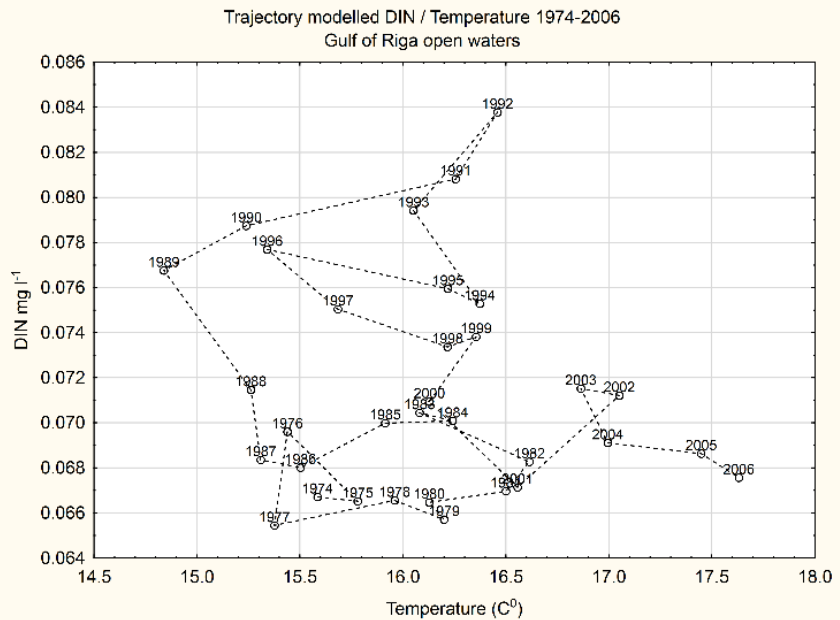
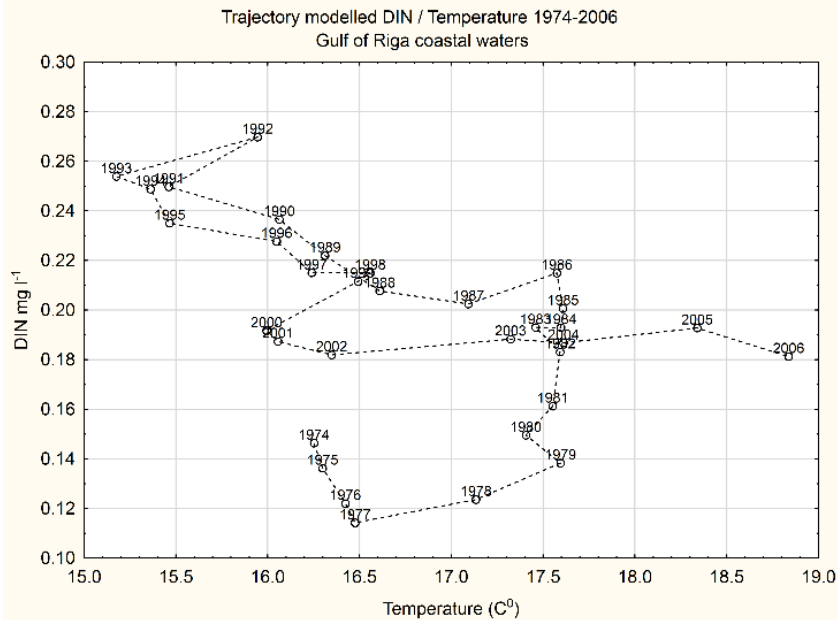
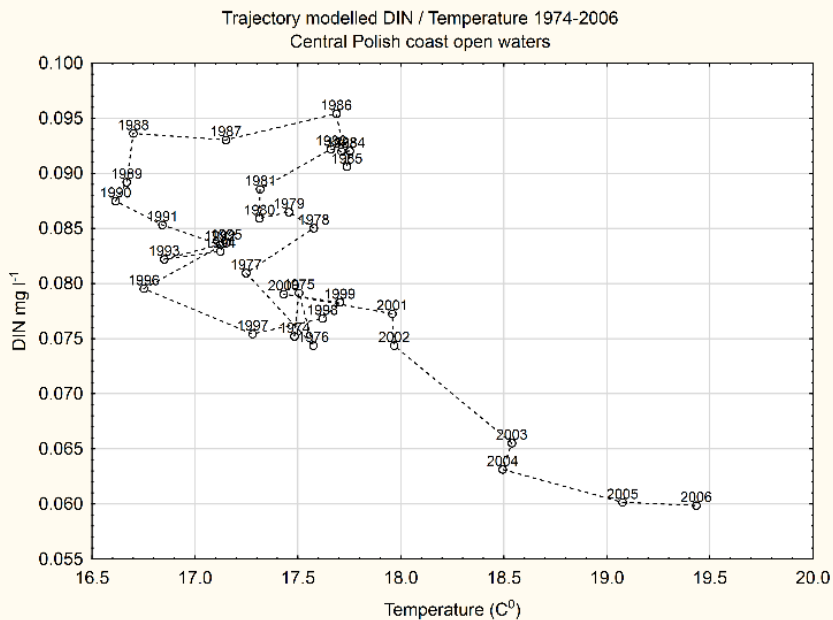
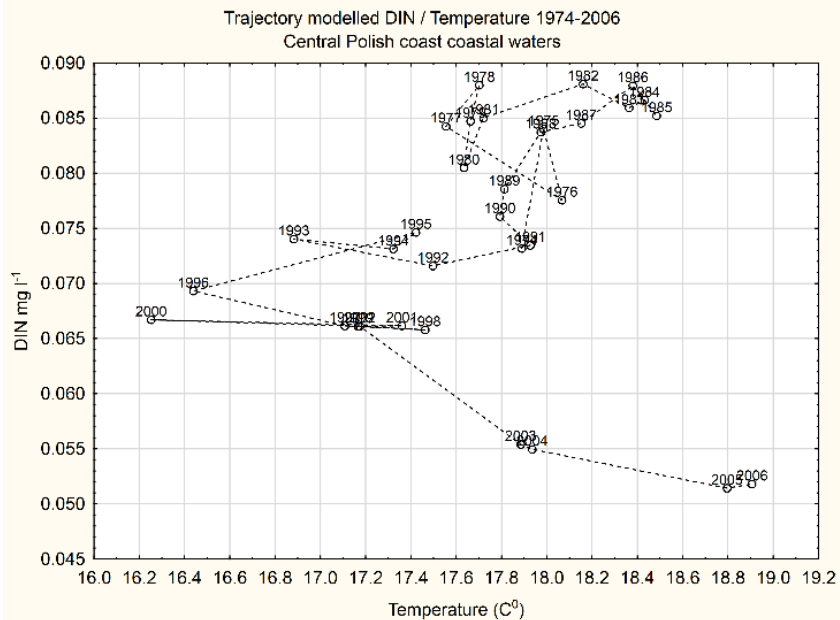
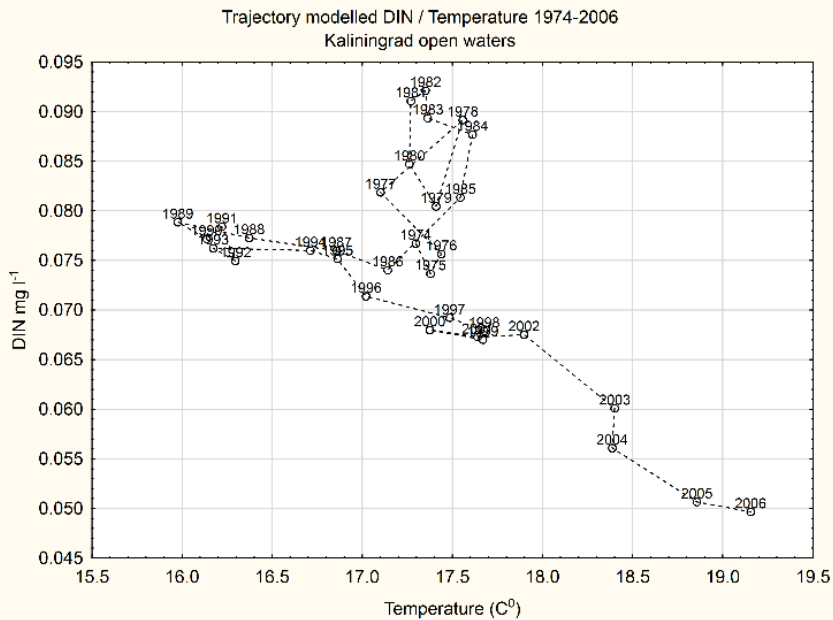
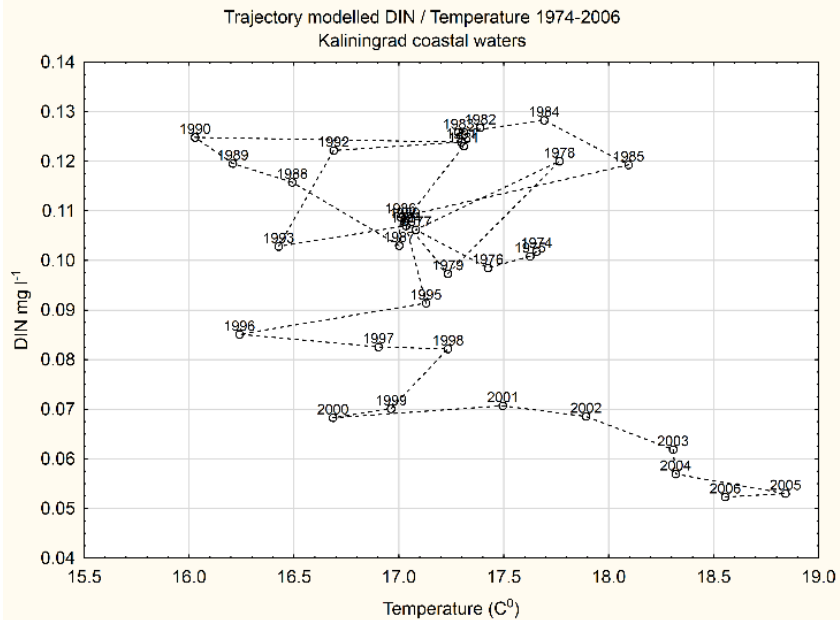
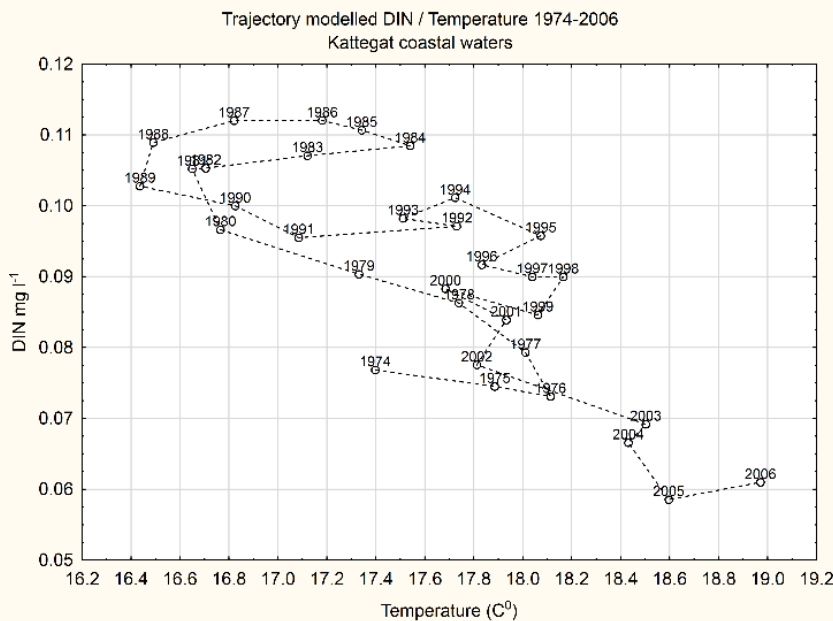
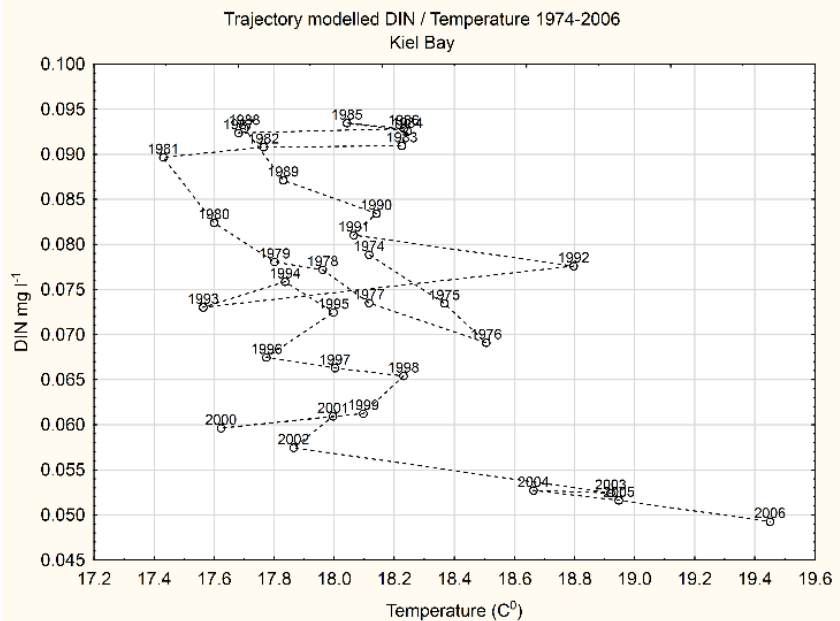
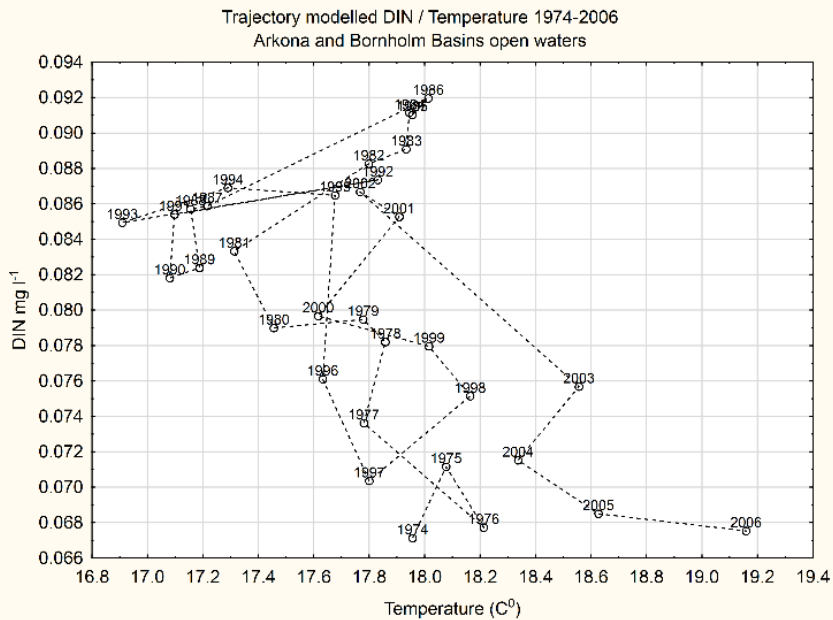
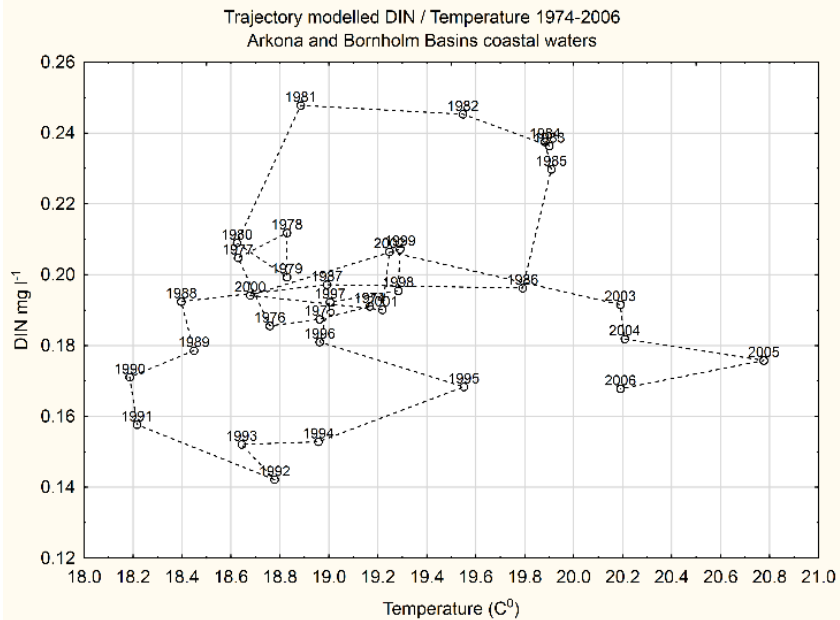


Figure 3. Trends in measured surface temperatures during the summer months (July–September) 1970–2010. Dotted curves are 5-year moving average.







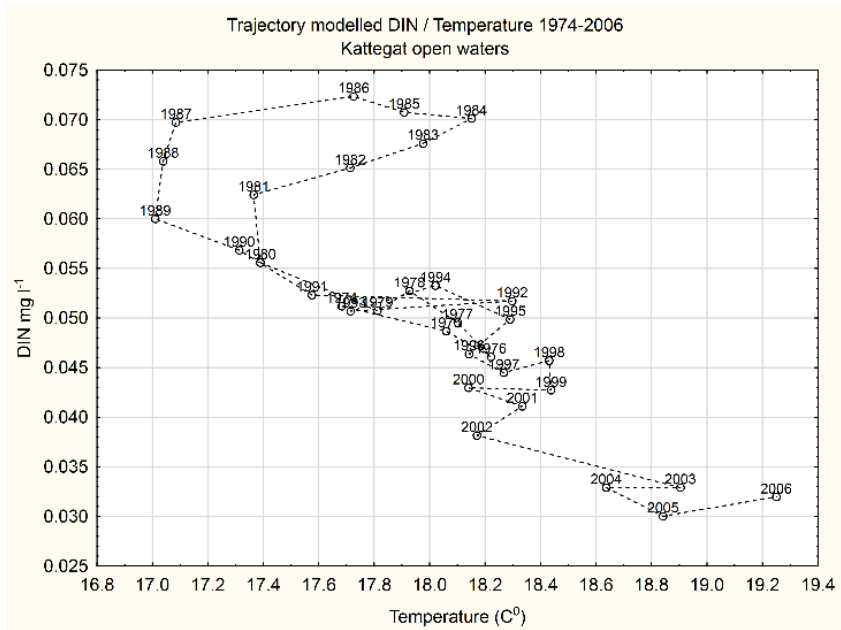


Figure 4. Time trajectories of the relationship between modelled surface temperatures (July–September) and nitrate concentrations (winter DIN), based 5-year moving averages.

### **3.6.6 Recommendations**

The trends in summer sea surface temperatures for the Baltic Sea between 1970 and 2010 indicate a long-term increasing trend rather than a shift in temperature levels after 1989. The year of 1989 has been suggested as identifying a major regime shift (Österblom et al. 2007, Casini and Hjelm 2009, Möllmann et al. 2009), yet see Yletyinen et al. (2016) for a critical re-assessment of ecosystem changes induced by the shift.

The results of the trajectory analyses will be useful for designing the scenarios for both the hindcasts and forecasts of the ecosystem models in WP4 and WP5. Scenarios based on the period after 2001 may be useful to assess the impact of temperature increase on benthic productivity by running the models with temperatures from the period prior to 2001. The period of relatively stable surface temperatures before 1996 will be useful for running scenarios demonstrating the impact of varying levels of nitrogen concentrations on benthic productivity.

Although overall trends in summer surface temperature and winter DIN between 1970 and 2010 seem coincidental, the recent trends towards both lower nitrogen concentrations and higher sea temperatures may continue over the medium term, hence giving rise to future ecosystem responses, which differ from responses to each driver independently. With the large-scale decrease in concentrations of nitrogen changes in the distribution and biomass of submerged vegetation and benthic macrofauna are expected. The current observations indicate signs of increased cover of macroalgae in deeper waters and a drastic decline in the biomass of filter-feeding macrofauna (Riemann et al. 2016) as well as in the number of benthic feeding waterbirds (Skov et al. 2011). One of the key questions to be answered in BIO C3 with the ecosystem modelling and assessments undertaken in WP2, WP3, WP4 and WP5 is whether the potential for the Baltic Sea to compensate the loss in benthic productivity due to declining nutrient concentrations will be affected under the current and future temperature increases.

### **3.7 Relationships between Baltic Sea inflows and physical and biochemical parameters (P12)**

*Helén C. Andersson, Kari Eilola, H.E. Markus Meier & Elin Almroth Rosell,  
Swedish Meteorological and Hydrological Institute*

#### **3.7.1 Abstract/highlights**

Saltwater inflows from the North Sea to the Baltic Sea occur frequently. However, the inflows large and saline enough to ventilate the deeper layers happen infrequently and their occurrences, or lack of them, play a large role in the extension of hypoxic areas below the halocline. This in turn exerts crucial control on the Baltic Sea biogeochemistry and ecosystem. We have investigated possible future changes of the dynamics of the inflows by exploring the impact of anticipated future sea level changes on the dynamics of those inflows. A suite of idealized experiments suggests that rising sea level is associated with intensified ventilation as saltwater inflows become stronger, longer, and more frequent. Expressed quantitatively as a salinity increase in the deep central Baltic Sea, we find that a sea level rise of 1 m triggers a saltening of more than 1 PSU. This substantial increase in ventilation is the consequence of the increasing cross section in the Danish Straits amplified by a reduction of vertical mixing.

Further, we studied the impact of dense saltwater inflows on the phosphorus dynamics in the Baltic Sea. Phosphorus has been discussed to be a key nutrient for the eutrophication of the Baltic Sea (Conley et al. 2009). Model simulations showed that the coasts of the NorthWest Gotland Basin and the Gulf of Finland, the Estonian coast in the East Gotland Basin are regions where tracers from below the halocline are primarily lifted up above the halocline. After 1 year tracers are accumulated at the surface along the Swedish east coast and at the western and southern sides of Gotland. Elevated concentrations are also found east and southeast of Gotland, in the northern Bornholm Basin and in the central parts of the East Gotland Basin. The annual supplies of phosphorus from the deeper waters to the productive surface layers are estimated to be of the same order of magnitude as the waterborne inputs of phosphorus to the entire Baltic Sea. The model results suggest that regionally the impact of



these nutrients may be quite large, and the largest regional increases in surface concentrations are found after large inflows. However, the overall direct impact of major Baltic inflows on the annual uplift of nutrients from below the halocline to the surface waters is small because vertical transports are comparably large also during periods without major inflows. Our model results suggest that phosphorus released from the sediments between 60 and 100 m depth in the East Gotland Basin contributes to the eutrophication, especially in the coastal regions of the eastern Baltic Proper.

A number of studies have shown that the sediments play an important role in controlling the phosphorus supply to the pelagic realm as they regionally act as an internal source or sink for dissolved phosphate (Emeis et al. 2000, Lukkari et al. 2009, Viktorsson et al. 2012, 2013). Phosphate has the ability to adsorb on hydrated metal oxides, e.g. iron (III) oxy hydroxides (oxides), which build up in the oxidized sediment layer. Large amounts of phosphate can thus build up in the sediment during oxic bottom water conditions. During anoxic periods the oxides reductively dissolve, which prevents further adsorption of phosphate to iron oxides and the previously adsorbed phosphorus is released to the pore water in the sediment and can thus diffuse to the water column (Froelich 1988, Mortimer 1941, 1942, Sundby et al. 1992). Thus, the low retention capacity of phosphorus in the sediment during anoxic conditions and the limited vertical circulation and ventilation of the bottom water leads to high phosphate concentrations in the anoxic bottom water. Here we have utilized an approach to model the oxygen dependent phosphate release by implementing formulations of the oxygen penetration depths (OPD) and mineral bound inorganic phosphorus pools into a biogeochemical model of the Baltic Sea. The phosphorus dynamics and the oxygen concentrations in the Baltic Proper sediment were studied during the period 1980–2008. The impact from oxygen consumption on the determination of the OPD was found to be largest in the coastal zones where also the largest OPD are found. In the deep water the low oxygen concentrations mainly determine the OPD. Highest modelled release rate of phosphate from the sediment is about  $59 \times 10^3 \text{ t P year}^{-1}$  and is found on anoxic sediment at depths between 60–150 m, corresponding to 17 % of the Baltic proper total area. The deposition of organic and inorganic phosphorus on sediments with oxic bottom water is larger than the release of phosphorus, about  $43 \times 10^3 \text{ t P year}^{-1}$ . For anoxic bottoms the release of total phosphorus during the investigated period is larger than the deposition, about  $19 \times 10^3 \text{ t P year}^{-1}$ . In total the net

Baltic proper sediment sink is about  $23.7 \times 10^3$  t P year<sup>-1</sup>. The estimated phosphorus sink efficiency of the entire Baltic Sea is on average about 83 % during the period.

### **3.7.2 Progress and (if applicable) deviations from the work plan**

The objective of the studies were to investigation on how the frequency and magnitude of deep-water inflow events determines volume and variance of salinity and temperature under the halocline, the vertical uplift of nutrients, deep-water oxygen levels and sediment fluxes of nutrients, using observations and model results from historical baselines to present. The work has proceeded according to plan and have resulted in three published, peer-reviewed papers:

Hordoir, R., Axell, L., Löptien, U., Dietze, H., Kuznetsov, I., 2015: Influence of sea level rise on the dynamics of salt inflows in the Baltic Sea. *J. Geophys. Res. Oceans*, 120, doi:10.1002/2014JC010642. (Appendix 3)

Eilola, K., Almroth-Rosell, E., Meier, H.E.M., 2014: Impact of saltwater inflows on phosphorus cycling and eutrophication in the Baltic Sea: a 3D model study. *Tellus A* 2014, 66, 23985, <http://dx.doi.org/10.3402/tellusa.v66.23985>. (Appendix 4)

Almroth-Rosell, E., Eilola, K., Kuznetsov, I., Hall, P.O.J., and Meier, H.E.M., 2015: A new approach to model oxygen dependent benthic phosphate fluxes in the Baltic Sea. *J. Marine Syst.*, 144, 127-141. (Appendix 5)

### **3.7.3 Deviations from the work-plan**

None

### **3.7.4 Introduction**

The semi-enclosed Baltic Sea basin has a hampered water exchange with adjacent seas. Hence, river inflows from the highly industrialized countries of the large catchment area determine its brackish characteristic and render it vulnerable to anthropogenic eutrophication. The Baltic Sea is highly stratified and its lower layers can only receive oxygen by salinity intrusions finding their way through three narrow passages linking the Baltic with the North Sea; the Little Belt, the Great Belt and the Öresund. The straits have different vertical cross sections with the middle strait (Great Belt) being the broadest and deepest and hosting the

largest share of the water exchange. The inflowing water is typically characterized by a relatively high salinity and high oxygen content. Thus, saltwater inflows from the North Sea are a vital source of oxygen for the Baltic Sea and the whole ecosystem is impacted by their frequency and intensity. Salt inflows directly influence the salinity structure of the Baltic Sea (Lass and Matthäus 1996, Meier and Kauker 2003, Meier 2007). They also influence biological processes such as cod spawning (Stigebrandt et al. 2014) and the ventilation of the deeper layers of the Baltic Sea is crucial to macrobenthic organisms (Gogina and Zettler 2010). Previous studies have shown that the frequency of saltwater inflows has decreased during the recent decades, particularly in the period between 1983 and 1993 (Lass and Matthäus 1996). Saltwater inflows are also suspected to decrease in a future climate due to an increase of the runoff into the Baltic Sea (Meier et al. 2006). Hypoxia is nowadays a severe environmental problem for the Baltic Sea, reaching a point where even geoengineering solutions are under discussion (Stigebrandt et al. 2014). Additionally, the high nutrient content of the Baltic Sea together with increased temperatures suggest that the lower layers are prone to reach a state of hypoxia more often and with a greater extent (Meier et al. 2012).

The impact of sea level rise, an expected consequence of climate change, on the Baltic Sea haline dynamics has, so far, not been investigated, and one challenging question is to determine how the Baltic Sea salt inflow dynamics respond to a significant sea level increase: the aim of the study was to address this issue.

Oxygen deficiency in the deep waters of the Baltic is a problem that also influences eutrophication by the redox dependent phosphorus (P) fluxes from the sediments (Conley et al. 2009). This causes a large variability of P concentrations in the deeper parts of the Baltic Sea. In fact, the large scale variations of the pools of inorganic P caused by the intermittent major Baltic inflows may be up to two orders of magnitude larger than the variations in the external P input (e.g. Savchuk 2010). Measurements of nutrients and oxygen in the Baltic Sea have been done for more than 100 yr with regular monitoring starting in the 1950s, though the earliest nutrient measurements from the beginning of the last century are regarded as unreliable. The central part of the Eastern Gotland Basin, which has the longest historical data records, is often used as a representative area for studies of the basic physical and biogeochemical dynamics in the Baltic Sea. Schneider (2011) studied the changes in the mean phosphate ( $\text{PO}_4$ ) and total inorganic carbon (CT) below 150 m depth in the East Gotland Deep after the major Baltic inflow in 2003. He observed a drop of  $\text{PO}_4$  by 39 % within 6

weeks after the inflow and a further drop to a minimum of 60 % within 1 year. The CT concentrations that are not redox sensitive dropped similarly to  $\text{PO}_4$  due to dilution during the initial weeks (Schneider 2011). Because of on-going organic matter mineralization, CT concentrations started to increase again already in the autumn when the water exchange slowed down. The release of  $\text{PO}_4$  from the sediment was, however, according to Schneider (2011) most likely very small after the inflow when the water turned from anoxic to oxic. A possible explanation for this is that the  $\text{PO}_4$  can bind to hydrated metal oxides (e.g. Fe) in the Baltic Sea sediments as discussed, e.g. by Mort et al. (2010) and Schneider (2011). An overview of the present knowledge about mechanisms driving the physical dynamics and mixing processes of the inflowing waters and the vertical transports of salt and nutrients to the surface layers is given in the review by Reissmann et al. (2009), but all details of the processes are still not fully understood. One example is the passive vertical transports of dissolved P from the deep waters to the surface layers, which needs further attention as pointed out by Reissmann et al. (2009). Further aims of our studies were therefore to perform high-resolution model experiments to simulate the renewal of the East Gotland Deep water and to follow the fate of the accumulated pools of P in the Baltic deep water. We investigated the impacts of modelled inflows that occurred during the period 1961–2009, when the stagnant deep water usually became anoxic and rich in phosphate before the next deep water renewal took place (e.g. Stigebrandt and Gustafsson 2007), and used passive tracer experiments to examine the role of water masses from different regions and different depth layers. The aim was to investigate if there are specific regions where the deep water usually is lifted above the halocline, and also, if there are regions where we might expect a possible addition to the spring primary production from the excess phosphorus annually lifted up from the layers below the halocline. The relative importance of inflows on the average uplift of tracers was quantified from a set of years having stronger and weaker inflows respectively, compared to years with no inflows.

Not only external supplies of nutrients from land and atmosphere contribute to the increasing eutrophication, but also internal loads, i.e. the impact from an intensified recycling of nutrients in the sediment (Conley et al. 2002, Stigebrandt et al. 2014). Gustafsson et al. (2012) estimated that external phosphorus loads increased by a factor of 5 from 1850 to around 1980. After 1980 external phosphorus loads started to decrease, but the phosphorus efflux from the sediments and the phosphorus pool in the water continued to increase.

The deep water in the southern and central basins of the Baltic Sea is separated from the surface water by a permanent halocline at a depth of about 60 m, which prevents vertical circulation and ventilation of the bottom water. Only major water inflows can oxygenate the deep waters in the basins. The inflowing water replaces the anoxic and phosphate rich bottom water in the deeper part of the basins, which is lifted up to more shallow water depths. The vertical transport and mixing of the deep bottom water due to major Baltic inflows (MBI) have been discussed in earlier studies (e.g. Reissmann et al. 2009, Schneider 2011). During the stagnant periods, between the major inflows, the oxygen concentrations in the deep water decrease with time, often until depletion. Further, Jilbert et al. (2011) suggested that preferential phosphorus mineralization with respect to carbon, may be a key player besides the mineral bound redox dependent phosphorus dynamics. Sediment that has been anoxic for a longer period might get the accumulated pool of mineral bound inorganic phosphorus depleted.

The release of phosphate will then depend on the supply and degradation of organic matter and the mineralization rate of organic phosphorus (Viktorsson et al. 2012). Today, about 40 % of the total bottom area in the Baltic proper (including the Gulf of Riga and the Gulf of Finland) is estimated to be overlain by hypoxic (dissolved  $O_2$  concentrations less than  $2 \text{ ml l}^{-1}$  or  $91 \mu\text{M}$ ) or anoxic bottom water (Hansson and Andersson 2013). In contrast to soft water lakes marine waters also have a sink for iron. Saline water contains sulfate which is used during bacterial anaerobic decomposition of organic material. The produced hydrogen sulfide reacts with iron and precipitates as minerals, e.g. FeS or pyrite  $\text{FeS}_2$  (Skoog et al. 1996, Blomqvist et al. 2004). Iron (III) oxides and phosphate form aggregates with the molar (Fe:P) ratio of 2:1 (Gunnars and Blomqvist 1997, Gunnars et al. 2002). If the molar ratio is less than two, the phosphate can escape from the sediment without binding to iron(III)oxides. The produced FeS and  $\text{FeS}_2$  acts as a sink of iron and may thus lead to a reduced retention capacity of phosphate in the sediment (Blomqvist et al. 2004). The depth of the oxidized sediment layer, and hence the amount of hydrated metal oxides available for phosphorus adsorption, depends on the oxygen concentrations in the bottom water and also on the oxygen consumption rate in the sediment (Cai and Sayles 1996). Hence, if the oxygen penetration depth is large more iron can transform to iron (III) oxides and larger fractions of the mineralized phosphorus may be adsorbed. The relative importance of oxygen consumption rate, compared to the importance of bottom water oxygen concentration, on the actual oxygen

penetration depth as well as the sink efficiency of phosphorus in the Baltic Sea will therefore be investigated.

### **3.7.5 Methods and results**

The analyses of the impact of sea-level rise on the Baltic inflows are based on the NEMO-Nordic configuration developed at SMHI (Swedish Meteorological and Hydrological Institute) which has been used in previous studies (under the name BaltiX) (Hordoir et al. 2013, Godhe et al. 2013). NEMO-Nordic is a coupled ocean-sea ice model based on the NEMO ocean engine (Madec 2010). Its domain includes the entire Baltic Sea basin, and a major part of the North Sea. NEMO-Nordic has two open boundaries: a meridional one located in the English Channel between Brittany and Cornwall, and a zonal one between Scotland and Norway (Hordoir et al. 2013). Since we use a resolution of 2 nautical miles, it is sometimes difficult to give each critical section of the Danish Straits its true width. Therefore, we have instead made each critical cross sections of each strait fit its actual measured size. To reach this goal, we have slightly modified either the depth or the width of each critical cross section, so that the surface of each critical cross section fits its actual size. This has been done with the goal to find the best compromise that modifies as little as possible depth or width. NEMO-Nordic uses a fully nonlinear explicit free surface, based on the approach described by Adcroft and Campin (2004). Partial steps are used in order to obtain a good consistency between the input bathymetry and that utilized by the model. We use a time-splitting approach that computes a barotropic and a baroclinic mode, as well as the interaction between them.

For the biogeochemistry studies we used the coupled physical-biogeochemical RCO-model, Rossby Centre Ocean model (Meier et al. 2003). RCO is used with a horizontal resolution of 3.7 km (2 nautical miles) and with 83 vertical levels with layer thicknesses of 3 m. In the model the maximum depth amounts to 249 m. The Swedish Coastal and Ocean Biogeochemical model (SCOBI; Eilola et al. 2009) describe the dynamics of nitrate, ammonium, phosphate, phytoplankton, zooplankton, detritus, and oxygen. Phytoplankton consists of three algal groups representing diatoms, flagellates and others, and cyanobacteria (corresponding to large, small and nitrogen fixing cells). The growth rates depend on nutrient concentrations, irradiance, and water temperature. The modelled cyanobacteria also have the ability to fix molecular nitrogen. Organic matter sinks and enters the sediment containing benthic nitrogen and phosphorus. The sediment processes include oxygen dependent nutrient

regeneration and denitrification as well as permanent burial of nutrients. Resuspension of organic matter depends on the combined effects of waves and current induced shear stress (Almroth-Rosell et al. 2011).

The study showed that a moderate mean sea level rise modifies the long-term dynamics of salt inflows in the Baltic Sea. In a 46 year hindcast simulation of NEMO-Nordic, the bottom salinity in the deepest parts of the Baltic Sea increases by 0.3 PSU for an anticipated sea level rise of 0.5 m (Fig. 1, e0.5). This salinity increase reaches values of more than 1 PSU for a mean sea level rise of 1.5 m (Fig. 1, e1.5). These increases in the deep salinity indicate an increase in the ventilation of the deep parts of the Baltic Sea even for a modest sea level rise.

Sea level rises trigger deep salinity biases, but no diverging temporal trends. Hence, apparently, on the time scales and magnitudes considered here, increased deep salinity does not weaken consecutive inflows.

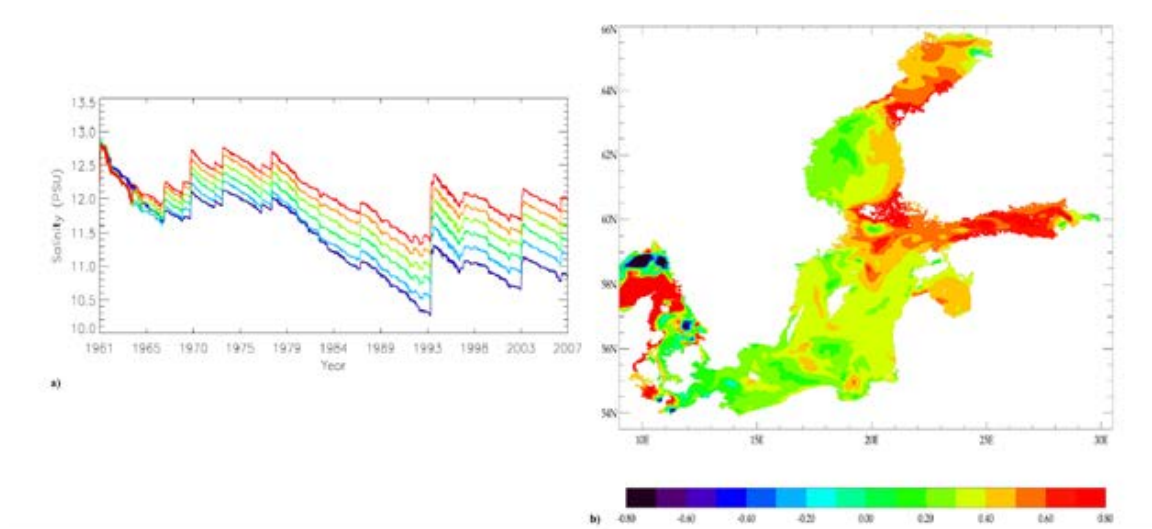


Figure 1. (a) Deep salinity (in PSU) at 250 m at BY15 from 1961 to 2007 for experiments with sea level rise of 0 m (e0) to 1.5 m (e1.5), from blue to red respectively. (b) Changes in sea surface salinity between e1.5 and e0 after 10 years of simulation (from Hordoier et al. 2015).

The destiny of the deep water due to MBI in the Baltic proper was investigated in the tracer study. Regionally, the direct impact on the uplift of nutrients from waters below the halocline to surface waters due to MBI can be quite large, but the overall direct impact is small because comparably large vertical transports occur also in years without MBI. The impact from the

East Gotland Deep water on eutrophication in the Baltic Sea is expected to be small because the volume of water below 150 m is small.

The modelled monthly mean of the net phosphate release from the sediment at depth below 150 m in the Eastern Gotland Basin was in the range of 200 and 350 t P month<sup>-1</sup> in the beginning of the periods 1990–1998 and 2000–2008, respectively (Fig. 2). In 1993, 1994, 1997 and 2003 large decreases in the phosphate release rates are observed, which coincidence with MBIs. Also in 2001 there was an inflow, which resulted in a decrease in the modelled phosphate release rate. Due to the MBI in 2003 the modeled net release even becomes negative during 2004, i.e. phosphate is taken up by the sediment. In the beginning of 2005 the net phosphate release rate increases again. Modelled net uptake of phosphate from the water to the sediment is only found in the period from May 2003 to June 2004 and to a very low extent, on average 2.9 t P month<sup>-1</sup>, which in total corresponds to about 40 t phosphorus. The total phosphorus pool in the water the month before the MBI was  $26 \times 10^3$  t P. Thus, the uptake of phosphate by the sediment corresponded to only 0.15 % of the total phosphorus content in the bottom water (N150 m depth), and can thus be concluded to play a minor role in the decreased bottom water phosphate concentrations. This uptake is much lower compared to the uptake calculated in the study by Schneider (2011), in which it was concluded that the immediate decrease in phosphate and dissolved inorganic carbon concentrations due to the MBI in the beginning of 2003 was caused to 66 % by dilution of the incoming water and to 33 % of adsorption to newly formed iron (III) oxides on the sediment surface.

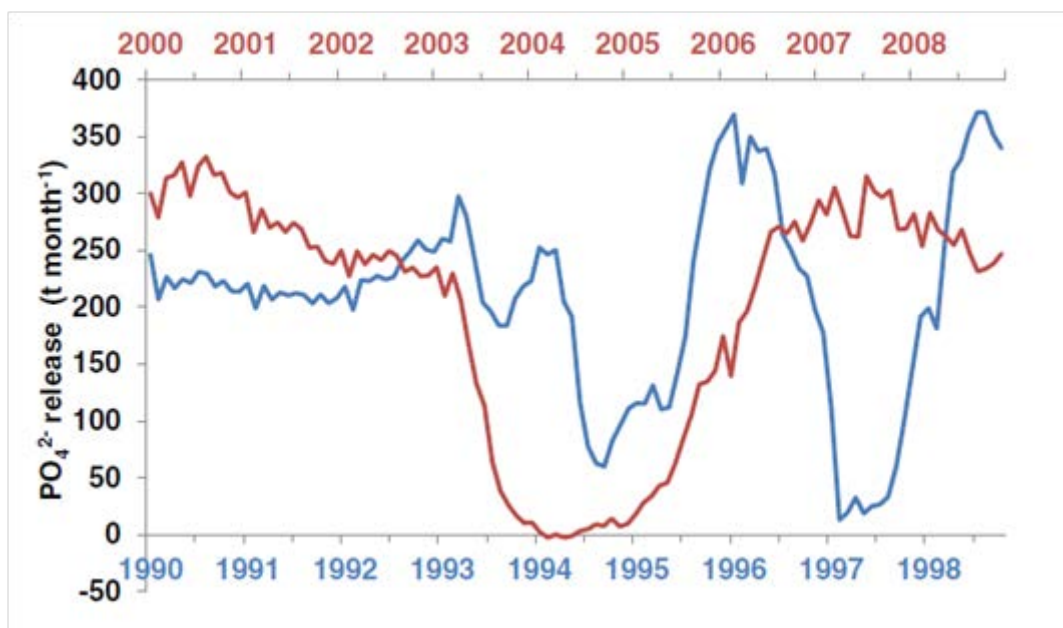




Figure 2. Monthly mean of the phosphate release ( $\text{t P month}^{-1}$ ) from sediment to water column during two different time periods, 1990–1998 (blue) and 2000–2008 (red) in the Eastern Gotland Basin (from Almroth-Rosell et al. 2015).

### 3.7.6 Recommendations

The effect of sea level rise on the overall haline structure of the Baltic Sea is an aspect needed to be further investigated, in addition to the coupling of stronger salt inflows with biogeochemistry and e.g. the cod reproductive volume that is influenced by both the salinity and oxygen conditions. From this perspective, it is difficult to make a forecast just based on these results. However, one might expect the following features. First, added saltwater inflows usually carry oxygen to the deepest parts of the Baltic Sea, but this added oxygen content is usually consumed within a time scale of 1 or 2 years (Feistel et al. 2008). However, added salinity in the deepest parts of the Baltic Sea also leads to stronger stratification which suggests on longer time periods that the oxygen content might actually decrease. A consequence could be a higher release of phosphorus from the bottom sediments.

The phosphate release rate from the sediment was shown to drastically decrease and even become negative as a result of Major Baltic Inflows. However, the decrease in the bottom water concentrations of phosphate due to the MBI is mainly explained by dilution. The uptake of phosphate by the sediment from the water column was in this study concluded to be negligible.

In the model experiment it was also found that about 85 % of the tracer mass was removed due to dilution effects which also is a larger dilution effect compared to that obtained by Schneider (2011). Sediment uptake of phosphate from the water column at a normally anoxic station which became oxic for a period has been measured in situ by Viktorsson et al. (2012).

The time-scale for how long this uptake of phosphate may take place was, however, not studied why this is a question for future investigations. The overall direct impact of major Baltic inflows on the annual uplift of nutrients from below the halocline to the surface waters is small because the processes causing vertical transports are comparably large also in the cases with no major inflows. The impact from the East Gotland Deep water on eutrophication in the Baltic Sea is hence expected to be small because the volume below 150 m is small. The results point out needs for more research. It was shown by Eilola et al. (2012) that the

exchanges of nutrients between the shallow and deeper waters may intensify in a warmer future climate and the regional effects may therefore become even more accentuated. The physical dynamics and the processes driving the regional patterns of uplifted deep water to the surface layers are, however, still not well understood. The regional effects e.g. on the ecosystems and acidification from uplifted nutrients and other contents (e.g. hydrogen sulfide) of the uplifted deep water also need further attention.

### **3.8 Habitat sensitivity to eutrophication of selected pelagic species in the Baltic Sea (P1)**

*Burkhard von Dewitz, GEOMAR*

#### **3.8.1 Abstract/highlights**

Eutrophication and less frequent inflow events in the last decades resulted in severe expansions of hypoxic and anoxic regions in the deep basins in the Baltic Sea. Many species were impacted by a reduction of their area of distribution and quality of their habitat. In this study a high resolution hydrodynamic coupled sea ice-ocean model was used to investigate in hindcast the sensitivity of the habitat of several pelagic species to eutrophication only. With this approach the differences in habitat expansion and/or habitat quality introduced only through eutrophication could be assessed. Results suggested that habitats in the eastern Baltic Proper with the sub basins Gdansk Deep and Gotland Basin are more sensitive to changes in eutrophication than the Bornholm Basin and the western Baltic. With decreasing eutrophication and with the cascading effect in adjacent basins the eastern areas showed large potential to provide suitable habitats for Eastern Baltic cod and European flounder reproduction. In the Bornholm Basin area the spawning habitat quality for cod was significantly impacted by the effects of eutrophication. In particular the surviving chances of eggs and larvae spawned by young females of the stock are decreasing with increasing eutrophication while old females were found to be less affected. The inflow events stay however the most influential mechanism determining habitat extensions and quality in the Baltic Sea. Decreasing eutrophication could however damp the effect of less frequent inflow events in the future.

#### **3.8.2 Progress and (if applicable) deviations from the work plan**

All planned model exercises have been completed and the findings about the impact of eutrophication on the spawning habitat extensions and quality of Eastern Baltic cod in the Bornholm Basin including the effect of age of the female spawner on the parameters, are being prepared for publication.

### **3.8.3 Deviations from the work-plan**

None.

### **3.8.4 Introduction**

The Baltic Sea is one of the largest semi-enclosed brackish waters in the world with a water surface area of 377,400 km<sup>2</sup> (Sjoeberg 1992). The topography features a series of basins separated by sills (Fig. 1; Kullenberg and Jacobsen 1981) The Gulf of Bothnia and the Gulf of Riga can be seen as internal fjords, while the Baltic Proper and the Gulf of Finland consists of several deep basins with open connections. The oceanography of the Baltic Sea is mainly determined by the North Atlantic and European continental large scale climatic conditions (Lehmann et al. 2002). The topographical and meteorological factors (e.g. wind, precipitation and temperature) influence the ratio of the two main water sources of the Baltic Sea (river runoff and saline water inflows from the North Sea) and their interactions.

Within the Baltic Sea the hypoxic and anoxic areas on the seafloor are expanding rapidly in the last decades (Carstensen et al. 2014, Lehmann et al. 2014) erasing any benthic macro fauna and flora from vast areas in the eastern Baltic Proper. Besides these severe impacts on the benthic community pelagic habitats are also impacted by hypoxia and the general oxygen reduction (Schulz et al. 2007, Hinrichsen et al. 2007, Yakushev et al. 2011). The vertical stratification of the pelagic zone is especially amplifying the oxygen depletion. Only major Baltic inflows (MBIs) can transport substantial amounts of oxygenated water masses horizontally from the Kattegat and Skagerrak area into the deep parts of the Baltic Sea replenishing them with oxygen (Lehmann et al. 2002, 2014). All other import of oxygen from the surface is very limited. The halocline between low saline water in the mixed surface layer and high saline water in the deep parts of the Basins acts as barrier and separator cutting the pelagic zone into two distinct water masses. The depletion of oxygen within the enclosed water body at the bottom is driven by the respiration of organisms degrading biotic material (Fonselius 1970). Increasing eutrophication in the system leads to higher biomass loads reaching the deep basins and faster consumption of available oxygen (Laine et al. 1997).

In this study a high resolution sea ice-ocean model with realistic atmospheric forcing was used to perform a hindcast sensitivity study on pelagic habitats to eutrophication in the Baltic

Sea. Expansions and characteristics of habitats defined by abiotic thresholds were investigated in respect of their differences between three different levels of eutrophication.

### **3.8.5 Methods and Results**

#### **3.8.5.1 Hydrodynamic and habitat modelling**

The Basis for the hydrodynamical modelling was the Kiel Baltic Sea Ice-Ocean Model (BSIOM, Lehmann and Hinrichsen 2000, Lehmann et al. 2002). Its horizontal resolution was 2.5 km and consisted in the vertical of 60 levels. The model domain included the Baltic Sea, Kattegat and Skagerrak. It was complemented by an oxygen consumption sub-model producing oxygen property fields for the entire Baltic Sea with the same resolution (Lehmann et al. 2014). It uses idealized primary production levels represented as a factor in the oxygen tracer to calculate depletion rates on the 3D model grid points. To force the hydrographical model a realistic atmospheric forcing was chosen with the ERA-Interim reanalysis fields (Dee et al. 2011). These are available at a temporal resolution of 6 hours and have been downloaded on a regular grid of  $0.5^\circ \times 0.5^\circ$ . The database consisted of surface air pressure, precipitation, cloudiness, and air- and dew point temperatures at 2 m height. These data fields were further interpolated to be used as forcing for the model grid points. Wind speed and direction at 10 m height were calculated from geostrophic winds with respect to different degrees of roughness on the open sea and off the coast (Bumke et al. 1998). BSIOM forcing functions, such as wind stress, radiation and heat fluxes were calculated according to Rudolph and Lehmann (2006). Additionally, river runoff was prescribed from a monthly mean runoff data set (Kronsell and Andersson 2012).

As acclimatization and stabilization period the model setup was run from 1971 until 1998 with steadily increasing eutrophication. The above described primary production factor in the oxygen sub-model was for that purpose additively increased from 0.5 to 1 by a factor of 0.018 per year, following idealized in vivo findings of shifting eutrophication within this period (Wasmund et al. 2001). Subsequently beginning from the first of January 1998 until the end of 2015 the model was run three times with identical climate forcing but with different modulations of the primary production factor in the model. In the first run the primary production factor was kept constant at 1 for the whole period. In the second and third run the

factor was continuing to increase and decrease respectively by 0.018 per year. Daily values of the parameters salinity, temperature and oxygen were compiled from these three sensitivity runs on the entire model grid and interpolated for a monthly resolution.

Habitat modelling was performed with R (R Development Core Team 2011) and FORTRAN on the compiled data of the three sensitivity runs of the hydrographical model from 1998 to 2015. For all modelled habitats a hydrographical oriented classification for horizontal separation of the Baltic Proper into its sub basin was used to analyse habitat characteristics on a basin scale. The overall used separation is shown in Fig. 1. The used polygons in this separation were loosely orientated on the ICES subdivisions for the Baltic Sea with some adaptations for a better fit to hydrographical and topographical features in the area.

For habitat modelling established thresholds for habitat boundaries in regard to abiotic parameters of salinity, temperature and oxygen were used. The modelling exercises for habitats of pelagic species of the Baltic Sea comprised: The reproductive volume of Eastern Baltic cod (*Gadus morhua*); horizontal expansions of the reproductive habitat of *Pseudocalanus acuspes* and the European flounder (*Platichthys flesus*); the area expansions of the cod juvenile settlement habitat; and cod spawning habitat expansions and quality for eggs and larvae spawned by different aged females on the corresponding water density levels (including larval migration activity (LVMA) and oxygen depending egg survival). In the following sections first the methods used to compile the habitat data and then the results of these modeling exercises are shown.

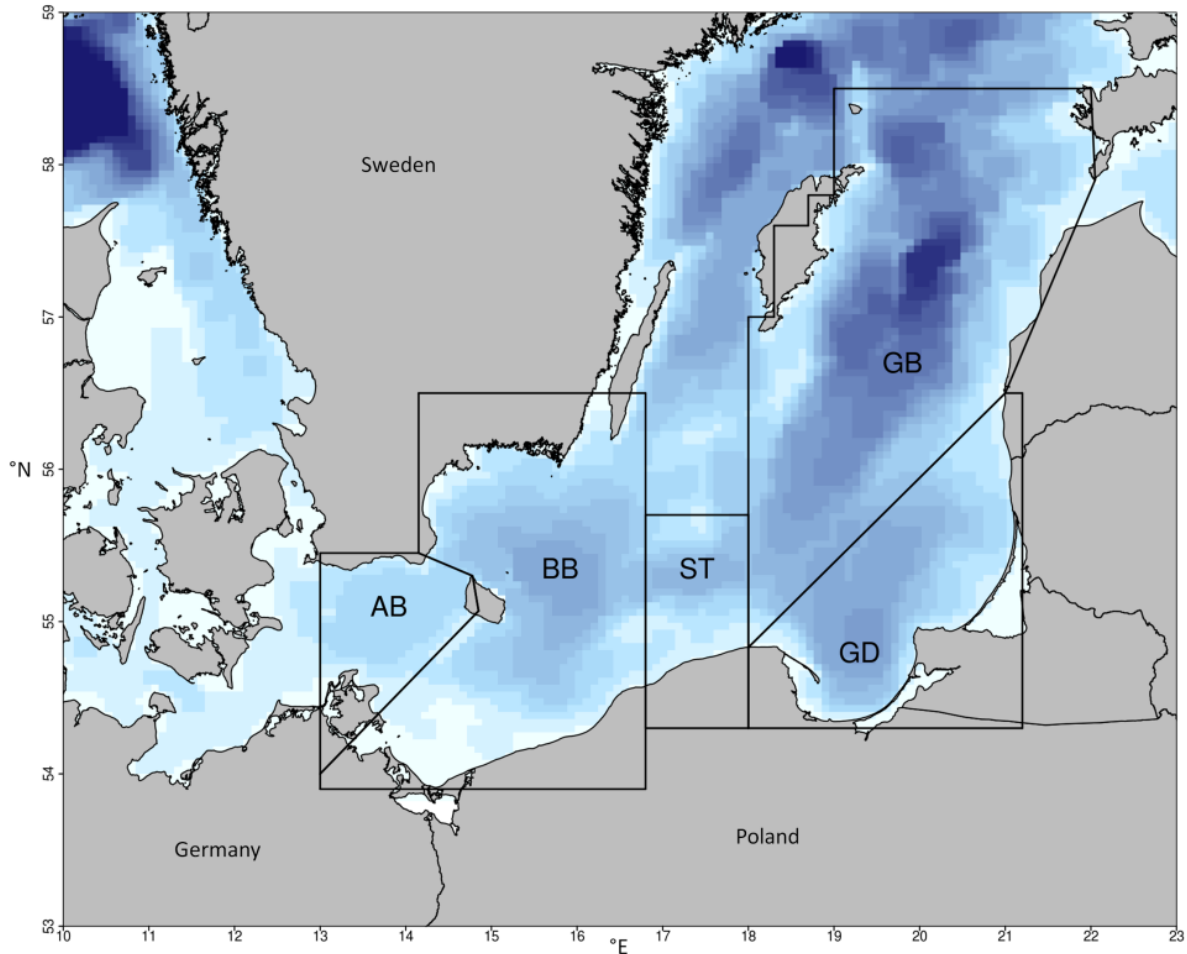


Figure 1. Area definitions for Basins used in the analysis. Horizontal boundaries for the separation of the Baltic Proper area into sub basins are depicted by black polygons. Basin names are abbreviated by “AB” for Arkona Basin, “BB” for Bornholm Basin, “ST” for Stolpe Trench, “GD” for Gdansk Deep and “GB” for Gotland Basin.

### 3.8.5.2 Impact of eutrophication on the reproductive volume of Eastern Baltic cod (*Gadus morhua*)

For calculating the reproductive volume for Eastern Baltic cod the classical definition taken from Hinrichsen et al. (2007) were used defining the reproductive volume as that volume of water with a salinity >11 PSU, an oxygen level of > 2 ml l<sup>-1</sup> and a temperature > 1.5 °C .

The reproductive volume of Eastern Baltic Cod showed strong variations in all investigated areas (see Fig. 2). Impulses introduced by inflow events frequently increased the RV in all areas strongly but was found to reach the more eastern spawning areas of Gdansk Deep and Gotland Basin with a certain delay. These Impulses are commonly followed by a strong

decrease in Volume introduced by depletion of the oxygen content over time. In general the Bornholm Basin was found to remain after these decreases above ca 100 km<sup>3</sup>, while the RV in the Gdansk Deep and Gotland Basin got in the majority of cases reduced to 0 again. For the Bornholm Basin and the Gdansk Deep eutrophication was found to impact the RV very little and only during the decreasing periods or stagnating periods in case of the Bornholm Basin. Increasing eutrophication results here in decreasing the amount of time it takes the RV to come back to the value from before the increasing impulse. In the Bornholm Basin eutrophication impacts the level on which the RV remains during this window if the period exceeds a few months. The differences though are marginal seen in relation to the total amount of available habitat.

The Gotland Basin shows different dynamics in respect to eutrophication than the other investigated areas (see Fig. 2). Here the increase of RV from the inflow events depends on eutrophication. Less eutrophication results in a slightly stronger increase of RV. Most probably due to the fact that the newly inflowing water masses to the Gotland Basin passes preceding Basins before reaching the Gotland Basin. Therefore an increase of eutrophication decreases the amount of oxygen being passed on to this most eastern area resulting in a slightly lower level of RV. In the end of the time series the two strong inflow events in winter 2013/2014 and 2014/2015 amplify the previously described effect of eutrophication determining the amount of oxygen renewal in the east of the Baltic Sea. Here for the decreasing eutrophication run the RV in the Gotland Basin reaches in the spawning period of 2015 a three times higher level (~700 km<sup>3</sup>) than for the steady eutrophication run to that time (~230 km<sup>3</sup>). Also compared with the results of the whole time period in all three basins this level is unmatched, showing the potential of the eastern Baltic to provide spawning habitat at a low eutrophication stage.

In conclusion eutrophication impacts the reproductive volume of Eastern Baltic cod in a considerable amount only in the more eastern part of the Baltic. Here the RV is most sensible to the cascading effect of oxygen loss of newly introduced oxygen rich water masses from MBIs during their passage through the preceding basins.



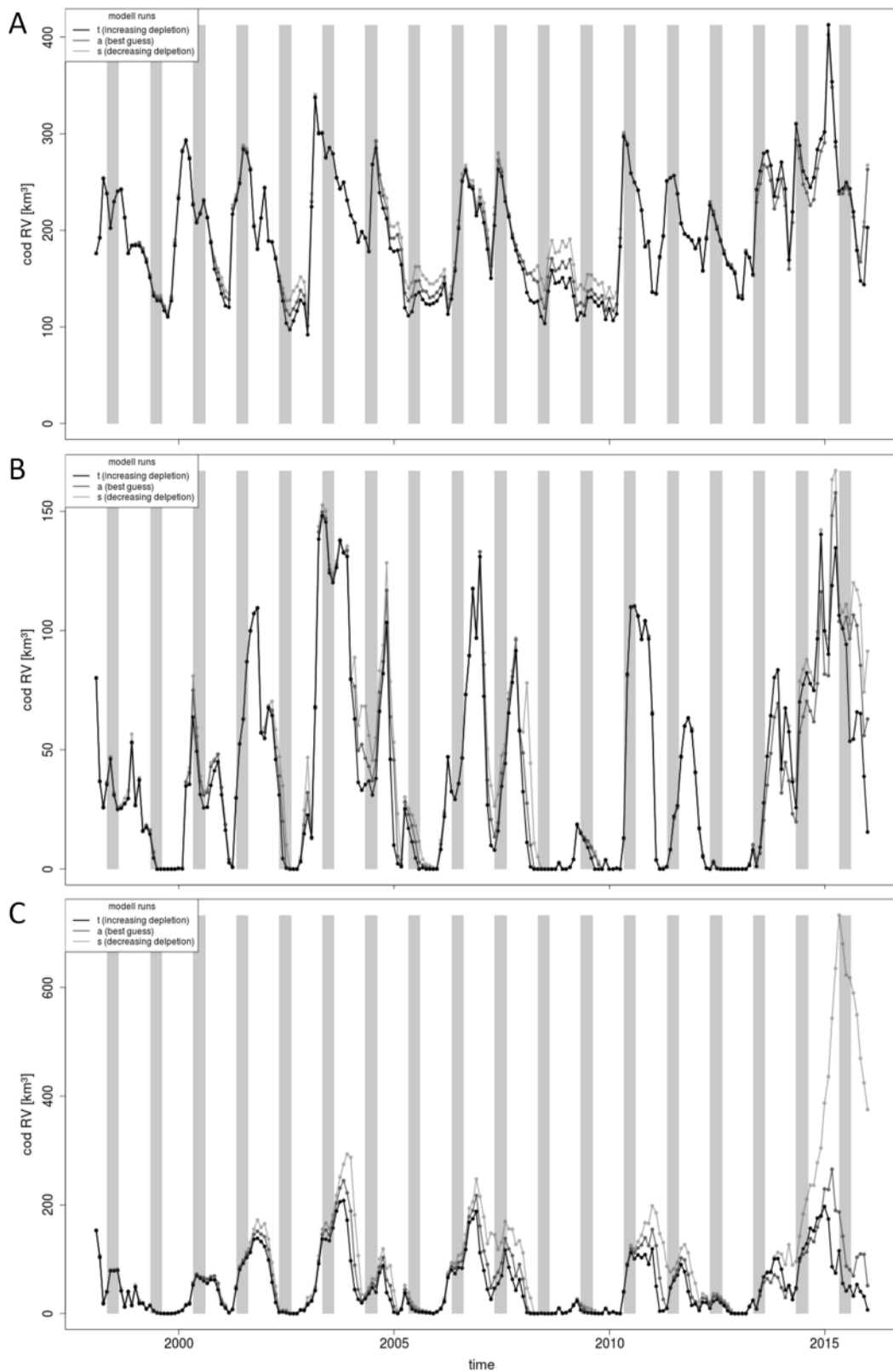


Figure 2. Time series of monthly values of reproductive volume of Eastern Baltic Cod in (A) the Bornholm Basin, (B) the Gdansk Deep and (C) the Gotland Basin. The three eutrophication sensitivity runs represented by colour intensity with run a (“best guess”; steady

eutrophication) in grey, run t (“increasing eutrophication”) in black and run s (“decreasing eutrophication”) in light grey. Spawning periods of cod indicated by grey vertical boxes.

Sections 3.8.5.3 and 3.8.5.4 were removed because they are under embargo until manuscript is published. If there is interest in the data, contact with Burkhard von Dewitz (bdewitz@geomar.de)





















#### **3.8.5.5 Impact of eutrophication on *Pseudocalanus acuspes* Reproductive habitat area extensions**

Schmidt (2006) described the reproduction volume of *Pseudocalanus acuspes* to be limited by hydrographical conditions. Due to the oceanic origin of this copepod species, egg sac carrying females seek higher saline waters in depth of the basin where at least 0.88 ml l<sup>-1</sup> oxygen

content is available. After Schmidt a boundary of 13.25 PSU was seldom vertical transcended towards the surface. These findings were used as thresholds to calculate the horizontal area expansions of the habitat for the three eutrophication hydrodynamic model runs described in 3.8.5.1. Results for the Gdansk Deep and Gotland Basin area east of the Bornholm Basin revealed only very little availability of the habitat during the modelled time period in the years 2003 and 2015 (results not shown). Within the Bornholm Basin however the reproductive volume was always available between 1998 and 2015 (Fig. 9).

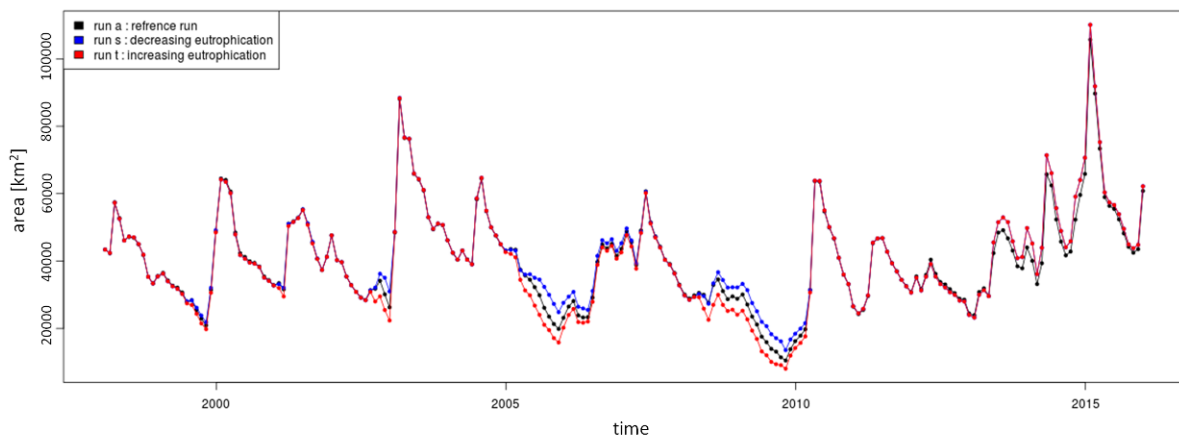


Figure 9. Time series of monthly values of area expansion of the reproductive volume of *Pseudocalanus acuspes* in the Bornholm Basin with colours indicating results derived from the eutrophication sensitivity hydrodynamic model runs. Time series in red colour represents increasing eutrophication, black colour steady eutrophication and blue colour decreasing eutrophication.

The impact of eutrophication on the area expansion of the reproductive volume of *Pseudocalanus acuspes* was found to be very weak. Only during the prolonged stagnation periods within the years 2005/06 and 2008/09 less eutrophication resulted into a slight higher area of the habitat. The very low threshold of oxygen for this habitat makes it very robust to slight changes in eutrophication. Only if very severe climate changes would get paired with a high increase of eutrophication the reproduction of this species could be impacted.

### 3.8.5.6 Impact of eutrophication on the horizontal expansion of the reproductive habitat of the European Flounder (*Platichthys flesus*)

Modeling exercises on the reproductive volume of the European Flounder (*Platichthys flesus*) were conducted with thresholds for abiotic factors taken from Ustups et al. (2012; after

Plikshs 1993). The resulting data grids from the hydrodynamic model runs with different levels of eutrophication were vertically interpolated and according to the thresholds for salinity of  $\geq 10.7$  and oxygen of  $\geq 2 \text{ ml l}^{-1}$  processed to habitat distribution maps for the entire model domain. Using the horizontal basin classification (Fig. 1) time series for mean horizontal expansions of the habitat were compiled. The results are shown for the three most important basins in the Baltic Proper the Bornholm Basin, the Gdansk Deep and the Gotland Basin in Figure 10.

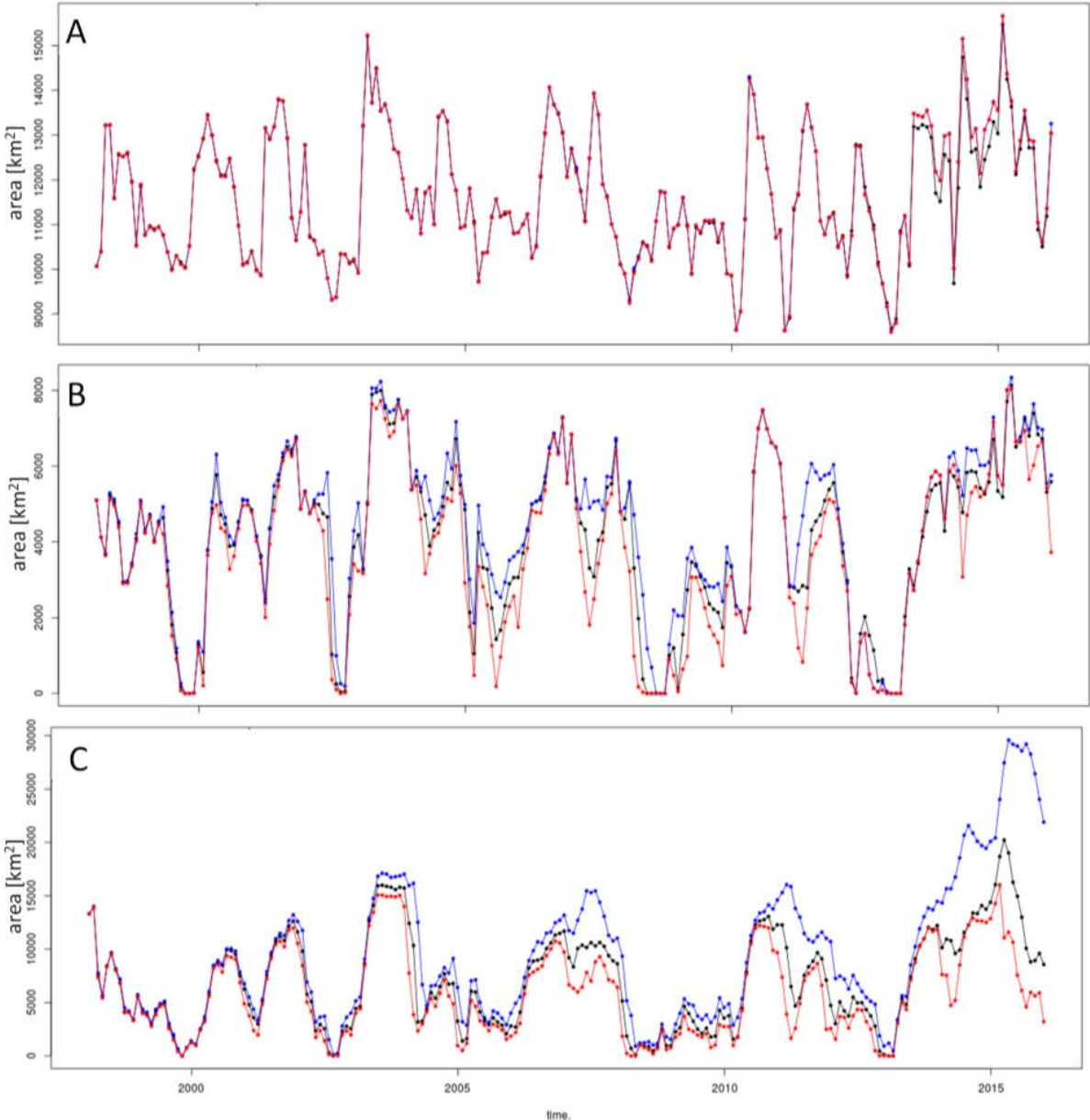


Figure 10. Time series of monthly values of area expansion of the reproductive volume of the European flounder (*Platichthys flesus*) in (A) the Bornholm Basin, (B) the Gdansk Deep and

(C) Gotland Basin area. Time series resulting from experimental eutrophication model runs indicated by colours, with “best guess” steady eutrophication in black, “increasing eutrophication” in red and “decreasing eutrophication” in blue.

The expansions of the reproductive volume of the European flounder were found to vary in all basins substantially during the modelled time period. While the Bornholm Basin showed results to be varying between ~8500 and 15500 km<sup>2</sup>, the expansion of the reproductive habitat in the Gdansk Deep and Gotland Basin were reduced to close to 0 km<sup>2</sup> five times over during the modelled period. These lows were usually lasting only for a few months before newly introduced oxygen improved the situation drastically within 4 to 5 months pushing the expansion area to 4000 to 7000 km<sup>2</sup> and 4000 to 14000 km<sup>2</sup> for the Gdansk Deep and Gotland Basin, respectively.

An impact of eutrophication on the habitat expansions were found for the Gdansk Deep and the Gotland Basin (Fig. 10). The Bornholm Basin proved to be robust to changes in eutrophication in for this habitat. Although the possibility that severe change could also affect this area can not be excluded with the performed study. Within the Gdansk area a lower level of eutrophication resulted in slight improvements of the habitat expansion during several periods. For the Gotland Basin a cascading effect like already described above for the RV of Eastern Baltic cod was found again. Here a lower eutrophication level results in larger improvements of the habitat expansion because the water lateral introduced through MBIs was less reduced in its oxygen content during the passage through the preceding basins. Most evident is this effect during the last 3 years of the modelled time period where two MBIs resulted in a difference of the habitat expansion of 13000 km<sup>2</sup> between the model runs with steady eutrophication and decreasing eutrophication in the end of 2015.

### **3.8.6 Recommendations**

In a preceding literature research for this study a lack of knowledge was found regarding Baltic specific physical tolerance levels of pelagic organisms. Most of the information we have about habitat characteristics, also put together in Task 1.1 of this project, is derived from field observations giving chosen preferences of abiotic parameter levels at best. To produce possible distribution maps and species composition scenarios for the pelagic habitat in the Baltic through modelling exercises this gap would be needed to be closed.

Older females of Eastern Baltic cod have in terms of contribution to spawning and recruitment in the stock better chances and a more robust habitat to their disposal. Due to the high fishing pressure on these old and big females their abundance is shrinking drastically in the last decades. Preferably new fishing techniques or methods are needed to put the highest fishing pressure on the middle aged fishes of 5 to 6 years of age. This would give the stock the highest chances for a yearly good recruitment and a long existence in the warming and freshening Baltic Sea.

## 4 References

- Adcroft, A., Campin, J.-M. 2004. Re-scaled height coordinates for accurate representation of free-surface flows in ocean circulation model. *Ocean Modelling*, 7, 269–284.
- Alheit, J., Möllmann, C., Dutz, J., Kornilovs, G., Loewe, P., Mohrholz, V., Wasmund, N. 2005. Synchronous ecological regime shifts in the central Baltic and the North Sea in the late 1980s. *ICES Journal of Marine Science*, 62, 1205–15.
- Almroth-Rosell, E., Eilola, K., Hordoir, R., Meier, H.E.M., Hall, P. 2011. Transport of fresh and resuspended particulate organic material in the Baltic Sea - a model study. *Journal of Marine Systems*, 87, 1–12.
- Almroth-Rosell, E., Eilola, K., Kuznetsov, I., Hall, P., Meier, H.E.M. 2015. A new approach to model oxygen dependent benthic phosphate fluxes in the Baltic Sea. *Journal of Marine Systems*, 144, 127–141. DOI:10.1016/j.jmarsys.2014.11.007.
- Andersen, J. H., Carstensen, J., Conley, D.J., Dromph, K., Fleming-Lehtinen, V., Gustafsson, B.G., Josefson, A.B., Norkko, A., Villnäs, A., Murray, C. 2015. Long-term temporal and spatial trends in eutrophication status of the Baltic Sea. *Biological Reviews*. doi: 10.1111/brv.12221.
- Anderson, D.M., Burkholder, J.M., Cochlan, W.P., Glibert, P.M., Gobler, C.J., Heil, C.A., Kudela, R.M., Parsons, M.L., Rensel, J.J.E., Townsend D.W., Trainer V.L., Vargo G.B. 2008. Harmful algal blooms and eutrophication: Examining linkages from selected coastal regions of the United States. *Harmful Algae*, 8, 39–53.



- AquaNIS. 2016. Information system on aquatic non-indigenous and cryptogenic species. URL: <http://www.corpi.ku.lt/databases/aquanis>. (11.01.2016).
- BACC. 2008. Assessment of climate change for the Baltic Sea, 1–479.
- Blomqvist, S., Gunnars, A., Elmgren, R. 2004. Why the limiting nutrient differs between temperate coastal seas and freshwater lakes: a matter of salt. *Limnology and Oceanography*, 49, 2236–2241.
- Bumke, K., Karger, U., Hasse, L., Niekamp, K. 1998. Evaporation over the Baltic Sea as an example of a semi-enclosed sea. *Contributions to Atmospheric Physics*, 71, 249–261.
- Cai, W.-J., Sayles, F.L. 1996. Oxygen penetration depths and fluxes in marine sediments. *Marine Chemistry*, 52, 123–131.
- Cardinale, M., Casini, M., Arrhenius, F. 2002. The influence of biotic and abiotic factors on the growth of sprat (*Sprattus sprattus*) in the Baltic Sea. *Aquatic Living Resources*, 15, 273–281.
- Carstensen, J., Sánchez-Camacho, M., Duarte, C.M., Krause-Jensen, D., Marbà, N. 2011. Connecting the Dots: Responses of Coastal Ecosystems to Changing Nutrient Concentrations. *Environmental Science & Technology*, 45, 9122–32.
- Casini, M., Hjelm, J. 2009. Trophic cascades promote threshold-like shifts in pelagic marine ecosystems. *Proceedings of the National Academy of Sciences of the United States of America*, 106, 197–202.
- Casini, M., Bartolino, V., Molinero, J.C., Kornilovs, G. 2010. Linking fisheries, trophic interactions and climate: Threshold dynamics drive herring *Clupea harengus* growth in the central Baltic Sea. *Marine Ecology Progress Series*, 413, 241–252.
- Cederwall, H., Elmgren, R. 1990. Biological Effects of eutrophication in the Baltic Sea, particularly the coastal zone. *Ambio*, 19, 109–112.
- Chabot, D., Dutil, J.D. 1999. Reduced growth of Atlantic cod in non-lethal hypoxic conditions. *Journal of Fish Biology*, 55, 472–491.
- Clarke, K.R., Warwick, K.M. 1994. Change in marine communities: an approach to statistical analysis and interpretation. National Environment Research Council, UK, Swindon, Wilts
- EC (2007) Council regulation (EC) no. 708/2007 of 11 June 2007 concerning use of alien

- and locally absent species in aquaculture. Official Journal of the European Union L, 168, 1–17.
- Conley, D.J., Humborg, C., Rahm, L., Savchuk, O.P., Wulff, F. 2002. Hypoxia in the Baltic Sea and Basin-Scale changes in phosphorous and biogeochemistry. *Environmental Science & Technology*, 36, 5315–5320.
- Conley, D.J., Björck, S., Bonsdorff, E., Carstensen, J., Destouni, G., Gustafsson, B.G., Hietanen, S., Kortekaas, M., Kuosa, H., Meier, M.H.E., Müller-Karulis, B., Nordberg, K., Norkko, A., Nürnberg, G., Pitkänen, H., Rabalais, N.N., Rosenberg, R., Savchuk, O.P., Slomp, C.P., Voss, M., Wulff, F., Zillen, L. 2009. Hypoxia-related processes in the Baltic Sea. *Environmental Science & Technology*, 43, 3412–3420.
- Crain, C.M., Kroeker, K., Halpern, B.S. 2008. Interactive and cumulative effects of multiple human stressors in marine systems. *Ecology Letters*, 11, 1304–1315.
- Díaz, R.J., Rosenberg, R. 2008. Spreading dead zones and consequences for marine ecosystems. *Science*. 321, 926–929.
- Dee, D.P., Uppala, S.M., Simmons, A.J., Berrisford, P., Poli, Kobayashi S., Andrae, U., Balmaseda, M.A., Balsamo, G., Bauer, P., Bechtold, P., Beljaars, A.C.M., van de Berg, L., Bidlot, J., Bormann, N., Delsol, C., Dragani, R., Fuentes, M., Geer, A.J., Haimberg, L., Healy, S.B., Hersbach, H., Holm, E.V., Isaksen, L., Kallberg, P., Köhler, M., Matricardi, M., McNally, A.P., Monge-Sanz, B.M., Morcrette, J.-J., Park, B.-K., Peubey, C., de Rosnay, P., Tavolato, C., Thepaut, J.N., Vitrat, F. 2011. The ERA-Interim reanalysis: configuration and performance of the data assimilation system. *Quarterly Journal of the Royal Meteorological Society*, 137, 553–597.
- Duarte, C.M. 1995. Submerged aquatic vegetation in relation to different nutrient regimes. *Ophelia*, 41, 87–112.
- EC. 2007. Council regulation (EC) no. 708/2007 of 11 June 2007 concerning use of alien and locally absent species in aquaculture. Official Journal of the European Union L, 168, 1–17.
- EC. 2008. Directive 2008/56/EC of the European Parliament and of the Council of 17 June 2008 establishing a framework for community action in the field of marine environmental

- policy (Marine Strategy Framework Directive). Official Journal of the European Union L, 164, 19–40.
- EC. 2011. Our life insurance, our natural capital: an EU biodiversity strategy to 2020. Communication from the Commission of the European Parliament, the Council, the Economic and Social Committee and the Committee of the Regions COM (2011) 244, Brussels, Belgium.
- EC. 2014. Regulation (EU) No 1143/2014 of the European Parliament and of the Council of 22 October 2014 on the prevention and management of the introduction and spread of invasive alien species. Official Journal of the European Union L, 317, 35–55.
- EC 2015. Mobility and Transport. Infrastructure - TEN-T - Connecting Europe. Corridors  
URL: [http://ec.europa.eu/transport/themes/infrastructure/ten-t-guidelines/corridors/index\\_en.htm](http://ec.europa.eu/transport/themes/infrastructure/ten-t-guidelines/corridors/index_en.htm) (11.06.2016)
- Edelist, D., Rilov, G., Golani, D., Carlton, J.T., Spanier, E. 2012. Restructuring the Sea: profound shifts in the world's most invaded marine ecosystem. *Diversity and Distributions*, 19, 69–77.
- Eero, M. 2012. Reconstructing the population dynamics of sprat (*Sprattus sprattus balticus*) in the Baltic Sea in the 20th century. *ICES Journal of Marine Science*, 69, 1010–1018.
- Eilola, K., Meier, H.E.M., Almroth, E. 2009. On the dynamics of oxygen, phosphorus and cyanobacteria in the Baltic Sea: A model study. *Journal of Marine Systems*, 75, 163–184.
- Eilola, K., Almroth-Rosell, E., Dieterich, C., Fransner, F., Höglund, A., Meier, H.E.M. 2012. Modeling nutrient transports and exchanges of nutrients between shallow regions and the open Baltic Sea in present and future climate. *AMBIO*, 41, 574–585, DOI: 10.1007/s13280-012-0319-9.
- Eilola, K., Almroth-Rosell, E., Meier, H.E.M. 2014. Impact of saltwater inflows on phosphorus cycling and eutrophication in the Baltic Sea. A 3D model study. *Tellus A*, 66, 23985, <http://dx.doi.org/10.3402/tellusa.v66.23985>.
- Emeis, K.C., Struck, U., Leipe, T., Pollehne, F., Kunzendorf, H., Christiansen, C. 2000. Changes in the C, N, P burial rates in some Baltic Sea sediments over the last 150 years – relevance to P regeneration rates and the phosphorus cycle. *Marine Geology*, 167, 43–59.

- Feistel, R., Nausch, G., Wasmund, N. (eds) 2008. State and Evolution of the Baltic Sea, 1952–2005: A Detailed 50-Year Survey of Meteorology and Climate, Physics, Chemistry, Biology, and Marine Environment. Wiley, Hoboken, New Jersey.
- Feistel, R., Weinreben, S., Wolf, H., Seitz, S., Spitzer, P., Adel, B., Nausch, G., Schneider, B., Wright, D.G. 2010. Density and Absolute Salinity of the Baltic Sea 2006–2009. *Ocean Science*, 6, 3–24.
- Folino-Rorem, N.C., Darling, J.A., D’Ausilio, C.A. 2008. Genetic analysis reveals multiple cryptic invasive species of the hydrozoan genus *Cordylophora*. *Biological Invasions*, 11, 1869–1882.
- Fonselius, F.S. 1970. On the stagnation and recent turnover of the water in the Baltic. *Tellus*, 22, 533–544.
- Froelich, P.N. 1988. Kinetic control of dissolved phosphate in natural rivers and estuaries – a primer on the phosphate buffer mechanism. *Limnology and Oceanography*, 33, 649–668.
- Godhe, A., Egardt, J., Kleinhans, D., Sundqvist, L., Hordoir, R., Jonsson, P. 2013. Seascape analysis reveals regional gene flow patterns among populations of a marine planktonic diatom. *Proceedings of the Royal Society B*, 280, doi:10.1098/rspb.2013.1599.
- Gogina, M., Zettler, M. L. 2010. Diversity and distribution of benthic macrofauna in the Baltic Sea: Data inventory and its use for species distribution modelling and prediction. *Journal of Sea Research*, 64, 313–321.
- Gorokhova, E., Lehtiniemi, M., Viitasalo-Frösen, S., Haddock, S.D.H. 2009. Molecular evidence for the occurrence of ctenophore *Mertensia ovum* in the northern Baltic Sea and implications for the status of the *Mnemiopsis leidyi* invasion. *Limnology and Oceanography*, 54, 2025–2033.
- Grosholz, E.D., Ruiz, G.M. 2009. Multitrophic effects of invasions in marine and estuarine systems. In: Rilov, G., Crooks, J.A., Jeffrey, A. (eds). *Biological invasions in marine ecosystems. Ecological, management, and geographic perspectives*. Springer, Series: Ecological Studies, 204, pp 109–116.
- Gunnars, A., Blomqvist, S. 1997. Phosphate exchange across the sediment-water interface when shifting from anoxic to oxic conditions an experimental comparison of freshwater and brackish-marine systems. *Biogeochemistry*, 37, 203–226.

- Gunnars, A., Blomqvist, S., Johansson, P., Andersson, C. 2002. Formation of Fe (III) oxyhydroxide colloids in freshwater and brackish seawater, with incorporation of phosphate and calcium. *Geochimica et Cosmochimica Acta*, 66, 745–758.
- Gustafsson, B.G., Blenckner, T., Eilola, K., MacKenzie, B., Meier, H.E.M., Müller-Karulis, B., Neumann, T., Niiranen, S., Rhoija-Airola, T., Savchuk, O., Schenk, F., Tomczak, M., Zorita, E. 2012. Reconstructing the development of Baltic Sea eutrophication 1850–2000. *Ambio*, 41, 534-548.
- Hansson, M., Andersson, L. 2013. Oxygen survey in the Baltic Sea 2013 – extent of anoxia and hypoxia, 1960–2013. REPORT OCEANOGRAPHY No. 49. Swedish Meteorological and Hydrological Institute. URL: [http://www.smhi.se/polopoly\\_fs/1.35317!Oxygen\\_timeseries\\_1960\\_2013\\_final.pdf](http://www.smhi.se/polopoly_fs/1.35317!Oxygen_timeseries_1960_2013_final.pdf).
- HELCOM. 2007. Baltic Sea action plan. Helsinki: HELCOM.
- HELCOM. 2010. Ecosystem Health of the Baltic Sea 2003–2007: HELCOM Initial Holistic Assessment. Baltic Sea Environment Proceedings No. 122. HELCOM, Helsinki.
- HELCOM. 2013. Joint HELCOM/OSPAR Guidelines for the Contracting Parties of OSPAR and HELCOM on the granting of exemptions under International Convention for the Control and Management of Ships' Ballast Water and Sediments, Regulation A-4. Adopted by HELCOM Ministerial Meeting, 3 October 2013 in Copenhagen and OSPAR Agreement 2013-09.
- Hinrichsen, H.H., Voss, R., Wieland, K., Koster, F., Andersen, K.H., Margonski, P. 2007. Spatial and temporal heterogeneity of the cod spawning environment in the Bornholm Basin, Baltic Sea. *Marine Ecology Progress Series*, 345, 245–254.
- Hordoir, R., Dieterich, C., Basu, C., Dietze, H., Meier, H.E.M. 2013. Freshwater outflow of the Baltic Sea and transport in the Norwegian current: A statistical correlation analysis based on a numerical experiment. *Continental Shelf Research*, 64, 1–9.
- Hordoir, R., Axell, L., Löptien, U., Dietze, H., Kuznetsov, I. 2015. Influence of sea level rise on the dynamics of salt inflows in the Baltic Sea. *Journal of Geophysical Research. Oceans*, 120, doi:10.1002/2014JC010642.
- Hulme, P. 2015. Invasion pathways at a crossroad: policy & research challenges for managing alien species introductions. *Journal of Applied Ecology*, 52, 1418–1424.

- Hägg, H.E., Lyon, S.W., Wällstedt, T., Mörth, C.-M., Claremar, B., Humborg, C. 2014. Future nutrient load scenarios for the Baltic Sea due to climate and lifestyle changes. *Ambio*, 43, 337–351.
- Hüssy, K. 2011. Review of western Baltic cod (*Gadus morhua*) recruitment dynamics. *ICES Journal of Marine Science* 2011, 68, 1459–1471.
- ICES. 2014. Report of the Baltic Fisheries Assessment Working Group (WGBFAS), 3-10 April 2014, ICES HQ, Copenhagen, Denmark. ICES CM 2014/ACOM:10. 834 pp.
- ICES. 2015a. Special Request Advice Baltic Sea Ecoregion. HELCOM request on pressure from fishing activity (based on VMS/logbook data) in the HELCOM area relating to both seafloor integrity and management of HELCOM MPAs. ICES Advice 2015, Book 1.
- ICES. 2015b. Report of the Working Group on Introductions and Transfers of Marine Organisms (WGITMO), 18–20 March 2015, Bergen, Norway. ICES CM 2015/SSGEPI:10.
- IMO. 2004. International Convention for the Control and Management of Ships' Ballast Water and Sediments. URL: <http://www.imo.org>. (20.12.2015).
- Jilbert, T., Slomp, C., Gustafsson, B.G., Boer, W. 2011. Beyond the Fe-P-redox connection: preferential regeneration of phosphorus from organic matter as a key control on Baltic Sea nutrient cycles. *Biogeosciences*, 8, 1699–1720.
- Josefson, A.B., Rasmussen, B. 2000. Nutrient retention by benthic macrofaunal biomass of Danish estuaries: importance of nutrient load and residence time. *Estuarine, Coastal and Shelf Science*, 50, 205–216.
- Katsanevakis, S., Wallentinus, I., Zenetos, A., Leppäkoski, E., Çinar, M.E., Oztürk, B., Grabowski, M., Golani, D., Cardoso, A.C. 2014. Impacts of invasive alien marine species on ecosystem services and biodiversity: a pan-European review. *Aquatic Invasions*, 9, 391–423.
- Kelley, D. 2011. Analysis of Oceanographic Data. Kelley, R package 'oce': Analysis of Oceanographic data, R package. URL: <https://cran.r-project.org/web/packages/oce/>
- Kemp, W.M., Boynton, W.R., Adolf, J.E., Boesch, D.F., Boicourt, W.C., Brush, G., Cornwell, J.C., Fisher, T.R., Glibert, P.M., Hagy, J.D., Harding, L.W., Houde, E.D., Kimmel, D.G., Miller, W.D., Newell, R.I.E., Roman, M.R., Smith, E.M., Stevenson, J.C.

2005. Eutrophication of Chesapeake Bay: Historical trends and ecological interaction. *Marine Ecology Progress Series*, 303, 1–29.
- Kjørboe, T., Møhlenberg, F., Nøhr, O. 1980. Feeding, particle selection and carbon adsorption in *Mytilus edulis* in different mixtures of algae and resuspended bottom material. *Ophelia*, 19, 193–205.
- Köster, F.W., Mollmann, C., Hinrichsen, H.H., Wieland, K., Tomkiewicz, J., Kraus, G., Voss, R., Makarchouk, A., MacKenzie, B.R., St. John, M.A., Schnack, D., Rohlf, N., Linkowski, T., Beyera, J.E. 2005. Baltic cod recruitment - the impact of climate variability on key processes. *ICES Journal of Marine Science*, 62, 1408–1425.
- Kronsell, J., Andersson, P. 2012. Total regional runoff to the Baltic Sea. HELCOM Indicator Fact Sheets 2011. URL: <http://www.helcom.fi/environment2/ifs>.
- Kullenberg, G., Jacobsen, T.S. 1981. The Baltic Sea - An outline of its physical oceanography. *Marine Pollution Bulletin*, 12, 183–186.
- Laine, A.O., Sandler, H., Andersin, A.B., Stigzelius, J. 1997. Long term changes of macrozoobenthos in the Eastern Gotland Basin and the Gulf of Finland (Baltic Sea) in relation to the hydrographical regime. *Journal of Sea Research* 38, 135–159.
- Lass, H. U., Matthäus, W. 1996. On temporal wind variations forcing salt water inflows into the Baltic Sea. *Tellus Series A: Dynamic Meteorology and Oceanography*, 48, 663–671.
- Lehmann, A., Hinrichsen, H.-H. 2000. On the thermohaline variability of the Baltic Sea. *Journal of Marine Systems*, 25, 333–357.
- Lehmann, A., Krauß, W., Hinrichsen, H.-H. 2002. Effects of remote and local atmospheric forcing on circulation and upwelling in the Baltic Sea. *Tellus*, 54A, 299–316.
- Lehmann, A., Hinrichsen, H. H., Getzlaff, K., Myrberg, K. 2014. Quantifying the heterogeneity of hypoxic and anoxic areas in the Baltic Sea by a simplified coupled hydrodynamic-oxygen consumption model approach. *Journal of Marine Systems*, 134, 20–28.
- Lehtiniemi, M., Ojaveer, H., David, M., Galil, B., Gollasch, S., McKenzie, C., Minchin, D., Occhipinti-Ambrogi, A., Olenin, S., Pederson, J. 2015. Dose of truth – monitoring marine non-indigenous species to serve legislative requirements. *Marine Policy*, 54, 26–35.

- Lima, F.P., and Wethey, D.S. 2012. Three decades of high-resolution coastal sea surface temperatures reveal more than warming. *Nature Communications*, 3, 704.
- Lukkari, K., Leivuori, M., Vallius, H., Kotilainen, A. 2009. The chemical character and burial of phosphorus in shallow coastal sediments in the northeastern Baltic Sea. *Biogeochemistry*, 94, 141–162.
- Madec, G. 2010. NEMO ocean engine, version 3.3, Note du Poole de modelisation de l'Inst. Pierre-Simon Laplace 27, Inst. Pierre-Simon Laplace, Paris. URL: <http://www.nemoocean.eu/>.
- Margonski, P., Hansson, S., Tomczak, M.T., Grzebielec, R. 2010. Climate influence on Baltic cod, sprat, and herring stock–recruitment relationships. *Progress in Oceanography*, 87, 277–288.
- Meier, H.E.M., Döscher, R., Faxén, T. 2003. A multiprocessor coupled ice-ocean model for the Baltic Sea: Application to salt inflow. *Journal of Geophysical Research*, 108, 3273.
- Meier, H.E.M., Kauker, F. 2003. Modeling decadal variability of the Baltic Sea: 2. Role of freshwater inflow and large-scale atmospheric circulation for salinity. *Journal of Geophysical Research*, 108, 3368.
- Meier, H.E.M., Kjellström, E., Graham, L.P. 2006. Estimating uncertainties of projected Baltic Sea salinity in the late 21st century. *Geophysical Research Letters*, 33, L15705,
- Meier, H.E.M. 2007. Modeling the pathways and ages of inflowing salt- and freshwater in the Baltic Sea. *Estuarine, Coastal and Shelf Science*, 74, 717–734.
- Meier, H.E.M., Hordoir R., Andersson, H., Dieterich, C., Eilola, K., Gustafsson, B., Höglund, A., and Schimanke, S., 2012. Modeling the combined impact of changing climate and changing nutrient loads on the Baltic Sea environment in an ensemble of transient simulations for 1961–2099, *Climate Dynamics*, 39, 2421–2441.
- Micheli, F. 1999. Eutrophication, fisheries, and consumer-resource dynamics in marine pelagic ecosystems. *Science*. 285, 1396–1399.
- Millero, F. J., Kremling, K. 1976. Densities of Baltic Sea waters. *Deep-Sea Research*, 23, 1129–1138.



- Mort, H. P., Slomp, C. P., Gustafsson, B. G. Andersen, T. J. 2010. Phosphorus recycling and burial in Baltic Sea sediments with contrasting redox conditions. *Geochimica et Cosmochimica Acta*, 74, 1350–62.
- Mortimer, C.H. 1941. The exchange of dissolved substances between Mud and water in lakes. *Journal of Ecology*, 29, 280–329.
- Mortimer, C.H. 1942. The exchange of dissolved substances between mud and water in lakes. *Journal of Ecology*, 30, 147–201.
- Möllmann, C., Kornilovs, G., Fetter, M., Köster, F.W. 2005. Climate, zooplankton, and pelagic fish growth in the central Baltic Sea. *ICES Journal of Marine Science*, 62, 1270–1280.
- Möllmann, C., Diekmann, R., Müller-Karulis, B., Kornilovs, G., Plikshs, M., Axe, P. 2009. Reorganization of a large marine ecosystem due to atmospheric and anthropogenic pressure: a discontinuous regime shift in the Central Baltic Sea. *Global Change Biology*, 15, 1377–1393.
- Nixon, S.W., Buckley, B.A. 2002. “A strikingly rich zone”—Nutrient enrichment and secondary production in coastal marine ecosystems. *Estuaries*, 25, 782–796.
- Oesterwind, D. (Ed.), Dewitz, B. von, Döring, R., Eero, M., Goti, L., Kotta, J., Nurske, J., Ojaveer, H., Rau, R., Skov, H., Stepputtis, H., and Zaiko, H., 2016. Review on (existing knowledge of) patterns and dynamics of drivers of biodiversity (species, communities, habitats) across Baltic Sea ecosystems in space and time including socio-economy. BIO-C3 WP 3.1 Report. Thünen Institute of Baltic Sea Fisheries.
- Ojaveer, H., Galil, B.S., Minchin, D., Olenin, S., Amorim, A., Canning-Clode, J., Chainho, P., Copp, C.H., Gollasch, S., Jelmert, A., Lehtiniemi, M., McKenzie, C., Mikuš, J., Miossec, L., Occhipinti-Ambrogi, A., Pećarević, M., Pederson, J., Quilez-Badia, G., Wijsman, J.W.M., Zenetos, A. 2014. Ten recommendations for advancing the assessment and management of nonindigenous species in marine ecosystems. *Marine Policy*, 44, 160–165.
- Ojaveer, H, Kotta, J. 2015. Ecosystem impacts of the widespread non-indigenous species in the Baltic Sea: literature survey evidences major limitations in knowledge. *Hydrobiologia*, 750, 171–185.

- Olenin, S., Minchin, D. 2011. Biological introductions to the systems: macroorganisms. In: Wolanski, E., McLusky, D.S. (eds) *Treatise on Estuarine and Coastal Science* 8, Academic Press, Waltham, pp 149–183.
- Olenin, S., Narščius, A., Minchin, D., David, M., Galil, B., Gollasch, S., Marchini, A., Occhipinti-Ambrogi, A., Ojaveer, H., Zaiko, A. 2014. Making non-indigenous species information systems practical for management and useful for research: an aquatic perspective. *Biological Conservation*, 173, 98–107.
- Österblom, H., Hansson, S., Larsson, U., Hjerne, O., Wulff, F., Elmgren, R., Folke, C. 2007. Human-induced trophic cascades and ecological regime shifts in the Baltic Sea. *Ecosystems*, 10, 877–889.
- Palialexis, A., Cardoso, A.C., Tsiamis, K., Alemany, F., Cheilari, A., Guerin, L., Hoppe, K., Kabuta, S., Mavri, B., Miossec, L., Ojaveer, H., Orlando-Bonaca, M., Ouerghi, A., Tidbury H. 2015. Report of the JRC's Descriptor 2 workshop in support to the review of the Commission Decision 2010/477/EU concerning MSFD criteria for assessing Good Environmental Status for NIS, EUR 27714
- Plikshs, M., Kalejs, M., Graumann, G. 1993. The influence of environmental conditions and spawning stock size on the yearclass strength of the eastern Baltic cod. *ICES CM* 1993/J:22.
- Poloczanska, E.S., Babcock, R.C., Butler, A., Hobday, A.J., Hoegh-Guldberg, O., Kunz, T.J., Matear, R., Milton, D.A., Okey, T.A., Richardson, A.J. 2007. Climate change and Australian marine life. *Oceanography and Marine Biology: an Annual Review*. 45, 407–478.
- R Development Core Team. 2011. *R: A language and environment for statistical computing*. R Foundation for Statistical Computing, Vienna, Austria. ISBN 3-900051-07-0, URL: <http://www.R-project.org/>.
- Rasmussen, E.K. 2015. Development of ecosystem models. Input to BIO-C3 WP 2.1. DHI.
- Reissmann, J.H., Burchard, H., Feistel, R., Hagen, E., Lass, H.U., Mohrholz, V., Nausch, G., Umlauf, L., Wiczorek, G. 2009. Vertical mixing in the Baltic Sea and consequences for eutrophication\_a review. *Progress in Oceanography*, 82, 47–80.

- Riemann, B., Carstensen, J., Dahl, K., Fossing, H., Würgler, J., Jakobsen, H., Josefson, A.B., Krause-Jensen, D., Markager, S., Stæhr, P.A., Timmermann, K., Windolf, J., Andersen, J.H. 2016. Recovery of Danish coastal ecosystems after reductions in nutrient loading: A holistic ecosystem approach. *Estuaries and Coasts*, 39, 82–97.
- Rohlf, N. 1999. *Verhaltensänderungen der Larven des Ostseedorsches (Gadus morhua callarias) während der Dottersackphase*. Kiel: Inst. für Meereskunde, Abt. Fischereibiologie. Dissertation. Berichte aus dem Institut für Meereskunde an der Christian-Albrechts-Universität Kiel; Nr.312. doi:10.3289/IFM\_BER\_312.
- Rudolph, C., Lehmann, A. 2006. A model-measurements comparison of atmospheric forcing and surface fluxes of the Baltic Sea. *Oceanologia*, 48, 333–380.
- Ruiz, G.M., Fofonoff, P.W., Steves, B.P., Carlton, J.T. 2015. Invasion history and vector dynamics in coastal marine ecosystems: A North American perspective. *Aquatic Ecosystem Health and Management*, 8, 299–311.
- Savchuk, O.P. 2010. Large-scale dynamics of hypoxia in the Baltic Sea. In: *Chemical Structure of Pelagic Redox Interfaces: Observation and Modelling. The Handbook of Environmental Chemistry* (ed. E. Yakushev). Springer-Verlag, Berlin. pp. 137–160.
- Schmidt, J. 2006. Small and meso-scale distribution patterns of key copepod species in the Central Baltic Sea and their relevance for larval fish survival. Ph.D. thesis. Univ. of Kiel.
- Schneider, B. 2011. PO<sub>4</sub> release at the sediment surface under anoxic conditions: a contribution to the eutrophication of the Baltic Sea? *Oceanologia*, 53, 415–529.
- Schulz, J., Mollmann, C., Hirche, H. J. 2007. Vertical zonation of the zooplankton community in the Central Baltic Sea in relation to hydrographic stratification as revealed by multivariate discriminant function and canonical analysis. *Journal of Marine Systems*, 67, 47–58.
- Siegel, H., Gerth, M., Tschersich, G. 2006. Sea surface temperature development of the Baltic Sea in the period 1990–2004. *Oceanologia*, 48, 119–131.
- Sjoeberg, B. (ed). 1992. Sea and coast. The National Atlas of Sweden. Stockholm, Sweden: Almqvist and Wiksell International: 128.
- Skoog, A., Hall, P.O.J., Hulth, S., Paxeus, N., Van Der Loeff, M.R., Westerlund, S. 1996. Early diagenetic production and sediment-water exchange of fluorescent dissolved

- organic matter in the coastal environment. *Geochimica et Cosmochimica Acta*, 60, 3619–3629.
- Skov, H., Heinänen, S., Žydelis, R., Bellebaum, J., Bzoma, S., Dagys, M., Durinck, J., Garthe, S., Grishanov, G., Hario, M., Kieckbusch, J. J., Kube, J., Kuresoo, A., Larsson, K., Luigujoe, L., Meissner, W., Nehls, H. W., Nilsson, L., Petersen, I.K., Roos, M. M., Pihl, S., Sonntag, N., Stock, A., Stipniece, A. 2011. Waterbird populations and pressures in the Baltic Sea. Nordic Council of Ministers. TemaNord. 2011:550.
- Skov, H., Zydelis, R., Heinänen, S. 2011. Responses of waterbird populations to broad scale regime shifts in the Baltic Sea. *Proceed. World Conference on Marine Biodiversity*, Aberdeen, UK.
- Soetaert, K., Petzoldt, T., Meysman, F. 2012. marelac: Tools for Aquatic Sciences. R package version 2.1.1, URL: <http://CRAN.R-project.org/package=marelac/2012>.
- Stigebrandt, A., Gustafsson, B.G. 2007. Improvement of Baltic proper water quality using large-scale ecological engineering. *Ambio*, 36, 280–286.
- Stigebrandt, A., Rosenberg, R., Råman Vinnå, L., Ödalen, M. 2014. Consequences of artificial deepwater ventilation in the Bornholm Basin for oxygen conditions, cod reproduction and benthic biomass—A model study. *Ocean Science Discussion*, 11, 1783–1827.
- Suikkanen, S., Pulina, S., Engström-Öst, J., Lehtiniemi, M., Lehtinen, S., Brutemark, A. 2013. Climate Change and Eutrophication Induced Shifts in Northern Summer Plankton Communities. *PLoS ONE* 8(6): e66475.
- Sundby, B., Gobeil, C., Silverberg, N., Mucci, A. 1992. The phosphorus cycle in coastal marine sediments. *Limnology and Oceanography*, 37, 1129–1145.
- Tornroos, A., Bonsdorff, E. 2012. Developing the multitrait concept for functional diversity: lessons from a system rich in functions but poor in species. *Ecological Applications*, 22, 2221–2236.
- UNEP. 2011. The strategic plan for biodiversity 2011–2020 and the Aichi biodiversity targets. UNEP/CBD/COP/DEC/X/2, 29 October 2010, Nagoya, Japan. COP CBD Tenth Meeting. [www.cbd.int/decisions/cop/?m=cop-10](http://www.cbd.int/decisions/cop/?m=cop-10) (20.12.2015)

- Ustup, D., Müller-Karulis, B., Bergstrom, U., Makarchouk, A., Sics, I. 2012. The influence of environmental conditions on early life stages of flounder (*Platichthys flesus*) in the central Baltic Sea. *Journal of Sea Research*, doi:10.1016/j.seares.2012.05.001
- Vallin, L., Nissling, A. 2000. Maternal effects on egg size and egg buoyancy of Baltic cod, *Gadus morhua* - Implications for stock structure effects on recruitment. *Fisheries Research*, 49, 21–37.
- Viktorsson, L., Almroth-Rosell, E., Tengberg, A., Vankevich, R., Neelov, I., Isaev, A., Kravtsov, V., Hall, P.O.J. 2012. Benthic phosphorus dynamics in the gulf of Finland, Baltic Sea. *Aquatic Geochemistry*, 18, 543–564.
- Viktorsson, L., Ekeröth, N., Nilsson, M., Kononets, M., Hall, P.O.J. 2013. Phosphorus recycling in sediments of the central Baltic Sea. *Biogeosciences*, 10, 3901–3916.
- Wasmund, N., Andrushaitis, A., Łysiak-Pastuszek, E., Müller-Karulis, B., Nausch, G., Neumann, T., Ojaveer, H., Olenina, I., Postel, L., Witek, Z. 2001 Trophic Status of the South-Eastern Baltic Sea: A Comparison of Coastal and Open Areas. *Estuarine Coastal and Shelf Science*, 53, 849–864.
- Yakushev, E.V., Kuznetsov, I.S., Podymov, O.I., Burchard, H., Neumann, T., Pollehne, F. 2011. Modeling the influence of oxygenated inflows on the biogeochemical structure of the Gotland Sea, central Baltic Sea: Changes in the distribution of manganese. *Computers & Geosciences*, 37, 398–409.
- Yletyinen, J., Bodin, Ö., Nordström, M., Weigel, B., Bonsdorff, E., Blenckner, T. 2016. Regime shifts in marine communities: a complex systems perspective on food web dynamics. *Proceedings of the Royal Society B*. 283, 20152569.

## 5 List of appendices

**Appendix I:** Impact of increased eutrophication on production of forage fish in the 20th century (P2) (Eero, M., Andersson, H.C., Almroth-Rosell, E., MacKenzie, B.R. 2016. Has eutrophication promoted forage fish production in the Baltic Sea? *Ambio*, DOI 10.1007/s13280-016-0788-3).

**Appendix II:** Current status of non-indigenous species (NIS) in the Baltic Sea (P6) (Ojaveer, H., Olenin, S., Narščiū, A., Florin, A-B., Ezhova, E., Gollasch, S., Jensen, K.R., Lehtiniemi, M., Minchin, D., Normant-Saremba, M. and Strāke, S. Dynamics of biological invasions and pathways over time: a case study of a temperate coastal sea.)

**Appendix III:** Relationships between Baltic Sea inflows and physical and biochemical parameters (P12) (Hordoir, R., Axell, L., Löptien, U., Dietze, H., Kuznetsov, I., 2015: Influence of sea level rise on the dynamics of salt inflows in the Baltic Sea. *J. Geophys. Res. Oceans*, 120, doi:10.1002/2014JC010642)

**Appendix IV:** Relationships between Baltic Sea inflows and physical and biochemical parameters (P12) (Eilola, K., Almroth-Rosell, E., Meier, H.E.M., 2014: Impact of saltwater inflows on phosphorus cycling and eutrophication in the Baltic Sea: a 3D model study. *Tellus A* 2014, 66, 23985, <http://dx.doi.org/10.3402/tellusa.v66.23985>)

**Appendix V:** Relationships between Baltic Sea inflows and physical and biochemical parameters (P12) (Almroth-Rosell, E., Eilola, K., Kuznetsov, I., Hall, P.O.J., and Meier, H.E.M., 2015: A new approach to model oxygen dependent benthic phosphate fluxes in the Baltic Sea. *J. Marine Syst.*, 144, 127-141)

## APPENDIX I

REPORT

# Has eutrophication promoted forage fish production in the Baltic Sea?

Margit Eero, Helén C. Andersson, Elin Almroth-Rosell,  
Brian R. MacKenzie

Received: 21 December 2015 / Revised: 26 March 2016 / Accepted: 26 April 2016

**Abstract** Reducing anthropogenic nutrient inputs is a major policy goal for restoring good environmental status of coastal marine ecosystems. However, it is unclear to what extent reducing nutrients would also lower fish production and fisheries yields. Empirical examples of changes in nutrient loads and concurrent fish production can provide useful insights to this question. In this paper, we investigate to what extent a multi-fold increase in nutrient loads from the 1950s to 1980s enhanced forage fish production in the Baltic Sea. We use monitoring data on fish stock dynamics covering the period of the nutrient increase, combined with nutrient concentrations from a 3-dimensional coupled physical-biogeochemical ocean model. The results suggest that nutrient enrichment enhanced the biomass level of forage fish by up to 50 % in some years and areas due to increased body weight of fish. However, the trends in fish biomasses were generally decoupled from changes in nutrient concentrations.

**Keywords** Nutrients · Fish production · Recruitment · Body weight

## INTRODUCTION

Anthropogenic nutrient enrichment and resulting eutrophication is considered as one of the major human perturbations to marine ecosystems worldwide (e.g. Carpenter et al. 1998; Smith et al. 1999). Eutrophication is generally associated with negative impacts on the environment, such as toxic algal blooms, degradation of habitats, oxygen

deficiency and fish kills (e.g. Kemp et al. 2005; Anderson et al. 2008; Díaz and Rosenberg 2008). Consequently, minimizing human-induced eutrophication is necessary in order to achieve good environmental status of marine ecosystems. The historical, non-impacted status is often used as a basis for defining targets for nutrient reductions (e.g. HELCOM 2007). In this context, it is relevant to consider whether lowering nutrient concentrations to historical in some cases oligotrophic levels would involve tradeoffs in terms of potentially reduced fish production and subsequent fisheries yields.

The main undoubted effect of nutrient enrichment is elevated levels of primary production (e.g. Kerr and Ryder 1992). Regarding the effect of nutrients on secondary production, the views and evidences are diverse. Up to a certain level of nutrients, positive effects on fish production can be expected following the principles of an agricultural model, where the amount of production is determined by the food available (Nixon and Buckley 2002). However, the cascading effects of changes in nutrients and primary productivity on fish biomasses are often not apparent in empirical data or are difficult to demonstrate (Micheli 1999). However, several studies comparing nutrient levels or primary production with fish production or fisheries yields suggest that such relation may exist (e.g. Ware and Thomson 2005; Chassot et al. 2007, 2010).

The Baltic Sea offers a unique opportunity for such investigations due to long time series of observational data on fish production that span over a period of substantial increase in nutrient inputs. In the Baltic Sea, eutrophication first became an issue after World War II, when intensified agriculture with high fertilizer usage, lack of proper wastewater treatment and atmospheric deposition caused a dramatic nutrient-load increase over a few decades from the 1950s to 1980s (Jansson and Dahlberg 1999; Elmgren

**Electronic supplementary material** The online version of this article (doi:10.1007/s13280-016-0788-3) contains supplementary material, which is available to authorized users.



2001). Catches of forage fish, i.e. sprat (*Sprattus sprattus*) and herring (*Clupea harengus*), increased simultaneously from about 100 kt in the first half of the 1950s to above 500 kt in the mid-1980s, which could be considered as an effect of increased nutrient inputs (e.g. Österblom et al. 2007). However, fisheries landings can be influenced by various other mechanisms besides resource availability (Mcowen et al. 2015). A recent reconstruction of sprat dynamics, in fact, revealed a substantial decline in sprat biomass from the late 1960s to 1980s (Eero 2012), in contrast to increasing nutrient concentrations (Fig. 1). Dedicated analyses of individual components of fish production are therefore needed in order to elucidate the potential effects of increased nutrient availability.

In this paper, we assemble observational evidence for changes in recruitment (i.e. production of offspring) and individual growth of major forage fish species in the Baltic Sea, i.e. sprat and herring in the period from the 1950s to 1980s. We combine this information with nutrient concentrations from a 3-dimensional coupled physical-bio-geochemical ocean model and investigate whether positive effects of nutrient enhancement on fish production potentially occurred. The present study provides useful insights to whether reduced fish production can be expected if historical trophic status of the sea is restored, and can contribute to defining good environmental status in a wider ecosystem context.

## MATERIALS AND METHODS

### Data sources

Fish biomasses are determined by a combination of recruitment, individual growth and mortality. Nutrients are expected to impact on adult fish biomass mainly via recruitment and growth, while biomasses of forage fish in the Baltic Sea are additionally heavily influenced by mortality due to fishing and predation by cod (Köster et al. 2003). In order to minimize the effect of mortality interfering with biomass dynamics, we investigated the potential effect of nutrient increase separately on recruitment and growth. The analyses used biomass and recruitment estimates of sprat that were available back to the 1950s (Eero 2012), separately for three sub-regions, i.e. (i) Western Baltic and Bornholm Basin, (ii) Gdansk and Gotland Basins and (iii) northern (N) Baltic Proper (Fig. 2). The borders for the sub-regions were defined based on the Subdivisions used in ICES, and are further referred to as southwest (SW), southeast (SE) and northern (N) Baltic Proper, respectively. For herring, estimates of population dynamics covering the period of nutrient increase from the 1950s to 1980s were available only for the northern Baltic Proper (Ojaveer 2003). Growth was represented by mean body weight of fish with observations originating roughly from the same sub-regions as the biomass and recruitment

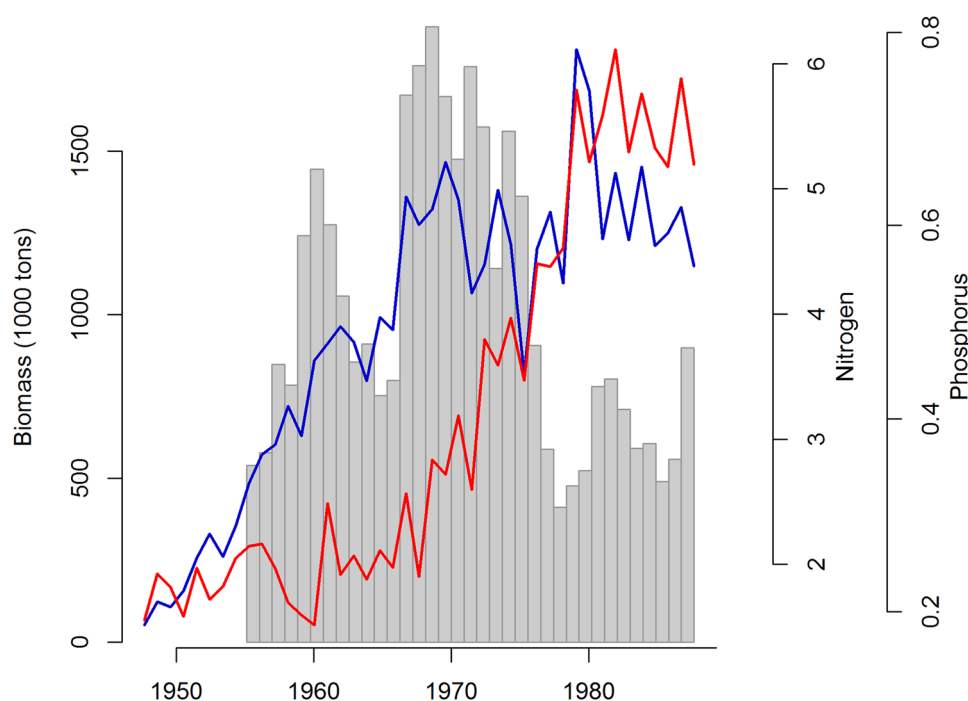


**Fig. 1** Development of winter nitrogen (blue line) and phosphorus (red line) concentrations ( $\text{mmol m}^{-3}$ ) in the Baltic Sea (average of sub-areas, based on results from this study) in comparison with trends in sprat biomass (bars) (Eero 2012)

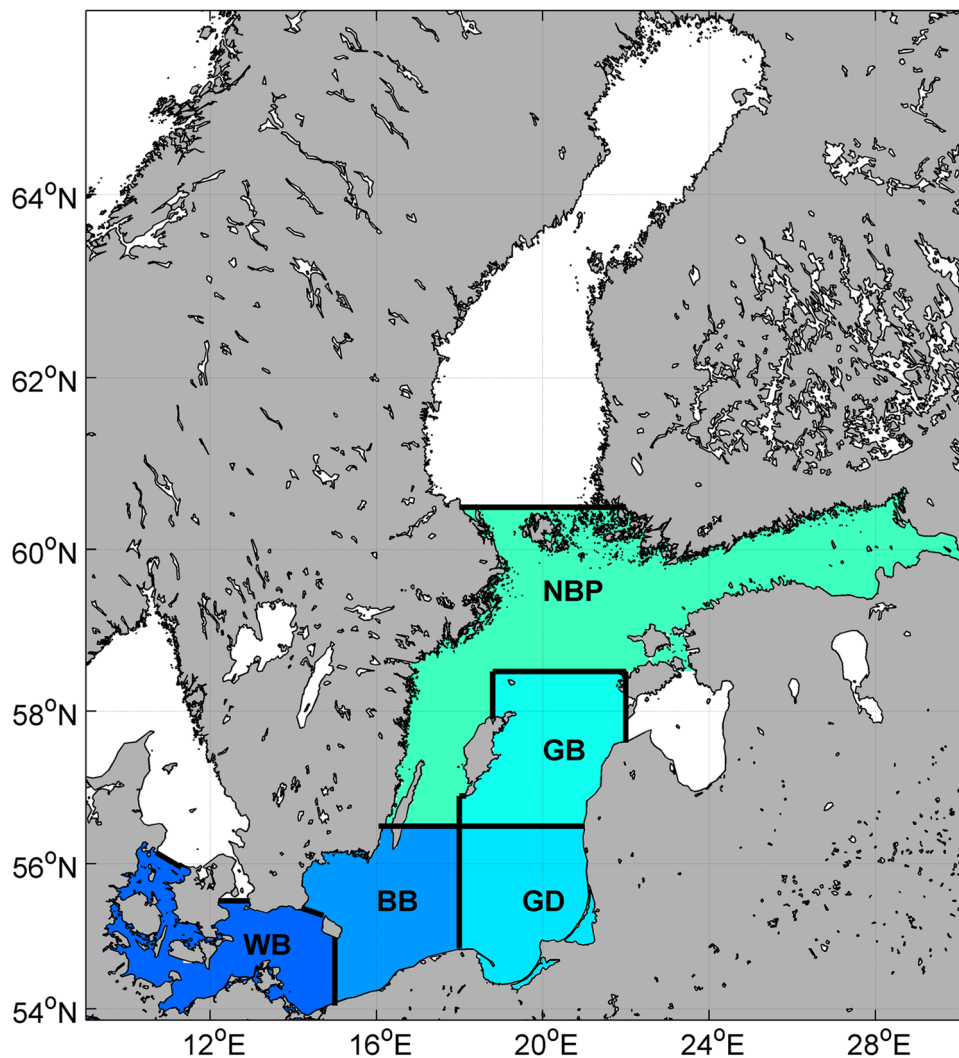


**Fig. 2** Map of the Baltic Sea showing the sub-regions referred to in the paper: *WB* Western Baltic; *BB* Bornholm Basin; *GD* Gdansk Deep; *GB* Gotland Basin; and *NBP* Northern Baltic Proper

estimates. The temporal and spatial coverage of the data used and data sources are provided in Table S1.

Recruitment and mean weight of sprat and herring in the Baltic Sea are influenced by a number of environmental and ecological factors, in addition to the potential effect of nutrients. Environmental variables used in the analyses (Table S1) included sea surface temperature (SST) and average temperature and salinity in the 0–50 m water layer. Additionally, the Baltic Sea environmental index (BSE) was used, which consists of the Arctic oscillation index, the salinity between 120 and 200 m in the Gotland Sea, the integrated river runoff into the Baltic Sea and the relative vorticity of geostrophic wind over the Baltic Sea area (Dippner et al. 2012). Average winter values (December–February) of nitrogen (Nc) and phosphorus (Pc) concentrations in the surface layers (0–9 m) at different sub-areas (Fig. S1) were extracted from the Swedish Coastal and

Ocean Biogeochemical model coupled to the Rossby Centre Ocean circulation model (RCO-SCOB). The model system is described in Eilola et al. (2009) and Meier et al. (2003) and has been used in various ocean-climate and process studies. A brief description of the model is provided in the electronic supplementary material.

#### Analyses of changes in mean body weight of fish

Annual mean weight ( $W$ ) of fish, averaged over specific age classes (Table S1), was used to represent inter-annual changes in body weight. This is following similar approach as used by Casini et al. (2010), as the trends in mean weights of different age-groups of a species were similar. Previous studies focusing on recent decades have related the weight of sprat and herring in the Baltic Sea to temperature, salinity and sprat abundance via intra-specific

competition (Cardinale et al. 2002; Möllmann et al. 2005; Casini et al. 2010). Based on this knowledge, at first step, region-specific temperature and salinity at 0–50 m depth in spring–summer and sprat abundance were included as explanatory variables for mean weight of both sprat and herring in all sub-areas, in addition to Nc and Pc. Analyses of temporal changes in mean weight were conducted using multiple linear regressions that have a generic form:

$$W = a_0 + a_1 * \text{Var1} + a_2 * \text{Var2} + \varepsilon, \quad (1)$$

where  $a_0$ ,  $a_1$  and  $a_2$  are model parameters and Var1 and Var2 are explanatory variables. The number of elements in specific models depends on the number of explanatory variables (*Var*) included. Non-significant variables were removed from final models, except for Nc and Pc that were kept in order to demonstrate their level of significance.

### Recruitment analyses

Recruitment of forage fish in the Baltic Sea, especially sprat, shows high inter-annual variability. Earlier studies covering the period from the 1970s onwards have identified a number of processes and variables influencing sprat recruitment, such as climate variability, transport of larvae, food availability and predation on early life stages (Voss et al. 2012 and references therein). Also, the size of the parent stock is traditionally considered to affect the amount of offspring. Among the variables investigated, sprat recruitment in a Baltic wide scale has been found to be most correlated with SST in summer that affects the recruitment possibly via impacting on feeding and growth of early life stages (e.g. Margonski et al. 2010). SST has also been found to influence herring recruitment in the central Baltic Sea (Margonski et al. 2010). In a more coastal environment, such as the Gulf of Riga, herring recruitment has been related to the Baltic Sea index (BSI), which is the difference of normalized sea level pressures between Oslo, Norway and Szczecin, Poland (Lehmann et al. 2002). Based on this knowledge, region-specific SST in summer (August), Baltic Sea environmental index (BSE) and spawning stock biomass (SSB) were included as explanatory variables in recruitment (*R*) models, both for sprat and herring. We used the more recently developed climate index BSE that shows a better performance than other climate indices such as BSI (Dippner et al. 2012). Additionally, Nc and Pc were included in recruitment models to explore their significance in explaining recruitment fluctuations. A standard stock-recruitment model (Ricker 1954) was applied, incorporating environmental variables. The model has a generic form:

$$R = a * \text{SSB} * \exp(b * \text{SSB} + c * \text{env}), \quad (2)$$

where  $a$ ,  $b$  and  $c$  are model parameters, and *env* represents an environmental variable. The number of elements in specific models depends on the number of environmental variables (*env*) included. Similarly to the analyses of mean weight, non-significant variables were removed from final models, except for Nc and Pc that were kept in order to demonstrate their significance levels.

### Quantifying the contribution of nutrient increase in the 1950s–1980s to sprat biomass

In a next step, we calculated what the biomass of sprat in the Baltic Sea in the period from the 1950s to 1990s would have been if the observed nutrient increase would not have taken place, using the results from the mean weight and recruitment analyses described above. To eliminate the effect of nutrient increase in the 1950s–1980s, the nutrient concentrations in this period were kept constant at the level estimated for the beginning of the analysed time series. These adjusted nutrient concentrations were then entered in the regression models for mean weight (described above) to derive the adjusted fitted values for mean weight ( $W_{\text{fitted\_adj}}$ ). The ratio between  $W_{\text{fitted\_adj}}$  and the fitted weights from the original model using the realized nutrient levels ( $W_{\text{fitted}}$ ) was used as a factor to adjust the observed mean weights ( $W_{\text{obs}}$ ):

$$W_{\text{adj}} = W_{\text{obs}} * \frac{W_{\text{fitted\_adj}}}{W_{\text{fitted}}}. \quad (3)$$

Changes in mean weight impact on biomass in two ways, i.e. (i) directly, as a larger body weight of individual fish results in a higher biomass, and (ii) indirectly through recruitment, given that a larger spawner biomass produces a higher recruitment. To account for the indirect effects of changes in mean weight on recruitment, the stock-recruitment models (described above) were fitted again using the spawner biomass values adjusted for  $W_{\text{adj}}$  ( $\text{SSB}_{\text{adj}}$ ). The ratio between the fitted recruitment ( $R_{\text{fitted\_adj}}$ ) from the model using  $\text{SSB}_{\text{adj}}$  and the recruitment from the model with observed SSB ( $R_{\text{fitted}}$ ) was used as a factor to adjust the observed recruitment values ( $R_{\text{obs}}$ ):

$$R_{\text{adj}} = R_{\text{obs}} * \frac{R_{\text{fitted\_adj}}}{R_{\text{fitted}}}. \quad (4)$$

These analyses did not account for direct impacts of nutrient increase on recruitment as nutrients were not found to explain significant amounts of variability in recruitment dynamics in the recruitment analyses described above (see “Results” section).

Finally, simulations of sprat stock development from the 1950s to 1990s were performed using the adjusted mean

weight ( $W_{\text{adj}}$ ) and recruitment values ( $R_{\text{adj}}$ ) corresponding to constant nutrient concentrations at the level of the 1950s. The simulations used observed stock numbers in 1956 as a starting point and applied fishing and natural mortalities from the original stock assessments for the three sub-regions, i.e. SW, SE and N Baltic Proper (Eero 2012). The stock numbers were projected forward in time using the standard stock numbers at age equation (e.g. Haddon 2001).

## RESULTS

### Nutrient concentrations and mean body weight of sprat and herring

The nutrient levels estimated from the RCO-SCOB1 model show a fivefold increase in nitrogen concentration (Nc) from the 1950 to early 1970s, after which concentrations fluctuated without a trend. The concentration of phosphorus (Pc) was relatively stable from the 1950s to 1970s, but increased three to four times from the beginning of the 1970s to the first half of the 1980s when it levelled off (Fig. 1). The increase is visible in all areas of the Baltic Sea, although the absolute levels vary by sub-regions (Figs. S1, S2).

The mean body weight of sprat (average of ages 3–6) in SW and SE Baltic Sea was approximately 10–15 % higher in the 1970s–1980s compared to the early 1950s (Fig. 3a, b). A more pronounced increase in mean weight was recorded in the northern Baltic Proper, where an average sprat was up to 1.7 times heavier in the mid-1980s compared to the early 1960s (Fig. 3c). A similar increase in mean weight (average of ages 2 and 4) was recorded for herring in the northern Baltic, where the data extending back to 1948 show stable mean weights until the mid-1960s and an increase to approximately 1.5 times higher weights in the 1970s (Fig. 3d). The positive trends in both sprat and herring body weight in the 1970s–1980s coincided with the pronounced increase in Pc. Accordingly, Pc was found to explain significant amount of variability in mean weight of both sprat and herring in all sub-areas (Table 1). Nc was significant only for herring in the northern Baltic Sea. Changes in sprat weight in SE and N Baltic were additionally found to be correlated with temperature and sprat abundance, respectively (Table 1).

### Nutrient concentrations and recruitment of sprat and herring

Sprat recruitment models including SSB and SST as explanatory variables explained significant amounts of recruitment variability in all three sub-regions in the Baltic

Proper. In the northernmost area, including additionally BSE as an explanatory variable significantly improved the explained variability in recruitment (Table 2). For herring in the northern Baltic, SST was not found to be significant and the final model therefore only included SSB and BSE as explanatory variables. Nc and Pc did not appear significant in any of the recruitment models. The effect of nutrients on recruitment was tested both on longer (1957–2010) and shorter time series until 1987 (results not shown), with similar results. Indirectly, the nutrient increase was found to have affected recruitment via mean weight of individual fish (see above) that enhanced the biomass, which in turn influenced recruitment.

The fitted recruitment models were able to describe sprat recruitment dynamics relatively well in SW and SE Baltic Proper (Fig. 4a, b). In the north, the magnitude of variation between year-classes and single events of outstanding year-classes were often not well captured by the recruitment model that generally underestimated recruitment in these years (Fig. 4c). These strong year-classes occurred mainly in the beginning of the time series and are therefore unlikely resulting from increased nutrients but probably are related to some other unaccounted processes. For herring, major long-term variations in recruitment were captured by SSB and BSE (Fig. 4d). The residuals of the recruitment models did not reveal significant trends ( $p < 0.1$ ) for any of the areas or species, besides sprat in the northern Baltic, where recruitment was underestimated in the beginning of the time series in the 1960s, resulting in a significant trend from positive to negative residuals (Fig. S3).

### Impact of nutrient increase on sprat biomass

The increase in nutrients from the 1950s to 1980s coincided with increased body weight of both sprat and herring. Changes in body weight of individual fish modify the biomass directly. Additionally, given that a larger SSB produces a higher recruitment, the increase in mean body weight promotes the stock further via enhanced recruitment. Both of these processes were taken into account when simulating sprat biomass dynamics under stable nutrient concentrations from the 1950s. The simulated biomass dynamics in terms of major fluctuations in stock size were similar to the estimates from original stock assessment (Fig. 5a–c). However, the proportional difference between the two time series increased from the 1950s to 1980s and reached up to 50 % (in the 1980s) higher observed sprat biomass in northern Baltic Sea compared to the simulated scenario with no increase in nutrients (Fig. 5f). The relative effect of nutrient increase on biomass was lower in SW and SE, up to 30 and 40 %, respectively

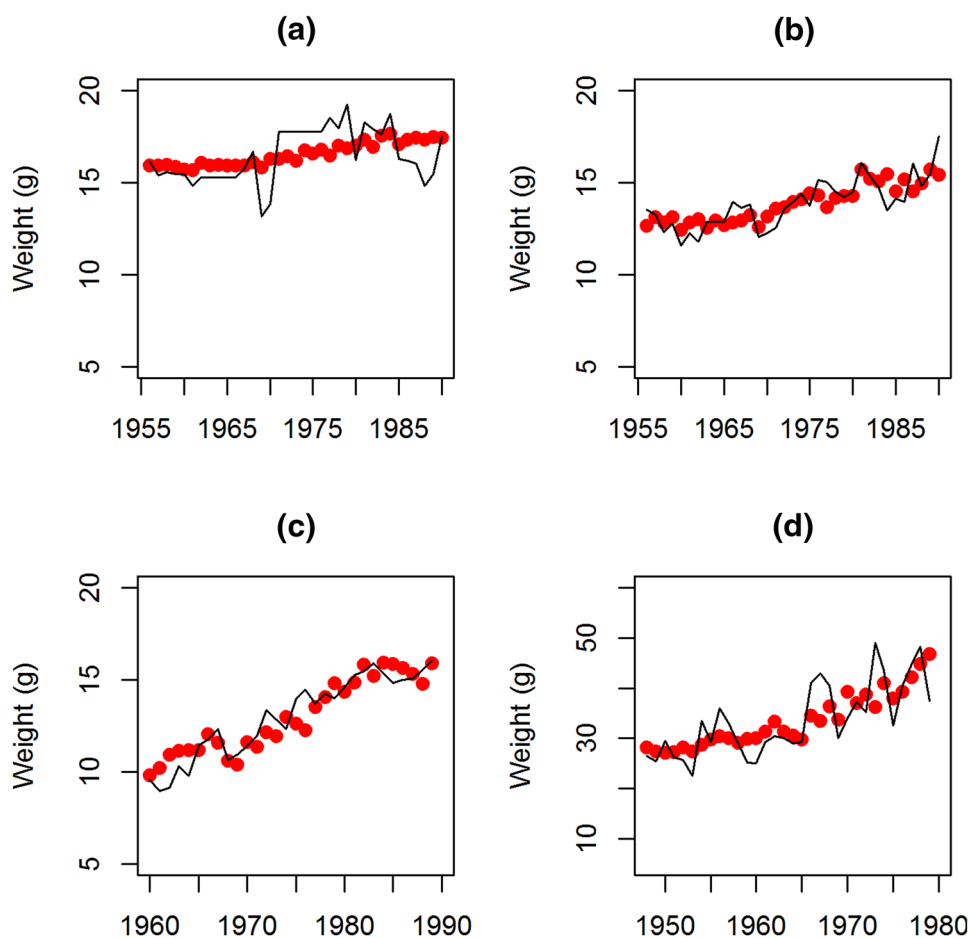


**Fig. 3** Mean weight of sprat (a–c) and herring (d) predicted from regression models (red dots) compared to the observed values (lines) in southwestern (a), southeastern (b) and northern (c, d) areas in the Baltic Proper

**Table 1** The variables significantly ( $*p < 0.05$ ) correlated with mean weight of sprat and herring in southwestern (SW), southeastern (SE) and northern (N) areas of the Baltic Proper in the period from the 1950s to 1990s. The level of significance ( $p$  value) of nitrogen (Nc) and phosphorus (Pc) concentrations is presented for all regression models

Species	Area	Years	Variables	$p$ value
Sprat	SW	1953–1990	Nc	>0.1
			Pc	<0.01*
Sprat	SE	1954–1990	Nc	>0.1
			Pc	<0.01*
			Temperature	0.093
Sprat	N	1960–1989	Sprat abundance	<0.05*
			Nc	>0.1
			Pc	<0.01*
Herring	N	1948–1979	Nc	<0.05*
			Pc	<0.01*

(Fig. 5d, e). In a scale of the entire Baltic Sea, our simulations of sprat dynamics applying constant nutrient concentrations resulted in up to 40 % lower biomass (in the 1980s) compared to the observed level.

## DISCUSSION

Marine fish species in the Baltic Sea are living at conditions close to their tolerance boundaries and their

**Table 2** The variables explaining significant ( $*p < 0.05$ ) amount of variability in sprat and herring recruitment in southwestern (SW), southeastern (SE) and northern (N) areas of the Baltic Proper (spawning stock biomass (SSB), seas surface temperature (SST), Baltic Sea environmental index (BSE)). The level of significance ( $p$  value) of nitrogen (Nc) and phosphorus (Pc) concentrations is presented for all recruitment models

Species	Area	Years	Variables	$P$ value
Sprat	SW	1957–2010	SSB, SST	<0.01*
		1957–2010	Nc	>0.1
		1957–2010	Pc	>0.1
Sprat	SE	1957–2010	SSB, SST	<0.01*
		1957–2010	Nc	>0.1
		1957–2010	Pc	>0.1
Sprat	N	1957–2010	SSB	0.041*
		1957–2010	SST	<0.01*
		1957–2010	BSE	0.019*
		1957–2010	Nc	>0.1
		1957–2010	Pc	>0.1
Herring	N	1949–1998	SSB, BSE	<0.01*
		1949–1998	Nc	>0.1
		1949–1998	Pc	>0.1

productivity is influenced by a number of hydrographic and ecosystem drivers (e.g. MacKenzie et al. 2007). Separating out the cause and effect may be possible under controlled experiments, for example in lakes, but is generally extremely difficult in open sea ecosystems. Therefore, large enough contrast in time series is essential to possibly be able to identify an ecosystem response to a change in driver, which would not be detectable at small-scale variability. For this reason, we focus this study on the years from the 1950s to 1980s when the most pronounced increase in nutrient concentrations took place, expecting that if nutrient enrichment has enhanced fish production in the Baltic Sea, this would likely be best detectable in this period. After that, nutrient concentrations stabilized (Fig. 1), while the hydrographic status of the Baltic Sea changed due to lack of frequent major inflows since the late 1980s, which in combination with high nutrient concentrations led to increased hypoxic areas (Meier 2007; Conley et al. 2009). Thus, from this period onwards the negative effects of high nutrient concentrations likely dominate. This is another reason why we focus on the period from the 1950s to 1980s, as we are interested in elucidating whether positive effects of nutrient increase on forage fish production potentially occurred.

There is strong evidence that a massive increase in anthropogenic nutrient load to the Baltic Sea has led to increased spread of hypoxia, decreased water transparency and increased summer cyanobacteria blooms (Andersen et al. 2015 and references therein). The biological effects associated with the onset of increased nutrient discharges are also well documented for coastal zone (Cederwall and

Elmgren 1990 and references therein). However, it has been surprisingly difficult to convincingly demonstrate the biological changes, for example in phytoplankton and zooplankton biomasses, resulting from increased nutrient availability in the open Baltic Proper, in the period from the 1950s to 1980s (see Elmgren 1989; Cederwall and Elmgren 1990 and references therein for a review). This is because few observational series exist that have used identical methods with a sufficient sampling intensity. A few studies have demonstrated an increase in primary production resulting from eutrophication, though the dataserries often started only from the 1970s (Kononen and Niemi 1984; Wulff et al. 1986). Polish data show an increase in zooplankton biomass from the 1950s to 1970s (Cederwall and Elmgren 1990). However, several shorter zooplankton series from other parts of the Baltic Sea have failed to show significant trends, and a reconstruction of mesozooplankton dynamics in different basins of the open Baltic Proper from the 1960s onwards did not reveal increasing trends in zooplankton biomasses until the 1980s (Möllmann et al. 2000). This is probably because zooplankton biomass is greatly influenced by other factors, e.g. variations in water temperature and salinity (Möllmann et al. 2000). A clearly demonstrated biological effect of the increased nutrients was the 3- to 5-fold increase in macrobenthic biomass between 1920/1923 and 1976/1977 in shallower waters not impacted by anoxia (Cederwall and Elmgren 1980).

We recognize that nutrients are not directly influencing secondary production but via food web interactions at lower trophic levels (Sommer et al. 2002). Thus, ideally, the

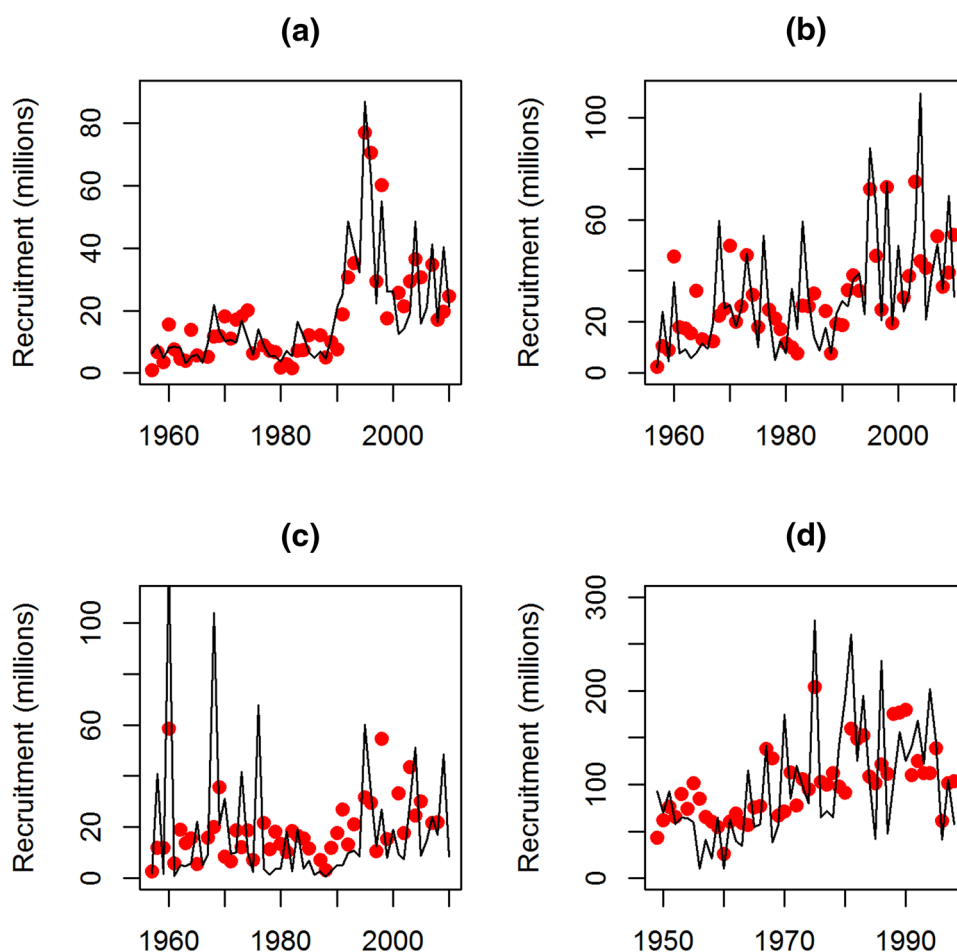


**Fig. 4** Recruitment of sprat (a–c) and herring (d) predicted from stock-recruitment models (*red dots*) compared to the estimates from stock assessment (*lines*) in southwestern (a), southeastern (b) and northern (c, d) areas in the Baltic Proper

investigations of how nutrients have affected fish production should follow the signals of nutrient increase through the entire food web. Due to lack of consistent time series on lower trophic levels covering the period of major nutrient increase, we have chosen an alternative approach in this study. In our approach, we took into account the drivers that have been shown in the literature to have most explanatory power in describing variations in mean weight and recruitment of sprat and herring, and explored whether the remaining unexplained variability could be ascribed to a process with a strong positive trend over time, possibly associated with the observed increase in nutrient concentrations. We evaluated the potential effects of nutrient increase separately on recruitment and mean body weight of fish, which, to our knowledge, has not been done earlier for the open Baltic Sea. Furthermore, in several earlier analyses addressing eutrophication effect on fish stocks (e.g. Österblom et al. 2007), the perception of fish stock dynamics before the 1970s has largely been based on landings that increased in parallel with intensified

eutrophication (Fig. S4). However, changes in fishing intensity and fishing methods that coincided with the onset of eutrophication in the Baltic Sea make the use of landings data as an indicator for changes in fish production difficult (Hansson et al. 2007).

The effect of nutrient concentrations on fish abundances is likely species specific and the effects mediated by recruitment (Massol et al. 2007). In our analyses, recruitment variations of sprat and herring were not associated with the strong increase in nutrient concentrations. Complex processes and interactions involved in regulating food availability and thereby survival of early life stages, such as temporal mismatch between fish larvae and their prey organisms and/or inter-specific competition for prey (Voss et al. 2012) can have contributed to the lack of direct coupling between nutrient increase and recruitment success. In recent decades, most of the variability in especially sprat recruitment has been explained by climatic variables, such as temperature (e.g. Margonski et al. 2010). Our results suggest that climate variability was a dominating

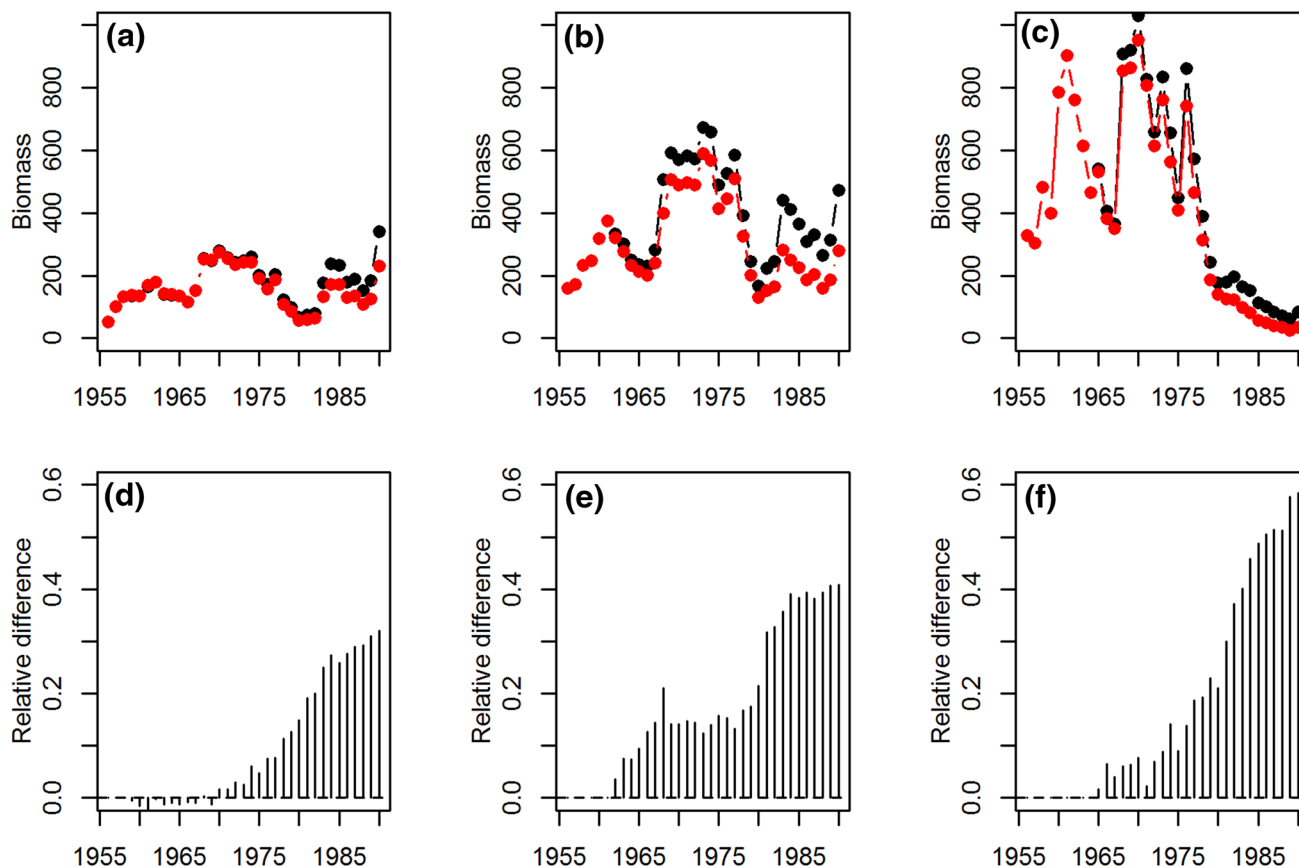


**Fig. 5** Upper panels simulated sprat biomass (red line) applying constant nutrient concentrations from the 1950s compared to the observed biomass (black line) as estimated from stock assessment (Eero 2012). Lower panels proportional difference between the observed and simulated sprat biomass. The results are shown separately for southwestern (a, d), southeastern (b, e) and northern (c, f) areas of the Baltic Proper

factor in regulating major variations in year-class strength also historically. We recognize that a number of other processes affect fish recruitment that were not taken into account in our analyses, for example intra-specific competition for zooplankton. These unaccounted processes likely constitute the unexplained part of recruitment variability in our analyses. The residuals from recruitment models did not indicate that these unaccounted processes could be associated with nutrient increase. Earlier investigations on cod showed that nutrient increase possibly had a minor positive contribution to cod recruitment in the 1980s (Eero et al. 2011), which suggests that nutrient concentrations may impact different parts of the food web differently.

For adult fish, nutrient enrichment likely improved feeding conditions evidenced by the increased mean body weight of both sprat and herring from the 1950s to 1980s. This is in line with increased fat content in sprat in the southeastern Baltic Sea (Elwertowski et al. 1974). The weights of both sprat and herring in the Baltic Sea have undergone large variations over time, including a substantial decline in the 1990s (Casini et al. 2011 and

references therein). The reasons for this are not fully understood, but the processes likely involved include climate variability affecting the abundance of favoured prey items and competition (Casini et al. 2011). Due to complexity of the processes affecting fish growth, it cannot be excluded that the increase in body weight from the 1950s to 1980s coincidentally occurred in parallel with increased nutrients without being a direct effect of it. This would imply that the contribution of nutrient enrichment to mean weight and thereby to biomass of forage fish may be less than suggested by our analyses. For example, competition for food is represented only by sprat abundance in our analyses, while total clupeid abundance may as well be important. However, long time series of herring abundance are not available for all parts of the Baltic Sea and previous studies have identified significant effect of sprat abundance on growth of both sprat and herring (Möllmann et al. 2005; Casini et al. 2010).

The almost twofold increase of mean body weight of fish in some areas led to up to 40 % higher sprat biomass in the entire Baltic Sea in the 1980s than would have been the case at mean weight values corresponding to constant



nutrient levels from the 1950s (Fig. 5). This supports the findings, for example, from Black Sea where a dramatic increase in nutrient loads in the 1970s appeared to benefit the anchovy (Knowler 2007). Furthermore, positive relations between nutrients and fish biomasses have been found in lakes and semi-enclosed seas (Hanson and Leggett 1982; Bernotas 2002). In contrast, a meta-analysis of experimental and field data concluded that the effects of changes in nutrient availability and primary productivity rarely cascaded upward to affect biomasses of marine pelagic consumers (Micheli 1999). Our results also provide support to the latter hypothesis, as the nearly linear increase in mean weight of fish in parallel with the increase in nutrient concentrations did not translate into a similar trend in biomass. In fact, the sprat biomass declined substantially from the late 1960s–1980s, especially in the northern Baltic Sea, reaching record low levels in the 1980s when the nutrient concentrations were highest (Fig. 1). This is because growth is just one of the processes regulating fish biomasses that additionally are modified by recruitment variability and removals due to predation and fishing (Fig. 6). The decline in sprat biomass in the 1970s was mainly due to a combination of unfavourable climatic conditions for recruitment and high predation pressure from cod (Köster et al. 2003).

In summary, although our analyses suggest that the nutrient increase enhanced the level of sprat biomass via mean weight, this effect appears relatively minor compared to the more than fivefold fluctuations in sprat biomass that have occurred over time due to other drivers (Fig. 1). This makes it difficult to predict future trajectories of fish biomasses resulting from nutrient reduction, as these will probably largely depend on combinations of other drivers. However, nutrient concentrations will likely modify the

biomass levels possible to reach under given ecosystem and environmental conditions.

## CONCLUSIONS

The state of the Baltic Sea similar to that before the onset of major industrialization in the 1950s is used as a basis for defining targets for nutrient reductions to restore the good ecological status of the Baltic Sea (HELCOM 2007). Empirical evidence suggests that nutrient increase from the 1950s to 1980s enhanced the level of forage fish biomass (up to 40 % in our analyses) in the Baltic Sea via increased body weight of the fish. Thus, nutrient reduction likely will affect the level of lows and peaks in future biomasses. However, major trends in sprat biomass in past decades have occurred independently of nutrient dynamics, largely driven by climate and top-down control (predation, fishing). This suggests that future biomass trajectories may not follow changes in nutrient dynamics, but will probably largely depend on other prevailing ecosystem and climate conditions. Furthermore, future nutrient levels and availability for biological production are difficult to predict due to long response times to reduced nutrient loads (e.g. Conley et al. 2009), combined effects of changing climate and nutrient loads (Hägg et al. 2014) and the uncertainty of whether the nutrient loading objectives themselves can be achieved by all Baltic countries.

**Acknowledgments** This work was supported by the European Community's Seventh Framework Programme (FP7/2007–2013) under Grant Agreement No. 266445 for the project Vectors of Change in Oceans and Seas Marine Life, Impact on Economic Sectors (VECTORS) and resulted from the BONUS BIO-C3 project supported by BONUS (Art 185), funded jointly by the EU and Innovation Fund Denmark and the Swedish Research Council for Environment, Agricultural Sciences and Spatial Planning (Formas) (219-2013-2041). Support was also received by the Norden Top-level Research Initiative sub-programme "Effect Studies and Adaptation to Climate Change" through the Nordic Centre for Research on Marine Ecosystems and Resources under Climate Change (NorMER).

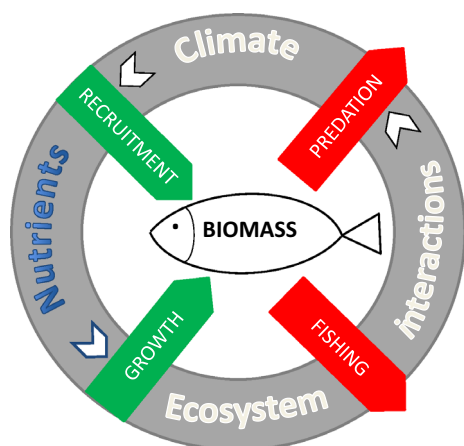


**Fig. 6** Schematic illustration of the main processes impacting on fish biomass (growth, recruitment, predation, fishing) and the pathway through which nutrients increase may have impacted on forage fish biomasses in the Baltic Sea (i.e. via growth), based on the results of this study

## REFERENCES

- Andersen, J.H., J. Carstensen, D.J. Conley, K. Dromph, V. Fleming-Lehtinen, B.G. Gustafsson, A.B. Josefson, A. Norkko, et al. 2015. Long-term temporal and spatial trends in eutrophication status of the Baltic Sea. *Biological Reviews*. doi:10.1111/brv.12221.
- Anderson, D.M., J.M. Burkholder, W.P. Cochlan, P.M. Glibert, C.J. Gobler, C.A. Heil, R.M. Kudela, M.L. Parsons, et al. 2008. Harmful algal blooms and eutrophication: Examining linkages from selected coastal regions of the United States. *Harmful Algae* 8: 39–53.
- Bernotas, E. 2002. Changes in fish biomass under impact of a thermal effluent and eutrophication in Lake Druksiai. *Acta Zoologica Lituanica* 12: 242–253.

- Cardinale, M., M. Casini, and F. Arrhenius. 2002. The influence of biotic and abiotic factors on the growth of sprat (*Sprattus sprattus*) in the Baltic Sea. *Aquatic Living Resources* 15: 273–281.
- Carpenter, S.R., N.F. Caraco, D.L. Correll, R.W. Howarth, A.N. Sharpley, and V.H. Smith. 1998. Nonpoint pollution of surface waters with phosphorus and nitrogen. *Ecological Applications* 8: 559–568.
- Casini, M., V. Bartolino, J.C. Molinero, and G. Kornilovs. 2010. Linking fisheries, trophic interactions and climate: Threshold dynamics drive herring *Clupea harengus* growth in the central Baltic Sea. *Marine Ecology Progress Series* 413: 241–252.
- Casini, M., G. Kornilovs, M. Cardinale, C. Möllmann, W. Grygiel, P. Jonsson, T. Raid, J. Flinkman, and V. Feldman. 2011. Spatial and temporal density dependence regulates the condition of central Baltic Sea clupeids: Compelling evidence using an extensive international acoustic survey. *Population Ecology* 53: 511–523.
- Cederwall, H., and R. Elmgren. 1980. Biomass increase of benthic macrofauna demonstrates eutrophication of the Baltic Sea. *Ophelia* 1: 287–304.
- Cederwall, H., and R. Elmgren. 1990. Biological effects of eutrophication in the Baltic Sea, particularly the coastal zone. *Ambio* 19: 109–112.
- Chassot, E., F. Mélin, O. Le Pape, and D. Gascuel. 2007. Bottom-up control regulates fisheries production at the scale of eco-regions in European seas. *Marine Ecology Progress Series* 343: 45–55.
- Chassot, E., S. Bonhommeau, N.K. Dulvy, F. Mélin, R. Watson, D. Gascuel, and O. Le Pape. 2010. Global marine primary production constrains fisheries catches. *Ecology Letters* 13: 495–505.
- Conley, D.J., S. Björck, E. Bonsdorff, J. Carstensen, G. Destouni, B.G. Gustafsson, S. Hietanen, M. Kortekaas, et al. 2009. Hypoxia-related processes in the Baltic Sea. *Environmental Science and Technology* 43: 3412–3420.
- Díaz, R.J., and R. Rosenberg. 2008. Spreading dead zones and consequences for marine ecosystems. *Science* 321: 926–929.
- Dippner, J.W., G. Kornilovs, and K. Junker. 2012. A multivariate Baltic Sea environmental index. *Ambio* 41: 699–708.
- Eero, M., B.R. MacKenzie, F.W. Köster, and H. Gislason. 2011. Multi-decadal responses of a cod (*Gadus morhua*) population to human-induced trophic changes, exploitation and climate variability. *Ecological Applications* 21: 214–226.
- Eero, M. 2012. Reconstructing the population dynamics of sprat (*Sprattus sprattus balticus*) in the Baltic Sea in the 20th century. *ICES Journal of Marine Science* 69: 1010–1018.
- Eilola, K., H.E.M. Meier, and E. Almroth. 2009. On the dynamics of oxygen, phosphorus and cyanobacteria in the Baltic Sea: A model study. *Journal of Marine Systems* 75: 163–184.
- Elmgren, R. 1989. Man's impact on the ecosystem of the Baltic Sea: Energy flows today and at the turn of the century. *Ambio* 18: 326–331.
- Elmgren, R. 2001. Understanding human impact on the Baltic Sea ecosystem: changing views in recent decades. *Ambio* 30: 222–231.
- Elwertowski, J., M. Giedz, and J. Maciejczyk. 1974. Changes of fat content in Baltic sprat during the past 25 years. *ICES CM Document H*: 14.
- Haddon, M. 2001. *Modelling and quantitative methods in fisheries*. Florida: Chapman & Hall/CRC.
- Hanson, J.M., and W.C. Leggett. 1982. Empirical prediction of fish biomass and yield. *Canadian Journal of Fisheries and Aquatic Sciences* 39: 257–263.
- Hansson, S., O. Hjerne, C. Harvey, J.F. Kitchell, S.P. Cox, and T.E. Essington. 2007. Managing Baltic Sea fisheries under contrasting production and predation regimes: Ecosystem model analyses. *Ambio* 36: 265–271.
- Hägg, H.E., S.W. Lyon, T. Wällstedt, C.-M. Mörth, B. Claremar, and C. Humborg. 2014. Future nutrient load scenarios for the Baltic Sea due to climate and lifestyle changes. *Ambio* 43: 337–351.
- HELCOM. 2007. *Baltic Sea action plan*. Helsinki: HELCOM.
- Jansson, B.O., and K. Dahlberg. 1999. The environmental status of the Baltic Sea in the 1940s, today and in the future. *Ambio* 28: 312–319.
- Kemp, W.M., W.R. Boynton, J.E. Adolf, D.F. Boesch, W.C. Boicourt, G. Brush, J.C. Cornwell, T.R. Fisher, et al. 2005. Eutrophication of Chesapeake Bay: Historical trends and ecological interaction. *Marine Ecology Progress Series* 303: 1–29.
- Kerr, S.R., and R.A. Ryder. 1992. Effects of cultural eutrophication on coastal marine fisheries: A comparative approach. In *Marine coastal eutrophication: The response of marine transitional systems to human impact: Problems and perspectives for restoration: Proceedings of an international conference*, ed. R.A. Vollenweider, R. Marchetti, and R. Viviani, 599–614. Amsterdam: Elsevier Science Publishers B.V.
- Knowler, D. 2007. Estimation of a stock–recruitment relationship for Black Sea anchovy (*Engraulis encrasicolus*) under the influence of nutrient enrichment and the invasive comb-jelly, *Mnemiopsis leidyi*. *Fisheries Research* 84: 275–281.
- Kononen, K., and Å. Niemi. 1984. Long-term variation in the phytoplankton composition at the entrance to the Gulf of Finland. *Ophelia* 3: 101–110.
- Köster, F.W., C. Möllmann, S. Neuenfeldt, M. Vinther, M.A.S. John, J. Tomkiewicz, R. Voss, H.-H. Hinrichsen, et al. 2003. Fish stock development in the central Baltic Sea (1974–1999) in relation to variability in the environment. *ICES Marine Science Symposia* 219: 294–306.
- Lehmann, A., W. Krauss, and H.-H. Hinrichsen. 2002. Effects of remote and local atmospheric forcing on circulation and upwelling in the Baltic Sea. *Tellus A* 54: 299–316.
- MacKenzie, B.R., H. Gislason, C. Möllmann, and F.W. Köster. 2007. Impact of 21st century climate change on the Baltic Sea fish community and fisheries. *Global Change Biology* 13: 1348–1367.
- Margonski, P., S. Hansson, M.T. Tomczak, and R. Grzebielec. 2010. Climate influence on Baltic cod, sprat, and herring stock–recruitment relationships. *Progress in Oceanography* 87: 277–288.
- Massol, F., P. David, D. Gerdeaux, and P. Jarne. 2007. The influence of trophic status and large-scale climatic change on the structure of fish communities in Perialpine lakes. *Journal of Animal Ecology* 76: 538–551.
- Mcowen, C.J., W.W.L. Cheung, R.R. Rykaczewski, R.A. Watson, and L.J. Wood. 2015. Is fisheries production within Large Marine Ecosystems determined by bottom-up or top-down forcing? *Fish and Fisheries* 16: 623–632.
- Meier, H.E.M., R. Döscher, and T. Faxén. 2003. A multiprocessor coupled ice–ocean model for the Baltic Sea: Application to salt inflow. *Journal of Geophysical Research* 108: 3273.
- Meier, H.E.M. 2007. Modeling the pathways and ages of inflowing salt- and freshwater in the Baltic Sea. *Estuarine, Coastal and Shelf Science* 74: 610–627.
- Micheli, F. 1999. Eutrophication, fisheries, and consumer-resource dynamics in marine pelagic ecosystems. *Science* 285: 1396–1399.
- Möllmann, C., G. Kornilovs, M. Fetter, and F.W. Köster. 2005. Climate, zooplankton, and pelagic fish growth in the central Baltic Sea. *ICES Journal of Marine Science* 62: 1270–1280.
- Möllmann, C., G. Kornilovs, and L. Sidrevics. 2000. Long term dynamics of main mesozooplankton species in the central Baltic Sea. *Journal of Plankton Research* 22: 2015–2038.

- Nixon, S.W., and B.A. Buckley. 2002. "A strikingly rich zone"—Nutrient enrichment and secondary production in coastal marine ecosystems. *Estuaries* 25: 782–796.
- Ojaveer, E. 2003. Baltic herring. In *Fishes of Estonia*, ed. E. Ojaveer, E. Pihu, and T. Saat, 58–79. Tallinn: Estonian Academy Publishers (in Estonian).
- Österblom, H., S. Hansson, U. Larsson, O. Hjerne, F. Wulff, R. Elmgren, and C. Folke. 2007. Human-induced trophic cascades and ecological regime shifts in the Baltic Sea. *Ecosystems* 10: 887–889.
- Ricker, W.E. 1954. Stock and recruitment. *Journal of the Fisheries Research Board of Canada* 11: 559–623.
- Smith, V.H., G.D. Tilman, and J.C. Nekola. 1999. Eutrophication: Impacts of excess nutrient inputs on freshwater, marine, and terrestrial ecosystems. *Environmental Pollution* 100: 179–196.
- Sommer, U., H. Stibor, A. Katchakis, F. Sommer, and T. Hansen. 2002. Pelagic food web configurations at different levels of nutrient richness and their implications for the ratio fish production: Primary production. *Hydrobiologia* 484: 11–20.
- Voss, R., M.A. Peck, H.-H. Hinrichsen, C. Clemmesen, H. Baumann, D. Stepputtis, M. Bernreuther, J.O. Schmidt, et al. 2012. Recruitment processes in Baltic sprat—A re-evaluation of GLOBEC Germany hypotheses. *Progress in Oceanography* 107: 61–79.
- Ware, D.M., and R.E. Thomson. 2005. Bottom-up ecosystem trophic dynamics determine fish production in the northeast Pacific. *Science* 308: 1280–1284.
- Wulff, F., G. Aertebjerg, G. Nicolaus, Å. Niemi, P. Ciszewski, S. Sculz, and W. Kaiser. 1986. The changing pelagic ecosystem of the Baltic Sea. *Ophelia* 4: 299–319.
- Address:** National Institute for Aquatic Resources, Technical University of Denmark, Jægersborg Allé 1, 2920 Charlottenlund, Denmark.  
e-mail: mee@aqua.dtu.dk
- Helén C. Andersson** is head of the Oceanographic Research Unit at the Swedish Meteorological and Hydrological Institute (SMHI). Her research interest is within the physical and biogeochemical dynamics of the sea, with special emphasis on water quality and impact of climate variability.  
**Address:** Swedish Meteorological and Hydrological Institute, 601 76 Norrköping, Sweden.  
e-mail: helen.andersson@smhi.se
- Elin Almroth-Rosell** is a researcher at the Swedish Meteorological and Hydrological Institute (SMHI). She is mainly working with biogeochemical modelling in the Baltic Sea and has special interests in the benthic processes.  
**Address:** Swedish Meteorological and Hydrological Institute, 601 76 Norrköping, Sweden.  
e-mail: elin.almroth.rosell@smhi.se
- Brian R. MacKenzie** is a professor of Marine Fish Population Ecology, at the National Institute for Aquatic Resources, Technical University of Denmark (DTU Aqua). His research interests include natural and human impacts (fishing, climate change, eutrophication) on long-term dynamics of fish populations, food webs and ecosystems.  
**Address:** National Institute for Aquatic Resources, Technical University of Denmark, Jægersborg Allé 1, 2920 Charlottenlund, Denmark.  
e-mail: brm@aqua.dtu.dk

## AUTHOR BIOGRAPHIES

**Margit Eero** (✉) is a senior researcher at the Technical University of Denmark, DTU Aqua. Her research interests include understanding natural and human impacts on long-term changes in fish stocks with a special focus on the Baltic Sea.

## **APPENDIX II**

Appendix II was removed because it is under embargo until manuscript is published.  
If there is interest in the data, contact with Henn Ojaveer ([henn.ojaveer@ut.ee](mailto:henn.ojaveer@ut.ee)).









































































## **APPENDIX III**

## RESEARCH ARTICLE

10.1002/2014JC010642

## Influence of sea level rise on the dynamics of salt inflows in the Baltic Sea

Robinson Hordoir<sup>1</sup>, Lars Axell<sup>1</sup>, Ulrike Löptien<sup>2</sup>, Heiner Dietze<sup>2</sup>, and Ivan Kuznetsov<sup>3</sup>

## Key Points:

- Sea level rise increases the salinity of the Baltic Sea
- This increase is related to more frequent and stronger salt inflows
- One notices a decreased mixing and a bigger cross section in the Danish Straits

## Correspondence to:

R. Hordoir,  
robinson.hordoir@smhi.se

## Citation:

Hordoir, R., L. Axell, U. Löptien, H. Dietze, and I. Kuznetsov (2015), Influence of sea level rise on the dynamics of salt inflows in the Baltic Sea, *J. Geophys. Res. Oceans*, 120, doi:10.1002/2014JC010642.

Received 19 DEC 2014

Accepted 11 SEP 2015

Accepted article online 15 SEP 2015

<sup>1</sup>Department of Oceanography Research, SMHI, Norrköping, Sweden, <sup>2</sup>GEOMAR Helmholtz-Zentrum für Ozeanforschung, Kiel, Germany, <sup>3</sup>Institute of Coastal Research, Helmholtz-Zentrum Geesthacht, Geesthacht, Germany

**Abstract** The Baltic Sea is a marginal sea, located in a highly industrialized region in Central Northern Europe. Saltwater inflows from the North Sea and associated ventilation of the deep exert crucial control on the entire Baltic Sea ecosystem. This study explores the impact of anticipated sea level changes on the dynamics of those inflows. We use a numerical oceanic general circulation model covering both the Baltic and the North Sea. The model successfully retraces the essential ventilation dynamics throughout the period 1961–2007. A suite of idealized experiments suggests that rising sea level is associated with intensified ventilation as saltwater inflows become stronger, longer, and more frequent. Expressed quantitatively as a salinity increase in the deep central Baltic Sea, we find that a sea level rise of 1 m triggers a saltening of more than 1 PSU. This substantial increase in ventilation is the consequence of the increasing cross section in the Danish Straits amplified by a reduction of vertical mixing.

## 1. Introduction

The Baltic Sea is a semienclosed basin. River inflows from highly industrialized countries determine its brackish characteristic and render it vulnerable to anthropogenic eutrophication. It is a highly stratified estuary and its lower layers can only receive oxygen by salinity intrusions finding their way through three narrow passages linking the Baltic with the North Sea, the so-called Danish Straits. These three straits are called, from West toward East “Little Belt,” “Great Belt,” and “Öresund,” and have different vertical cross sections (Figure 1). The middle strait (Great Belt) is the broadest and deepest, hosting the largest share of the exchange.

The inflowing water is typically characterized by a relatively high salinity and a high oxygen content. Thus, saltwater inflows from the North Sea are a vital source of oxygen for the Baltic Sea and the whole ecosystem is impacted by their frequency and intensity.

Salt inflows directly influence the salinity structure of the Baltic Sea [Meier, 2007; Meier and Kauker, 2003; Meier et al., 2003; Lass and Matthäus, 1996]. They also influence biological processes such as cod spawning [Stigebrandt et al., 2014] and the ventilation of the deeper layers of the Baltic Sea is crucial to macrobenthic organisms [Gogina and Zettler, 2010]. Previous studies have shown that the frequency of saltwater inflows has decreased during the recent decades, particularly in the period between 1983 and 1993 [Lass and Matthäus, 1996]. Saltwater inflows are also suspected to decrease in a future climate due to an increase of the runoff into the Baltic Sea [Meier et al., 2006]. Hypoxia is nowadays a severe environmental problem for the Baltic Sea, reaching a point where even geoengineering solutions are under discussion [Stigebrandt et al., 2014]. Additionally, the high nutrient content of the Baltic Sea together with increased temperatures suggest that the lower layers are prone to reach a state of hypoxia more often and with a greater extent [Meier et al., 2012].

The impact of sea level rise on the Baltic Sea haline dynamics has, so far, not been investigated, and one challenging question is to determine how the Baltic Sea salt inflow dynamics respond to a significant sea level increase: the aim of this article is to address this issue. Based on a coupled ocean-sea ice model configuration with a fully nonlinear free surface, covering the Baltic Sea and the North Sea, we perform a suite of sensitivity experiments. We compare the dynamics of Baltic Sea salt inflows between a present-day sea level and several levels of sea level increase.

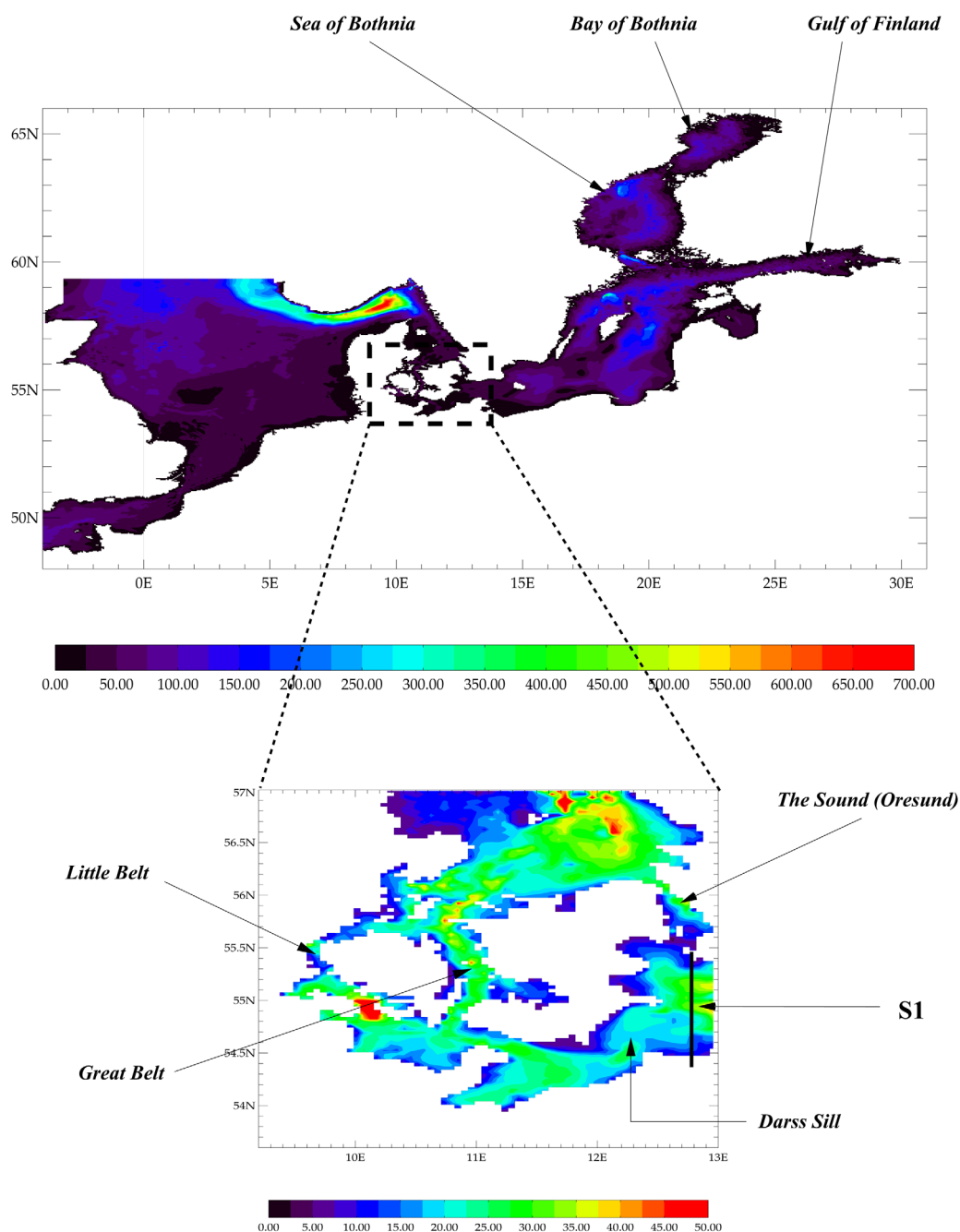


**Figure 1.** Geographical domain and color map of bathymetry (in m) of the NEMO-Nordic configuration, with zoom on the Danish Straits area between Denmark and Sweden, and position of the S1 cross section.

The second section of this article introduces the model setup and includes an evaluation of the haline dynamics. In the third section, we present the results of the sensitivity experiments. In the fourth section, we present a theoretical approach which tackles the problem from a process-orientated perspective. The fifth and final section comprises a final discussion and our conclusions.

## 2. Methodology

### 2.1. NEMO-Nordic: A NEMO-Based Ocean Modeling Configuration for Baltic and North Seas

Our analyses are based on the NEMO-Nordic configuration developed at SMHI (Swedish Meteorological and Hydrological Institute) which has been used in previous studies (under the name BaltiX) [Hordoir et al., 2013;

Godhe *et al.*, 2013]. NEMO-Nordic is a coupled ocean-sea ice model based on the NEMO ocean engine [Madec, 2010]. Its domain includes the entire Baltic Sea basin, and a major part of the North Sea (Figure 1, the critical area of the Danish Straits is also shown in detail). NEMO-Nordic provides sea level predictions in operational mode reaching a higher level of quality than that of the HIROMB system [Funkquist and Kleine, 2007; Axell *et al.*, 2014] used for operational predictions at SMHI, a system that NEMO-Nordic is intended to replace. The domain of NEMO-Nordic is similar to that of HIROMB. With 56 vertical levels, it has a resolution of approximately 2 nautical miles ( $\approx 3700$  m), and a vertical resolution of 3 m close to the surface, decreasing to 22 m at the bottom of the deepest part of the domain (Norwegian trench). NEMO-Nordic has two open boundaries: a meridional one located in the English Channel between Brittany and Cornwall, and a zonal one between Scotland and Norway [Hordoir *et al.*, 2013]. Since we use a resolution of 2 nautical miles, it is sometimes difficult to give each critical section of the Danish Straits its true width. Therefore, we have instead made each critical cross sections of each strait fit its actual measured size. To reach this goal, we have slightly modified either the depth or the width of each critical cross section, so that the surface of each critical cross section fits its actual size. This has been done with the goal to find the best compromise that modifies as little as possible depth or width.

NEMO-Nordic uses a fully nonlinear explicit free surface, based on the approach described by Adcroft and Campin [2004]. Partial steps are used in order to obtain a good consistency between the input bathymetry and that utilized by the model. We use a time-splitting approach that computes a barotropic and a baroclinic mode, as well as the interaction between them.

The barotropic mode is defined at the open boundary conditions using the Oregon State University Tidal Inversion Model [Egbert *et al.*, 1994; Egbert and Erofeeva, 2002] with 11 tidal harmonics defined both for sea level and barotropic tidal velocities. In addition, a simple coarse resolution barotropic storm surge model covering a large area of the Northern Atlantic basin provides wind-driven sea level that is added to the tidal contribution. The Levitus climatology [Levitus and Boyer, 1994] provides temperature and salinity data at the open boundary conditions. Simple radiation conditions are applied to calculate baroclinic velocities at these boundaries.

The surface boundary condition uses a bulk formulation based on Large and Yeager [2004]. The ocean model is coupled to the LIM3 sea ice model [Vancoppenolle *et al.*, 2008]. The sea-ice salinity is set to a constant value of  $10^{-3}$  PSU. A quadratic friction is applied at the bottom, and the drag coefficient is computed for each bottom grid cell based on a classical law-of-the-wall, with a constant bottom roughness of 3 cm.

NEMO-Nordic uses a TVD advection scheme with a modified leapfrog approach that ensures a very high degree of tracer conservation [Leclair and Madec, 2009]. It uses a  $k-\epsilon$  turbulence scheme to parameterize unresolved vertical turbulence [Umlauf and Burchard, 2003]. In addition, in order to obtain a stable long-term stratification for the Baltic Sea, the Galperin parameterization is used [Galperin *et al.*, 1988].

We apply a Laplacian isopycnal diffusion both for momentum and tracers with a diffusion parameter that is constant in time, but varies in space. Isopycnal viscosity is set to  $50 \text{ m}^2 \text{ s}^{-1}$  between the sea surface and a depth of 30 m, and to  $0.001 \text{ m}^2 \text{ s}^{-1}$  below 30 m. An additional strong isopycnal diffusion is used close to the Neva river inflow (Gulf of St. Petersburg) in order to avoid negative salinities. Our model does not necessitate any algorithm to artificially cut off spurious negative salinities.

We set the isopycnal diffusivity to 10% of the value of isopycnal viscosity, which proves to be a good compromise to insure a low viscosity and diffusivity while keeping the model barotropically and baroclinically stable.

However, this approach does not work well close to the bottom where higher diffusivity and viscosity would hamper salt inflows to the deepest layers of the Baltic Sea. Note that this is consistent with results from Dietze *et al.* [2014, Figure 15, bottom] who describe the antagonistic effects of viscosity. To obtain realistic results, we have set very low values for isopycnal diffusion and isopycnal viscosity below the mixed-layer depth. We also use a parameterization of the bottom boundary layer [Beckmann and Döscher, 1997] to ease the propagation of saltwater inflows between the Danish Straits and the deepest layers of the Baltic Sea. Sensitivity experiments showed that using a purely diffusive bottom boundary layer produces the best results to bring saltwater masses to the deepest parts of the Baltic Sea. Using a combination of advective and diffusive methods within the bottom boundary layer parameterization, or purely advective, produces



too much entrainment which defeats the purpose of the parameterization. Lateral boundaries do not create any friction as a free-slip option is used.

The model is driven by atmospheric forcing derived from a downscaled run of an ERA40 reanalysis for the period 1961–2007. The downscaling is based on the regional atmospheric model RCA3 [Samuelsson *et al.*, 2011] which uses the reanalysis data as boundary conditions. This atmospheric model output was used successfully as atmospheric forcing for a number of Baltic Sea models [Dietze *et al.*, 2014; Löptien and Meier, 2011; Löptien *et al.*, 2013].

A runoff database provides the river flow to NEMO-Nordic; it includes inter-annual variability for the Baltic Sea basin and is based on climatological values for the North Sea basin. The salinity of the river runoff is set to a constant value of  $10^{-3}$  PSU, which is the same value used for the sea-ice to avoid any negative salinity.

### 2.1.1. Evaluation of the Haline Dynamics of the Baltic Sea

Figure 2 shows climatological sea surface salinity (SSS hereafter) simulated from 1961 to 2007 by NEMO-Nordic, as well as the observed climatological SSS. The SSS is shown for March and July, which are the saltiest and freshest months of the year, respectively [Eilola and Stigebrandt, 1998; Hordoir and Meier, 2010]. The positions of the iso-salinity lines are in good agreement between the model and the observations, indicating that the model is capable of reproducing the seasonal cycle and the long-term averages in SSS. The isohalines follow the freshwater seasonal cycle, with a deeper penetration of salinity in March in the central Baltic Sea basin (Baltic proper), and a low penetration in July. These salinity changes are consistent with the strong wind-driven release of freshwater during spring, reported in earlier studies [Hordoir and Meier, 2010].

Using the SHARK database (Svensk Havsarkiv, SMHI, and other Swedish Institutes), we compare the haline structures of the simulation with measurements (Figure 3) at three measurement stations BY2 (Arkona), BY5 (Bornholm), and BY15 (Gotland Deep); their positions are indicated in Figure 2.

All of our simulations start with a spurious inflows. This is probably a consequence of the spatially homogeneous (and rather unrealistic) initial conditions of sea surface height. Right after the inflow, a spurious stagnation period with monotonically decreasing salinities succeeds. It is only after 1965 that the intrinsic model dynamics overcome the deficiencies in our (rather unconstrained) initial conditions and that the deep salinity of NEMO-Nordic starts to approach realistic conditions.

NEMO-Nordic reproduces the vertical structure of the Baltic Sea with some bias. Such biases are typical for z-level models. Dense water inflows penetrating the Baltic Sea follow the bottom and are well reproduced at the Arkona (BY2) measurement station.

After the first shelf break between the Arkona (BY2) and Bornholm (BY5) measurement stations, the dense water flow has problems to follow the bottom and drives excessive ventilation of the intermediate layers further up in the water column.

In order to compensate for this behavior, ocean models that include only the Baltic Sea like that of Meier [2007] have modified the bathymetry of the first subbasins in addition to using bottom boundary layer parameterizations [Beckmann and Döscher, 1997] as in the present model.

The slight overventilation of the intermediate layers is responsible for two features that appear at the BY15 measurement station (Gotland Deep), located in the deepest place of the Baltic Sea along the inflow pathway. First, the overall salinity structure at BY15 is well reproduced, but the depth of the halocline is too shallow, located between 40 m and 50 m, whereas it should be at 60 m according to measurements. This also suggests a slight overventilation at the level of the halocline or even above it. Second, the bottom salinity is underestimated, with a negative bias peaking at 1.5 PSU in 2007. The fact that the bias is highest at the end of the simulation is specifically related with the underestimated major saltwater inflow in 2003. It is not related with the length of the simulation. The bias at the end of stagnation period for example, or after the 1993 major salt inflow, is lower.

This means that the model is able to preserve the haline structure of the Baltic Sea over a long time period. The ability of the model to reproduce major saltwater inflows is a key feature indispensable to maintaining realistic salinity in the deeper layers. This ability varies as the 1993 major inflow is, for example, well reproduced in terms of amplitude, whereas the 2003 major inflow is not. In the latter case, previous experience with the RCO model [Meier *et al.*, 2003; Meier and Kauker, 2003] suggests this specific inflow is difficult to

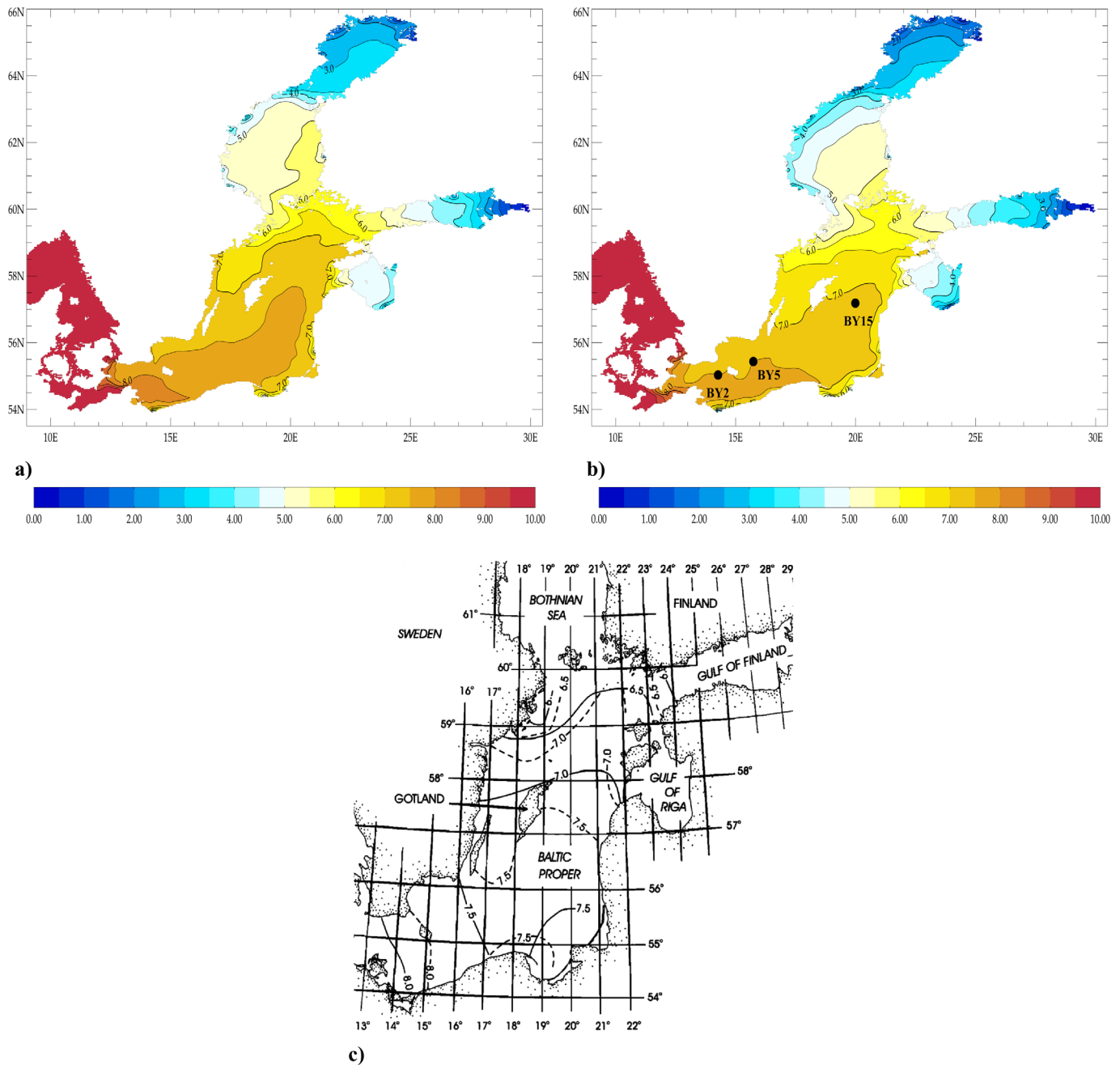


**Figure 2.** NEMO-Nordic simulated climatological sea surface salinities (in PSU) for the Baltic Sea for the months of (a) March and (b) July. (c) Observed climatological sea surface salinities [from Eilola and Stigebrandt, 1998]. Dashed lines, July; solid lines, March.

represent and cannot even be predicted based on the usual patterns in atmospheric circulation in contrast to other inflows [Schimanke *et al.*, 2014].

### 2.2. Sensitivity Experiments

Based on the NEMO-Nordic configuration run presented in section 2.1, we design a set of six experiments called e0, e0.5, e0.75, e1, e1.25, and e1.5. e0 is the reference experiment which corresponds to the standard long-term NEMO-Nordic simulation presented in section 2.1. The experiments e0.5, e0.75, e1, e1.25, and e1.5 differ from e0 only with respect to sea level. In each experiment, the mean sea level is increased by 0.5, 0.75, 1, 1.25, and 1.5 m for the experiments e0.5, e0.75, e1, e1.25, and e1.5, respectively. These values are

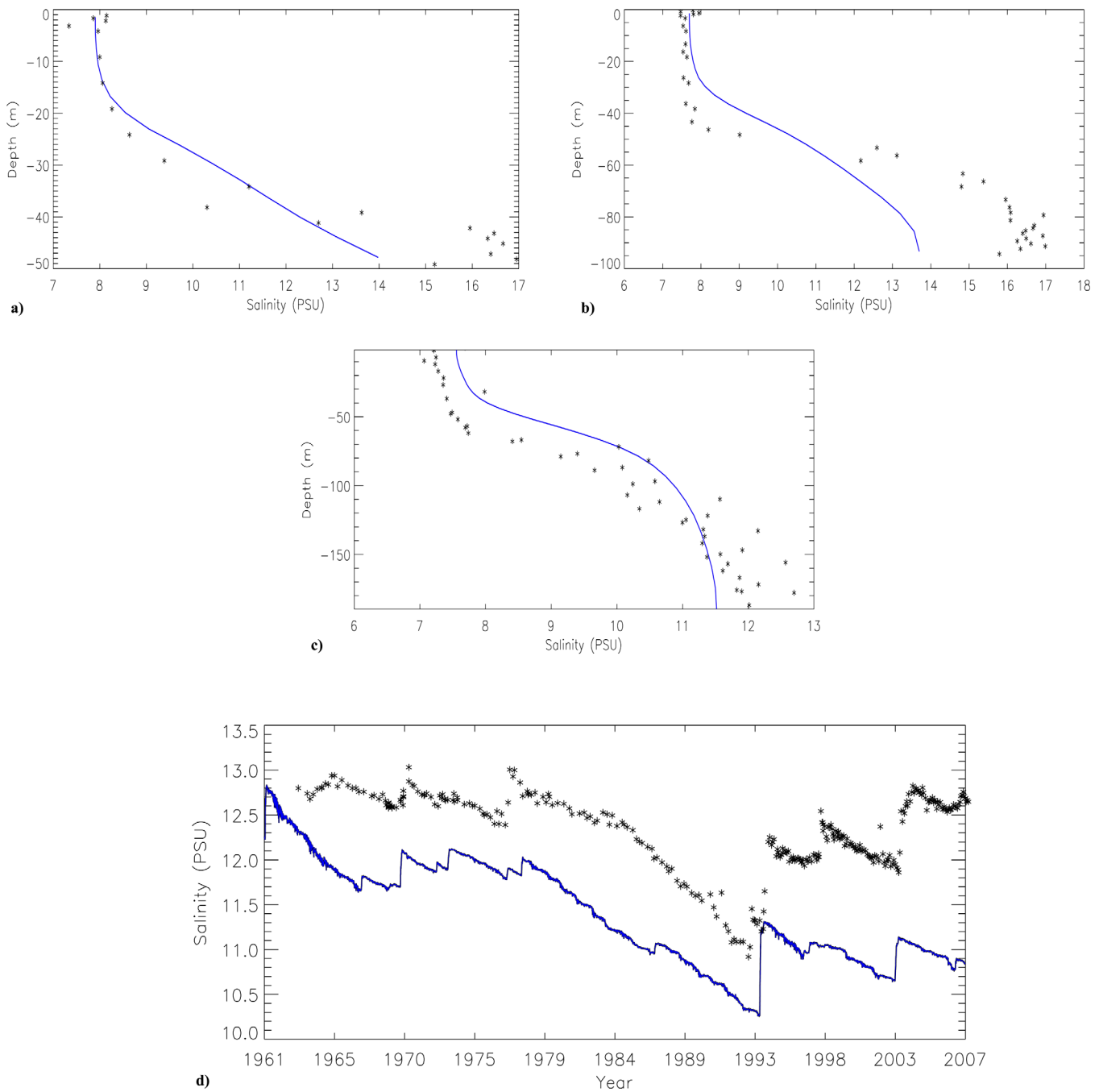


**Figure 3.** Salinity profiles (PSU) for the period 1961–2007 at stations (a) BY2, (b) BY5, and (c) BY15. (d) Deep salinity (PSU) at BY15 for the period 1961–2007.

taken based on the estimates made by *Blank et al.* [2012]. Their estimates suggest that there is a 95% chance that mean global sea level will increase by between 20 cm and 2 m by the end of the 21st century.

Although it remains to be shown how authoritative such forecasts are in general, this seems to be consistent with other studies, e.g., *Pfeffer et al.* [2008] project a sea level rise of 78 cm–2 m based on the kinematics of glacial melt and *IPCC* [2013] project a global sea level increase between 25 cm and 1 m. How these global averages will be modulated by local wind patterns in the Baltic and North Sea is, however, not well constrained yet.

In addition to winds, land uplift may also contribute locally to the rise of sea levels in Baltic and North Sea [Ekman and Mäkinen, 1996]. However, this increase does not affect significantly the region of the Danish Straits which is key to inflow dynamics.

For pragmatic reasons we explore in this study the effects of a sea level rises that are of similar magnitude than anticipated global averages. Specifically, we assume that an increase of 0.5 m would be close to a lower-case scenario, whereas a value of 1.5 m would be close to an upper-case scenario. The elevated sea levels are prescribed in the model by changing the initial and boundary conditions. As for the latter, we add a respective bias to the storm surge model. The sea level rise value is also added to the initial conditions.

### 2.3. Diagnostics

In order to quantify volume and salt exchanges, we estimate the mean daily fluxes at a cross section. It is a meridional cross section located at the entrance of the Baltic Sea, east of Darss Sill (Figure 1) named S1. It captures the entire exchange between the North Sea and the Baltic Sea.

For any cross section  $C_s$ , we define the following diagnostics:

$$F_v(t) = \int_{C_s} \mathbf{u}(\mathbf{x}, t) \cdot d\mathbf{C}_s, \quad (1)$$

where  $F_v(t)$  is the volume flux through the cross section  $C_s$ ,  $\mathbf{u}(\mathbf{x}, t)$  is the velocity vector field at position  $\mathbf{x}$  and at time  $t$ ;  $\mathbf{u}(\mathbf{x}, t)$  is integrated across the cross section  $C_s$  for which  $\mathbf{C}_s$  is the surface vector corresponding to the respective cross section.

To diagnose the haline flux at cross section  $C_s$  we define:

$$F_s(t) = \int_{C_s} s(\mathbf{x}, t) \mathbf{u}(\mathbf{x}, t) \cdot d\mathbf{C}_s, \quad (2)$$

where  $F_s(t)$  is the haline flux at cross section  $C_s$  and  $s(\mathbf{x}, t)$  is the salinity field at position  $\mathbf{x}$  and at time  $t$ .

Matthäus [2006] defines a major saltwater inflow as a flux of salinity higher or equal to 17 PSU across the meridional cross section located at the Darss sill (Figure 1) during five consecutive days in addition to a high stratification condition [Matthäus, 2006].

In the present work, the purpose is not to study the occurrence of major saltwater inflows, but rather to quantify changes in the process or occurrence of salt inflows from a general perspective, meaning that not only major salt inflows are taken into account. We therefore modify the criteria of Matthäus [2006]. In order to describe the entire flow, we have slightly shifted our Baltic Sea cross section from the Darss Sill toward the east. While we use a similar definition for the inflow salinity, we do not require that a salt inflow should last five consecutive days. However, it is still possible to extract the inflows based on these precise criteria from the diagnostics we define (section 3.3).

We define  $s_{inflow}(\mathbf{x}, t)$  as an inflow salinity field which value is:

$$\begin{aligned} s_{inflow}(\mathbf{x}, t) &= s(\mathbf{x}, t) \text{ if } s(\mathbf{x}, t) \geq 17PSU \\ s_{inflow}(\mathbf{x}, t) &= 0 \text{ if } s(\mathbf{x}, t) < 17PSU. \end{aligned} \quad (3)$$

This definition of  $s_{inflow}(\mathbf{x}, t)$  as a field yields the following definitions for the inflowing salt and volume fluxes, respectively:

$$\begin{aligned} F_{s_{inflow}}(t) &= \int_{C_s} s_{inflow}(\mathbf{x}, t) \mathbf{u}(\mathbf{x}, t) \cdot d\mathbf{C}_s \\ F_{v_{inflow}}(t) &= \int_{C_s} \delta(\mathbf{x}, t) \mathbf{u}(\mathbf{x}, t) \cdot d\mathbf{C}_s, \end{aligned} \quad (4)$$

with  $\delta(\mathbf{x}, t)$  defined as:

$$\begin{aligned} \delta(\mathbf{x}, t) &= 1 \text{ if } s_{inflow}(\mathbf{x}, t) \geq 17PSU \\ \delta(\mathbf{x}, t) &= 0 \text{ if } s_{inflow}(\mathbf{x}, t) < 17PSU. \end{aligned} \quad (5)$$

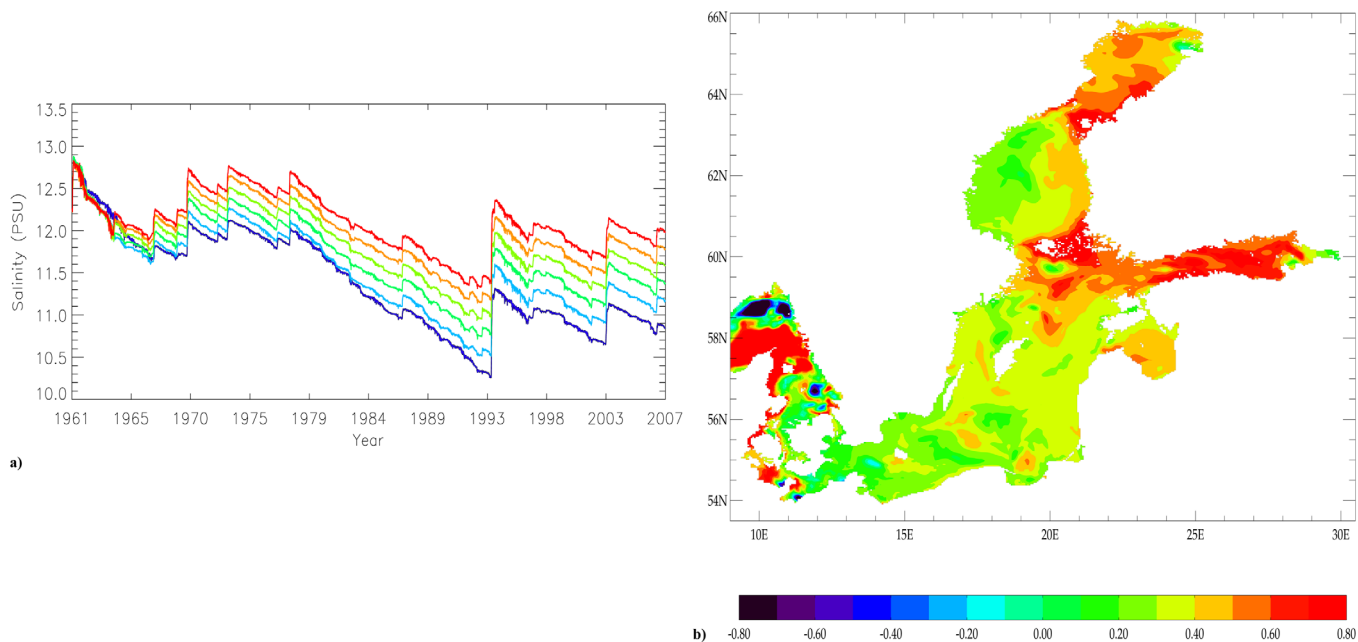


**Figure 4.** (a) Deep salinity (in PSU) at 250 m at BY15 from 1961 to 2007 for experiments e0, e0.5, e0.75, e1, e1.25, and e1.5, from blue to red, respectively. (b) Comparison of SSS between e1.5 and e0 after 10 years of simulation.

### 3. Results

Figure 4 depicts the differences in Baltic Sea SSS between the simulations e0 and e1.5 after 10 years of simulation. The Gulf of Finland as well as the Botnian Sea and Bothnian Bay show the most pronounced increases in SSS (Figure 1). The areas of the Baltic Sea with the highest surface salinity increases are disconnected from the North Sea by an area where the surface salinity increase is less pronounced.

Such a spatial pattern can only occur if an increased salt supply has been provided to the lower layers of the Baltic Sea and if some of that salt has found its way back to the surface in places of low stratification through the estuarine baroclinic circulation. The transfer of salinity through the permanent Baltic Sea halocline is a longer process.

Based on this set of sensitivity experiments and on the diagnostics designed in section 2.3, we investigate the reasons behind the increase of salinity of deep water created by a higher mean sea level. Specifically, we set out toward a mechanistic understanding of (1) if a higher mean sea level creates more deep water inflows into the Baltic Sea, or (2) if it increases the magnitude of inflows, or their salinity. Further, we aim to elucidate underlying mechanisms.

#### 3.1. Changes in Intensity of Inflow Events

As a first step, we analyze the changes in the mean intensity of salt inflows and try to understand how underlying processes change from experiments e0 to e1.5. For this purpose we analyze the changes in the mean values of  $F_{S_{inflow}}(t)$  and  $F_{V_{inflow}}(t)$  from experiments e0 to e1.5, whenever their value is not zero. We thus consider the changes in the inflow characteristics during inflow events.

Applying the diagnostics defined in section 2.3 for the time period 1966–2006 at section S1 yields Figure 5. Figure 5 indicates a clear increase in both strength and frequency of saltwater inflows in e1.5 compared with e0.

The increase of the mean intensity of inflows reaches 5, 7, 14, 17, and almost 24% for experiments e0.5, e0.75, e1, e1.25, and e1.5, respectively, compared with experiment e0.

The percentage of increase of variability of the barotropic flow across section S1 differs from the percentage of increase of intensity of inflows from experiment e0 to experiment e1.5. The percentage of increase of intensity of inflows follows a stronger trend: even if one considers the depth of the critical cross section of

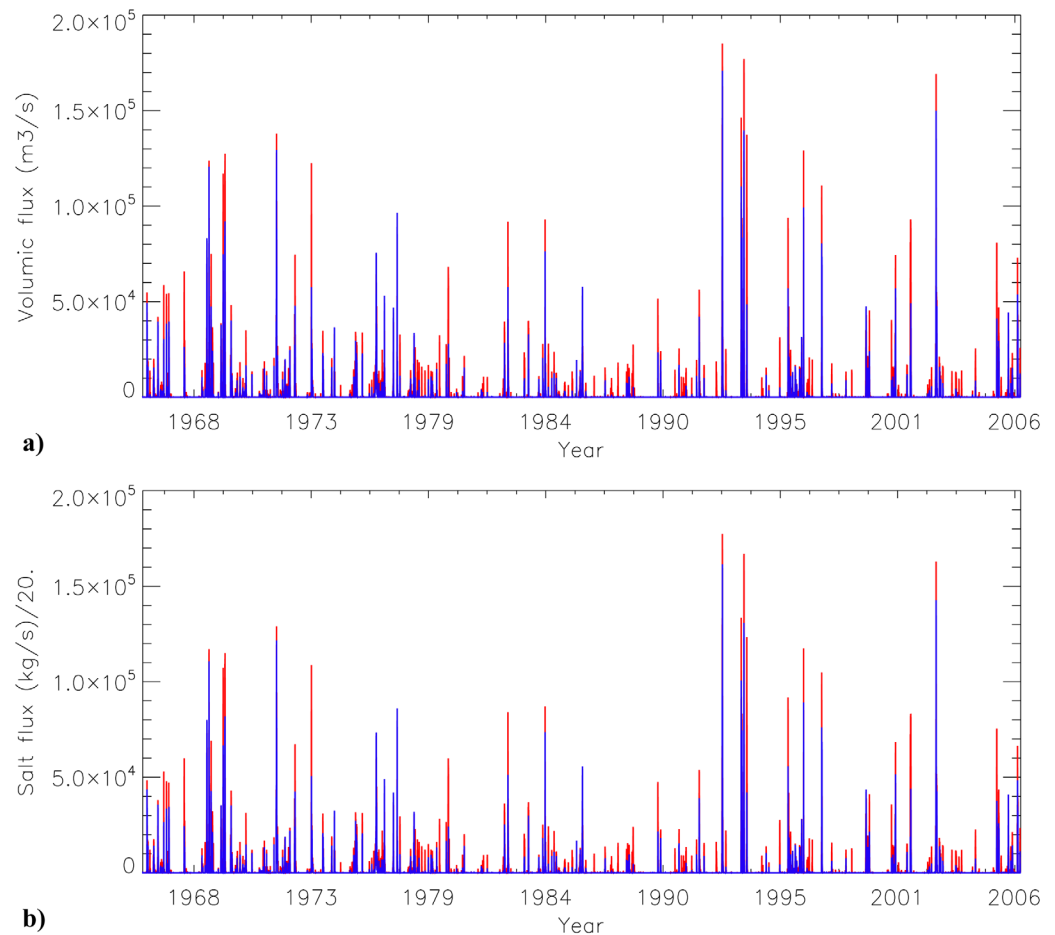


**Figure 5.** Comparison of volume and salt flux at cross section S1 for the reference experiment e0 (blue) and for the highest sea level increase experiment e1.5 (red). (a)  $F_{V_{inflow}}(t)$  in  $\text{m}^3 \text{s}^{-1}$ . (b)  $F_{S_{inflow}}(t)$  in  $\text{kg s}^{-1}$ .

the Great Belt, a sea level rise of 1.5 m creates an increase of the cross section area of only 7%. This fits with the increase of variability of the barotropic flow at section S1, which reaches 6.5% in the model. However, since the increase of intensity of inflows that corresponds to such a sea level rise reaches almost 24%, therefore an additional process must be involved (besides the increase in the cross section) in order to explain the increase of intensity of salt inflows.

A computation of the mean inflowing salinity for all the inflow events of the period and this for each scenario e0, e0.5, e0.75, e1, e1.25, and e1.5 gives, respectively, 18.22, 18.18, 18.18, 18.17, 18.17, and 18.16 PSU. Therefore, the mean salinity of inflow events does not change between the sensitivity runs: the increase in strength and frequency of  $F_{S_{inflow}}(t)$  one can notice in Figure 5 is only related with an increase in the strength of the inflows from a volume flux perspective.

### 3.2. Impact of Sea Level Increase on Mixing in the Danish Straits

Mixing in the Danish Straits is a critical process modulating salt inflows entering the Baltic. Most of the flow that creates salt inflows arrives in the Baltic Sea through the central channel of the Danish Straits (Great Belt) where entrainment rate estimates reach more than 70% [Kouts and Omstedt, 1993]. As a consequence, most of the saltier water arriving through the Great Belt is mixed with fresher water, and in a majority of cases is simply mixed with the upper and lighter mass of water, to finally be advected out of the Baltic Sea. Any change of mixing in this area can therefore lead to a dramatic change in the dynamics of saltwater inflows in the Baltic Sea.

Figure 6 shows the percentage of difference in vertical eddy diffusivity between experiments e1.5 and e0 for the Danish Straits area. Vertical eddy diffusivity is represented here as daily mean vertical

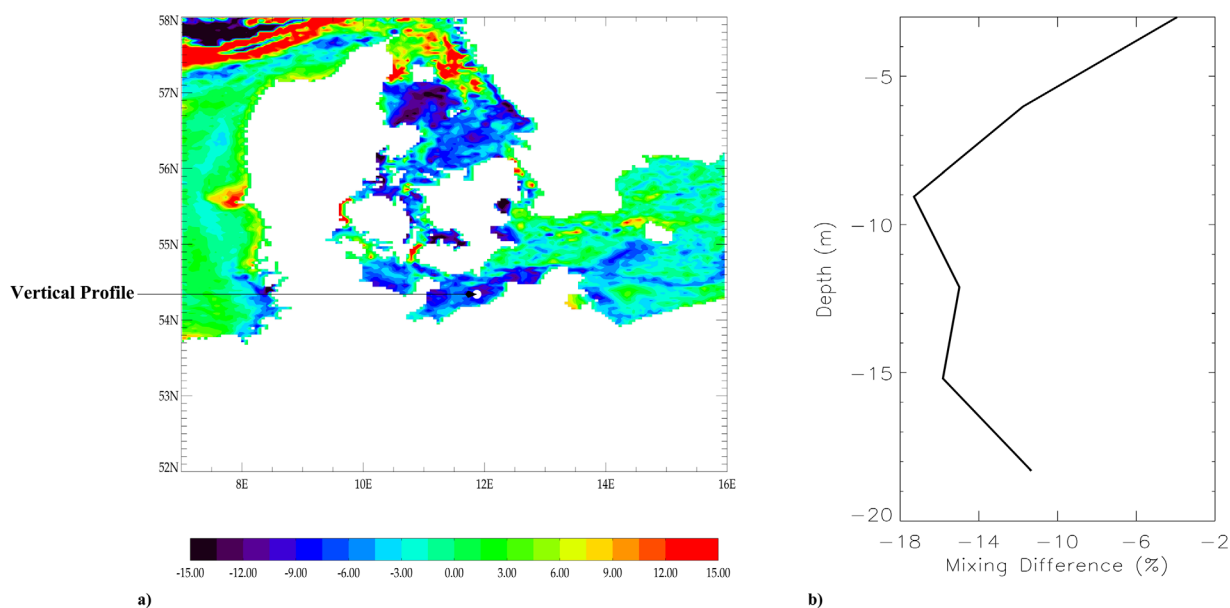


**Figure 6.** (a) Difference of mean vertically integrated vertical eddy diffusivity for year 1962, in % between experiments e1.5 and e0. (b) Difference of vertical eddy diffusivity at the point shown in the left figure.

turbulent eddy diffusivity as calculated from the  $k-\epsilon$  turbulence scheme, and averaged over the whole water column. We show the annual mean difference for 1962. We focus on a year at the beginning of the simulation, because we want to compare the simulations at a similar state of the ocean. In 1962, the state of the ocean is still similar in all sensitivity runs as they are not yet impacted by the differing inflow dynamics.

Figure 6 shows a strong decrease in vertical eddy diffusivity over the entire area of the Danish Straits. The decrease is especially pronounced along the main pathway of salt inflows, the Great Belt and the Darss Sill. Although some slight increase in vertical eddy diffusivity occurs in narrow straits, the mean decrease of vertical eddy diffusivity ranges from 5 to 10% depending on which extent of the Danish Straits area is considered. A decrease of the vertical eddy diffusivity can also be noticed in the South of Kattegat. A pronounced decrease in vertical eddy diffusivity occurs mainly in shallow areas. In deeper regions, a significant increase of vertical eddy diffusivity can be observed.

A vertical profile was chosen in the vicinity of the Darss Sill (Figure 6). There, the utmost damping of vertical eddy diffusivity as a consequence of the rising sea level is approximately 10–15 m below the surface. It is at this depth that the interface between higher fresher water masses and lower saltier water masses is located, and where the entrainment process takes place in the Danish Straits. Entrainment is a critical process of preconditioning the salt inflows in the Baltic Sea. It is still not comprehensively understood, but several studies have been made for the specific case of the Baltic Sea and the region of the Danish Straits. *Kouts and Omstedt* [1993], *Lass and Mohrholz* [2003], and especially *Arneborg et al.* [2007] provide us with the theoretical background which we use in the following.

Based on two different methods, *Arneborg et al.* [2007] computed an estimate of the entrainment parameter  $E$  describing the entrainment process that occurs in the Bornholm basin. It can be applied in regions where the flow is strongly influenced by geostrophy, which is the case for the Great Belt region and at the vicinity of section S1.

In their demonstration, *Arneborg et al.* [2007] have defined  $E$  as:

$$E = \frac{W_E}{U_s}, \quad (6)$$

where  $W_E$  is the entrainment velocity between the lower heavier mass of water, and the upper one of fresher and lighter water.  $U_s$  is a velocity explained hereafter.

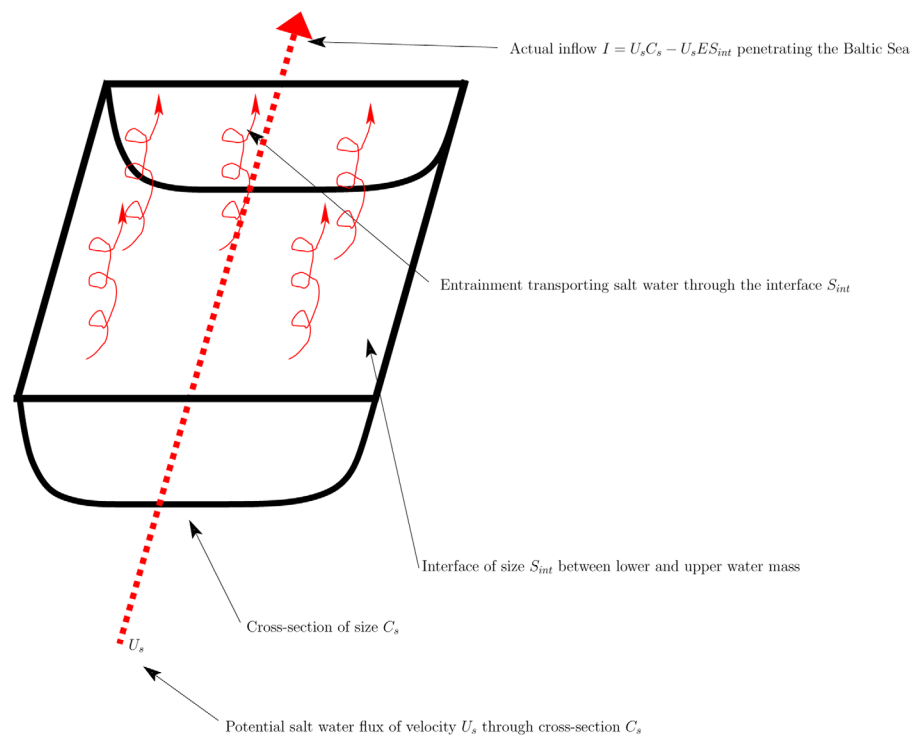


**Figure 7.** Schematic view of flow  $I$  through a cross section  $C_s$  of the Danish Straits. A potential inflow of velocity  $U_s$  flows below the horizontal section  $S_{int}$  located at the interface between ingoing and outgoing flows. This potential inflow is eroded with the entrainment rate  $E$  (red curved arrows).  $U_s C_s$  (in  $\text{m}^3 \text{s}^{-1}$ ) is the total volume flux of the potential inflow,  $I$  (in  $\text{m}^3 \text{s}^{-1}$ ) is the actual salt inflow that penetrates the Baltic Sea after the entrainment process that takes place in the Danish Straits has occurred. This entrainment process is described by the entrainment rate  $E$  (dimensionless).  $E$  describes the effect of deep saline water mixed to the surface where ultimately it will leave the Baltic Sea.

We now assume a system of inflowing water through the Danish Straits to reach a vertical cross section  $C_s$  located after the Danish Straits (in the Bornholm basin for example, similar to S1, Figure 1). For this system, we can define (equation (7)):

$$I = U_s C_s - U_s E S_{int}, \quad (7)$$

in which  $I$  is a volume flux of inflowing water through the cross section  $C_s$  with a velocity  $U_s$ .  $S_{int}$  represents the horizontal surface located at the interface between the mass of inflowing water that can potentially penetrate the Baltic Sea and the lighter water mass located above it. It has an entrainment parameter  $E$  (Figure 7). Our model results suggest that the salinity of water masses penetrating the Baltic Sea does not change with sea level rise, but that their frequency or their amplitude does (section 3.1). Hence, we take the point of view that entrainment is a process that erodes potential salt inflows upward, rather than mixing lighter water downward into a potential salt inflow. From a conservation perspective, both points of view are equivalent in our case: A salt inflow being mixed downward with lighter water cannot penetrate the Baltic Sea and will end up in the upper layer on its outgoing journey from the Baltic Sea. In the same manner, a potential salt inflow that is eroded upward mixes with lighter water in the upper layer, does not penetrate the Baltic Sea, and leaves the Baltic Sea.

For any potential salt inflow penetrating through the Danish Straits into the Baltic Sea with a velocity  $U_s$  through a strait of cross section  $C_s$ ,  $I$  is the flux that makes it through into the Baltic Sea after the entrainment process has eroded the incoming saltwater flow. This erosion takes place through the halocline of horizontal surface  $S_{int}$  with an entrainment rate  $E$ .  $I$  cannot be negative by definition: if the entrainment is too high, meaning in this case that  $E S_{int} > C_s$  then there is no possible inflow. In this case, all the potential inflow of dense water into the Baltic Sea is eroded and  $I$  is simply zero. However, for potential inflows making their way into the Baltic Sea, we also know based on literature surveys that most of their content is eroded [Kouts and Omstedt, 1993]. Therefore, for our reference experiment e0, this means that we can write:

$$E_0 S_{int} = \beta_0 C_s, \quad (8)$$



where  $\beta_0$  is the reference erosion rate for experiment e0, and  $E_0$  the associated entrainment rate. Introducing  $\beta_0$  allows re-writing the reference volume flux  $I(0)$ :

$$I(0) = U_s \frac{1 - \beta_0}{\beta_0} E_0 S_{int}. \quad (9)$$

We can define  $E_0, E_{0.5}, E_{0.75}, E_1, E_{1.25},$  and  $E_{1.5}$  as the entrainment parameters of experiments e0, e0.5, e0.75, e1, e1.25, and e1.5, respectively. We can also define the relative increase of inflowing fluxes  $I(h)/I(0)$  during inflow events as:

$$\frac{\delta I(h)}{I(0)} = \frac{S_{int}(E_h - E_0)}{C_s - E_0 S_{int}}, \quad (10)$$

which can be re-written as:

$$\frac{\delta I(h)}{I(0)} = \frac{\beta_0}{1 - \beta_0} \left( 1 - \frac{E_h}{E_0} \right). \quad (11)$$

Based on the relation found by *Arneborg et al.* [2007],  $E$  can be parameterized as (equation (12)):

$$E = a C_d K^b F_r^c, \quad (12)$$

in which  $a = 0.084, b = 0.6, c = 2.65, C_d$  is a drag coefficient,  $K$  is an estimate of the Ekman number of the flow, and  $F_r$  is the baroclinic Froude number. This baroclinic Froude number is defined as:

$$F_r = \frac{U_s}{\sqrt{g' D \cos \alpha_s}}, \quad (13)$$

where  $g'$  is the reduced gravity,  $D$  the thickness of the lower layer, and  $\alpha_s$  is the angle of the slope. The Ekman number of the flow  $K$  is defined as (equation (14)):

$$K = \frac{C_d U_s}{f' D}, \quad (14)$$

where  $C_d$  is a bottom drag coefficient and  $f' = f \cos \alpha_s$ , with  $f$  being the Coriolis parameter.

The theory presented by *Arneborg et al.* [2007] is based on a two-layer system. At the entrance of the Baltic Sea, we can assume that sea level rise affects only the lower layer of the system since the thickness of the upper one comes from the amount of river runoff rejected into the Baltic Sea and its eventual mixing within the basin. The thickness of the lower  $D$  is what varies in case of a mean variation of sea level. Based on the formulation of the entrainment parameter  $E$  and its relation with the Froude and Ekman numbers, equation (11) can be rewritten as:

$$\frac{\delta I(h)}{I(0)} = \frac{\beta_0}{1 - \beta_0} \left( 1 - \left( \frac{D_0}{D_h} \right)^{1.925} \right), \quad (15)$$

where  $D_0$  is the thickness of the lower layer for the reference experiment e0, and  $D_h$  is the thickness of the lower layer for an experiment of mean sea level rise  $h$ . Based on a thickness  $D_0$  of 12 m as in *Arneborg et al.* [2007], we compute the increase of inflow intensity predicted by this simple method and compare it to that predicted by our set of experiments for mean sea level increases of 0.5–1.5 m.

Since rising sea level additionally impacts the inflows by enlarging the cross section  $S_1$ , we additionally depict these anticipated changes in Figure 8. In order to get realistic results from this simple box model, we set  $\beta_0 = 0.5$  which is lower than even the lower bound (0.7) suggested by *Kouts and Omstedt* [1993]. However, the results of *Kouts and Omstedt* [1993] use a conceptual model based on long-term measurements, while we apply a 3-D ocean model that has a tendency to overestimate the stratification at the base of the mixed layer.

We notice that the increase of intensity of salt inflows follows the theory of *Arneborg et al.* [2007] for low sea level rise values. However, for higher sea level rise the addition of the barotropic variability at section  $S_1$  to the flow predicted by this theory provides a range that fits better with what is predicted by the model. When we extend our definition of inflows following the criterion of *Matthäus* [2006] which accounts for inflows only if they last at least five consecutive days then the results are different: the increasing trend follows closely that of the increase in barotropic variability at section  $S_1$ .

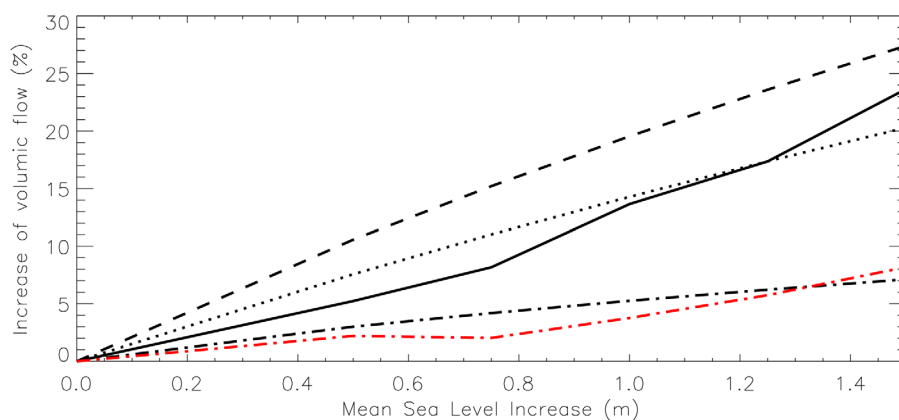


**Figure 8.** Plain line = mean volume inflow increase (%) for mean sea level increases of 0.5–1.5 m in simulations from e0 to e1.5. Dash-dotted line = increase in barotropic flow standard deviation (%) for the same set of experiments. Dotted line =  $\delta I(h)/I(0)$  as computed in equation (15). Dashed line =  $\delta I(h)/I(0)$  as computed in equation (15) to which the increase in barotropic flow standard deviation is added. Red dash-dotted line = increase in major Baltic Sea inflows (consecutive five day criteria taken into account).

### 3.3. Analysis of the Frequency of Inflow Events

So far we have concentrated on how the volume flux per inflow day changes with sea level rise. We now also present results on the number of inflow events and the increase in duration of the inflows. Our results indicate an increase in the number of days during which an inflow occurs, and additionally an increase in the mean duration of inflow events. This change is more difficult to address since it contains a higher degree of nonlinearity. It represents a change between a process (an inflow) that can exist and that is driven by an increase of sea level, and no inflow if no sea level increase occurs.

We present both the percentage of changes for the case of all salt inflow events (Figure 9), and the case of major Baltic Sea inflows with a duration of at least 5 days (Figure 10). In both cases, the number of salt inflows and the duration of salt inflows increase. The number of relatively short inflows (less than 5 days), which was already quite high, increases by a maximum of only 10%. In the same manner, major Baltic Sea inflows increase in length only by a maximum factor of 15% for a sea level rise of 1.5 m.

## 4. Discussion and Conclusion

In the present study, we investigate the effect of expected changes in global mean sea level on the processes governing salt inflows into the Baltic Sea. We show that a moderate mean sea level rise modifies the long-term dynamics of salt inflows in the Baltic Sea.

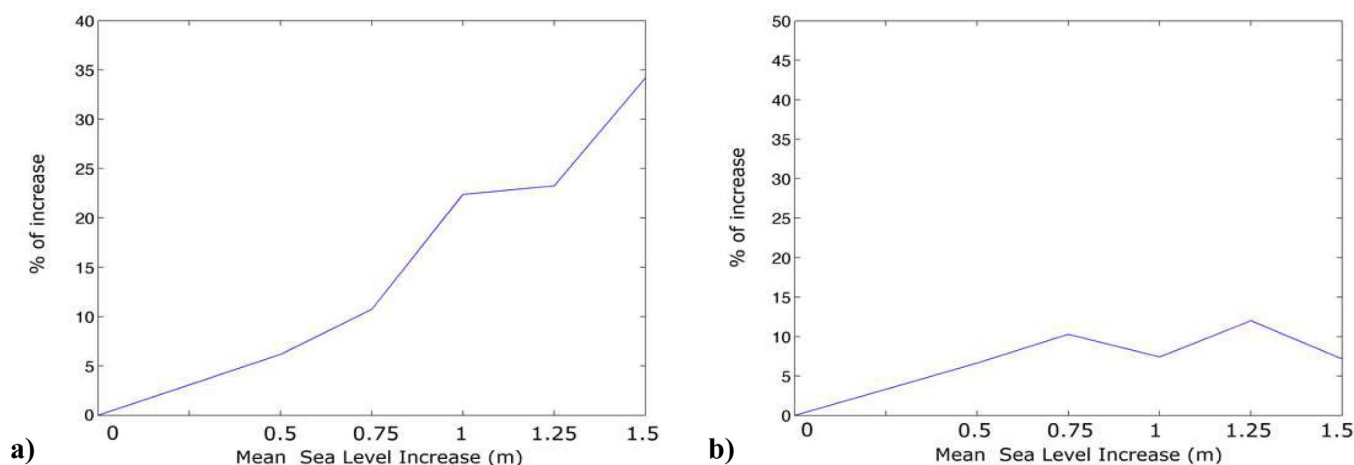


**Figure 9.** (a) Percentage of increase of length for salt inflow events of at least 1 day. (b) Percentage of increase in number of salt inflow events of at least 1 day.

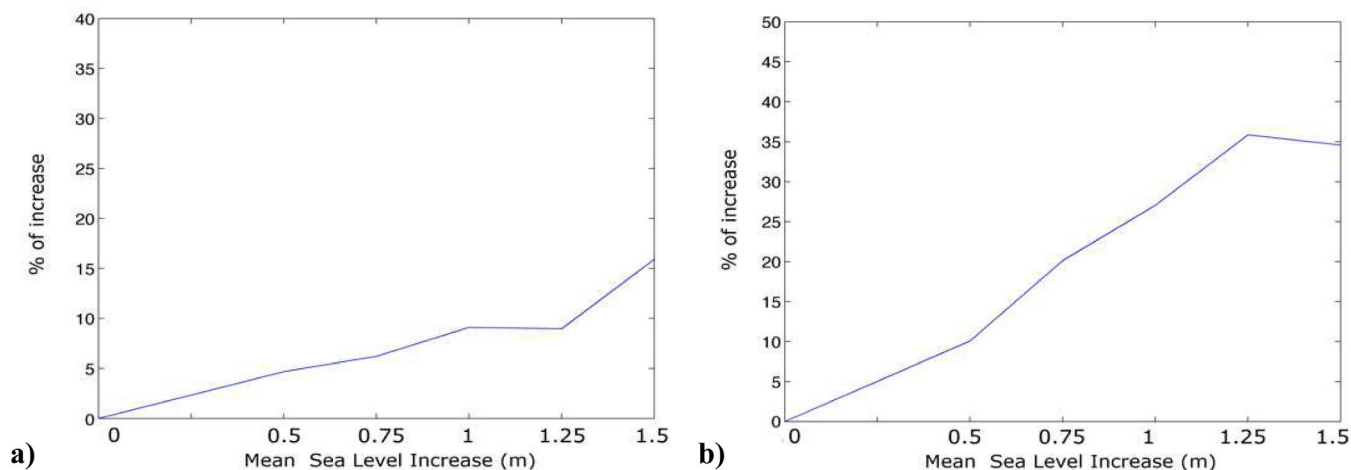


**Figure 10.** (a) Percentage of increase of length for salt inflow events of at least 5 days. (b) Percentage of increase in number of salt inflow events of at least 5 days.

In a 46 year hindcast simulation of NEMO-Nordic, the bottom salinity in the deepest parts of the Baltic Sea increases by 0.3 PSU for an anticipated sea level rise of 0.5 m. This salinity increase reaches values of more than 1 PSU for a mean sea level rise of 1.5 m. These increases in the deep salinity indicate an increase in the ventilation of the deep parts of the Baltic Sea even for a modest sea level rise.

Sea level rises trigger deep salinity biases, but no diverging temporal trends. Hence, apparently, on the time scales and magnitudes considered here, increased deep salinity does not weaken consecutive inflows.

We conclude that our results are robust, even though NEMO-Nordic overestimates the ventilation of intermediate layers and underestimates salinity transport to the deepest layers. Based on the argument that these model biases would rather weaken the simulated changes in the inflows instead of overestimating them, the model has a tendency to underestimate the amount of inflowing water that reaches the deepest parts of the Baltic Sea. It is the result of the vertical coordinate system and occurs mostly at shelf breaks: despite the bottom boundary layer parameterization, the model has difficulties representing slope currents in shelf break regions. This suggests that the model should also underestimate the impact of larger water masses penetrating the Baltic Sea.

Even though we illustrate the saltwater inflows become more frequent, longer, and more intense, we focus with our in-depth analysis on the intensity of inflows. Comparing compare the theoretical approach suggested by *Arneborg et al.* [2007] with the results of NEMO-Nordic, we find that:

1. The theoretical model presented by *Arneborg et al.* [2007] fits generally well for a given reference rate of erosion which is below that of observed values and with the simulated inflow increase for sea level rise from 0.5 to 1 m. This indicates that the inflow intensities were mainly impacted by a decrease of entrainment for these values. The increase of cross-sectional area does not appear to play a significant role for this range of sea level increase: the increase in the volume per day of saltwater inflows is much larger than the increase in standard deviation of the barotropic flow at section S1.
2. For larger anticipated mean sea level rise ranges, from 1.25 to 1.5 m, and beyond if one considers the slopes of curves of Figure 8, the reduction of entrainment in the Danish Straits alone cannot explain the increase in Baltic Sea salt inflows. This suggests the importance of another process. Adding the increase in standard deviation of the barotropic flow to the increase of inflows estimated from the reduction of the entrainment provides estimates of the increase in inflows that fit better to model results. This suggests that these two processes may simply add up (Figure 8) in the case of sea level rises exceeding 1.25 m. It is beyond the scope of this article to disentangle the respective contributions of the reduced entrainment and of the increased cross sections in the Danish Straits; also, because a comprehensive answer calls for an improved, higher-resolved representation of the Danish Straits. Further studies involving a better horizontal resolution of the Danish Straits area is therefore required.
3. If we consider only major inflows, as defined by *Matthäus* [2006], the highest-case scenario increases such inflows by 8%. In that case the increase of inflowing volume is highly correlated with the increase in standard deviation (Figure 8, red curve). As explained by *Schimanke et al.* [2014], major Baltic Sea inflows

are, to first order, barotropic phenomena driven by an emptying-refilling process of the Baltic Sea. As such they feature a lower sensitivity to a decrease of the mixing in the Danish Straits, and a rather high correlation with the increase in barotropic variability (which, in turn, is caused by the increase in cross section in the Danish Straits).

4. The decrease of mixing in the Danish Straits gives this area a stronger baroclinic behavior. This decrease of mixing enables stronger small inflows. The increase in cross section on the other hand affects the barotropic behavior of the Danish Straits, by also enabling stronger small inflows but also stronger major salt inflows into the Baltic Sea.

If we consider the changes of frequency and duration of inflow events, our results show an increase in the number of days during which inflow events occur, and indicate that the mean length of inflow events is affected regardless of the criteria that is chosen. The increase of frequency of major salt inflows reaches up to 35% for a mean sea level rise of 1.5 m, but their length increases only by a maximum of 15%.

For the rather frequent short inflow events, the frequency of inflows increases only by less than 10% for the most extreme case of sea level rise, but their length, that has more potential to become longer, increases by about 35%. It is difficult to interpret these findings which represent rather time-integrated metrics (in contrast to the previously presented dealt with volume fluxes). Even though, we conclude that the decrease of mixing is an essential factor determining the increase of frequency and length of Baltic Sea salt inflows: First, a decrease of mixing raises the probability that an inflowing water mass can penetrate through the Danish Straits and preserve its properties, hence increasing the probability of creating a salt inflow. Second, reduced mixing implies that the water masses at the beginning and at the end of the inflow process also have a larger probability to cross the Danish Straits while preserving their properties, thus increasing the duration of an inflow event.

This latter aspect and the effect of sea level rise on the overall haline structure of the Baltic Sea (i.e., which layers become saltier due to which process related with sea level rise), is an aspect we will further investigate in addition to the coupling of stronger salt inflows with biogeochemistry. From this perspective, it is difficult to make a forecast just based on these results. However, one can expect the following features. First, added saltwater inflows usually carry oxygen to the deepest parts of the Baltic Sea, but this added oxygen content is usually consumed within a time scale of 1 or 2 years [Nausch *et al.*, 2008]. However, added salinity in the deepest parts of the Baltic Sea also leads to stronger stratification which suggests on longer time periods that the oxygen content might actually decrease. A consequence could be a higher release of phosphorus from the bottom sediments [Almroth-Rosell *et al.*, 2015]. From this point of view, further investigation with the use of a coupled biogeochemistry model is our next target.

#### Acknowledgments

All the data used to compute the figures presented in this article are available by simple demand to the corresponding author. The NEMO-Nordic simulations were performed on the Linux cluster Krypton at the National Supercomputing Centre, Linköping University, Sweden. The authors wish to thank all the people who have contributed to the development of the NEMO-Nordic standalone, operational, and coupled configurations inside and outside SMHI. The study is part of the BIO-C3 project from BONUS, the joint Baltic Sea research and development programme (Art 185), funded jointly from the European Union's Seventh Programme for research, technological development, and demonstration and from the Swedish Research Council for Environment, Agricultural Sciences and Spatial Planning, FORMAS (219-2013-2041).

#### References

- Adcroft, A., and J.-M. Campin (2004), Re-scaled height coordinates for accurate representation of free-surface flows in ocean circulation model, *Ocean Modell.*, *7*, 269–284.
- Almroth-Rosell, E., K. Eilola, I. Kuznetsov, P. O. Hall, and H. M. Meier (2015), A new approach to model oxygen dependent benthic phosphate fluxes in the Baltic Sea, *J. Mar. Syst.*, *144*, 127–141.
- Arneborg, L., V. Fiekas, L. Umlauf, and H. Burchard (2007), Gravity current dynamics and entrainment—A process study based on observations in the Arkona Basin, *J. Phys. Oceanogr.*, *37*, 2094–2113, doi:10.1175/JPO3110.1.
- Axell, L., R. Hordoir, A. Jönsson, S. de Koster, Y. Liu, P. Ljungemyr, and P. Strömberg (2014), Verification of NEMO-Nordic: A setup for the Baltic Sea, technical report, Swed. Meteorol. and Hydrol. Inst.
- Beckmann, A., and R. Döscher (1997), A method for improved representation of dense water spreading over topography in geopotential-coordinate models, *J. Phys. Oceanogr.*, *27*, 581–591.
- Blank, R., J. Lubchenco, and R. Dietrick (2012), Global sea level rise scenarios for the united states national climate assessment, *NOAA Tech. Rep. OAR CPO-1*, Natl. Oceanic and Atmos. Admin., Clim. Program Off., Silver Spring, Md.
- Dietze, H., U. Lötjien, and K. Getzlaff (2014), MOMBA 1.1—A high-resolution Baltic Sea configuration of GFDL's modular ocean model geoscientific model development, *Geosci. Model Dev.*, *7*, 1713–1731, doi:10.5194/gmd-7-1713-2014.
- Egbert, G., A. Bennett, and M. Foreman (1994), TOPEX/POSEIDON tides estimated using a global inverse model, *J. Geophys. Res.*, *99*(C12), 24,821–24,852, doi:10.1029/94JC01894.
- Egbert, G. D., and S. Y. Erofeeva (2002), Efficient inverse modeling of barotropic ocean tides, *J. Atmos. Oceanic Technol.*, *19*(2), 183–204, doi:10.1175/1520-0426.
- Eilola, K., and A. Stigebrandt (1998), Spreading of juvenile freshwater in the Baltic proper, *J. Geophys. Res.*, *103*(C12), 27,795–27,807.
- Ekman, M., and J. Mäkinen (1996), Mean sea surface topography in the Baltic Sea and its transition area to the North Sea: A geodetic solution and comparisons with oceanographic models, *J. Geophys. Res.*, *101*(C5), 11,993–11,999, doi:10.1029/96JC00318.
- Funkquist, L., and E. Kleine (2007), HIROMB: An introduction to HIROMB, an operational baroclinic model for the Baltic Sea, *Rep. Oceanogr.*, *37*, Swed. Meteorol. and Hydrol. Inst., Norrköping, Sweden.
- Galperin, B., L. H. Kantha, S. Hassid, and A. Rosati (1988), A quasi-equilibrium turbulent energy model for geophysical flows, *J. Atmos. Sci.*, *45*, 55–62.

- Godhe, A., J. Egardt, D. Kleinhans, L. Sundqvist, R. Hordoir, and P. Jonsson (2013), Seascape analysis reveals regional gene flow patterns among populations of a marine planktonic diatom, *Proc. R. Soc. B*, *280*, doi:10.1098/rspb.2013.1599.
- Gogina, M., and M. L. Zettler (2010), Diversity and distribution of benthic macrofauna in the Baltic Sea: Data inventory and its use for species distribution modelling and prediction, *J. Sea Res.*, *64*(3), 313–321.
- Hordoir, R., and H. E. M. Meier (2010), Freshwater fluxes in the Baltic Sea—A model study, *J. Geophys. Res.*, *115*, C08028, doi:10.1029/2009JC005604.
- Hordoir, R., C. Dieterich, C. Basu, H. Dietze, and M. Meier (2013), Freshwater outflow of the Baltic Sea and transport in the Norwegian current: A statistical correlation analysis based on a numerical experiment, *Cont. Shelf Res.*, *64*, 1–9, doi:10.1016/j.csr.2013.05.006.
- IPCC (2013), Climate change 2013: The physical science basis, in *Working Group I Contribution to the Fifth Assessment Report*, edited by R. Feistel, G. Nausch, and N. Wasmund, *Rep. WGI AR5*. Tech. Support Unit, Univ. of Bern, Bern.
- Kouts, T., and A. Omstedt (1993), Deep water exchange in the Baltic proper, *Tellus, Ser. A*, *45*, 331–324.
- Large, W. G., and S. Yeager (2004), Diurnal to decadal global forcing for ocean and sea-ice models: The data sets and flux climatologies, *NCAR Tech. Note, NCAR/TN-460+STR*, CGD Div. of the Natl. Cent. for Atmos. Res.
- Lass, H. U., and W. Matthäus (1996), On temporal wind variations forcing salt water inflows into the Baltic Sea, *Tellus, Ser. A*, *48*, 663–671, doi:10.1034/j.1600-0870.1996.t01-4-00005.x.
- Lass, H. U., and V. Mohrholz (2003), On dynamics and mixing of inflowing saltwater in the Arkona Sea, *J. Geophys. Res.*, *108*(C2), 3042, doi:10.1029/2002JC001465.
- Leclair, M., and G. Madec (2009), A conservative leapfrog time stepping method, *Ocean Modell.*, *30*, 88–94, doi:10.1016/j.ocemod.2009.06.006.
- Levitus, S., and T. P. Boyer (1994), Salinity, in *World Ocean Atlas 1994, NOAA Atlas NESDIS*, vol. 3, 99 pp., U.S. Gov. Print. Off., Washington, D. C.
- Löptien, U., and H. E. M. Meier (2011), The influence of increasing water turbidity on the sea surface temperature in the Baltic Sea: A model sensitivity study, *J. Mar. Syst.*, *88*(2), 323–331, doi:10.1016/j.jmarsys.2011.06.001.
- Löptien, U., S. Martensson, H. E. M. Meier, and A. Höglund (2013), Long-term characteristics of simulated ice deformation in the Baltic Sea (1962–2007), *J. Geophys. Res. Oceans*, *118*, 801–815, doi:10.1002/jgrc.20089.
- Madec, G. (2010), NEMO ocean engine, version 3.3, *Note du Pôle de modélisation de l'Inst. Pierre-Simon Laplace 27*, Inst. Pierre-Simon Laplace, Paris. [Available at <http://www.nemo-ocean.eu/>.]
- Matthäus, W. (2006), The history of investigation of salt water inflows in the Baltic Sea—From the early beginning to recent results, *Mar. Sci. Rep.* *65*, Baltic Sea Res. Inst. (IOW), Ger. Inst. für Ostseeforschung Warnemünde, Rostock.
- Meier, H., R. Hordoir, H. Andersson, C. Dieterich, K. Eilola, B. Gustafsson, A. Höglund, and S. Schimanke (2012), Modeling the combined impact of changing climate and changing nutrient loads on the Baltic Sea environment in an ensemble of transient simulations for 1961–2099, *Clim. Dyn.*, *39*(9–10), 2421–2441, doi:10.1007/s00382-012-1339-7.
- Meier, H. E. M. (2007), Modeling the pathways and ages of inflowing salt- and freshwater in the Baltic Sea, *Estuarine Coastal Shelf Sci.*, *74*, 717–734.
- Meier, H. E. M., and F. Kauker (2003), Modeling decadal variability of the Baltic Sea: 2. Role of freshwater inflow and large-scale atmospheric circulation for salinity, *J. Geophys. Res.*, *108*(C11), 3368, doi:10.1029/2003JC001799.
- Meier, H. E. M., R. Döscher, and T. Faxén (2003), A multiprocessor coupled ice-ocean model for the Baltic Sea: Application to salt inflow, *J. Geophys. Res.*, *108*(C8), 3273, doi:10.1029/2000JC000521.
- Meier, H. E. M., E. Kjellström, and L. P. Graham (2006), Estimating uncertainties of projected Baltic Sea salinity in the late 21st century, *Geophys. Res. Lett.*, *33*, L15705, doi:10.1029/2006GL026488.
- Nausch, G., R. Feistel, and N. Wasmund (2008), *State and Evolution of the Baltic Sea, 1952–2005: A Detailed 50-Year Survey of Meteorology and Climate, Physics, Chemistry, Biology, and Marine Environment*, John Wiley, Hoboken, N. J.
- Pfeffer, W. T., J. T. Harper, and S. O'Neel (2008), Kinematic constraints on glacier contributions to 21st-century sea-level rise, *Science*, *321*, 1340–1343, doi:10.1126/science.1159099.
- Samuelsson, P., C. Jones, U. Willén, U. Ullerstig, S. Golvik, U. Hansson, C. Jansson, E. Kjellström, G. Nikulin, and K. Wyser (2011), The Rossby centre regional climate model RCA3: Model description and performance, *Tellus, Ser. A*, *63*, 4–23.
- Schimanke, S., C. Dieterich, and H. E. M. Meier (2014), An algorithm based on sea-level pressure fluctuations to identify major Baltic inflow events, *Tellus, Ser. A*, *66*, doi:10.3402/tellusa.v66.23452.
- Stigebrandt, A., R. Rosenberg, L. Råman Vinnå, and M. Ödalen (2014), Consequences of artificial deepwater ventilation in the Bornholm Basin for oxygen conditions, cod reproduction and benthic biomass—A model study, *Ocean Sci. Discuss.*, *11*(4), 1783–1827, doi:10.5194/osd-11-1783-2014.
- Umlauf, L., and H. Burchard (2003), A generic length-scale equation for geophysical turbulence models, *J. Mar. Syst.*, *61*, 235–265.
- Vancoppenolle, M., T. Fichefet, H. Goosse, S. Bouillon, G. Madec, and M. A. M. Maqueda (2008), Simulating the mass balance and salinity of arctic and Antarctic sea ice, *Ocean Modell.*, *27*(1–2), 33–53, doi:10.1016/j.ocemod.2008.10.005.

## **APPENDIX IV**

# Impact of saltwater inflows on phosphorus cycling and eutrophication in the Baltic Sea: a 3D model study

By KARI EILOLA<sup>1\*</sup>, ELIN ALMROTH-ROSELL<sup>1</sup> and  
H. E. MARKUS MEIER<sup>1,2</sup>, <sup>1</sup>*Swedish Meteorological and Hydrological Institute, Norrköping, Sweden;*  
<sup>2</sup>*Department of Meteorology, Stockholm University, Stockholm, Sweden*

(Manuscript received 5 February 2014; in final form 10 June 2014)

## ABSTRACT

The impact of dense saltwater inflows on the phosphorus dynamics in the Baltic Sea is studied from tracer experiments with a three-dimensional physical model. Model simulations showed that the coasts of the North West Gotland Basin and the Gulf of Finland, the Estonian coast in the East Gotland Basin are regions where tracers from below the halocline are primarily lifted up above the halocline. After 1 yr tracers are accumulated at the surface along the Swedish east coast and at the western and southern sides of Gotland. Elevated concentrations are also found east and southeast of Gotland, in the northern Bornholm Basin and in the central parts of the East Gotland Basin. The annual supplies of phosphorus from the deeper waters to the productive surface layers are estimated to be of the same order of magnitude as the waterborne inputs of phosphorus to the entire Baltic Sea. The model results suggest that regionally the impact of these nutrients may be quite large, and the largest regional increases in surface concentrations are found after large inflows. However, the overall direct impact of major Baltic inflows on the annual uplift of nutrients from below the halocline to the surface waters is small because vertical transports are comparably large also during periods without major inflows. Our model results suggest that phosphorus released from the sediments between 60 and 100 m depth in the East Gotland Basin contributes to the eutrophication, especially in the coastal regions of the eastern Baltic Proper.

*Keywords:* Phosphorus, eutrophication, saltwater inflows, biogeochemistry, Baltic Sea, numerical modelling

## 1. Introduction

The Baltic Sea is a semi-enclosed, brackish and shallow sea with a mean depth of 54 m and a limited water exchange with the open ocean (e.g. Leppäranta and Myrberg, 2009) (Fig. 1). The atmospheric forcing causes a large variability in motions and physical processes in the shallow Baltic Sea (e.g. Leppäranta and Myrberg, 2009). The freshwater supply from rivers causes large salinity gradients between the northern sub-basins and the entrance area and between the well-mixed brackish surface layer and the saltier bottom layer. Generally only intermittent major Baltic inflows with denser surface waters from Kattegat ventilate and oxygenate the deepest parts (Fischer and Matthäus, 1996). Oxygen deficiency is therefore a frequent problem that also influences eutrophication by the redox dependent phosphorus

(P) fluxes from the sediments (Conley et al., 2009). This causes a large variability of P concentrations in the deeper parts of the Baltic Sea (cf. Fig. 2). In fact, the large scale variations of the pools of inorganic P caused by the intermittent major Baltic inflows may be up to two orders of magnitude larger than the variations in the external P input (e.g. Savchuk, 2010).

Measurements of nutrients and oxygen in the Baltic Sea have been done for more than 100 yr with regular monitoring starting in the 1950s, though the earliest nutrient measurements from the beginning of the last century are regarded as unreliable (e.g. Fonselius and Valderrama, 2003; Feistel et al., 2008). The central part of the Eastern Gotland Basin (Fig. 1) which have the longest historical data records, is often used as a representative area for studies of the basic physical and biogeochemical dynamics in the Baltic Sea (e.g. Nausch et al., 2003; Stigebrandt and Gustafsson, 2007; Reissmann et al., 2009; Schneider, 2011). Schneider (2011) studied the changes in the mean phosphate ( $\text{PO}_4$ ) and total inorganic carbon ( $\text{C}_T$ ) below 150 m depth in the

\*Corresponding author.  
email: kari.eilola@smhi.se  
Responsible Editor: Johan Nilsson, Stockholm University, Sweden.

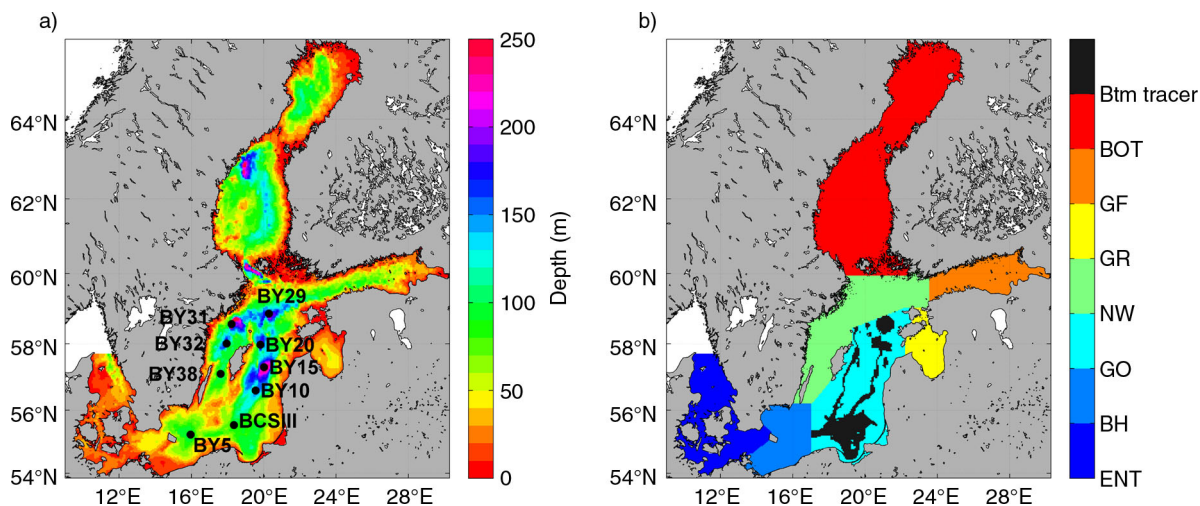


*Fig. 1.* Maps showing the RCO model bathymetry and nine standard monitoring stations (left, a) and the division of the model domain into Baltic Sea sub-basins (right, b). The bottom area at 60–99 m depth in the East Gotland Basin (black colour) used for the experiment with emulated sediment release of tracers (Btm tracer) is shown in the right panel. The model domain has an open boundary in the northern part of the Kattegat. Sub-basin abbreviations: Entrance area (ENT, including the Kattegat, the Danish sounds and the Arkona Basin), Bornholm Basin (BH), East Gotland Basin (GO), North-West Gotland Basin (NW), Gulf of Riga (GR), Gulf of Finland (GF) and the Gulf of Bothnia (BOT, including the Åland Sea, the Archipelago Sea, the Bothnian Sea and the Bothnian Bay). The volumes of the sub-basins are presented in Table 1. The Baltic Proper includes the NW, GO, BH and the Arkona Basin.

East Gotland Deep (BY15, see Fig. 1) after the major Baltic inflow in 2003. He observed a drop of  $\text{PO}_4$  from  $4.9 \mu\text{mol L}^{-1}$  to  $3.0 \mu\text{mol L}^{-1}$  (39%) within 6 weeks after the inflow and a further drop to a minimum of  $2.0 \mu\text{mol L}^{-1}$  (60%) within 1 yr. The  $\text{C}_T$  concentrations that are not redox sensitive dropped similarly to  $\text{PO}_4$  due to dilution during the initial weeks (Schneider, 2011). Because of on-going organic matter mineralisation,  $\text{C}_T$  concentrations started to increase again already in the autumn when the water exchange slowed down. The release of  $\text{PO}_4$  from the sediment was, however, according to Schneider (2011) most likely very small after the inflow when the water turned from anoxic to oxic. A possible explanation for this is that the  $\text{PO}_4$  can bind to hydrated metal oxides (e.g. Fe) in the Baltic Sea sediments as discussed, e.g. by Mort et al. (2010) and Schneider (2011).

P is a major nutrient that often limits productivity in the Baltic Sea and the sinking of P bound in organic matter mainly causes its downward transport. High-resolution model simulations have been used to study the transports and the sedimentation-resuspension dynamics of organic P (Almroth Rosell et al., 2011) as well as of the fate of river-borne P in the Baltic Sea (Radtke et al., 2012). Eilola et al. (2012) studied the horizontal transport patterns and the net exchange of P between the open sea and the regions shallower than 30 m depth in present climate as well as in climate-change scenarios. An overview of the present knowledge about mechanisms driving the physical dynamics

and mixing processes of the inflowing waters and the vertical transports of salt and nutrients to the surface layers is given in the review by Reissmann et al. (2009), but all details of the processes are still not fully understood. One example is the passive vertical transports of dissolved P from the deep waters to the surface layers, which needs further attention as pointed out by Reissmann et al. (2009).

The aim of the present paper is to perform high-resolution model experiments to simulate the renewal of the East Gotland Deep water and to follow the fate of the accumulated pools of P in the Baltic deep water. Previously Meier (2007) calculated the pathways and ages of various water masses in the Baltic Sea with the ocean circulation model RCO (Rossby Centre Ocean model) which is also used in the present study. For the surface layers, he found that mean ages associated to inflowing saline water from Kattegat ranged from about 26 yr in the south to 42 yr in the most northern Baltic Sea. Meier (2007) used the age tracing concept described by Delhez et al. (1999, 2004) and Deleersnijder et al. (2001). Radtke et al. (2012) combined the age concept with a source attribution technique to describe pathways and time scales between the input of nutrients to the Baltic Sea and their arrival in different sub-basins and the residence times of the nutrients in the ecosystem. They studied especially the discharges of the Oder, Vistula and Daugava rivers and found that after an average time of 1.4 yr, 95% of riverine nitrogen was lost by denitrification in sediments. The residence time of riverine phosphorus



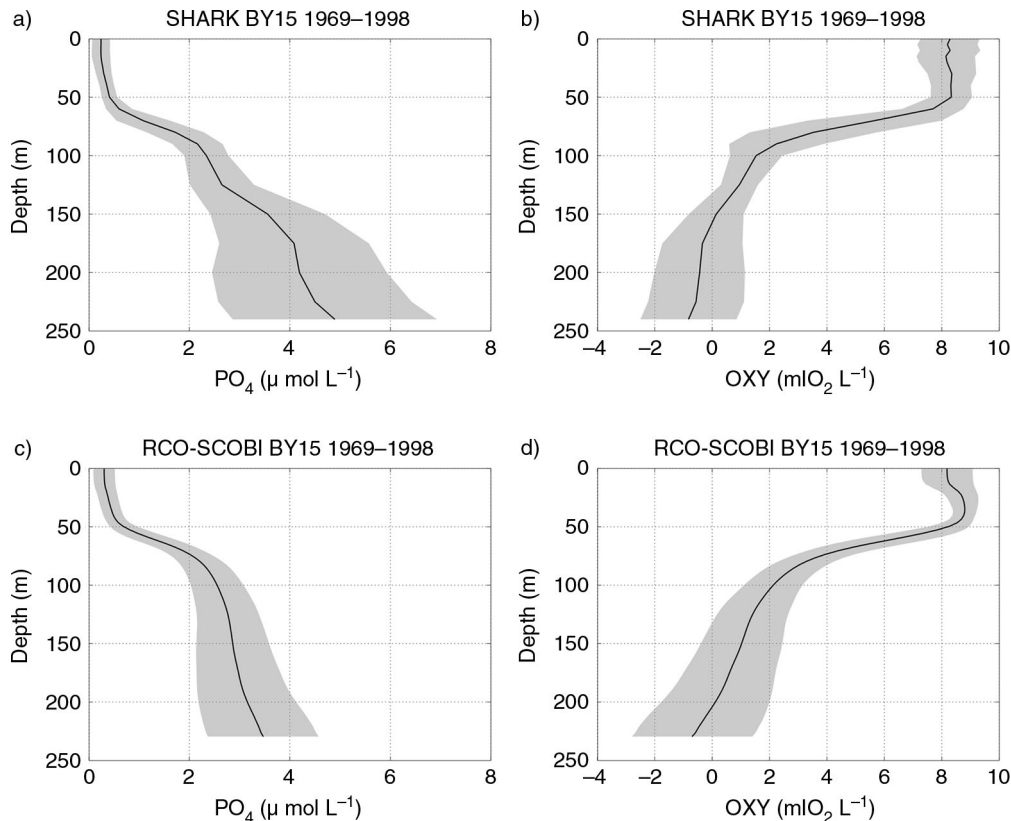


Fig. 2. Mean profiles and  $\pm 1$  standard deviation (grey shaded area) from GO (station BY15) in the period 1968–1998 of phosphate ( $\mu\text{mol PO}_4 \text{ L}^{-1}$ ) and oxygen ( $\text{ml O}_2 \text{ L}^{-1}$ ) in left and right panels, respectively. Observations (from the Swedish Oceanographic Data Centre (SHARK) at the Swedish Meteorological and Hydrological Institute, <http://www.smhi.se>) are shown in the upper panels (a and b) and the corresponding RCO-SCOBI results are shown in the lower panels (c and d).

exceeded the simulated period of 35 yr. These tracer techniques can be used to trace nutrients for long periods through the food web at the cost of additional state variables and copies of the equations involved in the biogeochemical cycles. A similar concept was used by Almroth-Rosell et al. (2011) to follow the transports of resuspended organic matter in the Baltic Sea.

We will investigate the impacts of modelled inflows occurring during the period 1961–2009, when the stagnant deep water usually became anoxic and rich in phosphate before the next deep water renewal took place (e.g. Stigebrandt and Gustafsson, 2007), and use passive tracer experiments to examine the role of water masses from different regions (Fig. 1) and different depth layers. This tracer study aims to investigate if there are specific regions where the deep water usually is lifted above the halocline, and also, if there are regions where we might expect a possible addition to the spring primary production from the excess phosphorus annually lifted up from the layers below the halocline. The relative importance of inflows on the average uplift of tracers will be quantified from a set of years having stronger and weaker inflows respectively, compared

to years with no inflows. The results from the present model study may support the planning of future field studies of vertical transports and mixing as well as the model developments in the Baltic Sea.

The paper is organised as follows. In Section 2, the model setup and details about the tracer methods are presented. The results of the modelled tracer dynamics are discussed in Section 3 and compared to the in-situ tracer experiment in 2007–2009 by Holtermann et al. (2012) and the data analysis of the inflow in 2003 by Schneider (2011). Finally the horizontal and vertical dispersion of the tracers are discussed and some concluding remarks are given.

## 2. Methods

### 2.1. Overview

The RCO (e.g. Meier et al., 2003; Meier, 2007), is coupled to the Swedish Coastal and Ocean Biogeochemical model (SCOBI) (e.g. Eilola et al., 2009; Almroth Rosell et al., 2011) that has been used in several applications for the Baltic Sea

(e.g. Eilola et al., 2012; Meier et al., 2012). The coupled model system has shown good performance compared to other Baltic Sea models and observations (Eilola et al., 2011) and the 30-yr (1969–1998) means and standard deviations of phosphate and oxygen are shown in comparison to the observations from the central Eastern Gotland Basin in Fig. 2. One may note that the main features of the stratification and variability are satisfactory reproduced though the position of the halocline is slightly too high in the water column as seen from the modelled stratification. The performance of the present model version and the dynamics of the halocline and its impact on hypoxia in the Baltic Sea are further discussed in detail by Väli et al. (2013).

The coupled model RCO-SCOBI is also used in the present study but the biogeochemical processing is not active and the SCOBI variables are used as passive tracers instead.

### 2.2. Coupled ice-ocean model

RCO is a Bryan-Cox-Semtner primitive equation circulation model with a free surface (Killworth et al., 1991) and open boundary conditions (Stevens, 1991) in the northern Kattegat (Fig. 1). It is coupled to a Hibler-type sea ice model (Hibler, 1979) with elastic-viscous-plastic rheology (Hunke and Dukowicz, 1997) and explicit representation of five undeformed and two deformed sea ice categories (Mårtensson et al., 2012). In the ocean model a flux-corrected, monotonicity preserving transport (FCT) scheme following Gerdes et al. (1991) is embedded to avoid overshooting of tracer concentration at large gradients due to numerical dispersion. Subgrid-scale mixing is parameterised using a turbulence closure scheme of the  $k$ - $\epsilon$  type with flux boundary conditions to include the effect of a turbulence enhanced layer due to breaking surface gravity waves and a parameterisation for breaking internal waves (Meier, 2001). The deep water mixing is assumed to be inversely proportional to the Brunt-Väisälä frequency with a proportionality factor  $\alpha = 1 \times 10^{-7} \text{ m}^2 \text{ s}^{-2}$  following Lass et al. (2003). As the layer thicknesses of the vertical grid are too large to resolve the bottom boundary layer (BBL) accurately, a BBL model is embedded to allow the direct communication between bottom boxes of the step-like topography (Beckmann and Döscher, 1997). The BBL model helps to improve the simulation of gravity-driven dense bottom flows (Meier et al., 2004). In this study RCO is used with a horizontal resolution of 3.7 km (2 nautical miles) and with 83 vertical levels with layer thicknesses of 3 m. In the model the maximum depth amounts to 249 m. For further details of the RCO model and the performance of relevant model variables compared to observations, the reader is referred to Meier (2001), Meier et al. (2003), Meier (2007) and Väli et al. (2013).

### 2.3. Regional climate data sets

The forcing of the ocean model for the period 1850–2009 is calculated from reconstructed atmospheric surface fields (Schenk and Zorita, 2012). The high-resolution daily fields are homogeneous and physically consistent by making use of both long-term records of European historical station data since 1850, and simulated atmospheric fields from a regional coupled atmosphere–ocean model over Northern Europe in the period 1958–2009, driven by re-analysis data at the lateral boundaries (Samuelsson et al., 2011). In this study, we focus on simulation results since 1960.

### 2.4. Tracer

The present study is based on experiments using passive tracers that follow the pathways of different water masses. This is also valid for the description of phosphorus transports from the deeper parts to the surface of the Baltic Sea as will be further discussed in Section 3.2.1. However, from this approach it is not possible to draw conclusions about the impact of biogeochemical processes on the uplifted phosphorus in the euphotic zone. Hence, source attribution and age following techniques needed for that task is out of the scope of the present study and will be addressed with the SCOBI model in future work.

Basically two main approaches are used in the present study. The first approach investigates the dispersion and the replacement of deep water tracers below 150 m depth in the East Gotland Basin and the second approach investigates the dispersion of tracers from below the halocline. The second approach is motivated by the fact that during recent times the oxygen-poor and phosphate-rich waters have reached high up in the water column and occupy thereby large volumes of the Baltic Proper (e.g. Reissmann et al., 2009; Hansson et al., 2013). The potential impact in the surface layers of uplifted tracers from below the halocline at about 70 m depth in the East Gotland Basin and the North-West Gotland Basin are therefore tracked by the tracer concentrations at 30 m depth 1 yr after the initiation. We will also track the fluxes to the upper 30 m, which correspond to the depth of the shallow areas discussed by Eilola et al. (2012). The tracer concentration at 60 m depth is evaluated after 6 months, in order to obtain a picture of the source regions just above the halocline layer.

The model was run continuously from 1960 to 2009 and the tracer was restarted with new fields of initialisation at some selected dates during the run. The initiation years (1960, 1964, 1969, 1975, 1979, 1992, 1997, 2002 and 2007) for tracers in the longer experiments were selected to cover periods having major inflows according to Table 10.2 in Feistel et al. (2008). In these experiments, we follow the

evolution of tracers during several years after initiation, until the next date when the initiation is reset again.

The inter-annual variability of tracer dynamics are evaluated from similar experiments but with tracers reset and initiated on January 1 every year. In these experiments the tracers are therefore followed during 1 yr after the initiation. A negligible fraction of the tracer leaves the Baltic Sea during the first year (0.06%) and still after 3 yr in the longer experiments on average only 2.5% of the tracer mass has been exported to the Skagerrak.

To clarify the impact of deep water inflows on the uplift of tracers, the annual experiments are divided into three cases representing average conditions during periods with no deep water inflows (1963, 1971, 1985, 1986, 1989, 1990, 2001, 2006), weaker inflows (1967, 1968, 1973, 1978, 1981, 1987, 2004, 2007) and stronger inflows (1969, 1970, 1977, 1980, 1993, 1994, 1997, 2003). The aim was to have a clear as possible separation without overlaps between the characteristics in the three cases (see Section 3.2).

For the investigation of the importance of different water masses on the East Gotland Deep water renewal we used 17 tracers to mark the water masses from the Eastern Gotland Basin (GO), the North-West Gotland Basin (NW), the Gulf of Bothnia (BOT), the Gulf of Finland (GOF), the Bornholm Basin (BH), and the entrance area (ENT) (Fig. 1). The initial concentration of the tracers was set to 1.0. The tracers from the GO and the NW were divided into five layers according to the vertical grid resolution of the model; 0–69 m (GO5 and NW5), 69–99 m (GO1 and NW1), 99–123 m (GO2 and NW2), 123–150 m (GO3 and NW3) and finally below 150 m depth (GO4 and NW4). According to the average vertical oxygen distribution (Fig. 2b) the

selected ranges from deeper waters correspond approximately to the layers in the halocline and just below the halocline, in the redoxcline layer and in anoxic bottom waters. The volume of the water masses below the halocline containing tracers (Table 2) occupies about 30% of the total volume in the GO and NW volume (Table 1). The initial tracer mass is distributed fairly similar between the two basins, about 57% of the tracer mass in the GO and 43% in the NW basin. The tracers in the BH were divided into layers 0–51 m (BH4), 51–60 m (BH1), 60–69 m (BH2) and below 69 m (BH3). An additional tracer was used to emulate nutrient release from sediments at 60–99 m depth in GO (Btm tracer, see Fig. 1). In this case the tracer concentration was set to 1.0 when the water was in contact with the sediment in the selected areas.

### 3. Results and discussion

#### 3.1. Tracer dynamics after major Baltic inflows

*3.1.1. Renewal of Gotland Deep water.* During an inflow event the deep water is replaced and the old water is lifted up to the overlying layers as seen, e.g. after the inflow in 2003 (Reissmann et al., 2009). In this case the oxygen poor and phosphate rich waters were lifted from 100 m depth to about 70 m depth. The effect is seen from the tracer GO4 (Fig. 3a) which is lifted up and diluted by the intruding new water masses and spread through the halocline towards the surface layers after an inflow. A noteworthy result is the low surface-layer tracer concentration (Fig. 3a), less than about 0.5% of the initial concentration, caused by the dispersed Gotland Deep water. This is due to the small

Table 1. The total volume and the surface layer volume (0–30 m) of the Baltic Sea sub-basins (in km<sup>3</sup>)

Basin name	Basin Nr	Abbreviation	Total volume	Volume 0–30 m
Total Baltic Sea	1	TB	22 562	10 297
Kattegat <sup>a</sup>	2	KA	485	397
The Sound <sup>a</sup>	3	OR	23	23
The Belt Sea <sup>a</sup>	4	BE	420	419
Arkona Basin <sup>a</sup>	5	AR	406	314
Bornholm Basin	6	BH	1749	1002
East Gotland Basin	7	GO	6953	2679
North-West Gotland Basin	8	NW	4791	1738
Gulf of Riga	9	GR	431	366
Gulf of Finland	10	GF	1118	703
Archipelago Sea <sup>b</sup>	11	AS	49	49
Åland Sea <sup>b</sup>	12	AL	327	104
Bothnian Sea <sup>b</sup>	13	BS	4353	1715
Bothnian Bay <sup>b</sup>	14	BB	1455	787

The basin names and abbreviations used in the text are shown together with the corresponding basin numbers (Fig. 1).

<sup>a</sup>Included in the entrance area (ENT).

<sup>b</sup>Included in the Gulf of Bothnia (BOT).

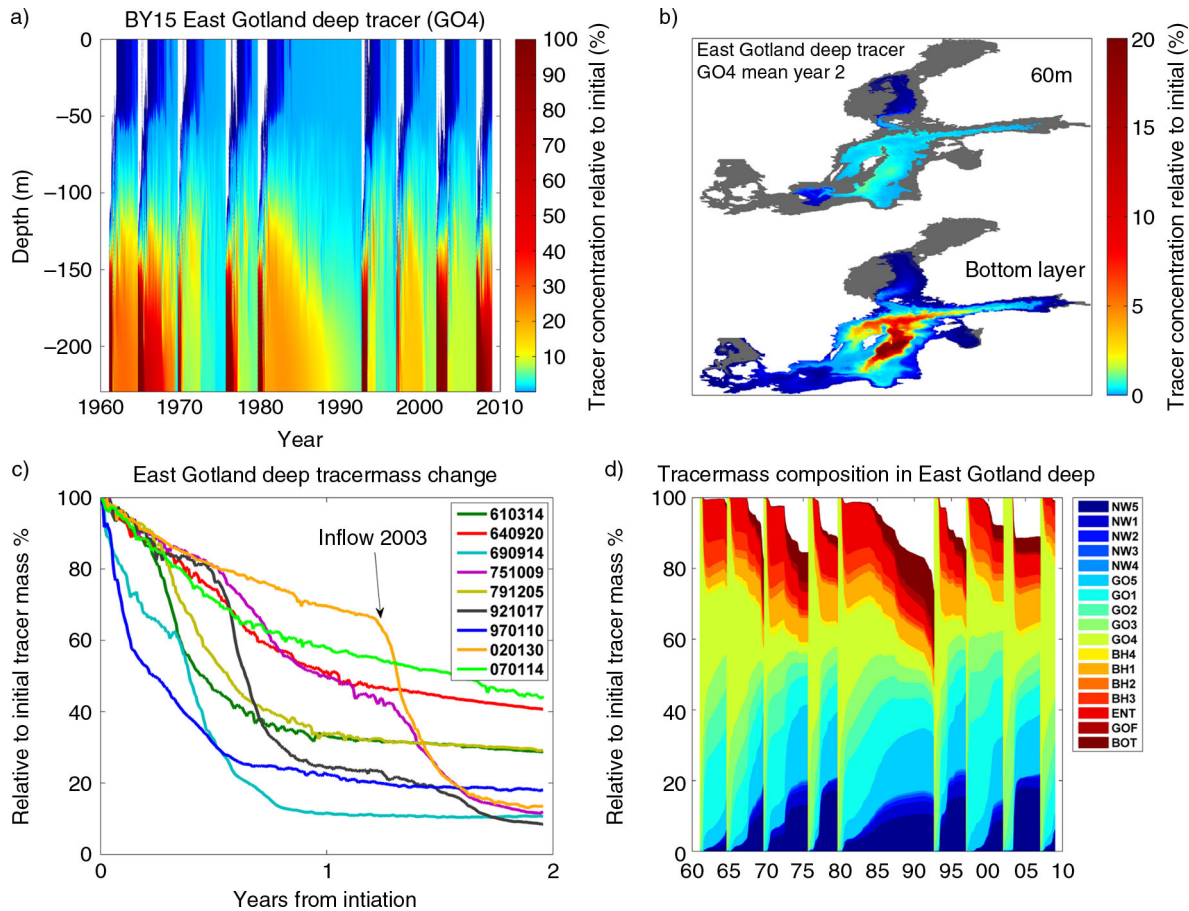


*Fig. 3.* Time series of vertical profiles of tracer GO4 at BY15 (upper left panel, a). Note the sharp gradient of colour scale used to separate the very low concentrations in panels a and b. The horizontal distribution (at 60 m depth and in the bottom layer) of the mean GO4 tracer concentration for all inflow cases 2 yr after the initiation dates is shown (in% of the initial concentration) (upper right panel, b). The decline after inflows of the GO4 tracer mass below 150 m depth is summarised in the lower left panel (c). The initiation date (see legend in Fig. 3c) was in each new tracer case defined by the first day when a water mass originating from BH was observed in the Gotland Deep. The arrow indicates the start of the large deep water inflow in 2003 depicted more than 1 yr after the tracer initiation in 2002. The lower right panel (d) shows temporal changes of the relative contributions from different water masses to the tracer mass in the Gotland Deep below 150 m (see explanation of legend abbreviations in methods). The tracer mass is shown relative to the initial tracer mass (i.e. at each initiation occasion GO4 is equal to 100%). White colour indicates the influence from undefined waters without tracers.

volume below 150 m depth in GO that causes the tracer concentration to reduce by almost a factor of 100 when the tracer mass is dispersed to the entire volume of NW and GO (Table 2). The tracer in the Gotland Deep is after 2 yr generally replaced by more than 50% by new water masses (Fig. 3c) and only 10 to 20% of the initial tracer remains after about 1 yr in the strongest inflow cases. In the more modest inflow cases there are still more than 50% of the initial tracer mass left in the Gotland Deep 1 yr after the initiation. The 2 yr time periods following the tracer initiations may, however, show several occasions with inflows of new deep water and especially the major events in 1977, 1993 and 2003 show large declines in tracer mass. This effect is exemplified in Fig. 3c by an arrow indicating the start of

the inflow in 2003. The average tracer composition in the Gotland Deep water 2 yr after the initialisation (Fig. 3d) consists of about 15% tracer mass from BH (90% from below 51 m), 10% from the entrance area, 9% from the NW, 4% from unmarked waters entering from the open boundary, rivers and the GR, and about 1% comes from the BOT and the GF. The largest contribution (about 61%) comes from GO, mainly from GO4 (19%) and GO1 (16%) and less from GO2 (9%), GO3 (9%) and GO5 (8%), respectively. In a natural situation, the concentrations in the deep water after inflows would largely depend on the blend of the actual nutrient and oxygen concentrations in these waters, but also on the release of nutrients and the oxygen consumption by ongoing mineralisation and decomposition of organic matter.

Table 2. The volume ( $\text{km}^3$ ) of the sub layers with tracer initialisation

Tracer layer	Depth range	Volume $\text{km}^3$	RTV
Sum all layers	69 m–bottom	3576	0.305
GO1	69 m–99 m	1182	0.101
NW1	69 m–99 m	890	0.076
GO2	99 m–123 m	424	0.036
NW2	99 m–123 m	320	0.027
GO3	123 m–150 m	263	0.022
NW3	123 m–150 m	197	0.017
GO4	150 m–bottom	174	0.015
NW4	150 m–bottom	125	0.011

The fraction of tracer water volume (RTV) relative to the total volume ( $11\,744\text{ km}^3$ ) of GO and NW (Table 1) is also shown.

In a later stage of the temporal development in the longer experiments one may also notice an increasing influence from tracers in the NW and the BOT as well as from the undefined waters.

### 3.1.2. Dispersion of the East Gotland deep water tracer.

Time scales of lateral homogenisation of tracers are short compared to the water residence time in the Baltic. The tracer release experiment by Holtermann et al. (2012) showed that the lateral dispersion of deep water occurs on time scales of a few months. The model results from the present study show that most of the spreading of the East Gotland deep water tracer takes place along the bottom layers of the Baltic and that significant concentrations (5–10% of the initial concentrations) of the tracer may be found to the north and the west of the island Gotland 2 yr after the tracer initiations (Fig. 3b). These dispersion results are in accordance with the findings from the tracer release experiment described by Holtermann et al. (2012). Small

tracer amounts emanating from the Gotland Deep may, however, also be found in the Gulf of Finland and the Gulf of Bothnia. The difference in the general dispersion pattern between weak and strong inflows is small but the concentrations differ since more tracers are removed from the deep water and transported to the northern Gotland Basin during the stronger inflows.

### 3.1.3. Comparing tracer and phosphate concentration changes in 2003.

It is not straightforward to compare the changes in tracer concentrations directly with surface layer  $\text{PO}_4$  concentrations since the latter depend on the seasonal biogeochemical cycles in the surface layers as well as on the horizontal and vertical gradients that have been built up during several years. However, as an example, in Fig. 4a we show the accumulation at 30 m depth of the tracers emanating from below 69 m depth in NW and GO. The tracer was initiated in January 2002 and the accumulation is calculated for the second year, i.e. year 2003 when a major inflow occurred. In this case the tracer has during the first year already built up some large-scale gradients also in the upper parts of the Baltic Sea. The observed changes therefore include both a fraction of the remaining tracers directly lifted up from below 69 m depth, as well as an addition of tracers from the previous year that are already available above the halocline in the beginning of 2003.

The results show an accumulation of tracer in NW and the areas surrounding the island Gotland, especially to the west and south. One may note that the increase in the northern and western parts correlates to areas where we observe increases of  $\text{PO}_4$  concentrations (Table 3) while the observations at the southern and eastern stations show unchanged or decreasing  $\text{PO}_4$  concentrations. These stations are more affected by the inflows of surface waters with lower  $\text{PO}_4$  concentrations from the entrance areas than by the uplifted

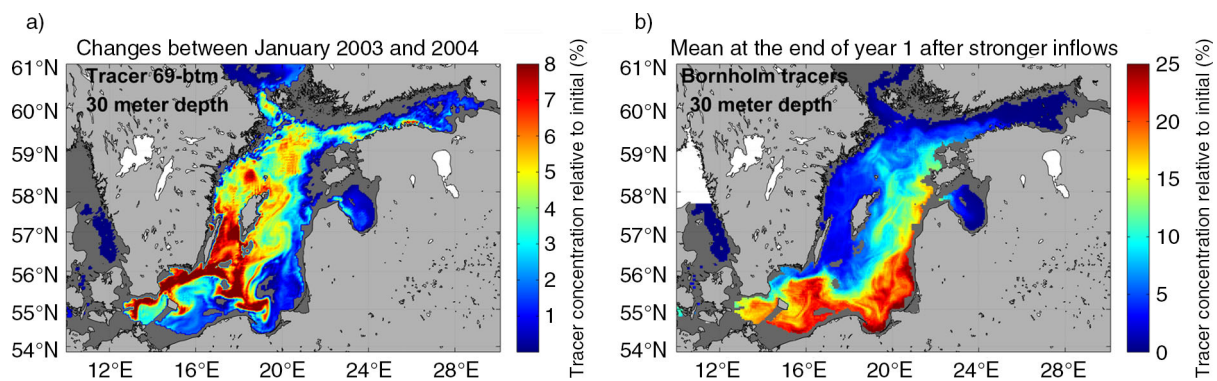


Fig. 4. The left panel shows the horizontal distribution of concentrations at 30 m depth of the tracers accumulated between the end of January 2003 and end of January 2004 (a). The sum of all GO and NW tracers initiated below 69 m are shown in% relative to the initial tracer concentration. The right panel shows the horizontal distribution at 30 m depth of the BH tracer concentration in the end of December (b). The mean for a sub set of years with stronger inflows is shown.

Table 3. Observed  $\text{PO}_4$  concentrations ( $\mu\text{mol L}^{-1}$ ) at 30 m depth in January 2003 and 2004

Station	2003	2004	Relative concentration%
BY31	0.50	0.91	182
BY32	0.50	0.93	186
BY38	0.50	0.82	164
BY5	0.54	0.45	83
BSIII	0.62	0.47	76
BY10	0.67	0.54	81
BY15	0.63	0.63	100
BY20	0.60	0.76	127
BY29	0.66	0.79	120

See positions of stations in Fig. 1. The last column shows the relative concentration in 2004 (in%) compared to the concentration in 2003.

lower layer water masses. The effect of inflows is illustrated by the average spreading pattern at 30 m depth of modelled Bornholm tracers 1 yr after the stronger inflows have taken place (Fig. 4b). The results show that BH tracers are flushed towards the east and occupy the southern and eastern parts of the Eastern Gotland Basin.

### 3.2. Annual tracer dynamics

3.2.1. *The deep water renewal in 2003.* The timing of the 2003 inflow was well reproduced by the model as seen from the intrusion of BH tracer mass below 150 m depth in the

East Gotland Basin (Fig. 5). The good correspondence with the observed salinity changes at 200 m depth in the central East Gotland Basin 2003 indicates that the temporal development of this inflow is also well simulated. According to the model experiment (Table 4), about 85% of the tracer mass was removed by the dilution effect during the first year after the 2003 inflow. Schneider (2011), however, estimated that only 2/3 of the  $\text{PO}_4$  removal was due to dilution while the rest was suggested to be a consequence of the precipitation of iron(III)-hydroxo-phosphates (Fe-P) at the sediment surface under oxic conditions.

The drop in  $\text{PO}_4$  concentration during 2003 was estimated in the present study from the model results combined with observations of  $\text{PO}_4$ . The weighted mean  $\text{PO}_4$  concentration of the different water masses contributing to the East Gotland Deep water at the end of 2003 is  $2.11 \mu\text{mol L}^{-1}$  (Table 4). The results agree well with the observed drop in mean  $\text{PO}_4$  concentrations from  $6.29 \mu\text{mol PO}_4 \text{ L}^{-1}$  in January 2003 to  $2.10 \mu\text{mol PO}_4 \text{ L}^{-1}$  in January 2004. The mean uptake of  $\text{PO}_4$  from the water column to hydrated metal oxides at the sediment surface is relatively small according to the analysis of sediment phosphorus fluxes in the model experiments by Almroth-Rosell et al. (2014). Hence, it is most likely that the drop in  $\text{PO}_4$  observed by Schneider (2011) is explained by dilution effects from the inflow and the increased mixing efficiency following the energy input from the inflow. The precipitation of  $\text{PO}_4$  from the water column to the sediment surface is therefore less than suggested by Schneider (2011) and the possible

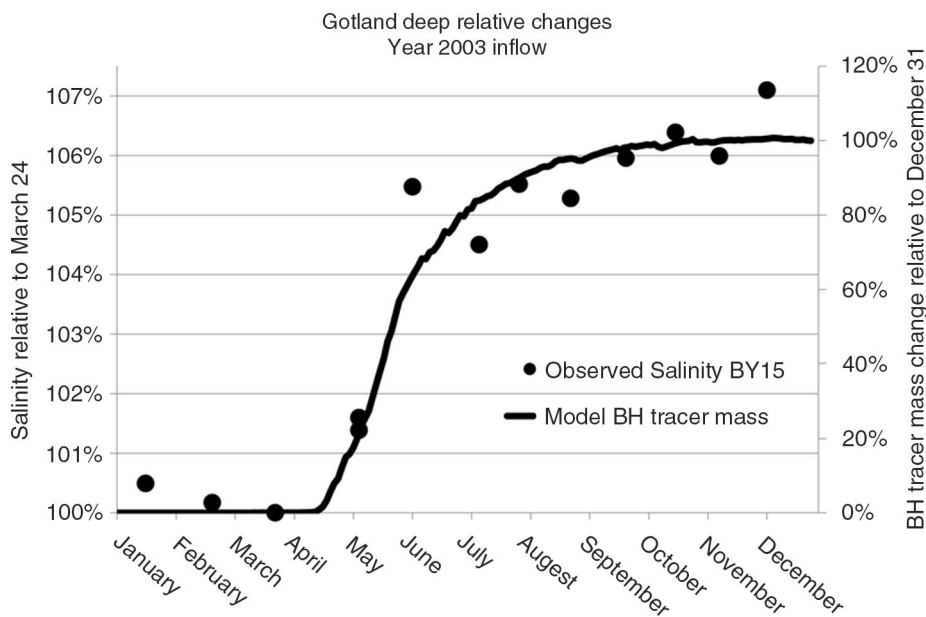


Fig. 5. The relative changes of salinity (observations from 200 m depth at station BY 15, SHARK data) and of the modelled inflow of BH tracer mass (51 m–btm) below 150 m depth in GO. The salinity change is shown relative to the situation just before the inflow while the tracer concentration (that is zero at start) is shown relative to the final concentration in order to make the results comparable.

*Table 4.* The relative contributions (RTV) from tracers found below 150 m in the East Gotland Deep at the end of 2003 and the mean PO<sub>4</sub> concentration of the inflowing waters estimated from SHARK observations (column 2, rows 1–6)

	RTV (%)	Mean PO <sub>4</sub> (μmol L <sup>-1</sup> )
1. GO1	18.7	2.27
2. GO2	8.0	3.13
3. GO3	5.4	3.66
4. BH 51–btm	10.1	0.97
5. ENT	18.9	0.40
6. Other	24.2	0.56
7. GO4	14.8	6.29
8. GO4 (Jan 2004)		2.10
9. Weighted mean	–	2.11

The mean PO<sub>4</sub> value (March–December) from 30 to 40 m depth in the Arkona Basin is used for the waters coming from the entrance area (ENT). The mean PO<sub>4</sub> value (March–December) from BY15 0–70 m is used as a proxy for other water masses (row 6). The mean PO<sub>4</sub> concentrations of the East Gotland Deep water in January 2003 and in January 2004 are shown in rows 7 and 8, respectively. The last row (9) shows the weighted mean calculated at the end of 2003 based on the relative contributions from different tracers.

precipitation of PO<sub>4</sub> to hydrated metal oxides in the water column is also of minor importance in accordance with the discussions by Schneider (2011). The tracer studies in the present paper may therefore be regarded as good representations of the possible pathways of PO<sub>4</sub> from the deeper parts to the surface layers of the Baltic Sea.

### 3.2.2. Inter-annual variability of the deep water renewal.

The deep water is subjected to stagnant periods, as in the 1980s when on average about 43% of the tracer mass is removed each year, and high-inflow years, like 1969 when up to 90% of the tracer mass is removed in the model experiment (Fig. 6). Stronger inflows show an annual mean tracer removal of more than 70%. Reissmann et al. (2009) suggested that the longer residence time of the deep water during stagnation periods results from the lack of energy imported by the inflows to the vertical mixing processes. The largest tracer decrease in the model experiments generally takes place during the month directly following the tracer initiation (not shown). A sensitivity experiment with a reset of tracer concentrations on July 1 every year shows that the changes during the first month are slightly larger on average if the experiment starts in January (–24% per month) compared to a start in July (–17% per month). The corresponding changes during the last months of the annual experiments show an average change of –3% and –7% per month in December and June, respectively. There are some differences between certain years in the annual changes of the two experiments (not shown) depending on

the timing of inflows and the fact that we study changes between winters in one case and summers in the other case, but the general results are similar. The rapid change of tracer mass in the beginning of the experiments is generally explained by quick erosion of the upper layers, which occupies most of the volume of the deep basin.

In case of stronger inflows the tracer mass may be replaced all the way to the deepest parts. This is exemplified by the tracer transects at the end of four different years (colour inlets in Fig. 6) of the experiment restarted in January. The monthly changes occasionally also show oscillations when the tracer mass is increased because the tracer is flushed back again to the GO deep water. This can be noticed when the remaining deep water tracer mass becomes low and the relative impact from recirculated tracers becomes larger. Hagen and Feistel (2004) measured during 1999–2002 the currents 20 m above the seafloor at about 200 m depth in the northeast part of the East Gotland Basin. They found a permanent northward current velocity of 3 cm/s and hourly along-slope fluctuations with peak values of –18 cm/s to +40 cm/s. The large-scale oscillations are forced, e.g. by inflow dynamics caused by varying sea level in Kattegat and atmospheric cyclones travelling across the Baltic Sea. The hydrodynamics behind the oscillations and the interactions between barotropic and baroclinic mechanisms are discussed more in detail by, e.g. Reissmann et al. (2009) and by Hagen and Feistel (2004).

### 3.2.3. Comparison with the in-situ tracer release experiment period 2007–2009.

The tracer release experiment by Holtermann et al. (2012) was performed in the years 2007–2009 when our model, in accordance with the in-situ data, indicates a relatively modest inflow period. This can be noticed both in the annual (Fig. 6) and the long term tracer experiments (Fig. 3c). At the end of 2008 the new tracer mass emanates mainly from the upstream basins and from the surface layers of the NW and GO (Fig. 3d). Only one third of the new tracer mass in the GO deep water comes from the depth range 69–150 m inside the GO. It is therefore possible that the modest inflow may have influenced the Holtermann et al. (2012) tracer mass experiment by advective processes. The 45–50% average removal rate of tracer mass in 2007–2008 (Fig. 5) also indicates that more energy might have been available for the dispersion of tracer mass during their tracer experimental period than during more stagnant periods as in 2006 or in the 1980s.

## 3.3. Horizontal and vertical fluxes of tracers

### 3.3.1. Dispersion of tracers from below the halocline.

The results show that the coasts of NW, and GF, and in case

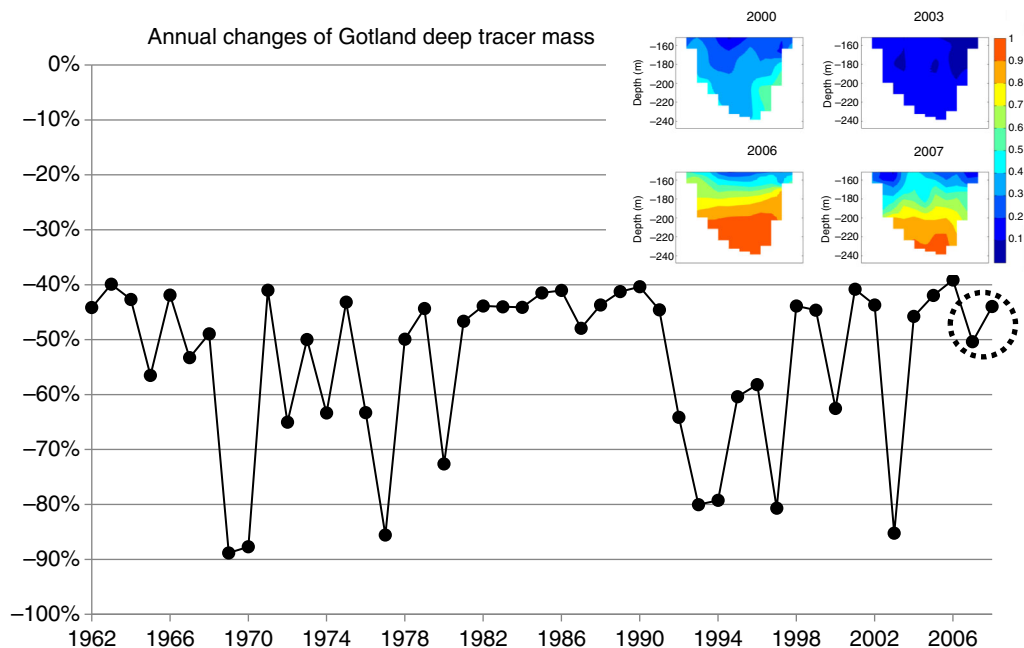


Fig. 6. Annual changes (relative to the initial value reset on January 1 every year) of tracer mass (GO4) in Gotland Deep (large solid dots). The dotted circle indicates the Baltic Sea tracer experiment period in 2007–2009 by Holtermann et al. (2012). The colour inlets show W–E transects ( $\sim$ E19.6°–E20.4°) in the central GO ( $\sim$ N57.3°) of the tracer concentration profiles (150 m–btm) at the end of December in the years 2000, 2003, 2006 and 2007.

of inflows also the Estonian coast in GO, are regions where we after 6 months at 60 m depth find tracers lifted up from below the halocline (Fig. 7, left column). Under situations with poor oxygen conditions below the halocline in the Baltic Proper these bottom areas may therefore potentially be affected by an advection of poisonous anoxic and phosphate rich waters from the deeper parts. A common signature of all annual cases in Fig. 7 (right column) is a focus of tracers along the Swedish east coast and at the western and southern sides of Gotland. Differences between the cases are in general mainly explained by increased concentrations when inflows occur, with the largest impact obtained in the stronger inflow cases. The highest tracer concentrations are found along the rim of the NW basin indicating the influence from bottom topography on the rate of vertical tracer spreading which was also pointed out by Holtermann et al. (2012). The results differ partly from those presented by Meier (2007) because he marked inflowing water with a salinity larger than 17 in the Arkona Basin instead of old deep water that is lifted up by the inflowing water as in this study. On average during the 24 yr period studied by Meier (2007), the locations with upward fluxes across the halocline of the heavier water were scattered. In agreement with the present study, however, relatively large upward fluxes were found in the Northern Basin north of Gotland island and at the western coast of Gotland.

In this study, elevated concentrations are also found east and south east of Gotland, in the northern Bornholm Basin and in the central parts of the GO Basin. These results may be explained by the southward transports of nutrients along the Swedish coast that continues to the south and to the west along the Swedish coast, into the Bornholm Basin and further into the Arkona Basin (Eilola et al. 2012). Another branch of the southward transport joins the cyclonic circulation in the central Baltic Proper. In total, about 9% of all initial tracers mass below 69 m in the GO and NW is found in the upper 30 m of the total Baltic Sea (TB) 1 yr after the stronger inflows (Fig. 8). This number is about 15% higher than in the case with no inflows while the tracer content in the NW is up to 29% higher in the cases with inflows (Table 5). The uplifted amount of NW tracer is about 20% larger during the stronger inflow cases with a 40% increased contribution in the North-West Gotland Basin compared to the cases with no inflows.

If we assume an average concentration below the halocline of about  $3.0 \mu\text{mol PO}_4 \text{ L}^{-1}$ , similar to 2003, an annual amount of about  $29 \times 10^3$  and  $25 \times 10^3$  tons of  $\text{PO}_4$  will be added to the surface layers in the strong inflow cases and cases with no inflows, respectively. Hence, the annual supplies of P from the deep parts directly to the productive surface layers are of the same order of magnitude as the waterborne inputs of P to the entire Baltic Sea (HELCOM, 2011). Regionally the impact may be quite large (Fig. 7).



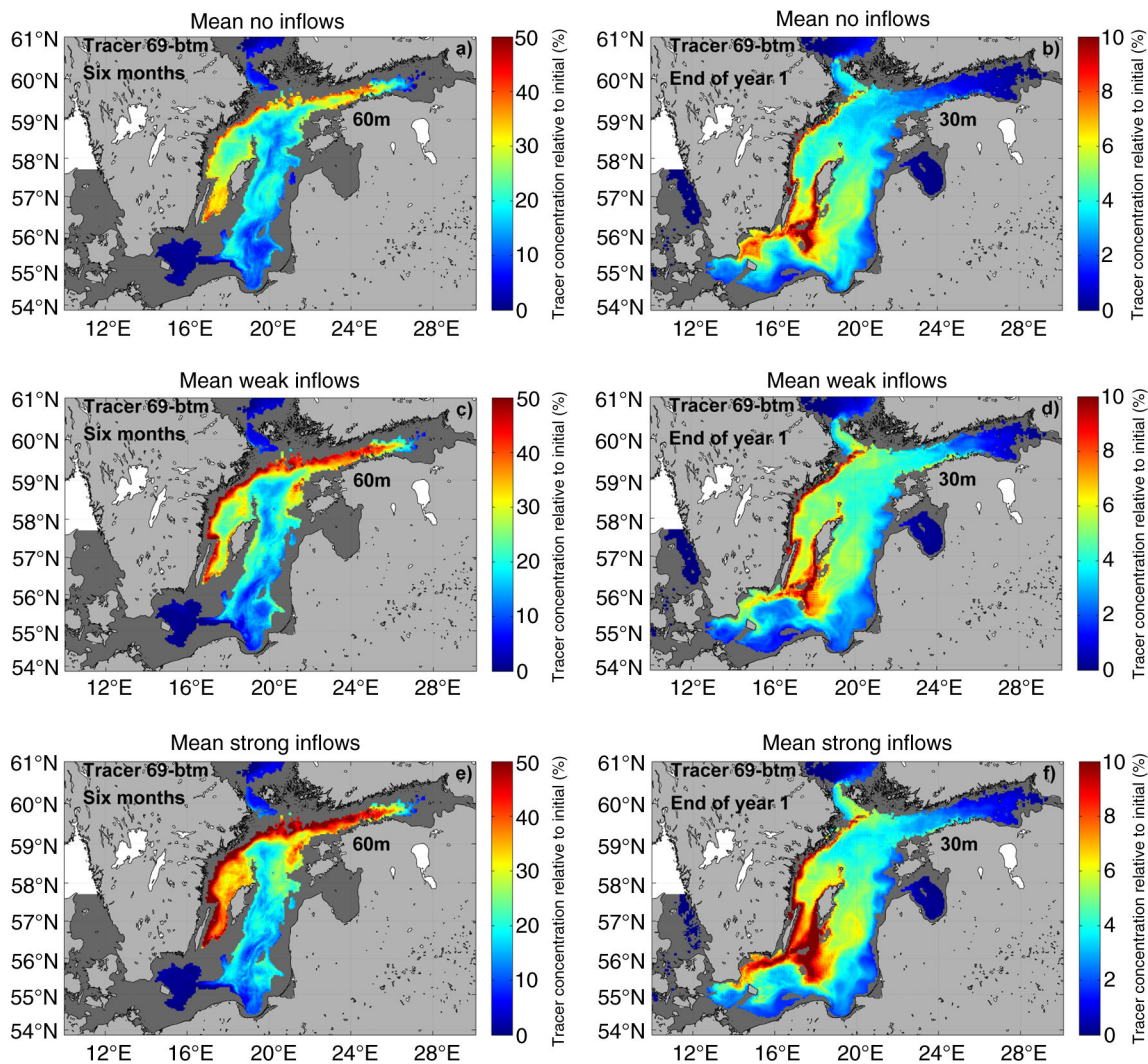


Fig. 7. The horizontal distribution of the mean tracer concentration at 60 m depth in end of June (left column) and at 30 m depth in the end of December (right column) from periods with no deep water inflows (upper panels, a and b), weaker inflows (middle panels, c and d) and with stronger inflows (lower panels, e and f). Note different scales of colour bars. The sum of all GO and NW tracers initiated below 69 m are shown.

Concentrations from 10% up to about 25%, corresponding to  $0.3\text{--}0.75\ \mu\text{mol PO}_4\ \text{L}^{-1}$ , may be found at 30 m depth in the coastal regions between the Swedish mainland and Gotland. Concentration increases of up to 10% (corresponding to  $0.3\ \mu\text{mol PO}_4\ \text{L}^{-1}$ ) between the cases with no inflows and cases with strong inflows may locally be found (not shown) in the same regions with a focus southwest of Gotland island. Using the numbers from Tables 2 and 5 together with the 0–30 m volume of the NW and GO basins ( $4417\ \text{km}^3$ ) an average concentration in the surface layer of North-West and East Gotland basins of about  $0.13\text{--}0.15\ \mu\text{mol PO}_4\ \text{L}^{-1}$  is calculated. The additional supply of  $\text{PO}_4$  from strong inflows therefore gives only a minor average absolute  $\text{PO}_4$  increase ( $0.02\ \mu\text{mol PO}_4\ \text{L}^{-1}$ ) compared to the

cases with no inflows. The overall direct impact of major Baltic inflows on the uplift of nutrients from the deepest layers to the surface waters is small because the processes causing vertical transports are comparably large also in the cases with no major inflows as will be further discussed in Section 3.3.3.

*3.3.2. Dispersion of the bottom tracer.* The potential impact of uplifted bottom tracer emulating phosphorus release from sediments at 60 to 99 m depth in GO (see Fig. 1) on surface layer concentrations, is studied by the tracer concentrations observed at 30 m depth. These sediments correspond to the areas where Eilola et al. (2012) found the

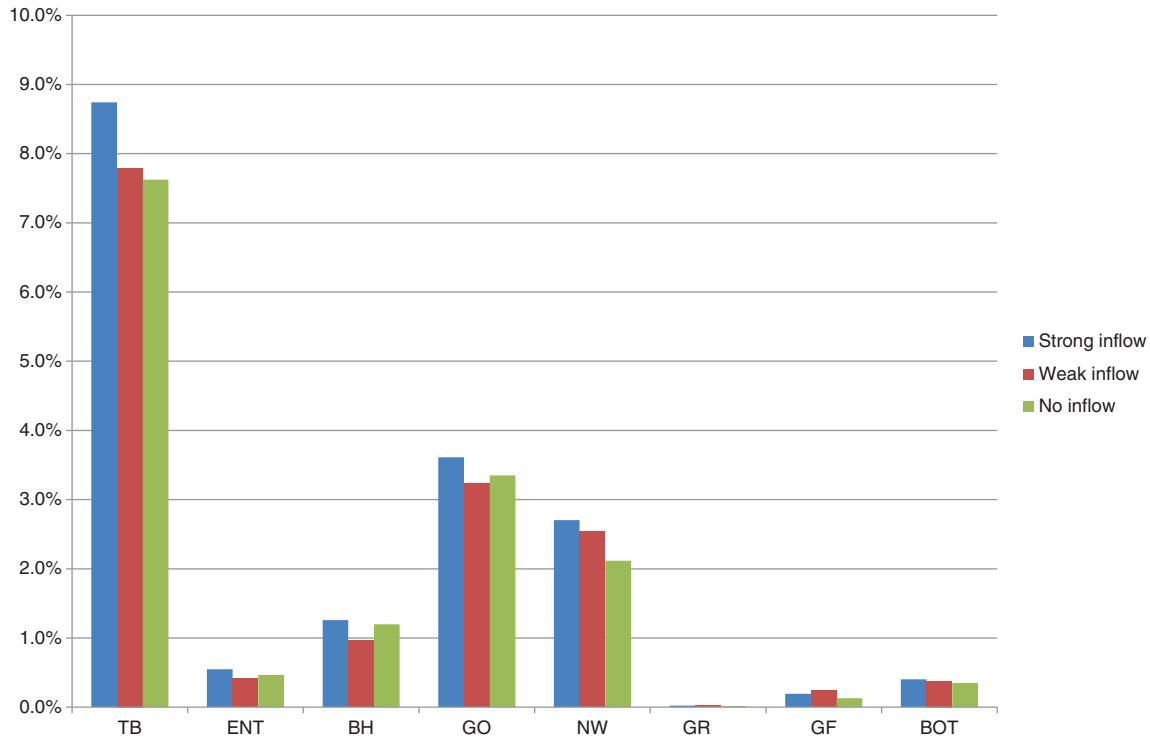


Fig. 8. The mean integrated amount of tracer from all GO and NW tracers initiated below 69 m (in% of the total initial mass) accumulated in the upper 30 m of the entire Baltic Sea (TB) and the sub-basins 1 yr after the initiation dates (end of December) in years with strong, weak or no inflow cases.

largest exports of phosphate in their model experiments. The detailed analysis of sediment fluxes by Almroth-Rosell et al. (2014) showed that this export is caused by large phosphorus release from areas with anoxic sediments that may be found between 60 and 150 m depth in the model. An important

feature of these bottom tracers (Fig. 9) is the accumulation at the eastern coasts of the GO basin. Due to the high vertical dispersion along the Baltic Sea bottoms, a considerable fraction of the phosphorus released from the sediments below the halocline may reach the surface layer and

Table 5. The mean integrated amount of tracer (in% of the total initial mass) accumulated in the upper 30 m of the total Baltic Sea (TB) and the sub-basins 1 yr after the initiation dates (end of December) in years with strong, weak or no inflow cases (cf. Fig. 6)

%	TB	ENT	BH	GO	NW	GR	GF	BOT
Strong inflow	8.7	0.5	1.3	3.6	2.7	0.0	0.2	0.4
Weak inflow	7.8	0.4	1.0	3.2	2.5	0.0	0.2	0.4
No inflow	7.6	0.5	1.2	3.3	2.1	0.0	0.1	0.4
GO tracer strong	6.0	0.2	0.5	3.9	1.3	0.0	0.1	0.0
GO tracer weak	5.6	0.1	0.4	3.5	1.4	0.0	0.1	0.1
GO tracer no inflow	5.5	0.2	0.5	3.5	1.2	0.0	0.0	0.0
NW tracer strong	12.4	1.0	2.3	3.3	4.6	0.0	0.4	0.9
NW tracer weak	10.7	0.8	1.7	2.9	4.0	0.0	0.5	0.8
NW tracer no inflow	10.4	0.9	2.1	3.1	3.3	0.0	0.3	0.8
Bottom tracer no inflow	100.0	1.5	4.7	71.0	19.8	1.2	1.1	0.7
Bottom tracer weak inflow	98.1	1.4	4.6	67.9	20.6	1.2	1.7	0.8
Bottom tracer strong inflow	87.7	1.7	4.6	60.9	17.8	1.1	1.1	0.5

The 'Strong', 'Weak' and 'No inflow' rows show the relative contribution from all GO and NW tracers initiated below 69 m. The rows 'GO tracer' and 'NW tracer' show the individual relative fraction of uplifted GO and NW tracers (in% of the initial mass in each sub basin). The rows 'Bottom tracer' shows the relative contribution of bottom tracers accumulated in the upper 30 m (in% of the mean tracer mass 0–30 m in the TB in the no inflow case).

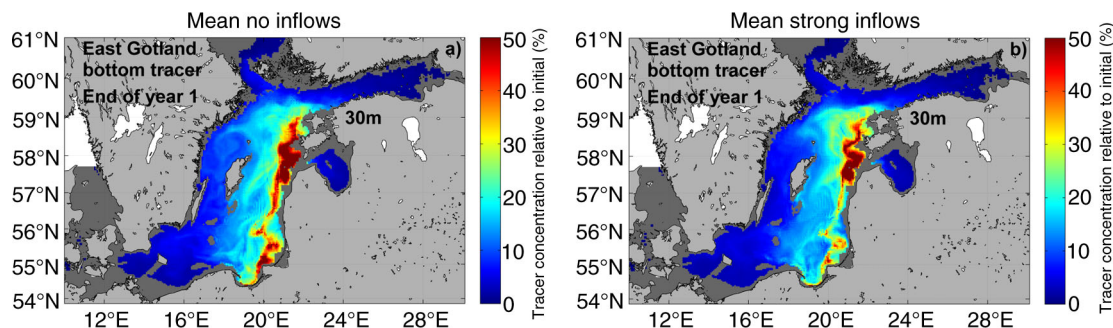


Fig. 9. The horizontal distribution at 30 m depth of the mean bottom tracer concentration (emulating phosphorus released from sediments at 60–99 m depth in GO see Fig. 1) in the end of December from periods with no deep water inflows (left, a) and with stronger inflows (right, b). The tracer concentration is shown relative to the constant bottom concentration set at the sediment interface. No larger differences were seen between the cases with no or only weak inflows (not shown).

contribute to eutrophication especially in the coastal regions of the eastern Baltic Proper. Both the amounts of bottom tracers in the upper 30 m in the GO basin and its total amount in TB are reduced in the cases of inflows (Table 5). After strong inflows there is a weakening of the tracer concentrations in the south eastern parts of the Baltic Proper which was also noticed from the integrated tracer mass in Table 5. The reason of these reductions is partly due to the intrusion of water from the Bornholm Basin that flushes the eastern parts of the Baltic Proper (Fig. 4b) and hampers the uplift of bottom tracers.

**3.3.3. Transport processes.** In this section possible mechanisms that may cause the observed regional differences in the modelled uplift of tracers from the deeper layers of the Baltic Proper are discussed. The layers below the halocline are regularly ventilated by inflows from the entrance area as illustrated by concentration differences along the East Gotland transect of the tracer from below 51 m depth in the Bornholm Basin (Fig. 10a and b). Actually, it has been shown that major parts of the regular inflows are interleaved in or below the halocline layer with maximum transports at about 100 m depth (e.g. Stigebrandt, 1987; Meier and Kauker, 2003). Hence, the energy supplied to the dilution of tracers at about 150 m depth (discussed in Section 3.2.2) is most likely generated by these inflows. Earlier Reissman et al. (2009) pointed out that horizontal advection of saline water below the halocline is a dominating process for temporal changes and associated transports in the central Baltic Sea. A variety of possible processes such as near bottom currents, breaking internal waves and eddies causing turbulent vertical mixing through the halocline in the Baltic Sea were also discussed by Reissman et al. (2009). The importance of coastal upwelling was mentioned but the lack of large-scale quantifications limited the understanding about its importance.

The relatively small differences in total uplifted tracers between years with strong inflows compared to years with no inflows (Section 3.3.1) point to the importance of a large, not inflow related source of energy, most likely from the wind forcing upwelling, vertical mixing and the most frequent inflows that ventilate the halocline layer. The west-to-east transects in the end of 2003 and 2006 (Fig. 10c and d) show clearly examples on how the tracer from below the halocline is ascending towards the surface at the Swedish coast. The results are similar for both years even though there was a major inflow in 2003. There is an average south-westerly wind in the northern Baltic Proper ( $N58.8^\circ$ ), similar between the years 2003 and 2006 (wind direction  $8-30^\circ$ , wind speed about  $2 \text{ m s}^{-1}$ ). This wind causes an Ekman transport towards east and southeast at the ocean surface. As a consequence upwelling of water along the western boundary is found. The effect is exemplified by data at one grid point (Table 6) describing the first occasions with observed rapid increase of tracer concentrations closer to the surface at the Swedish coast of the section  $N58.8^\circ$  (Fig. 10c and d). One may note that the upper depth level with 15% tracer concentration was uplifted by more than 20 m during 6 d with dominating south and westerly winds. This has a large impact on the dispersion of tracers since the uplifted tracers become more exposed to the intense mixing taking place at the surface especially during winter time. A possible reason for the preferential uplift of tracers along the Swedish coasts is therefore the frequent occasions with upwelling that are forced by the predominant south-westerly winds in the Baltic Sea (Myrberg and Andrejev, 2003). Gidhagen (1987) noted that at the Swedish coast, upwelling may occur from depths of 20–40 m and cover areas up to 100 km along the coast and spreading 5–20 km into the sea. Correspondingly, at the coasts along the eastern Gotland Basin downwelling may occur due to eastward wind-driven transports (e.g. Kowalewski and Ostrowski, 2005). Downwelling may slow down the annual mean uplift of tracers.

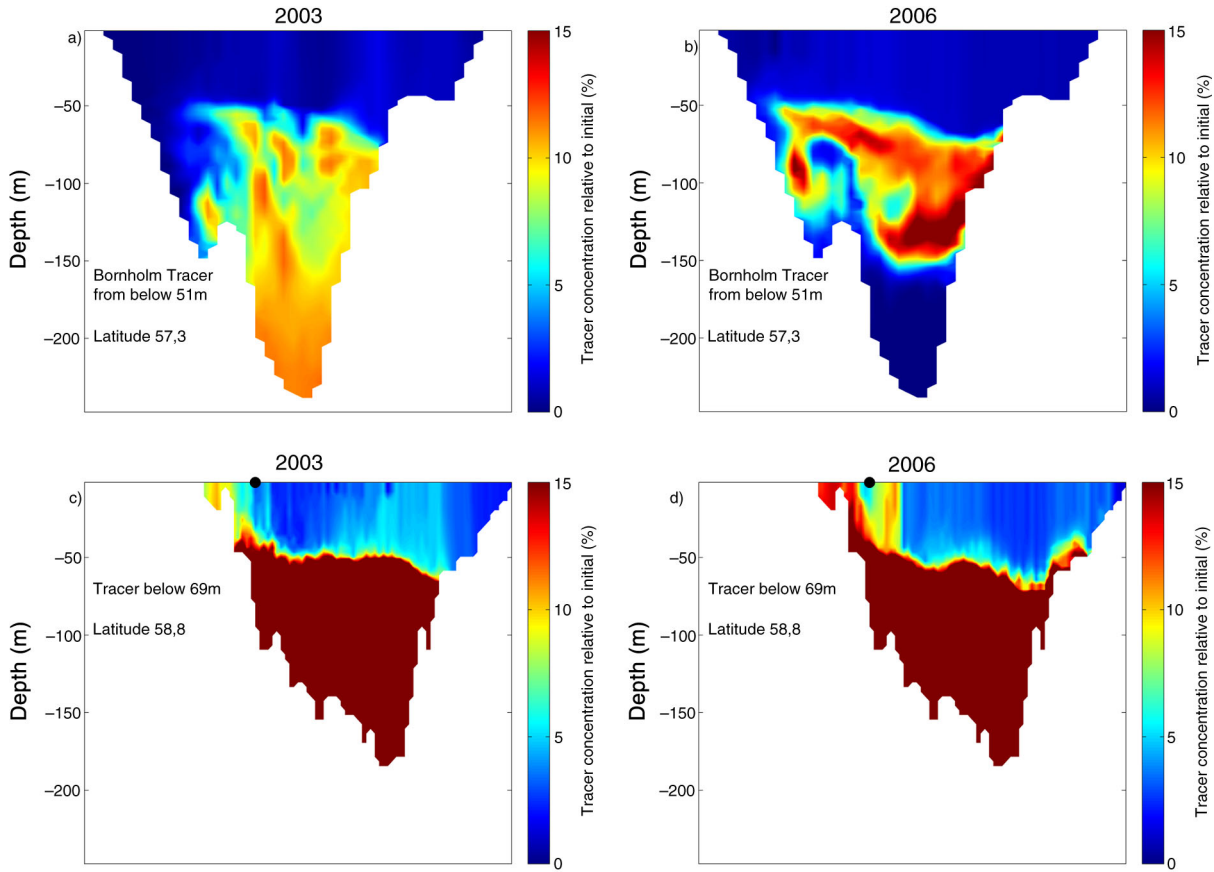


Fig. 10. West-to-east transects at the end of December in the years 2003 (left) and 2006 (right). The upper panels (a and b) show the Bornholm tracer (from below 51 m) concentrations between Gotland and Latvia at about  $N57.3^\circ$  (in% of the initial concentration). The lower panels (c and d) show the tracer (from below 69 m) concentrations between Sweden and Estonia at about  $N58.8^\circ$  (in% of the initial concentration). The black dots shown at surface level depict the position studied in Table 6.

This explains why, in combination with the spreading of tracer-free water from the Bornholm Basin along the eastern parts of the Baltic Proper (Fig. 4b), the uplift of tracers is less intense in this region (Fig. 7).

Our results indicate that the impact from wind stress is an important factor, but a comprehensive investigation about the possible mechanisms causing the observed model results is out of the scope of the present paper. Coastal upwelling is a common feature in the entire Baltic Sea and there is a need for research about its causes and impacts on the transport of nutrients and harmful substances as discussed by Lehmann and Myrberg (2008). The role of upwelling is usually studied from temperature variations during the summer while there is less information available regarding upwelling during winter because the surface layer is homogenised due to storms and convection. Future work might therefore include detailed studies of how intense and deep reaching and how frequent up- and downwelling is along the western and eastern coasts in the model. The work may follow, e.g. the modelling concept

of Kowalewski and Ostrowski (2005) and include also ground truth information from in-situ experiments and remote sensing products.

Table 6. Changes of the upper level (H) of the 15% concentration of the bottom tracer below 69 m.

Date	Delta H (m)	Wind direction ( $^\circ$ )	Wind speed ( $\text{ms}^{-1}$ )
11 Jan 2003	–	16	5.9
13 Jan 2003	12	10	11.9
15 Jan 2003	18	121	8.5
17 Jan 2003	24	6	5.9
7 Jan 2006	–	236	4.1
9 Jan 2006	6	58	6.8
11 Jan 2006	15	18	7.7
13 Jan 2006	21	28	7.0

Model data were extracted from a position at about  $N58.8^\circ E18.3^\circ$  (cf. Fig. 10c and d). The first occasions with an observed rapid increase in level H in early January 2003 and 2006 are shown. The uplift is discretised due to the vertical grid resolution (3 m) and the 2-d output of the model run.

## 4. Conclusions

### 4.1. The deep water renewal

- The study of the renewal of the East Gotland Deep water below 150 m depth showed that, on average, 2 yr after the inflows almost 50% of the tracer mass in the deep East Gotland Basin came from tracer enriched water in the Bornholm Basin and the East Gotland Basin below the halocline (from depths less than 150 m). About 30% originated from well oxygenated surface waters and the rest 20% was remaining old GO deep water.

### 4.2. Uplift of tracers above the halocline

- We found that the coasts of the North West Gotland Basin and the Gulf of Finland, and in case of inflows also the Estonian coast in the East Gotland Basin, are regions where tracers from below the halocline are primarily lifted up above the halocline.

### 4.3. Uplift of tracers to the surface layer

- After 1 yr, tracers are accumulated at the surface along the Swedish east coast and at the western and southern sides of Gotland. Elevated concentrations are also found east and southeast of Gotland, in the northern Bornholm Basin and in the central parts of the East Gotland Basin.
- The model results indicate that the uplift of tracers along the Swedish coasts is likely caused by upwelling forced by south-westerly winds, but further studies are needed to clarify details of these processes.

### 4.4. Impact on eutrophication

- The annual supplies of phosphorus from the layers below the halocline directly to the productive surface layers are estimated to be of the same order of magnitude as the waterborne inputs of phosphorus to the entire Baltic Sea. The model results suggest that regionally the impact may be quite large but more sophisticated tracer experiments similar to Delhez et al. (2004) and Radtke et al. (2012) are needed to follow the nutrient tracers through the processes of biogeochemical cycling.

- The overall direct impact of major Baltic inflows on the annual uplift of nutrients from below the halocline to the surface waters is small because the processes causing vertical transports are comparably large also in the cases with no major inflows.
- The impact from the East Gotland Deep water on eutrophication in the Baltic Sea is expected to be small because the volume below 150 m is small.

### 4.5. Bottom tracer and sediment release

- Because of the high dispersion along the bottom in the Baltic, much of the phosphorus released from the sediments between 60 and 100 m depth in the East Gotland Basin may contribute to eutrophication especially in the coastal regions of the eastern Baltic Proper.

## 5. Acknowledgements

The research presented in this study is part of the Baltic Earth programme (Earth System Science for the Baltic Sea region, see <http://www.baltex-research.eu/balticearth>) and was funded by the Swedish Research Council for Environment, Agricultural Sciences and Spatial Planning (FORMAS) within the projects 'Impact of accelerated future global mean sea level rise on the phosphorus cycle in the Baltic Sea' (grant no. 214-2009-577) and 'Impact of changing climate on circulation and biogeochemical cycles of the integrated North Sea and Baltic Sea system' (grant no. 214-2010-1575). Additional support came from Stockholm University's Strategic Marine Environmental Research Funds 'Baltic Ecosystem Adaptive Management (BEAM)' and from the Norden Top-level Research Initiative sub-programme 'Effect Studies and Adaptation to Climate Change' through the 'Nordic Centre for Research on Marine Ecosystems and Resources under Climate Change (NorMER)'. In its final phase the research leading to these results received also funding from BONUS, the joint Baltic Sea research and development programme (Art 185), funded jointly from the European Union's Seventh Programme for research, technological development and demonstration and from FORMAS (grant no. 219-2013-2041).

The RCO model simulations were performed on the climate computing resources 'Ekman' and 'Vagn' jointly operated by the Centre for High Performance Computing (PDC) at the Royal Institute of Technology (KTH) in Stockholm and the National Supercomputer Centre (NSC) at Linköping University. 'Ekman' and 'Vagn' are funded by a grant from the Knut and Alice Wallenberg foundation.

We would like to acknowledge two anonymous reviewers for their constructive comments.

## References

- Almroth-Rosell, E., Eilola, K., Hordoir, R., Meier, H. E. M. and Hall, P. 2011. Transport of fresh and resuspended particulate organic material in the Baltic Sea – a model study. *J. Mar. Syst.* **87**, 1–12.
- Almroth-Rosell, E., Eilola, K., Kuznetsov, I., Hall, P. O. J. and Meier, M. 2014. The Baltic Sea sediment oxygen conditions and phosphorus dynamics – a 3D model study. *J. Mar. Syst.* Submitted.
- Beckmann, A. and Döscher, R. 1997. A method for improved representation of dense water spreading over topography in geopotential-coordinate models. *J. Phys. Oceanogr.* **27**, 581–591.
- Conley, D. J., Björck, S., Bonsdorff, E., Carstensen, J., Destouni, G. and co-authors. 2009. Hypoxia-related processes in the Baltic Sea. *Environ. Sci. Technol.* **43**(10), 3412–3420.
- Deleersnijder, E., Campin, J.-M. and Delhez, E. J. M. 2001. The concept of age in marine modelling: I. Theory and preliminary results. *J. Mar. Syst.* **28**, 229–267.
- Delhez, É. J., Lacroix, G. and Deleersnijder, E. 2004. The age as a diagnostic of the dynamics of marine ecosystem models. *Ocean Dynam.* **54**(2), 221–231.
- Delhez, E. J. M., Campin, J.-M., Hirst, A. C. and Deleersnijder, E. 1999. Toward a general theory of the age in ocean modelling. *Ocean Model.* **1**, 17–27.
- Eilola, K., Almroth-Rosell, E., Dieterich, C., Fransner, F., Höglund, A. and co-authors. 2012. Modeling nutrient transports and exchanges of nutrients between shallow regions and the open Baltic Sea in present and future climate. *Ambio.* **41**(6), 574–585. DOI: 10.1007/s13280-012-0319-9.
- Eilola, K., Gustafson, B. G., Kuznetsov, I., Meier, H. E. M., Neumann, T. and co-authors. 2011. Evaluation of biogeochemical cycles in an ensemble of three state-of-the-art numerical models of the Baltic Sea. *J. Mar. Syst.* **88**, 267–284.
- Eilola, K., Meier, H. E. M. and Almroth, E. 2009. On the dynamics of oxygen, phosphorus and cyanobacteria in the Baltic Sea; a model study. *J. Mar. Syst.* **75**, 163–184.
- Feistel, R., Nausch, G. and Wasmund, N. eds. 2008. *State and Evaluation of the Baltic Sea, 1952–2005. A Detailed 50-Year Survey of Meteorology and Climate, Physics, Chemistry, biology, and Marine Environment.* John Wiley & Sons, Hoboken, NJ, USA.
- Fischer, H. and Matthaus, W. 1996. The importance of the Drogden Sill in the Sound for major Baltic inflows. *J. Mar. Syst.* **9**, 137–157.
- Fonselius, S. and Valderrama, J. 2003. One hundred years of hydrographic measurements in the Baltic Sea. *J. Sea Res.* **49**, 229–241.
- Gerdes, R., Köberle, C. and Willebrand, J. 1991. The influence of numerical advection schemes on the results of ocean general circulation models. *Clim. Dynam.* **5**, 211–226.
- Gidhagen, L. 1987. Coastal upwelling in the Baltic Sea – satellite and in situ measurements of sea surface temperatures indicating coastal upwelling. *Estuar. Coast. Shelf Sci.* **24**, 449–462.
- Hagen, E. and Feistel, R. 2004. Observations of low-frequency current fluctuations in deep water of the Eastern Gotland Basin/Baltic Sea. *J. Geophys. Res.* **109**, C03044. DOI: 10.1029/2003JC002017.
- Hansson, M., Andersson, L., Axe, P. and Szaron, J. 2013. Oxygen survey in the Baltic Sea 2012, Extent of anoxia and hypoxia 1960–2012. *Report Oceanography 46*, Swedish Meteorological and Hydrological Institute, Norrköping, Sweden, 20 pp. ISSN: 0283-1112.
- HELCOM. 2011. The Fifth Baltic Sea Pollution Load Compilation (PLC-5) Balt. *Baltic Sea Environment Proceedings*. No. 128. Helsinki Commission, Finland, 217 pp.
- Hibler, W. D. 1979. A dynamic thermodynamic sea ice model. *J. Phys. Oceanogr.* **9**, 817–846.
- Holtermann, P. L., Umlauf, L., Tanhua, T., Schmale, O., Rehder, G. and co-authors. 2012. The Baltic Sea tracer release experiment: 1. Mixing rates. *J. Geophys. Res.* **117**, C01021. DOI: 10.1029/2011JC007439.
- Hunke, E. C. and Dukowicz, J. K. 1997. An elastic viscous plastic model for sea ice dynamics. *J. Phys. Oceanogr.* **27**, 1849–1867.
- Killworth, P., Stainforth, D., Webb, D. and Paterson, S. 1991. The development of a free-surface BryanCoxeSemtner ocean model. *J. Phys. Oceanogr.* **21**, 1333–1348.
- Kowalewski, M. and Ostrowski, M. 2005. Coastal up- and downwelling in the Southern Baltic. *Oceanologia.* **47**, 453–475.
- Lass, H.-U., Prandke, H. and Liljebladh, B. 2003. Dissipation in the Baltic proper during winter stratification. *J. Geophys. Res.* **108**(C6), 3187. DOI: 10.1029/2002JC001401.
- Lehmann, A. and Myrberg, K. 2008. Upwelling in the Baltic Sea – a review. *J. Mar. Syst.* **74**, S3–S12.
- Leppäranta, M. and Myrberg, K. 2009. *Physical Oceanography of the Baltic Sea.* Praxis Publishing, Chichester, UK. ISBN: 978-3-540-79702-9.
- Mårtensson, S., Meier, H. E. M., Pemberton, P. and Haapala, J. 2012. Ridged sea ice characteristics in the Arctic from a coupled multicategory sea ice model. *J. Geophys. Res.* **117**, C00D15. DOI: 10.1029/2010JC006936.
- Meier, H. E. M. 2001. On the parameterization of mixing in three-dimensional Baltic Sea models. *J. Geophys. Res.* **106**, 30997–31016.
- Meier, H. E. M. 2007. Modeling the pathways and ages of inflowing salt- and freshwater in the Baltic Sea. *Estuar. Coast. Shelf Sci.* **74**, 610–627.
- Meier, H. E. M., Andersson, H. C., Dieterich, C., Eilola, K., Gustafsson, B. G. and co-authors. 2012. Modeling the combined impact of changing climate and changing socio-economic development on the Baltic Sea environment in an ensemble of transient simulations for 1961–2099. *Clim. Dynam.* **39**, 2421–2441. DOI: 10.1007/s00382-012-1339-7.
- Meier, H. E. M., Döscher, R., Broman, B. and Piechura, J. 2004. The major Baltic inflow in January 2003 and preconditioning by smaller inflows in summer/autumn 2002: a model study. *Oceanologia.* **46**, 557–579.
- Meier, H. E. M., Döscher, R. and Faxen, T. 2003. A multi-processor coupled ice-ocean model for the Baltic Sea: application to salt inflow. *J. Geophys. Res.* **108**, 3273. DOI: 10.1029/2000JC000521.

- Meier, H. E. M. and Kauker, F. 2003. Modeling decadal variability of the Baltic Sea: 2. Role of freshwater inflow and large-scale atmospheric circulation for salinity. *J. Geophys. Res.* **108**(C11), 3368. DOI: 10.1029/2003JC001799.
- Mort, H. P., Slomp, C. P., Gustafsson, B. G. and Andersen, T. J. 2010. Phosphorus recycling and burial in Baltic Sea sediments with contrasting redox conditions. *Geochim. Cosmochim. Acta.* **74**, 1350–62.
- Myrberg, K. and Andrejev, O. 2003. Main upwelling regions in the Baltic Sea – a statistical analysis based on three-dimensional modelling. *Boreal Environ. Res.* **8**, 97–112.
- Nausch, G., Matthaus, W. and Feistel, R. 2003. Hydrographic and hydrochemical conditions in the Gotland Deep area between 1992 and 2003. *Oceanologia.* **45**(4), 557–569.
- Radtke, H., Neumann, T., Voss, M. and Fennel, W. 2012. Modeling pathways of riverine nitrogen and phosphorus in the Baltic Sea. *J. Geophys. Res. Oceans (1978–2012)* **117**(C9), C09024.
- Reissmann, J. H., Burchard, H., Feistel, R., Hagen, E., Lass, H. U. and co-authors. 2009. Vertical mixing in the Baltic Sea and consequences for eutrophication—a review. *Progr Oceanogr.* **82**(1), 47–80.
- Samuelsson, P., Jones, C. G., Willén, U., Ullerstig, A., Gollvik, S. and co-authors. 2011. The Rossby Centre Regional Climate model RCA3: model description and performance. *Tellus A.* **63**, 4–23.
- Savchuk, O. P. 2010. Large-scale dynamics of hypoxia in the Baltic Sea. In: *Chemical Structure of Pelagic Redox Interfaces: Observation and Modelling. The Handbook of Environmental Chemistry* (ed. E. Yakushev). Springer-Verlag, Berlin. pp. 137–160. DOI: 10.1007/698\_2010\_53.
- Schenk, F. and Zorita, E. 2012. Reconstruction of high resolution atmospheric fields for Northern Europe using analog-upscaling. *Clim. Past Discuss.* **8**, 819–868.
- Schneider, B. 2011. PO<sub>4</sub> release at the sediment surface under anoxic conditions: a contribution to the eutrophication of the Baltic Sea? *Oceanologia.* **53**(1–TI), 415–529.
- Stevens, D. P. 1991. The open boundary condition in the United Kingdom Fine-resolution Antarctic Model. *J. Phys. Oceanogr.* **21**, 1494–1499.
- Stigebrandt, A. 1987. A model of the vertical circulation of the Baltic deep water. *J. Phys. Oceanogr.* **17**, 1772–1785.
- Stigebrandt, A. and Gustafsson, B. G. 2007. Improvement of Baltic proper water quality using large-scale ecological engineering. *Ambio.* **36**, 280–286.
- Väli, G., Meier, H. E. M. and Elken, J. 2013. Simulated halocline variability in the Baltic Sea and its impact on hypoxia during 1961–2007. *J. Geophys. Res. Oceans.* **118**, 6982–7000. DOI: 10.1002/2013JC009192.

## **APPENDIX V**





# A new approach to model oxygen dependent benthic phosphate fluxes in the Baltic Sea



Elin Almroth-Rosell <sup>a,\*</sup>, Kari Eilola <sup>a</sup>, Ivan Kuznetsov <sup>a</sup>, Per O.J. Hall <sup>c</sup>, H.E. Markus Meier <sup>a,b</sup>

<sup>a</sup> Swedish Meteorological and Hydrological Institute, Norrköping, Sweden

<sup>b</sup> Department of Meteorology, Stockholm University, SE-106 91 Stockholm, Sweden

<sup>c</sup> University of Gothenburg, Department of Chemistry and Molecular Biology, Marine Chemistry, SE-412 96 Gothenburg, Sweden

## ARTICLE INFO

### Article history:

Received 17 March 2014

Received in revised form 25 September 2014

Accepted 17 November 2014

Available online 26 November 2014

### Keywords:

Phosphorus release

Oxygen penetration depth

Eutrophication

Saltwater inflow

Biogeochemical modelling

Baltic Sea

## ABSTRACT

The new approach to model the oxygen dependent phosphate release by implementing formulations of the oxygen penetration depths (OPD) and mineral bound inorganic phosphorus pools to the Swedish Coastal and Ocean Biogeochemical model (SCOBI) is described. The phosphorus dynamics and the oxygen concentrations in the Baltic proper sediment are studied during the period 1980–2008 using SCOBI coupled to the 3D-Rosby Centre Ocean model. Model data are compared to observations from monitoring stations and experiments. The impact from oxygen consumption on the determination of the OPD is found to be largest in the coastal zones where also the largest OPD are found. In the deep water the low oxygen concentrations mainly determine the OPD. Highest modelled release rate of phosphate from the sediment is about  $59 \times 10^3 \text{ t P year}^{-1}$  and is found on anoxic sediment at depths between 60–150 m, corresponding to 17% of the Baltic proper total area. The deposition of organic and inorganic phosphorus on sediments with oxic bottom water is larger than the release of phosphorus, about  $43 \times 10^3 \text{ t P year}^{-1}$ . For anoxic bottoms the release of total phosphorus during the investigated period is larger than the deposition, about  $19 \times 10^3 \text{ t P year}^{-1}$ . In total the net Baltic proper sediment sink is about  $23.7 \times 10^3 \text{ t P year}^{-1}$ . The estimated phosphorus sink efficiency of the entire Baltic Sea is on average about 83% during the period.

© 2014 The Authors. Published by Elsevier B.V. This is an open access article under the CC BY-NC-ND 3.0 license (<http://creativecommons.org/licenses/by/3.0/>).

## 1. Introduction

Phosphorus has been discussed to be a key nutrient for the eutrophication of the Baltic Sea (Conley et al., 2009). Not only external supplies of nutrients (phosphorus and nitrogen) from land and atmosphere contribute to the increasing eutrophication, but also internal loads, i.e. the impact from an intensified recycling of nutrients in the sediment (Conley et al., 2002; Stigebrandt et al., 2014). Gustafsson et al. (2012) estimated that external phosphorus loads increased by a factor of 5 from 1850 to around 1980. After 1980 external phosphorus loads started to decrease, but the phosphorus efflux from the sediments and the phosphorus pool in the water continued to increase. A number of studies have shown that the sediments play an important role in controlling the phosphorus supply to the pelagic realm as they regionally act as an internal source or sink for dissolved phosphate (Emeis et al., 2000; Lukkari et al., 2009b; Viktorsson et al., 2012, 2013).

The deep water in the southern and central basins of the Baltic Sea is separated from the surface water by a permanent halocline at a depth of about 60 m (Stigebrandt, 2001; Väli et al., 2013), which prevents vertical circulation and ventilation of the bottom water. Only major water inflows of dense surface water from Kattegat with higher salinity and oxygen can oxygenate the deep waters in the basins. The inflowing water replaces the anoxic and phosphate rich bottom water in the deeper part of the basins, which is lifted up to more shallow water depths (Eilola et al., 2014; Fischer and Matthäus, 1996; Reissmann et al., 2009; Schneider, 2011). The vertical transport and mixing of the deep bottom water due to MBI have been discussed in earlier studies (e.g. Reissmann et al., 2009; Schneider, 2011). The destiny of the deep water due to MBI in the Baltic proper was investigated in a tracer study by Eilola et al. (2014), who concluded that regionally the direct impact on the uplift of nutrients from waters below the halocline to surface waters due to MBI could be quite large, but that the overall direct impact was small because comparably large vertical transports occur also in years without MBI. The impact from the East Gotland Deep water on eutrophication in the Baltic Sea is expected to be small because the volume of water below 150 m is small (Eilola et al., 2014). During the stagnant periods, between the major inflows, the oxygen concentrations in the deep water decrease

\* Corresponding author at: Swedish Meteorological and Hydrological Institute, Sven Källfelts gata 15, SE-426 71 Västra Frölunda, Sweden. Tel.: +46 31 7518969.  
E-mail address: [elin.almroth.rosell@smhi.se](mailto:elin.almroth.rosell@smhi.se) (E. Almroth-Rosell).

with time, often until depletion (Lass and Matthäus, 2008, and references therein).

Phosphate has the ability to adsorb on hydrated metal oxides, e.g. iron(III) oxy hydroxides (oxides), which build up in the oxidized sediment layer. Large amounts of phosphate can thus build up in the sediment during oxic bottom water conditions. During anoxic periods the oxides reductively dissolve, which prevents further adsorption of phosphate to iron oxides and the previously adsorbed phosphorus is released to the pore water in the sediment and can thus diffuse to the water column (Froelich, 1988; Mortimer, 1941, 1942; Sundby et al., 1992). Thus, the low retention capacity of phosphorus in the sediment during anoxic conditions and the limited vertical circulation and ventilation of the bottom water leads to high phosphate concentrations in the anoxic bottom water. Further, Jilbert et al. (2011) suggested that preferential phosphorus mineralization with respect to carbon, may be a key player besides the mineral bound redox dependent phosphorus dynamics. However, with the present model setup this effect cannot be investigated. Sediment that has been anoxic for a longer period might get the accumulated pool of mineral bound inorganic phosphorus depleted. The release of phosphate will then depend on the supply and degradation of organic matter and the mineralization rate of organic phosphorus (Viktorsson et al., 2012). Today, about 40% of the total bottom area in the Baltic proper (including the Gulf of Riga and the Gulf of Finland) is estimated to be overlain by hypoxic (dissolved  $O_2$  concentrations less than  $2 \text{ ml l}^{-1}$  or  $91 \text{ } \mu\text{M}$ ) or anoxic bottom water (Hansson and Andersson, 2013). In contrast to soft water lakes marine waters also have a sink for iron. Saline water contains sulfate which is used during bacterial anaerobic decomposition of organic material. The produced hydrogen sulfide reacts with iron and precipitates as minerals, e.g.  $\text{FeS}$  or pyrite  $\text{FeS}_2$  (Blomqvist et al., 2004; Skoog et al., 1996). Iron(III)oxides and phosphate form aggregates with the molar (Fe:P) ratio of 2:1 (Gunnars and Blomqvist, 1997; Gunnars et al., 2002). If the molar ratio is less than two, the phosphate can escape from the sediment without binding to iron(III)oxides. The produced  $\text{FeS}$  and  $\text{FeS}_2$  acts as a sink of iron and may thus lead to a reduced retention capacity of phosphate in the sediment (Blomqvist et al., 2004; Lehtoranta et al., 2009). The salinity dependence of the phosphorus release capacity from the sediments in the Swedish Coastal and Ocean Biogeochemical model (SCOBI; Eilola et al., 2009; Marmefelt et al., 1999) was discussed by Eilola et al. (2009).

Field studies in the Gulf of Finland have shown that in spite of oxic/sub-oxic conditions in the water column there were high release rates of phosphate from the sediment (Conley et al., 1997; Lehtoranta and Heiskanen, 2003; Lehtoranta et al., 2009; Pitkanen et al., 2007). Lehtoranta and Heiskanen (2003) argued that a low availability of iron(III)oxides, due to limited vertical diffusion of iron(II) towards the oxidized surface layer of the sediment, limited the phosphorus adsorption and allowed for high release rates of phosphorus. According to Lehtoranta et al. (2009) the release of phosphate in spite of oxic bottom water was due to high deposition of organic material and that sulfate reduction and thus formation of  $\text{FeS}_2$  decreased the availability and recycling of iron in the sediment. Conley et al. (1997) concluded that the phosphorus content in the sediment was very high in the Gulf of Finland as compared to other Baltic Sea sediments. Also Hille (2005) discussed, based on measurements in the Baltic proper, that the high phosphorus flux rates correspond to sites with high accumulation rates of organic matter. Decomposition and oxidation rate of organic matter at these sites is therefore high. The depth of the oxidized sediment layer, and hence the amount of hydrated metal oxides available for phosphorus adsorption, depends on the oxygen concentrations in the bottom water and also on the oxygen consumption rate in the sediment (Cai and Sayles, 1996). Hence, if the oxygen penetration depth is large more iron can transform to iron(III)oxides and larger fractions of the mineralized phosphorus may be adsorbed. The importance of oxygen consumption rate on the oxygen diffusion and penetration into the sediment has not previously been accounted for in the state-

of-the-art model described by Eilola et al. (2011). Oxygen concentrations in the bottom water have usually been used to describe the status in the sediment.

The model system in the present study consists of the SCOBI model coupled to a three-dimensional high resolution ocean circulation model, the Rossby Centre Ocean model (RCO; Meier et al., 2003). The aim with this study was to further develop the description of the benthic phosphorus dynamics in SCOBI and to discuss the model results in comparison to available observations. A map of the horizontal variability of the oxygen penetration depth and the effects of major deep water inflows on the phosphate release in the Baltic proper will be described. The relative importance of oxygen consumption rate, compared to the importance of bottom water oxygen concentration, on the actual oxygen penetration depth as well as the sink efficiency of phosphorus in the Baltic Sea will be studied.

## 2. Material and methods

The Baltic Sea is a sensitive environment which is highly affected by the large amount of people living around its coast. Eutrophication with increased nutrient concentrations and, as a consequence, algae blooms and bottom anoxia has been observed during decades in the Baltic Sea. It is a landlocked sea that can be divided into several sub-basins connected by sills. The connection to the North Sea goes through the shallow Danish straits, Little Belt, Great Belt and Sound, and Kattegat. The model domain of the coupled RCO-SCOBI model system used in this study covers the entire Baltic Sea, including Kattegat (Fig. 1) and has been used in several applications for the Baltic Sea (e.g. Eilola et al., 2012, 2013; Meier et al., 2011, 2012a; Neumann et al., 2012; Skogen et al., 2014). The model system has shown good performance compared to other Baltic Sea models and observations (Eilola et al., 2011). In this study the main focus has been on the Baltic proper, including the Gotland, Bornholm and Arkona basins, and the Gulf of Riga and Gulf of Finland during the period 1980–2008.

### 2.1. The RCO-model

The RCO-model, Rossby Centre Ocean model (Meier et al., 2003), is a three-dimensional Bryan-Cox-Semtner primitive equation circulation model with a free surface (Killworth et al., 1991) and open boundary conditions (Stevens, 1991) in the northern Kattegat (Fig. 1). Subgrid-scale mixing is parameterized using a turbulence closure scheme of the  $k$ - $\epsilon$  type with flux boundary conditions to include the effect of a turbulence enhanced layer due to breaking surface gravity waves and a parameterization for breaking internal waves (Meier, 2001). The deep water mixing is assumed to be inversely proportional to the Brunt-Väisälä frequency with a proportionality factor  $\alpha = 1 \times 10^{-7} \text{ m}^2 \text{ s}^{-2}$  following Lass et al. (2003). As the layer thicknesses of the vertical grid are too large to resolve the bottom boundary layer (BBL) accurately, a BBL model is embedded to allow the direct communication between bottom boxes of the step-like topography (Beckmann and Döscher, 1997). The ocean model is coupled to a Hibler-type sea ice model (Hibler, 1979) with elastic-viscous-plastic rheology (Hunke and Dukowicz, 1997) and explicit representation of five undeformed and two deformed sea ice categories (Mårtensson et al., 2012). RCO is used with a horizontal resolution of 3.7 km (2 nautical miles) and with 83 vertical levels with layer thicknesses of 3 m. In the model the maximum depth amounts to 249 m. For further details of the RCO model and the performance of relevant model variables compared to observations the reader is referred to Meier (2001), Meier et al. (2003), Meier (2007) and Väli et al. (2013).

### 2.2. SCOBI

The Swedish Coastal and Ocean Biogeochemical model (SCOBI; Eilola et al., 2009) describe the dynamics of nitrate, ammonium,

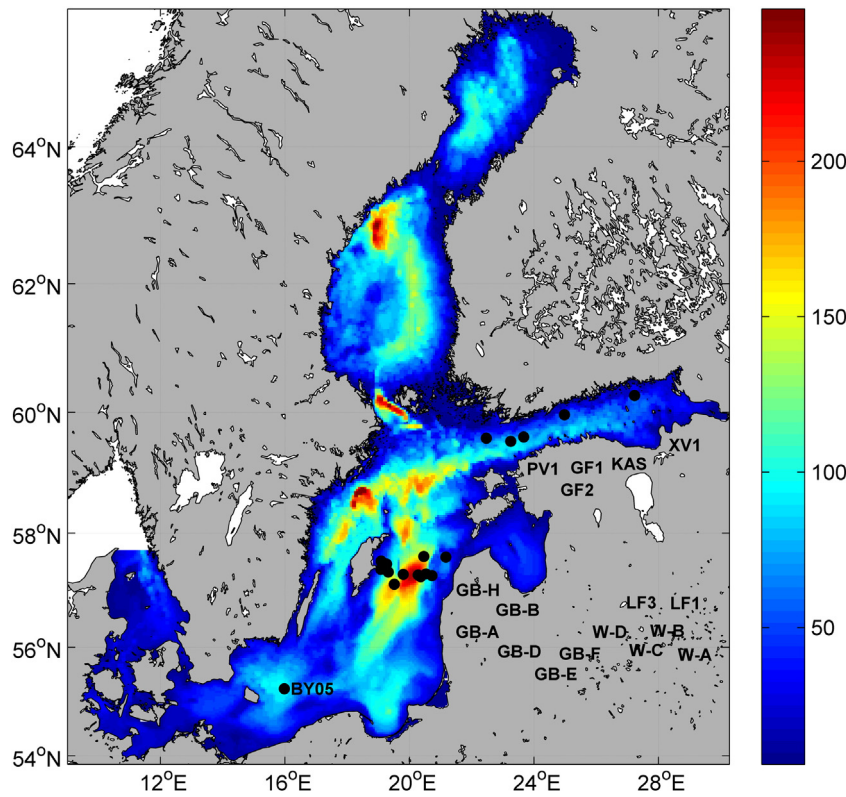


**Fig. 1.** The model domain of the RCO-SCOBI model covers the Baltic Sea, including Kattegat. The color bar shows the depth in meter and the black filled circles shows positions of the stations used for validation. The names of the stations in the Gulf of Finland and central Baltic proper are displaced to the right and down for clarity. The SMHI monitoring station BY15 has approximately the same position as GB-F and is not separately shown.

phosphate, phytoplankton, zooplankton, detritus, and oxygen. Phytoplankton consists of three algal groups representing diatoms, flagellates and others, and cyanobacteria (corresponding to large, small and nitrogen fixing cells). The growth rates depend on nutrient concentrations, irradiance, and water temperature. The modelled cyanobacteria also have the ability to fix molecular nitrogen. Organic matter sinks and enters the sediment containing benthic nitrogen and phosphorus. The sediment processes include oxygen dependent nutrient regeneration and denitrification as well as permanent burial of nutrients. Resuspension of organic matter depends on the combined effects of waves and current induced shear stress (Almroth-Rosell et al., 2011). In this study detritus is separated into different nitrogen and phosphorus pools in accordance with the description given by Savchuk (2002). The nutrient loads for the present run are identical to the historical loads described by Gustafsson et al. (2012). The sediment part in the SCOBI model has been further developed compared to the model described by Eilola et al. (2009) and Almroth-Rosell et al. (2011). New pelagic and sediment pools of inorganic phosphorus have been implemented to simulate the adsorption behavior of phosphate on e.g. iron(III)oxides, which in the sediment is regulated by the oxygen penetration depth (OPD).

Soetaert et al. (2000) tested five different levels of coupled sediment-water nutrient flux model complexity for continental shelf areas. The most complex model version (level 4) couples the water column processes to a vertically resolved biogeochemical sediment model (e.g. Reed et al., 2011). The results by Soetaert et al. (2000) suggested, however, that the vertically integrated dynamic sediment model (level 3) approach represent the best balance between computational demand and attained accuracy. The level 3 type model has been used with good results in the coupled physical-biogeochemical RCO-SCOBI model and other Baltic Sea models as well (Eilola et al., 2011). The aim is therefore to keep the basic structures of the SCOBI model formulations, described in Eilola et al. (2009) and Almroth-Rosell et al. (2011), for the new formulations to account for the oxygen penetration depth

and dynamics of inorganic phosphorus, described in Sections 2.2.1 and 2.2.2, respectively.

### 2.2.1. Oxygen penetration depth

The depth to which oxygen penetrates into the sediment depends on the rate of oxygen consumption in the sediment and the diffusive transport of oxygen from the bottom water to the sediment (Cai and Sayles, 1996). The OPD is calculated using Eq. (1) from Cai and Sayles (1996), who showed that this estimation of OPD describes well the situation in continental marginal seas. This equation describes the OPD at steady state pore water oxygen profiles and a homogenous depth distribution of carbon decomposition in the OPD layer with no bioirrigation included. In frontal areas with highly variable oxygen concentrations in the bottom water the equation might therefore temporary give deviations from observations, but these occasions are believed to be of less importance for the long term study of the present paper.

$$OPD = 2\varnothing D_s \frac{[O_2]_{BW}}{F_{O_2}^0} \quad (1)$$

$$D_s = \frac{D}{1 - \ln(\varnothing^2)} \quad (2)$$

where OPD is the oxygen penetration depth in meter,  $\varnothing$  is the sediment porosity,  $[O_2]_{BW}$  is the bottom water oxygen concentration ( $\text{ml O}_2 \text{ l}^{-1}$ ),  $F_{O_2}^0$  is the oxygen flux to the sediment ( $\text{ml O}_2 \text{ m}^{-2} \text{ s}^{-1}$ ) and  $D_s$  is the diffusivity of oxygen in the sediment ( $\text{m}^2 \text{ s}^{-1}$ ).

Local sediment porosity is in the model grid described by three different values representing sediment types at accumulation bottoms (0.94), transport bottoms (0.85) and erosion bottoms (0.64). The bottom types were defined by the method described by Almroth-Rosell et al. (2011). The oxygen flux  $F_{O_2}^0$  is in the SCOBI model given by the

oxidation rate of organic matter and nitrification (of ammonia to nitrate) and the corresponding uptake of oxygen to the sediment. The oxygen penetration depth is properly described by this equation down to about 8 cm (Cai and Sayles, 1996). The porosity dependent diffusivity of oxygen in the sediment ( $D_s$ ) is described by Eq. (2) where  $D$  is the salinity ( $S$ ) and temperature ( $T$ ) dependent diffusivity for oxygen in water (Boudreau, 1996; Hall et al., 2007), which is calculated from Eq. (3). The Eqs. (3) and (4) were defined from the best polynomial fits to data from an oxygen diffusion table (Ramsing and Gundersen, 2014) based on calculations using more sophisticated equations (e.g. Broecker and Peng, 1974; Himmelblau, 1964; Li and Gregory, 1974).

$$D = A \cdot (1 - S \cdot B1 \cdot (B2 + B3 \cdot T)) \quad (3)$$

$$A = (C1 \cdot T^2 + C2 \cdot T + C3) \cdot C4 \quad (4)$$

where the salinity is in the range 0–35 and the water temperature in the range 0–30 °C. The values of the constants are shown in Table 1.

The relative impact of oxygen concentration and oxygen consumption on the magnitude of the OPDs was calculated from Eq. (5):

$$R = \frac{[O_2]^a / [O_2]^b}{F_{O_2}^b / F_{O_2}^a} \quad (5)$$

where  $[O_2]$  is the oxygen concentration and  $F_{O_2}^0$  is the oxygen consumption at yearly minimum OPD denoted by the superscripted letter  $a$  and at yearly maximum OPD denoted by the superscripted letter  $b$ . The equation was derived from Eq. (1) as  $OPD_{min}/OPD_{max}$  where the oxygen concentrations were clustered and compared to the oxygen fluxes. The ratio ( $R$ ) is higher than 1 when the oxygen consumption in the sediment controls the OPD and lower than 1 when it is the oxygen concentrations that determines the OPD. The temperature dependent sediment diffusivity is also a parameter that affects the OPD (Eq. (1)) and its relative contribution can be calculated in a similar way, using Eq. (5). Thus, instead of oxygen concentrations the modelled sediment diffusivity at the maximum OPD and minimum OPD, respectively, are used.

### 2.2.2. Benthic inorganic phosphorus

The new elements of the present SCOBI model are described below using formulations similar to the tables in the Appendix of Eilola et al. (2009). The source terms describing the change in time for each variable of the sediment model equations are described by changes in benthic organic phosphorus (PBT in Eq. (6)) and mineral bound inorganic phosphorus (BIP in Eq. (7)). The mineral bound inorganic phosphorus in the water (WIP) is followed in each discrete depth layer as a passive tracer without any biogeochemical sources or sinks in the water (WIP in Eq. (8)). The formulations of sediment resuspension of organic and mineral bound phosphorus are similar and follow in detail the formulations described by Almroth-Rosell et al. (2011) and Eilola et al. (2009), and will not be further discussed here. Also the sinking rate of WIP is similar

**Table 1**  
Constants of Eqs. (3) and (4).

Parameter	Value
B1	$35^{-1}$
B2	0.05
B3	0.00075
C1	0.000424
C2	0.042265
C3	1.105
C4	$10^{-9}$

**Table 2**  
List of biogeochemical state variables.

State variables	Description	Units
O <sub>2</sub>	Oxygen	ml O <sub>2</sub> l <sup>-1</sup>
OPD	Oxygen penetration depth	meter
PO <sub>4</sub>	Phosphate	mmol P m <sup>-3</sup>
WIP	Mineral bound phosphate in the water	mmol P m <sup>-3</sup>
PBT	Benthic organic phosphorus	mmol P m <sup>-2</sup>
BIP	Benthic inorganic phosphorus	mmol P m <sup>-2</sup>

to the sinking of detritus described by Eilola et al. (2009). The units of relevant variables of the present paper are listed in Table 2.

$$S_{PBT} = SINKI_{OP} - PBTOUT_{PO_4} - PBTOUT_{BIP} - SEDPLOSS - BURIAL_{PBT} \quad (6)$$

$$S_{BIP} = SINKI_{IP} + PBTOUT_{BIP} + SCAV_{PO_4} - LIBP_{PO_4} - SEDILOSS - BURIAL_{BIP} \quad (7)$$

$$S_{WIP} = SINKI_{IP} - SINKOUT_{IP} + SEDILOSS \quad (8)$$

The basic model concept of the new sediment model is illustrated in Fig. 2, where sinking organic phosphorus is deposited on the sediment and a pool of benthic organic phosphorus builds up. Organic matter is mineralized (Eq. (9)) and an oxygen penetration depth (OPD) dependent fraction (PRC) of the mineralized phosphorus (DCOMP<sub>PBT</sub>) is released directly to the overlying water (Eq. (10)). The salinity ( $S$ ) dependence of the PRC (Eilola et al., 2009) is not used in the present model setup. The remaining fraction (Eq. (11)) is added into the pool of BIP. Under anoxic conditions (OPD = 0) all the mineralized phosphorus is directly released to the overlying water (PRC = 1). Burial of PBT and BIP are similar and described by Eq. (14) and (15), respectively, and the values of the constants are shown in Table 3.

$$DCOMP_{PBT} = \alpha_{PBT} \cdot EXP(\beta_{PBT} \cdot T) \cdot PBT \quad (9)$$

$$PBTOUT_{PO_4} = PRC \cdot DCOMP_{PBT} \quad (10)$$

$$PBTOUT_{BIP} = (1 - PRC) \cdot DCOMP_{PBT} \quad (11)$$

$$PRC = \alpha_{PRC} - \delta_{PRC} \quad (12)$$

$$\delta_{PRC} = 1 / \left( 1 + a_{\delta} \cdot EXP \left( -b_{\delta} \cdot \left( \frac{OPD}{d_{\delta}} - c_{\delta} \right) \right) \right) \quad (13)$$

$$BURIAL_{PBT} = \alpha_{BUR} \cdot PBT \quad (14)$$

$$BURIAL_{BIP} = \alpha_{BUR} \cdot BIP \quad (15)$$

The basic ideas of the modelled mineral bound inorganic phosphorus dynamics follow Neumann and Schernewski (2008) and Reed et al. (2011). In order to account for the dynamics of changing strength of vertical gradients of phosphorus and oxygen in the sediment regulations according to the first order reaction kinetics was introduced. Hence, the release rate (LIBP<sub>PO<sub>4</sub></sub>) of PO<sub>4</sub> from the sediment (Eq. (16)) decreases as the sediment concentration of BIP decreases below a half saturation value. Similarly the release rate increases when the oxygen penetration depth decreases and reaches its maximum at anoxic conditions. At small OPD values, the half saturation value limits the amount of hydrated metal oxides available for phosphate adsorption. The values of the half saturation constants were evaluated from theoretical considerations and tested and calibrated against realistic values of sediment concentrations in a spread data-sheet model before the implementation into the RCO-SCOBI model. These calibration constants might be further studied and tuned in future experiments using a level 4 type of diagenetic model.

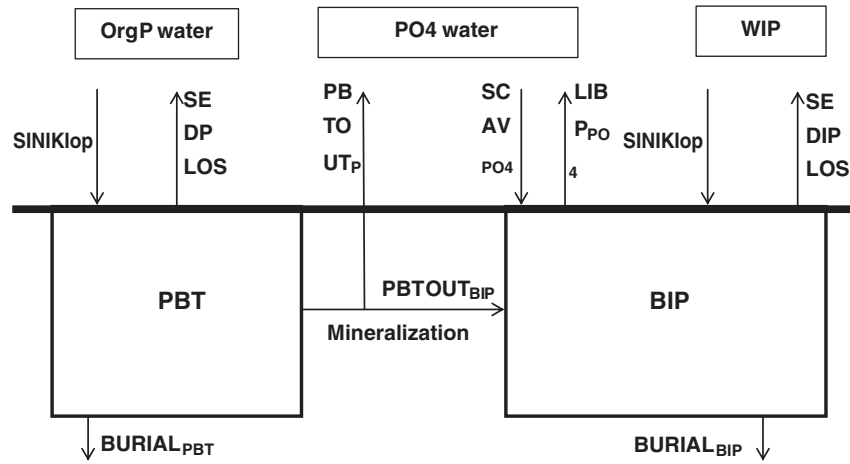


**Fig. 2.** The new benthic model concept of organic and mineral bound inorganic pools of phosphorus in SCOBI. Organic phosphorus from phytoplankton and detritus (including resuspended matter) are deposited on the sediment ( $SINKI_{op}$ ) and builds up the pool of benthic organic phosphorus (PBT). A fraction of the mineralized PBT is released directly to the overlying water ( $PBTOUT_{PO4}$ ) and the remaining fraction ( $PBTOUT_{BIP}$ ) adds to the sediment pool of mineral bound inorganic phosphorus (BIP). Mineral bound inorganic phosphorus from the water (WIP, only resuspended particles) is deposited on the sediment ( $SINKI_{IP}$ ) and adds to the pool of BIP. Phosphorus can be released from the pool of BIP to the overlying water ( $LIBP_{PO4}$ ) as well as become scavenged/adsorbed ( $SCAV_{PO4}$ ) from the water into the sediment. Burial occur from both the organic ( $BURIAL_{PBT}$ ) and inorganic ( $BURIAL_{BIP}$ ) pools of phosphorus. Resuspension may occur from both sediment pools of phosphorus ( $SEDPLOSS$  and  $SEDILOSS$ ).

The uptake of phosphate from the bottom water to the sediment ( $SCAV_{PO4}$ ) is regulated by interfacial reactions and phosphate diffusion across the sediment interface. The diffusion is driven by the gradient between the bottom water and the sediment pore water concentration at the sediment–water interface (cf. Eq. (3) in Reed et al., 2011). The formulation (Eq. (17)) may transfer  $PO4$  from the water to the sediment if the sediment is under saturated with BIP with regard to the amount of hydrated metal oxides available for phosphate adsorption. This situation may occur e.g. after a period with anoxic conditions when most BIP have been released to the overlying water and BIP decreases below the half saturation value. The uptake requires, however, also that the oxygen penetration depth is deep enough to produce an active oxidized layer. This is regulated by the half saturation value of OPD. The values of the constants are shown in Table 4.

$$LIBP_{PO4} = \alpha_{LIBP} \cdot \frac{BIP}{BIP + \beta_{LIBP}} \cdot \left(1 - \frac{OPD}{OPD + \eta_{LIBP}}\right) \cdot BIP \quad (16)$$

$$SCAV_{PO4} = \alpha_{SCAV} \cdot \left(1 - \frac{BIP}{BIP + \beta_{LIBP}}\right) \cdot \frac{OPD}{OPD + \eta_{LIBP}} \cdot PO4_{water} \quad (17)$$

The transfer rate ( $\alpha_{SCAV}$ ) of phosphate from the water to the sediment ( $m s^{-1}$ ) is regulated by the sediment porosity and the temperature ( $^{\circ}C$ ) dependent phosphate diffusivity ( $m^2 s^{-1}$ ) formula ( $D'$ ) adopted from Krom and Berner (1980).

$$\alpha_{SCAV} = D_{PO4} \cdot \frac{\phi}{\Delta X} \quad (18)$$

**Table 3**  
Constants and units of Eqs. (9)–(15).

Parameter	Unit	Value	Description
$\alpha_{PBT}$	$day^{-1}$	0.0005	Mineralization rate, of benthic organic phosphorus, at 0 $^{\circ}C$
$\beta_{PBT}$	$^{\circ}C^{-1}$	0.15	PBT mineralization temperature dependence
$\alpha_{PRC}$	-	1.15	Constant in benthic redox dependence of phosphate
$a_6$	-	0.5	Constant in benthic redox dependence of phosphate
$b_6$	$l ml^{-1}$	1.5	Constant in benthic redox dependence of phosphate
$c_6$	$ml l^{-1}$	0.7	Constant in benthic redox dependence of phosphate
$d_6$	$m^{-1} (ml l^{-1})^{-1}$	$6.164 \times 10^{-4}$	Constant in benthic redox dependence of phosphate
$\alpha_{BUR}$	$day^{-1}$	$2.8/1.8/1.4/1.0 \times 10^{-4}$	Burial rate in the Bothnian Sea/Gulf of Finland/Bothnian Bay/Elsewhere

$$D_{PO4} = \frac{D'}{1 - \ln(\phi^2)} \quad (19)$$

$$D' = C1_{SCAV} + C2_{SCAV} \cdot (T - C3_{SCAV}) \quad (20)$$

The length scale of the diffusion gradient  $\Delta X$  was set to 1 cm (0.01 m) and the values of the constants are shown in Table 5.

### 2.3. Model validation

The pelagic modelled oxygen and phosphate concentrations are validated qualitatively by comparison of long time series of the model results and data from the central Baltic proper. Observations from the database Svenskt HavsARKiv (SHARK, 2014) at SMHI are used for validation. Hydrogen sulfide concentrations are both in the models and in the observations represented by “negative oxygen” equivalents ( $1 ml H_2S l^{-1} = -2 ml O_2 l^{-1}$ ) (Fonselius and Valderrama, 2003)

Modelled OPDs in SCOBI have been validated through comparison with observed OPD found in the literature for the Eastern Gotland Basin (Steenbergh et al., 2011; Wenzhöfer et al., 2002), and to calculated OPD according to formulations from Cai and Sayles (1996) using observation data of bottom water oxygen concentrations and benthic oxygen fluxes together with known porosity (Viktorsson et al., 2013; Nilsson et al., unpublished results; M. Kononets, pers. comm.). Observation data for the OPD have preferentially been chosen because both P-fluxes and oxygen penetration depths from the same study site at the same occasion are included. Stations used for validation are shown in Fig. 1.

**Table 4**  
Constants of Eqs. (16) and (17).

Parameter	Unit	Value	Description
$\alpha_{\text{LIBP}}$	$\text{day}^{-1}$	0.01	Maximum release rate of benthic inorganic phosphorus
$\beta_{\text{LIBP}}$	$\text{mmol m}^{-2}$	484	Half saturation value of BIP
$\eta_{\text{LIBP}}$	meter	$10^{-4}$	Half saturation value of OPD

### 3. Results and discussion

#### 3.1. Validation of model results

Validation processes of large scale biogeochemical models are complicated and include many variables. It is not only the variability of the weather, but the statistics (mean, standard deviation, etc.) or the climate which needs to be simulated correctly. The nutrient and oxygen concentrations at certain times are much influenced by the characteristics of the hydrodynamic model, such as the timing of inflows or the vertical stratification. The chronology between observed and modelled concentrations may therefore differ. For the present study it is desirable that the model captures the characteristic dynamics of oxygen and phosphate concentrations in the deepest water layer.

##### 3.1.1. Variability of oxygen and phosphate concentrations

Modelled oxygen and phosphate concentrations have been compared to observations from monitoring stations (Eilola et al., 2009) and results from the present model version from the stations BY05 and BY15 (for locations see Fig. 1) in the bottom water are shown (Fig. 3). Generally the model captures the long-term variability of oxygen and phosphate concentrations in the Baltic proper.

In the bottom water (90 m depth) and ten meters above bottom at station BY05 the variability of phosphate concentrations is satisfactory reproduced (Fig. 3) during large parts of modelled period. However, during a few occasions e.g. at the end of the 1980s and from about 2006 and forward the concentrations are too low because the modelled oxygen concentrations were not low enough during these periods (Fig. 3). About ten meters above the bottom the oxygen mean value is too high compared to observations, which probably is due to the a weakness in the simulation of the stratification (Väli et al., 2013). These higher oxygen concentrations do, however, not seem to affect significantly the oxygen concentrations at the bottom most water layer at this station. Overall are the dynamics of oxygen and phosphate concentrations at station BY05 reasonably reproduced (Fig. 3).

At BY15 are the stagnation periods as well as the consequences from deep water inflows (1970, 1976, 1993 and 2003) captured by the model both at the bottom most layer (240 m) and at about 100 m depth (Fig. 3). During the stagnation periods the oxygen concentrations decrease while the phosphate concentrations in the deep water increase. However, the modelled phosphate concentrations in the bottom most layer are lower compared to observations, which is clearly seen during the stagnation period 1983–1993. The increase in phosphate concentrations levels off from the mid-1980s much because the modelled benthic inorganic phosphorus pool becomes depleted (not shown). The modelled oxygen concentrations follow the observations at both 240 m and 100 m depth, with the exception in the end of the period where the modeled oxygen does not capture the observed, fast depletion of oxygen.

**Table 5**  
Constants of Eq. (20).

Parameter	Value
$C1_{\text{SCAV}}$	$7.34 \times 10^{-10}$
$C2_{\text{SCAV}}$	$0.16 \times 10^{-10}$
$C3_{\text{SCAV}}$	25

The long-time average profiles (1980–2008) of the modelled and observed phosphate and oxygen concentrations at station BY15 (Fig. 4) confirm that the model manages to capture the oxygen and phosphate dynamics. However, below the halocline oxygen and phosphate concentrations are too high and too low, respectively, with largest differences closest to the bottom.

A comprehensive validation of the physics is presented by Väli et al. (2013).

##### 3.1.2. Oxygen penetration depth

The model seems to simulate oxygen penetration depth with reliable magnitude and variability. However, there are differences between model results and observations (Table 6) that will be discussed below. The OPD in a coastal zone is in general of the magnitude of millimeters (Glud, 2008) and fluctuates depending on the bottom water oxygen concentrations and the amount of organic material. E.g. Rasmussen and Jørgensen (1992) found seasonal variations of the OPD in Aarhus Bay in the range from  $-5.1$  mm during winter to  $-1.2$  mm during spring. During summer the OPD was between  $-1.3$  and  $-2.5$  mm. However, there are some general problems when model results are compared to observations, especially for measurements in the sediment. One important factor is the size of the horizontal grid and the lack of spatial variation in each grid cell of the model. Observations are made on a very limited spatial scale which is assumed to represent a larger area, while the horizontal resolution of the present model system is about 3.7 km. This causes the differences between the observed and modelled water depths at some of the stations (Table 6). It is also important to remember that the model results in Table 6 are monthly means while the observations are snapshots at specific dates, or at the most averages of snapshots from two or maximum three measurement occasions. The limited number of observations restricts the possibilities to perform a statistical evaluation. It would therefore be desirable to have more observations of OPD to be able to do a more comprehensive validation in the future.

Largest difference between modelled and observed OPD is found at station GB-A (Table 6) which is a station in the Eastern Gotland Basin at about 60 m depth with oxic bottom water (Viktorsson et al., 2013). The estimated observation of OPD at this station is  $-1.5$  mm while the modelled monthly mean value for the same month is as deep as  $-21$  mm. The limited numbers of measurements of the OPD make it hard to determine whether or not they are representative as well as the fact that the observed OPD is estimated from observations of oxygen concentrations and consumption instead of a direct measurement. The estimation is on the other hand calculated in the same way as the modelled OPD (Eq. (1)). Another important factor is that the bottom depth in the model at this station (45 m) is in the ventilated waters above the modelled halocline, why the oxygen concentrations and the OPD are higher.

At the stations GB-B and Kasuuni the difference between modelled and observed OPD was in the range from  $-2.4$  mm to  $-3.1$  mm, thus the modelled OPD was underestimated. The Kasuuni station is classified as transport/accumulation bottom at about 55 m water depth (Almroth et al., 2009; Viktorsson et al., 2012) but in the model the water depth is larger, 66 m. The modelled halocline in the Gulf of Finland is too strong and shallow, approximately at about 50 m depth (Meier, 2007; Väli et al., 2013). The water exchange, and hence, the supply of oxygen below the halocline is much less effective than in the surface layers above. This can be one of the reasons why the modelled OPD is zero at Kasuuni, while the observations show non-zero OPDs. At GB-B the modelled and observed depths are about 70 m, which approximately coincide with the depth of the fluctuating halocline in the Baltic proper (Väli et al., 2013). The bottom water at this station may therefore often shift between anoxic and oxic conditions. This is reflected in the variability of the modelled OPD (Fig. 5, left). It is not possible to simulate the exact timing and amplitude of observed OPD variations with a large-scale model although the variability of the model well captures

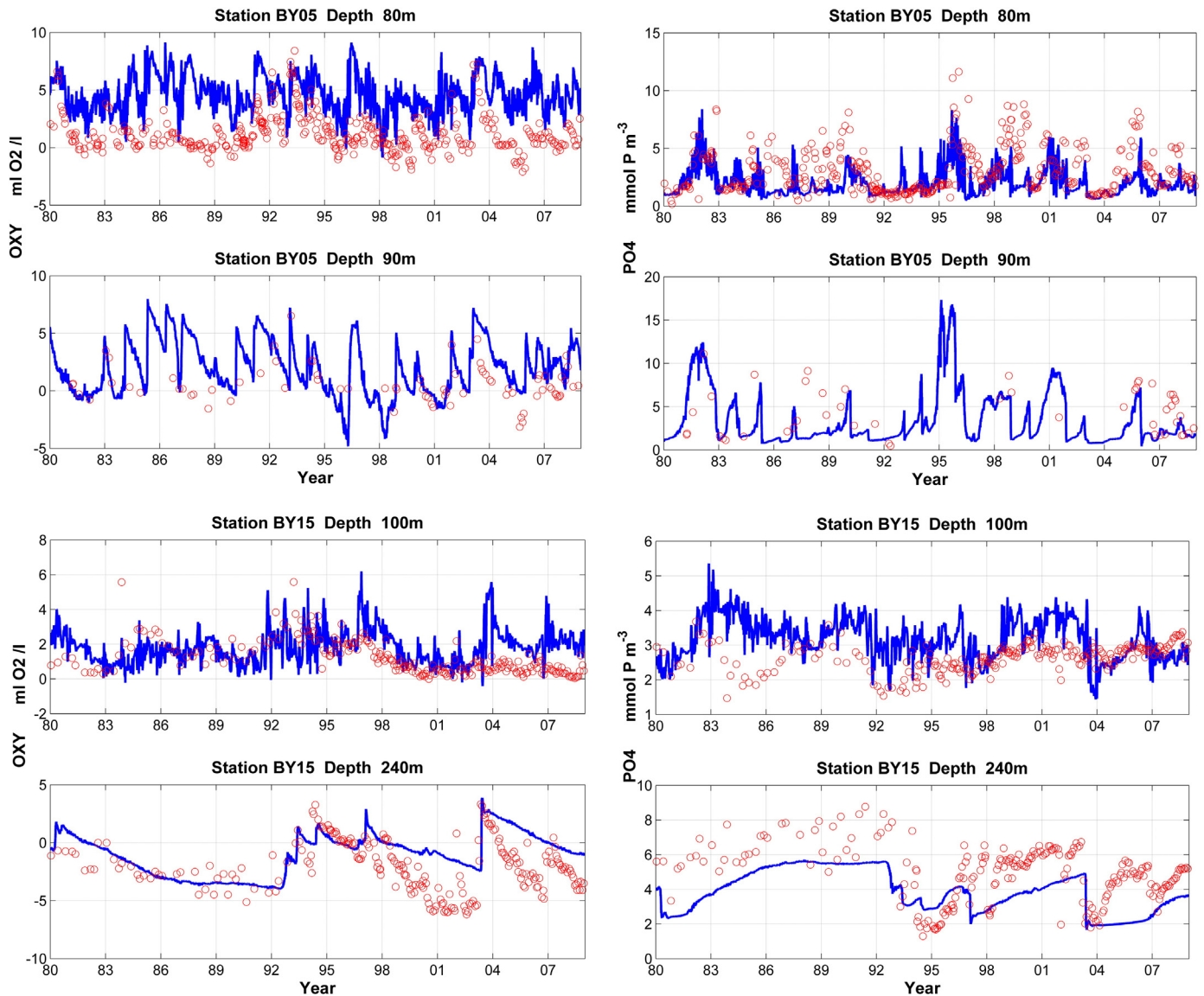


**Fig. 3.** Modelled (line) bottom water concentrations of oxygen ( $\text{ml l}^{-1}$ ) (left) and phosphate ( $\text{mmol m}^{-3}$ ) (right) are compared to observations (circles) at the stations BY05 in the Bornholm Basin (top), and BY15 (bottom) in the Eastern Gotland Basin, during the period 1980–2008.

the magnitudes of the observed OPD. A similar fluctuating pattern can be observed for station W-B (Fig. 5, right). The observed and modelled water depth at W-B is about 120 m. Due to the restricted water exchange the bottom water has low oxygen concentrations with shallow OPD, at the most about 2 mm for the period 1980–2008. The bottom water often becomes anoxic during long periods with zero OPD as a result.

### 3.1.3. Phosphate release from sediment

The oxygen conditions in the sediment affect the release of phosphate from the sediment to the overlying water and the bottom water phosphate concentration. Most observations of phosphate concentrations in the bottom water fit within the variability of the modelled (1980–2008) phosphate concentrations depicted at different OPD (Fig. 6A). The mean phosphate release rates from the sediment to the water column is low with a small standard deviation at large oxygen penetration depths (Fig. 6B), which is in accordance with observations. There is also an uptake of phosphate by the sediment, which is seen by observations (Fig. 6B) for OPD > 1 mm depth in the sediment. These occasions are not captured by the variability of the model results as

seen from the modelled standard deviation, but the modelled minimum values shows that the model has the capability to a low uptake of phosphate from the water column. Some observations show high phosphate release rates also under oxic conditions in the sediment, which is not captured by the variability (standard deviation) of the model. However, the maximum release rates of phosphate at different OPD shows that the model has the capacity to also capture higher release rates both at oxic conditions and at zero OPD. It is difficult to judge whether these observations can be regarded as representative values for the monthly means or if the momentary measurements of sediment fluxes are influenced by temporary fluctuations in the bottom water oxygen concentrations. There are also challenges with measuring low phosphate fluxes (Almroth et al., 2009) that may affect the observations.

The long-term mean (1980–2008) of phosphate concentrations at different bottom water oxygen concentrations corresponds very well with the observations, that mainly are within the  $\pm 1$  standard deviation of the model results (Fig. 6C). The phosphate release from the sediment is very low at oxygen concentrations higher than about  $100 \text{ mmol m}^{-3}$  (Fig. 6D) and increases with oxygen depletion. The variability of modelled phosphate release at anoxic conditions captures

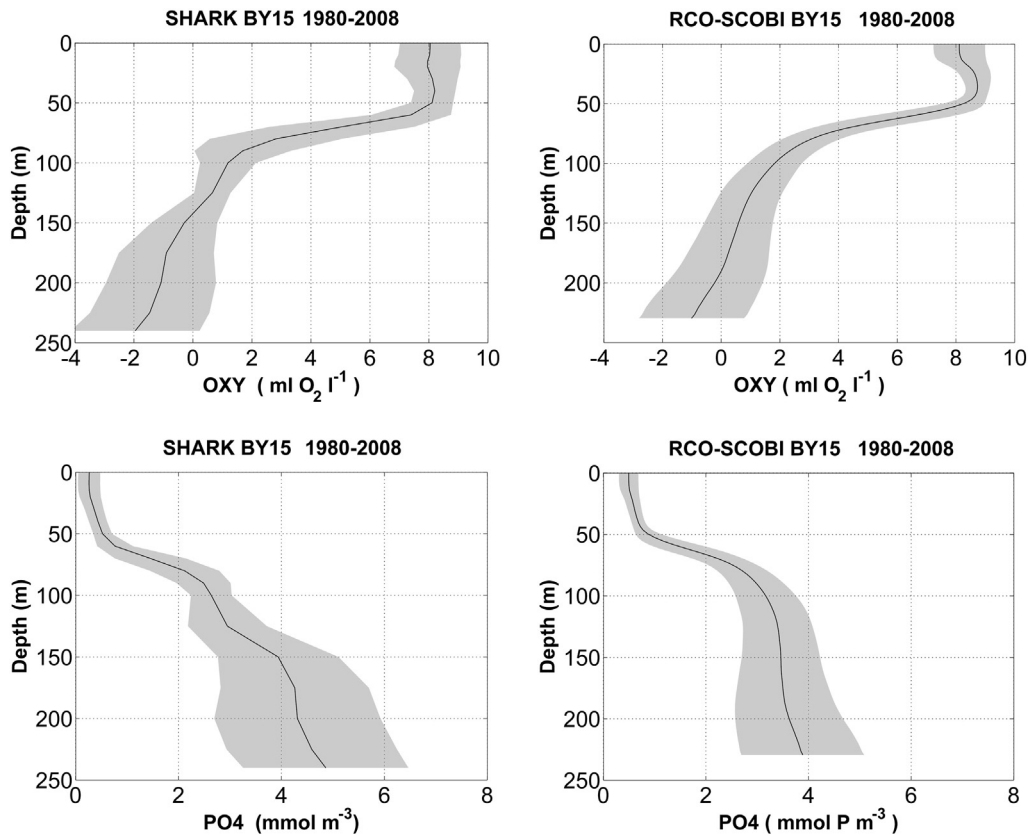


**Fig. 4.** The long-term (1980–2008) mean profiles of oxygen ( $\text{ml l}^{-1}$ ) and phosphate ( $\text{mmol m}^{-3}$ ) concentrations at station BY15 are shown by the black line in the top and low panels, respectively. The  $\pm 1$  standard deviation is shown by the grey shaded area. Observations are to the left and model results to the right.

well the variability of observed fluxes (Fig. 6D). The modelled maximum values of phosphate release rates show that the model capture also the high observed values. The results of the validation to *in situ* observations show that the model captures well the dynamics of oxygen and phosphate in the bottom water.

### 3.2. Spatial variation of the oxygen penetration depth

The spatial variability of the simulated OPD (Fig. 7) show highest values in shallow coastal zones, approximately at depth above the halocline. Lowest values are found in the deeper central basin,

**Table 6**

The mean observed oxygen penetration depth (OPD obs) and the standard deviation (STDV obs) for each field study at the different stations in the Gulf of Finland (GF) and Baltic proper (BP) with the observed (ObsDepth) and modelled (ModDepth) water depth during the given date (year; month). The model results are calculated as monthly mean (OPD mod) with the representative standard deviation (STDV mod). The difference between OPD obs and OPD mod is given as  $\Delta\text{OPD}$ . For location of the stations, see Fig. 1.

Basin	Station	Year	Month	Obs Depth (m)	Mod Depth (m)	OPD Obs (mm)	STDV Obs	OPD Mod (mm)	STDV Mod	$\Delta\text{OPD}$ (mm)
BP	GB-A <sup>2</sup>	2008	9	60	45	-2.9	0.3	-21.0	1.4	17.8
BP	GB-B <sup>2</sup>	2008	9	75	72	-5.3	0.2	-2.6	0.2	-2.7
BP	GB-D <sup>2</sup>	2008	9	128	123	0.0		0.0	0.00	0.0
BP	GB-E <sup>2</sup>	2008	9	180	165	0.0		0.0	0.02	0.0
BP	GB-F <sup>2</sup>	2008	9	210	216	0.0		0.0	0.00	0.0
BP	W-A <sup>3</sup>	1996	8	75	75	-1.5	0.0	-1.1	0.00	-0.4
BP	W-B <sup>3</sup>	1996	8	115	120	-1.5	0.0	0.0	0.00	-1.5
BP	W-C <sup>3</sup>	1996	8	155	165	-0.9	0.0	0.0	0.00	-0.9
BP	W-D <sup>3</sup>	1996	8	210	231	0.0	0.0	0.0	0.00	0.0
GF	GF1 <sup>2</sup>	2002	6	72	81	0.0		0.0	0.00	0.0
GF	GF2 <sup>2</sup>	2002	6	81	81	0.0		0.0	0.00	0.0
GF	PV1 <sup>1</sup>	2003	6	75	45	0.00	0.00	0.0	0.00	0.0
GF	PV1 <sup>1</sup>	2004	9	70	45	-1.9	0.2	0.0	0.00	-1.9
GF	PV1 <sup>1</sup>	2005	5	73	45	-0.6	0.2	0.0	0.00	-0.6
GF	XV1 <sup>1</sup>	2005	5	17	39	-1.8	0.4	-0.2	0.3	-1.6
GF	Kasuuni <sup>1</sup>	2003	7	53	66	-3.1	0.7	0.0	0.00	-3.1
GF	Kasuuni <sup>1</sup>	2004	9	54	66	-2.4	0.4	0.0	0.00	-2.4
GF	Kasuuni <sup>1</sup>	2005	5	54	66	-2.4	0.5	0.0	0.00	-2.4

<sup>1</sup> The observed OPD from these stations are calculated from oxygen data (Almroth et al., 2009).

<sup>2</sup> The observed OPD from these stations are calculated from unpublished data.

<sup>3</sup> The observed OPD from these stations are adopted from Wenzhöfer et al. (2002).



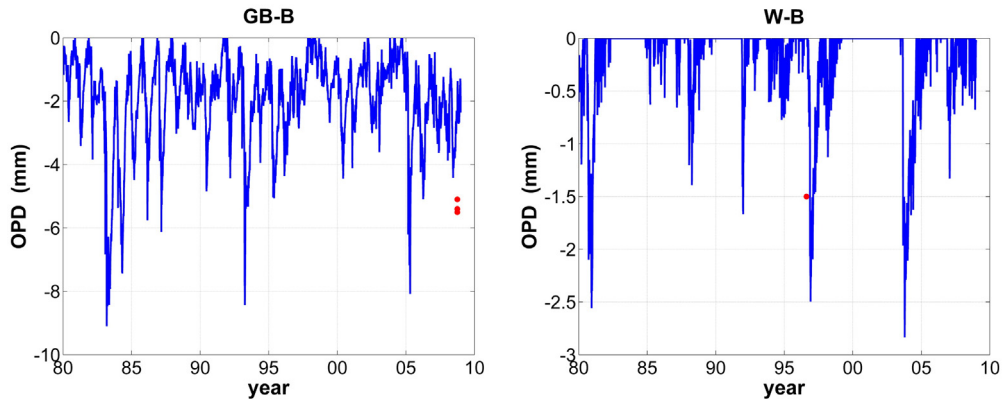


Fig. 5. The modelled (line) OPD (mm) at station GB-B (left) and at W-B (right) over time. Observations are shown as filled circles.

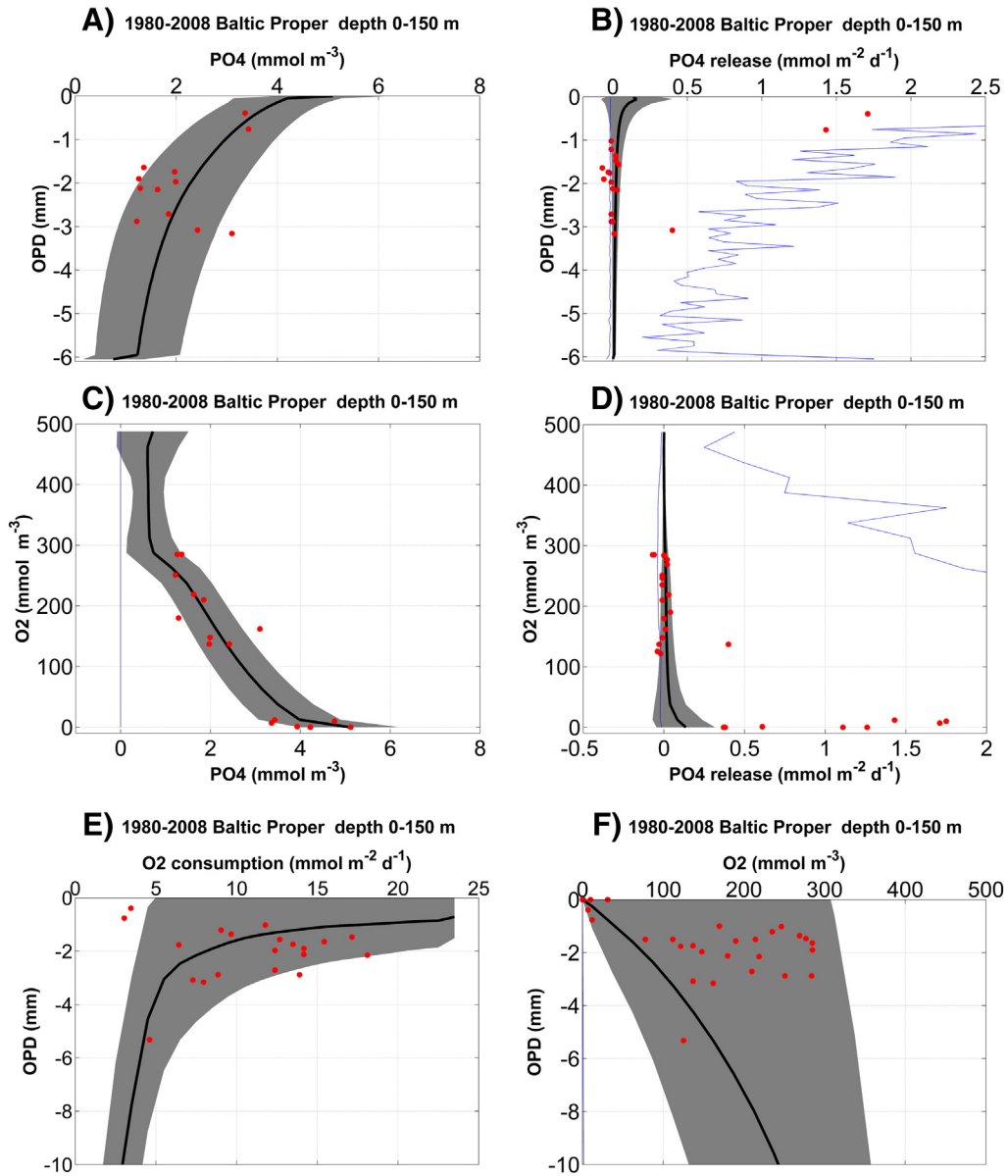
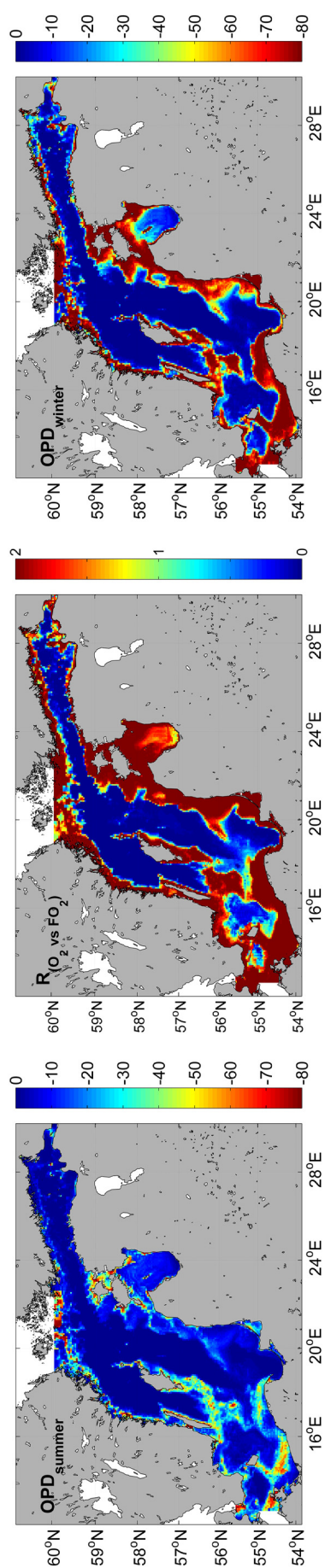


Fig. 6. The average values (black line) of the annual mean, during the period 1980–2008,  $\pm 1$  standard deviation (grey shaded area) of modelled; A) phosphate concentrations ( $\text{mmol m}^{-3}$ ) in the bottom water and B) phosphate release rates ( $\text{mmol m}^{-2} \text{d}^{-1}$ ) from the sediment to the overlying water for different oxygen penetration depths (mm); C) the phosphate concentrations ( $\text{mmol m}^{-3}$ ) and D) phosphate release rates ( $\text{mmol m}^{-2} \text{d}^{-1}$ ) from the sediment at different bottom water oxygen concentrations ( $\text{mmol m}^{-3}$ ); oxygen penetration depths (mm) for E) different oxygen consumptions ( $\text{mmol m}^{-2} \text{d}^{-1}$ ) in the sediment and F) oxygen concentrations ( $\text{mmol m}^{-3}$ ) in the bottom water. The thin black lines are the maximum and minimum values of the phosphate release rates during the period and filled circles are observations from different stations during the year 1996, 2002–2005 and 2008–2010.



**Fig. 7.** The spatial variability in the Baltic Proper of the August–September (left) and January–February (right) long term (1980–2008) monthly mean of OPD (mm) and the long-term mean of OPD from oxygen consumption versus oxygen concentrations (middle). The impact from the consumption and concentrations of oxygen on the OPD is equal at areas shown by green color. In areas with yellow–red colors the oxygen flux have larger impacts on the OPD compared to oxygen concentrations, while the turquoise–blue color shows areas where the oxygen concentrations controls the OPD.

where the oxygen concentration often is low. The seasonal variations show lowest long-term (1980–2008) monthly mean values of OPD (Fig. 7, left) during late summer and early fall (August–September), while the sediment still is enriched by organic material from algal blooms. This area is approximately the same as where the minimum oxygen concentrations are found (not shown). Largest mean OPD values (Fig. 7, middle) are mainly found during winter (January–February), before the productive season, thus before high deposition of organic material on the sediment surface. The seasonal variation of OPD has been shown also in field studies, e.g. in the study by Rasmussen and Jorgensen (1992) in the Aarhus Bay, in Denmark. They also found that the OPD decreased during spring/summer and then increased again during next winter when the fresh organic material was depleted. The largest OPD in the Baltic Sea found in literature is  $-40$  mm in the northern Bothnian Bay (Slomp et al., 2013). OPD down to  $-3.2$  mm has been found in other studies for the Baltic proper (Hietanen and Kuparinen, 2008; Steenbergh et al., 2011; Wenzhöfer et al., 2002), while the maximum OPD calculated from the observation data used in the present study was  $-5.5$  mm.

During storm events increased water mixing (improved oxygen conditions) and resuspension cause increased OPD. The immediate response in the model for changes in the consumption and concentration of oxygen in the OPD calculations can during resuspension events momentary lead to large OPD. Thus, during a resuspension event lasting for a day or more the organic material in the sediment is removed and by that the oxygen consumption decrease to very small values causing a maximum OPD (see Eq. (1)). However, the mean release rate of mineral bound phosphate is decreased by 90 % already at OPD of about  $-1$  mm (Eq. (16)).

The modelled largest mean OPD is reached at oxygen consumptions between  $>0$  and  $\leq 0.5$   $\text{mmol O}_2 \text{ m}^{-2} \text{ d}^{-1}$  and gets then rapidly shallower with increasing oxygen consumption (Fig. 6E). This is in accordance with the discussions from earlier studies (Conley et al., 1997; Lehtoranta and Heiskanen, 2003; Lehtoranta et al., 2009; Pitkanen et al., 2007) that high amounts of organic matter on the sediment surface can lead to decreased OPD and thus decreased phosphate retention capacity in the sediment, in spite of oxic bottom water. The OPDs at different bottom water oxygen concentrations are more variable (Fig. 6F), which also confirms that the OPD not necessary is large at high oxygen concentrations.

The mean (1980–2008) relative impact of oxygen concentration and oxygen flux on the magnitude of the OPDs in different areas (Fig. 7, right) showed that the oxygen consumption controlled the variability of OPD in the coastal zones. These are approximately at the same areas as where the large winter values of OPDs are found and where the seasonal variations seem to be large. The consumption of oxygen has generally a greater impact on the OPD than the temperature dependent sediment diffusivity (not shown).

### 3.3. Phosphate fluxes in the Baltic Proper

The net phosphate release rates from the sediment are calculated as long time means (1980–2008) for the whole Baltic Proper at four different depth levels (0–30, 30–60, 60–150 and  $>150$  m) during oxic and anoxic conditions. This categorization of depths is similar to what has been done in previous studies (Mort et al., 2010; Viktorsson et al., 2013).

The sum of deposition of organic and inorganic phosphorus on oxic sediments is at all depth levels larger than the release of phosphorus (Table 7). For anoxic bottoms the opposite is seen; the release of total phosphorus during this period is larger than the deposition of phosphorus. About  $43 \times 10^3$  t P year $^{-1}$  is taken up by the oxic sediments while about  $19 \times 10^3$  t P year $^{-1}$  is released from the anoxic sediments. In total the net Baltic proper sediment sink is then about  $23.7 \times 10^3$  t P year $^{-1}$ . The largest net loss (sources-sinks) of phosphate from

**Table 7**

The long term (1980–2008) mean of net phosphate release (PO4 Release) from the sediment to the overlying water, the net deposition of organic (OrgP Deposition) and inorganic (IorgP Deposition) phosphorus to the sediment and the burial of phosphorus is given for the different depth levels (Depth) during oxic and anoxic conditions in the Baltic Proper. The corresponding area to each depth level is given, as well as the fraction (%) of the total area which is 262,900 km<sup>2</sup>.

	Depth (m)	PO4 Release 10 <sup>3</sup> t P yr <sup>-1</sup>	OrgP Deposition 10 <sup>3</sup> t P yr <sup>-1</sup>	IorgP Deposition 10 <sup>3</sup> t P yr <sup>-1</sup>	Burial 10 <sup>3</sup> t P yr <sup>-1</sup>	Area km <sup>2</sup>	Area of tot %
OXIC	0–30	4.5	23.8	–15.2	4.1	85,400	32
	30–60	8.0	28.9	–10.5	8.2	70,800	27
	60–150	17.4	34.6	9.9	8.2	49,700	19
	>150	0.6	1.1	0.3	0.3	1970	0.8
ANOXIC	0–250	30.4	88.4	–15.5	20.7	208,000	79
	0–30	3.8	2.7	0.7	0.3	400	0.2
	30–60	8.5	3.7	2.6	1	2700	1
	60–150	59.4	30.7	12.8	5.3	43,800	17
	>150	5.5	4.0	1.1	0.6	8000	3
	0–250	77.0	41.0	17.1	7.2	54,900	21

the sediment to overlying water was about  $59 \times 10^3 \text{ t P year}^{-1}$  (Table 7) which corresponds to a phosphate release rate of  $0.12 \text{ mmol P m}^{-2} \text{ d}^{-1}$ . This flux was found on anoxic bottoms at depths between 60 and 150 m. On average these anoxic bottoms (Fig. 8, left) cover about 17% of the total area in the Baltic proper. During oxic conditions on this depth level the phosphate release was about  $17 \times 10^3 \text{ t P year}^{-1}$  (Table 7), which corresponds to a phosphate release rate of about  $0.03 \text{ mmol P m}^{-2} \text{ d}^{-1}$ . This release rate is in agreement with the observations found by Viktorsson et al. (2013) who measured a phosphate release rate of  $0.027 \text{ mmol P m}^{-2} \text{ d}^{-1}$  at the same depth level. In accordance with earlier studies (Jilbert et al., 2011; Koop et al., 1990; Mort et al., 2010) the highest phosphate fluxes are mainly found at periodically anoxic areas where the bottom water varies between oxic, hypoxic and anoxic oxygen conditions. Lowest release rates of phosphate,  $0.007 \text{ mmol P m}^{-2} \text{ d}^{-1}$ , were found at the oxic areas, of which 59% were found between surface and 60 m depth (Fig. 8, right) and 17% at the depth level 60–150 m (Table 7). Measurements at oxic sediments has shown a variability of phosphate fluxes that range from an uptake to the sediment of  $0.25 \text{ mmol P m}^{-2} \text{ d}^{-1}$  to a release up to  $0.36 \text{ mmol P m}^{-2} \text{ d}^{-1}$  (Conley et al., 1997; Koop et al., 1990; Laima et al., 2001; Lehtoranta and Heiskanen, 2003; Lukkari et al., 2009a; Pitkänen et al., 2001; Viktorsson et al., 2012, 2013). The spatial variability of the iron content in the Baltic Sea sediments is not well known and is therefore not included in the present model setup. The model therefore uses a spatially invariant half saturation constant (Table 4) that describes the limitation from hydrated metal oxides available for phosphate adsorption. A possible limitation in phosphate retention due to too low iron concentrations (relative to the need for phosphate binding) would under oxic conditions lead to higher effluxes of phosphate from the

model sediment. The model formulation may be further studied when more knowledge about the iron dynamics in the Baltic Sea becomes available.

At anoxic sediments below 150 m depth the model showed average phosphate release rates of about  $0.06 \text{ mmol P m}^{-2} \text{ d}^{-1}$ . The modelled release rates at anoxic sediments in the Baltic Proper ( $0.06\text{--}0.12 \text{ mmol P m}^{-2} \text{ d}^{-1}$ ) are within the large range of measured fluxes of phosphate at anoxic bottoms,  $0.001$  to  $1.75 \text{ mmol P m}^{-2} \text{ d}^{-1}$  (Hille, 2005; Jilbert et al., 2011; Lukkari et al., 2009a; Mort et al., 2010, Fig. 7; Viktorsson et al., 2012; Viktorsson et al., 2013).

As mentioned in Section 3.1.1 the deep water phosphate concentrations became too low when compared to measurements especially during the latter part of the stagnation period in the 1980s. At other depth levels no depletion of the benthic pools of phosphorus occurred. This is explained by the buildup of the pools during oxic conditions when more phosphorus is deposited on the sediment surface than is released. During the long anoxic period, however, the benthic pools of inorganic and organic phosphorus declined substantially and caused low release rates of phosphate. This shortcoming occurs in the deepest part of the Baltic proper where the mean anoxic bottom area at depth below 150 m represents only about 3% of the total bottom area why the impact is of minor importance for the Baltic Sea on the long term. The degradation rate of benthic organic matter in the present model has a shorter time scale on which the benthic pools of nutrients can be depleted (Meier et al., 2012a), compared to the model setup described by Eilola et al. (2009). The slower degradation rate of organic material in the sediment used in the model study by Eilola et al. (2009) lead to a larger pool of phosphorus which could be released on longer time scales. Stigebrandt et al. (2014) discussed whether there is a source of phosphate in the sediment that

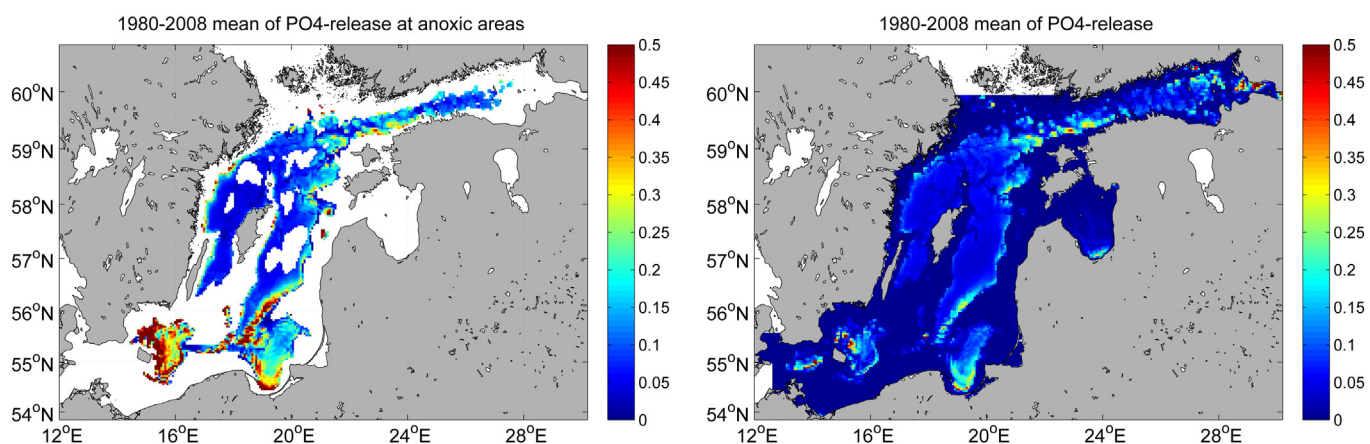


**Fig. 8.** The net long term mean (1980–2008) of phosphate release rate ( $\text{mmol m}^{-2} \text{ d}^{-1}$ ) at the depth 60–150 m during anoxic conditions (left) and on all depth levels and oxygen conditions (right).

was accumulated before the sediment became anoxic to be able to maintain the high phosphate release during longer anoxic periods. They mean that the phosphate source could consist of either organic phosphorus and/or a hydrous ferric phosphate mineral that undergoes very slow dissolution contributing to the long term phosphate release from the sediment in addition to the degradation of the deposited organic material from the water column. The importance of the degradation rate may be further studied from sensitivity experiments with the present model.

### 3.4. The Baltic Sea phosphorus sink

The balance between phosphorus loads to the Baltic Sea and the export of phosphorus to the Kattegat is determined by the sink efficiency in the Baltic Sea, i.e. how large fraction of the loads are permanently removed and stored within the Baltic Sea. The calculated phosphorus sink efficiency, was on average about 83 % during the period 1980 to 2008, i.e. about 17% of the average loads of phosphorus were exported from the Baltic Sea. The calculation of the net export to Kattegat ( $9.5 \times 10^3 \text{ t year}^{-1}$ ) is derived from the mass balance between the load from land, burial and change in the pools of phosphorus (cf. Meier et al., 2012b). The total annual supply of phosphorus to the Baltic Sea in the present simulation decreased from a maximum of  $74 \times 10^3 \text{ t year}^{-1}$  in 1980 to about  $35 \times 10^3 \text{ t year}^{-1}$  in 2008 and was on average  $54.4 \times 10^3 \text{ t year}^{-1}$  during the period. On average about  $50 \times 10^3 \text{ t year}^{-1}$  was permanently buried and removed from the sediment while the pools of active phosphorus in the water and sediment decreased by  $5.1 \times 10^3 \text{ t year}^{-1}$ . The decrease in phosphorus pools is caused by the imbalance between sources and sinks that was caused by the reduced phosphorus loads during the period.

Meier et al. (2012b) estimated for the period 1978–2007 from a model ensemble of three coupled physical–biogeochemical models the sink efficiency to 85 %. According to the numbers by Stigebrandt et al. (2014) the sink capacity was 88 % in year 1980 and decreased to 75 % in 2005. The calculation of the phosphorus sink efficiency is, however, somewhat delicate since it depends on the time period of consideration. There were drastic changes in the external loads of phosphorus after 1980 while the changes in total pools in the water and sediment are quite slow due to the large pools compared to the relatively slow burial and export to the Kattegat. The variability of the phosphorus pools in the water is large due to the varying oxygen conditions and exchanges with the sediment. However, the present results corresponds to the average sink capacity (82%) of the two years 1980 and 2005 estimated from the numbers presented by Stigebrandt et al. (2014). Hence, it is difficult to obtain accurate numbers just by judging from one single year and using information solely from the water column at a few stations in the Baltic proper. In order to obtain a representative figure of the sink efficiency, the calculation should preferably be performed during a period of equilibrium or cover a longer period accounting for the natural variability of inter-annual and decadal fluctuations caused by Baltic Inflows. Because of the long water residence time in the Baltic Sea also the pools in the Bothnian Sea and Bothnian Bay should be taken into consideration as the sediments here may act as sinks for phosphorus exported from the Baltic proper (e.g. Slomp et al., 2013).

The modelled sink efficiency for the periods 1980–1989 and 2000–2008 was 79% and 88%, respectively. Thus, the modelled sink efficiency increased from the 1980s to the 2000s in the present simulation. This result is in contradiction to the results by Stigebrandt et al. (2014) who saw decreased sink efficiency in 2005 compared to 1980. According to basin scale integrated observations (see Fig. 11 in Eilola et al., 2011) the phosphorus pool in the Baltic Proper increased from the late 1990s and accelerated rapidly after the Major Baltic Inflows (MBI) in 2003. The rapid increase after 2003 is not reproduced by the present simulation. The reason for the increased sink efficiency in the current simulation is much because phosphorus was retained on large areas with oxic sediments. These areas remained for the last part of the model run while observations indicated an increase of the hypoxic

and anoxic areas (Hansson and Andersson, 2013). Also the relatively high burial ( $50 \times 10^3 \text{ t year}^{-1}$ ), that causes decreasing sediment pools of phosphorus, partly describes the increased sink efficiency in the last part of the run. In the present model the burial rates of the inorganic and organic sediment pools are assumed equal (Eqs. (14), (15)), thus about two thirds of the buried phosphorus in sediment with oxic bottom water (Table 7) originates from the mineral bound pool. In sediment with anoxic condition about half of the buried phosphorus in the sediments originates from the mineral bound pool. It is possible that there should be differential burial rates of the different pools because of the quite different dynamic behavior of the inorganic and organic fractions of phosphorus in the sediment. Hence, a fraction of the buried inorganic phosphorus in the present run could for instance be transferred to the pool of mineral bound phosphorus and become available for release during anoxic conditions. The main conclusions of the present paper will however not be affected by this. More model experiments are needed to investigate further the details of this issue.

Studies in a fjord (Roskilde fjord), different estuaries (Humber and Ems) and river mouths (Ouse, Trent) show that the retention of phosphorus varies between 40 and 90% (Kamp-Nielsen, 1992; Sanders et al., 1997; Van Beusekom and De Jonge, 1998), while in the North sea a retention (burial) of the phosphorus load from land was calculated to only 2% (Brion et al., 2004). Thus, the estimated sink efficiency (80–85%) of the present Baltic Sea is in the higher range compared to other areas, which can be explained by the high residence time of the water in the Baltic Sea. The net export of phosphorus through estuaries was found to be inversely correlated with the mean residence time of the water system (Nixon et al., 1996).

In the future scenarios by Meier et al. (2012b) for the period 2069–2097, the estimated phosphorus sink efficiency becomes 67% in the reference scenario and 64% in the worst nutrient load case “the Business as Usual” scenario. According to the conclusions by Meier et al. (2012b) the reduced sink efficiency depends on the increased temperature. Higher water temperatures are projected to reduce oxygen concentrations due to lower solubility in warmer water and accelerate organic matter mineralization and oxygen consumption. Expanding anoxia increase the phosphate release rates from the sediments, and amplify the phosphorus recycling which will reduce the permanent removal of phosphorus from the ecosystem. Together with an accelerated pelagic recycling loop, this intensifies primary production and oxygen consumption and reinforces the phosphorus release from the sediments.

### 3.5. Phosphate dynamics during deep water inflows

The impact of major deep water inflows on oxygen conditions and release of phosphate from the sediment in the deep parts of the Baltic proper is studied using the present model setup. The decrease in deep water phosphate concentrations due to MBI (Fig. 3 and e.g. Conley

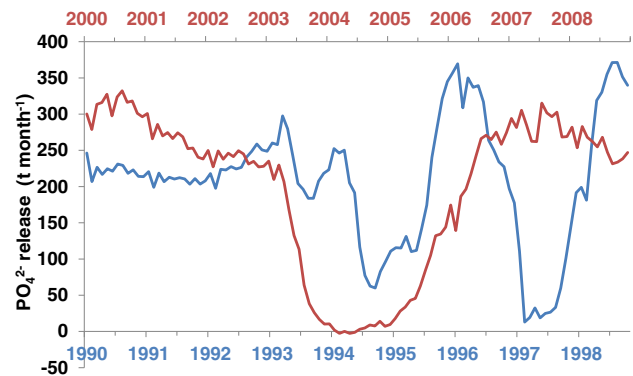


Fig. 9. Monthly mean of the phosphate release ( $\text{t P month}^{-1}$ ) from sediment to water column during two different time periods, 1990–1998 (blue) and 2000–2008 (red) in the Eastern Gotland Basin.

et al., 2002; Savchuk, 2013) is a result from a combination of dilution effects and decreased phosphate release from the sediment because of increased sediment retention capacity since the bottom water is oxygenated.

The modelled monthly mean of the net phosphate release from the sediment at depth below 150 m in the Eastern Gotland Basin was in the range of 200 and 350 t P month<sup>-1</sup> in the beginning of the periods 1990–1998 and 2000–2008, respectively (Fig. 9). In 1993, 1994, 1997 and 2003 large decreases in the phosphate release rates are observed, which coincidence with MBIs (Reissmann et al., 2009). Also in 2001 there was an inflow, which resulted in a decrease in the modelled phosphate release rate, which is observed in Fig. 9. Due to the MBI in 2003 the modeled net release even becomes negative during 2004, i.e. phosphate is taken up by the sediment. In the beginning of 2005 the net phosphate release rate increases again in agreement with the increased phosphate concentrations in the deep water shown in Fig. 3. Modelled net uptake of phosphate from the water to the sediment is only found in the period from May 2003 to June 2004 and to a very low extent, on average 2.9 t P month<sup>-1</sup>, which in total corresponds to about 40 t phosphorus. The total phosphorus pool in the water the month before the MBI was  $26 \times 10^3$  t P. Thus, the uptake of phosphate by the sediment corresponded to only 0.15 % of the total phosphorus content in the bottom water (>150 m depth), and can thus be concluded to play a minor role in the decreased bottom water phosphate concentrations. This uptake is much lower compared to the uptake calculated in the study by Schneider (2011), in which it was concluded that the immediately decrease in phosphate and dissolved inorganic carbon concentrations due to the MBI in the beginning of 2003 was caused to 66% by dilution of the incoming water and to 33% of adsorption to newly formed iron(III)oxides on the sediment surface. About seven month after the inflow Schneider (2011) stated that the C<sub>T</sub> started to increase again while the phosphate concentrations stayed on a low level. The phosphate concentrations started to increase in the beginning of 2005, which is in accordance with the increased phosphate release rate in 2005 seen in the present study. Eilola et al. (2014) found in their model experiment that about 85% of the tracer mass was removed due to dilution effects which also is a larger dilution effect compared to that obtained by Schneider (2011). Sediment uptake of phosphate from the water column at a normally anoxic station which became oxic for a period has been measured *in situ* by Viktorsson et al. (2012). The time-scale for how long this uptake of phosphate may take place was, however, not studied why this is a question for future investigations.

#### 4. Conclusions

The RCO-SCOBI model reproduces well the bottom water phosphate and oxygen concentrations in the Baltic proper during the studied period 1980–2008. In general the new approach to model benthic phosphorus captures much of the phosphate dynamics, and the oxygen penetration depths shows good results compared to observations.

Largest OPDs are found during winter time in the coastal zones, where also the impact from oxygen consumption on the determination of the OPD is found to be largest. During late summer the OPD decreases due to increased deposition of organic material on the sediment surface. Lowest OPD are found in the deeper parts of the basin where the oxygen concentrations often are low, which mainly determines the OPD at these areas. The temperature and salinity dependent sediment diffusivity had a relatively modest contribution to the determination of the OPD compared to the oxygen consumption and concentrations.

Highest modelled release rate of phosphate from the sediment to the overlying water is about  $59 \times 10^3$  t P year<sup>-1</sup>, which corresponds to a phosphate release rate of 0.12 mmol P m<sup>-2</sup> d<sup>-1</sup>. It is found on anoxic sediment in the depth layer between 60–150 m, which is an area that varies between presence of oxygen, hypoxia and anoxia. The sum of deposition of organic and inorganic phosphorus on oxic sediments is at all

depth levels larger than the release of phosphorus from the sediment. For anoxic bottoms the opposite is seen; the release of total phosphorus during the investigated period is larger than the deposition of phosphorus. In total the net Baltic proper sediment sink is about  $23.7 \times 10^3$  t P year<sup>-1</sup>. The estimated phosphorus sink efficiency of the entire Baltic Sea is on average about 83% during the period, i.e. about 17% of the average external loads are exported from the Baltic Sea.

The phosphate release rate from the sediment is shown to drastically decrease and even become negative as a result of Major Baltic Inflows, which transports oxygenated water to the previously anoxic bottoms in the Baltic proper. However, the decrease in the bottom water concentrations of phosphate due to the MBI is mainly explained by dilution. The uptake of phosphate by the sediment from the water column was in this study concluded to be negligible.

The number of available observations of Baltic Sea sediment oxygen penetration depth and sediment–water fluxes is limited, and more observations are needed to be able to do more comprehensive validations covering longer time periods and larger areas.

#### Acknowledgements

The research presented in this study is part of the Baltic Earth programme (Earth System Science for the Baltic Sea region, see <http://www.baltex-research.eu/balticearth>) and was funded by the Swedish Research Council for Environment, Agricultural Sciences and Spatial Planning (FORMAS) within the projects “Impact of accelerated future global mean sea level rise on the phosphorus cycle in the Baltic Sea” (grant no. 214-2009-577) and “Impact of changing climate on circulation and biogeochemical cycles of the integrated North Sea and Baltic Sea system” (grant no. 214-2010-1575). Additional support came from Stockholm University’s Strategic Marine Environmental Research Funds “Baltic Ecosystem Adaptive Management (BEAM)” and as part of the COCOA and BIO-C3 projects from the BONUS, the joint Baltic Sea research and development programme (Art 185), funded jointly from the European Union’s Seventh Programme for research, technological development and demonstration and from FORMAS.

The RCO model simulations were performed on the climate computing resources “Ekman” and “Vagn” jointly operated by the Centre for High Performance Computing (PDC) at the Royal Institute of Technology (KTH) in Stockholm and the National Supercomputer Centre (NSC) at Linköping University. “Ekman” and “Vagn” are funded by a grant from the Knut and Alice Wallenberg foundation.

#### References

- Almroth-Rosell, E., Eilola, K., Hordoir, R., Meier, H.E.M., Hall, P.O.J., 2011. Transport of fresh and resuspended particulate organic material in the Baltic Sea – a model study. *J. Mar. Syst.* 87, 1–12.
- Almroth, E., Tengberg, A., Andersson, J.H., Pakhomova, S.V., Hall, P.O.J., 2009. Effects of resuspension on benthic fluxes of oxygen, nutrients, dissolved inorganic carbon, iron and manganese in the Gulf of Finland, Baltic Sea. *Cont. Shelf Res.* 29, 807–818.
- Beckmann, A., Döscher, R., 1997. A method for improved representation of dense water spreading over topography in geopotential-coordinate models. *J. Phys. Oceanogr.* 27, 581–591.
- Blomqvist, S., Gunnars, A., Elmgren, R., 2004. Why the limiting nutrient differs between temperate coastal seas and freshwater lakes: a matter of salt. *Limnol. Oceanogr.* 49, 2236–2241.
- Boudreau, B.P., 1996. The diffusive tortuosity of fine-grained un lithified sediments. *Geochim. Cosmochim. Acta* 60, 3139–3142.
- Brion, N., Baeyens, W., De Galan, S., Elskens, M., Laane, R.P.M., 2004. The North Sea: source or sink for nitrogen and phosphorus to the Atlantic Ocean? *Biogeochemistry* 68, 277–296.
- Broecker, W.S., Peng, T.H., 1974. Gas exchange rates between air and sea. *Tellus* 26, 21–35.
- Cai, W.-J., Sayles, F.L., 1996. Oxygen penetration depths and fluxes in marine sediments. *Mar. Chem.* 52, 123–131.
- Conley, D., Björck, S., Bonsdorff, E., Carstensen, J., Destouni, G., Gustafsson, B., 2009. Hypoxia-related processes in the Baltic Sea. *Environ. Sci. Technol.* 43, 3412–3420.
- Conley, D.J., Humborg, C., Rahm, L., Savchuk, O.P., Wulff, F., 2002. Hypoxia in the Baltic Sea and basin-scale changes in phosphorus biogeochemistry. *Environ. Sci. Technol.* 36, 5315–5320.

- Conley, D.J., Stockenberg, A., Carman, R., Johnstone, R.W., Rahm, L., Wulff, F., 1997. Sediment-water nutrient fluxes in the gulf of Finland, Baltic Sea. *Estuar. Coast. Shelf Sci.* 45, 591–598.
- Eilola, K., Almroth-Rosell, E., Dieterich, C., Fransner, F., Höglund, A., Meier, H.M., 2012. Modeling nutrient transports and exchanges of nutrients between shallow regions and the open Baltic Sea in present and future climate. *Ambio* 41, 586–599.
- Eilola, K., Almroth-Rosell, E., Meier, H.E.M., 2014. Impact of saltwater inflows on phosphorus cycling and eutrophication in the Baltic Sea. A 3D model study. *Tellus A* 66, 23985.
- Eilola, K., Gustafsson, B.G., Kuznetsov, I., Meier, H.E.M., Neumann, T., Savchuk, O.P., 2011. Evaluation of biogeochemical cycles in an ensemble of three state-of-the-art numerical models of the Baltic Sea. *J. Mar. Syst.* 88, 267–284.
- Eilola, K., Meier, M.H.E., Almroth, E., 2009. On the dynamics of oxygen, phosphorus and cyanobacteria in the Baltic Sea; a model study. *J. Mar. Syst.* 75, 163–184.
- Eilola, K., Mårtensson, S., Meier, H., 2013. Modeling the impact of reduced sea ice cover in future climate on the Baltic Sea biogeochemistry. *Geophys. Res. Lett.* 40, 149–154.
- Emeis, K.C., Struck, U., Leipe, T., Pollehne, F., Kunzendorf, H., Christiansen, C., 2000. Changes in the C, N, P burial rates in some Baltic Sea sediments over the last 150 years – relevance to P regeneration rates and the phosphorus cycle. *Mar. Geol.* 167, 43–59.
- Fischer, H., Matthäus, W., 1996. The importance of the Drogden Sill in the Sound for major Baltic inflows. *J. Mar. Syst.* 9, 137–157.
- Fonselius, S., Valderrama, J., 2003. One hundred years of hydrographic measurements in the Baltic Sea. *J. Sea Res.* 49, 229–241.
- Froelich, P.N., 1988. Kinetic control of dissolved phosphate in natural rivers and estuaries – a primer on the phosphate buffer mechanism. *Limnol. Oceanogr.* 33, 649–668.
- Glud, R.N., 2008. Oxygen dynamics of marine sediments. *Mar. Biol. Res.* 4, 243–289.
- Gunnars, A., Blomqvist, S., 1997. Phosphate exchange across the sediment-water interface when shifting from anoxic to oxic conditions an experimental comparison of freshwater and brackish-marine systems. *Biogeochemistry* 37, 203–226.
- Gunnars, A., Blomqvist, S., Johansson, P., Andersson, C., 2002. Formation of Fe (III) oxyhydroxide colloids in freshwater and brackish seawater, with incorporation of phosphate and calcium. *Geochim. Cosmochim. Acta* 66, 745–758.
- Gustafsson, B., Schenk, F., Blenckner, T., Eilola, K., Meier, H.E.M., Müller-Karulis, B., Neumann, T., Ruoho-Airola, T., Savchuk, O., Zorita, E., 2012. Reconstructing the development of Baltic Sea eutrophication 1850–2006. *Ambio* 41, 534–548.
- Hall, P.O.J., Brunnegård, J., Hulth, G., Martin, W.R., Stahl, H., Tengberg, A., 2007. Dissolved organic matter in abyssal sediments: Core recovery artifacts. *Limnol. Oceanogr.* 52, 19–31.
- Hansson, M., Andersson, L., 2013. Oxygen survey in the Baltic Sea 2013 – extent of anoxia and hypoxia, 1960–2013. REPORT OCEANOGRAPHY No. 49. Swedish Meteorological and Hydrological Institute ([http://www.smhi.se/polopoly\\_fs/1.353171/Oxygen\\_timeseries\\_1960\\_2013\\_final.pdf](http://www.smhi.se/polopoly_fs/1.353171/Oxygen_timeseries_1960_2013_final.pdf)).
- Hibler, W.D., 1979. A dynamic thermodynamic sea ice model. *J. Phys. Oceanogr.* 9, 815–846.
- Hietanen, S., Kuparinen, J., 2008. Seasonal and short-term variation in denitrification and anammox at a coastal station on the Gulf of Finland, Baltic Sea. *Hydrobiologia* 596, 67–77.
- Hille, S., 2005. Sedimentary deposition and reflux of phosphorus (P) in the Eastern Gotland Basin and their coupling with P concentrations in the water column. *Oceanologia* 47, 663–679.
- Himmelblau, D.M., 1964. Diffusion of dissolved gases in liquids. *Chem. Rev.* 64, 527–550.
- Hunke, E.C., Dukowicz, J.K., 1997. An elastic-viscous-plastic model for sea ice dynamics. *J. Phys. Oceanogr.* 27, 1849–1867.
- Jilbert, T., Slomp, C., Gustafsson, B.G., Boer, W., 2011. Beyond the Fe-P-redox connection: preferential regeneration of phosphorus from organic matter as a key control on Baltic Sea nutrient cycles. *Biogeosci. Discuss.* 8.
- Kamp-Nielsen, L., 1992. Benthic-pelagic coupling of nutrient metabolism along an estuarine eutrophication gradient. *Hydrobiologia* 235–236, 457–470.
- Killworth, P.D., Webb, D.J., Stainforth, D., Paterson, S.M., 1991. The development of a free-surface Bryan-Cox-Semtner ocean model. *J. Phys. Oceanogr.* 21, 1333–1348.
- Koop, K., Boynton, W., Wulff, F., Carman, R., 1990. Sediment-water oxygen and nutrient exchanges along a depth gradient in the Baltic Sea. *Marine ecology progress series* 63. Oldendorf, pp. 65–77.
- Krom, M.D., Berner, R.A., 1980. The diffusion coefficients of sulfate, ammonium, and phosphate ions in anoxic marine sediments. *Limnol. Oceanogr.* 25, 327–337.
- Laima, M.J.C., Matthiesen, H., Christiansen, C., Lund-Hansen, L.C., Emeis, K.C., 2001. Dynamics of P, Fe and Mn along a depth gradient in the SW Baltic Sea. *Boreal Environ. Res.* 6, 317–333.
- Lass, H.-U., Matthäus, W., 2008. General oceanography of the Baltic Sea. In: Feistel, R., Nausch, G., Wasmund, N. (Eds.), State and evolution of the Baltic Sea, 1952–2005. John Wiley & Sons, Inc., New Jersey, p. 703.
- Lass, H.U., Prandke, H., Liljebladh, B., 2003. Dissipation in the Baltic proper during winter stratification. *J. Geophys. Res. Oceans* (1978–2012) 108.
- Lehtoranta, J., Ekholm, P., Pitkänen, H., 2009. Coastal eutrophication thresholds: a matter of sediment microbial processes. *Ambio* 38, 303–308.
- Lehtoranta, J., Heiskanen, A.-S., 2003. Dissolved iron: phosphate ratio as an indicator of phosphate release tooxic water of the inner and outer coastal Baltic Sea. *Hydrobiologia* 492, 69–84.
- Li, Y.-H., Gregory, S., 1974. Diffusion of ions in seawater and in deep-sea sediments. *Geochim. Cosmochim. Acta* 38, 703–714.
- Lukkari, K., Leivuori, M., Kotilainen, A., 2009a. The chemical character and behaviour of phosphorus in poorly oxygenated sediments from open sea to organic-rich inner bay in the Baltic Sea. *Biogeochemistry* 96, 25–48.
- Lukkari, K., Leivuori, M., Vallius, H., Kotilainen, A., 2009b. The chemical character and burial of phosphorus in shallow coastal sediments in the northeastern Baltic Sea. *Biogeochemistry* 94, 141–162.
- Marmefelt, E., Arheimer, B., Langner, J., 1999. An integrated biochemical model system for the Baltic Sea. *Hydrobiologia* 393, 45–56.
- Meier, H., 2001. On the parameterization of mixing in three-dimensional Baltic Sea models. *J. Geophys. Res. Oceans* (1978–2012) 106, 30997–31016.
- Meier, H.E.M., 2007. Modeling the pathways and ages of inflowing salt- and freshwater in the Baltic Sea. *Estuar. Coast. Shelf Sci.* 74, 610–627.
- Meier, H.E.M., Döscher, R., T., F., 2003. A multiprocessor coupled ice-ocean model for the Baltic Sea: Application to salt inflow. *J. Geophys. Res.* 108, 3273.
- Meier, H.E.M., Hordoir, R., Andersson, H.C., Dieterich, C., Eilola, K., Gustafsson, B.G., Höglund, A., Schimanke, S., 2012a. Modeling the combined impact of changing climate and changing nutrient loads on the Baltic Sea environment in an ensemble of present simulations for 1961–2099. *Clim. Dyn.* 39, 2421–2441.
- Meier, H.E.M., Müller-Karulis, B., Andersson, H., Dieterich, C., Eilola, K., Gustafsson, B., Höglund, A., Hordoir, R., Kuznetsov, I., Neumann, T., Ranjbar, Z., Savchuk, O., Schimanke, S., 2012b. Impact of climate change on ecological quality indicators and biogeochemical fluxes in the Baltic Sea: a multi-model ensemble study. *Ambio* 41, 558–573.
- Meier, H.M., Andersson, H.C., Eilola, K., Gustafsson, B.G., Kuznetsov, I., Müller-Karulis, B., Neumann, T., Savchuk, O.P., 2011. Hypoxia in future climates: A model ensemble study for the Baltic Sea. *Geophys. Res. Lett.* 38.
- Mort, H.P., Slomp, C.P., Gustafsson, B.G., Andersen, T.J., 2010. Phosphorus recycling and burial in Baltic Sea sediments with contrasting redox conditions. *Geochim. Cosmochim. Acta* 74, 1350–1362.
- Mortimer, C.H., 1941. The exchange of dissolved substances between Mud and water in lakes. *J. Ecol.* 29, 280–329.
- Mortimer, C.H., 1942. The exchange of dissolved substances between mud and water in lakes. *J. Ecol.* 30, 147–201.
- Mårtensson, S., Meier, H.E.M., Pemberton, P., Haapala, J., 2012. Ridged sea ice characteristics in the arctic from a coupled multicategory sea ice model. *J. Geophys. Res. Oceans* 117.
- Neumann, T., Eilola, K., Gustafsson, B., Müller-Karulis, B., Kuznetsov, I., Meier, H.M., Savchuk, O.P., 2012. Extremes of temperature, oxygen and blooms in the Baltic Sea in a changing climate. *Ambio* 41, 574–585.
- Neumann, T., Schernewski, G., 2008. Eutrophication in the Baltic Sea and shifts in nitrogen fixation analyzed with a 3D ecosystem model. *J. Mar. Syst.* 74, 592–602.
- Nixon, S., Ammerman, J., Atkinson, L., Berounsky, V., Billen, G., Boicourt, W., Boynton, W., Church, T., Ditoro, D., Elmgren, R., 1996. The fate of nitrogen and phosphorus at the land-sea margin of the North Atlantic Ocean. Nitrogen cycling in the North Atlantic Ocean and its Watersheds. Springer, pp. 141–180.
- Pitkänen, H., Kiiirikki, M., Savchuk, O.P., Raïke, A., Korpinen, P., Wulff, F., 2007. Searching efficient protection strategies for the eutrophied Gulf of Finland: The combined use of 1D and 3D modeling in assessing long-term state scenarios with high spatial resolution. *Ambio* 36, 272–279.
- Pitkänen, H., Lehtoranta, J., Råike, A., 2001. Internal nutrient fluxes counteract decreases in external load: the case of the estuarial eastern Gulf of Finland, Baltic Sea. *Ambio* 30, 195–201.
- Ramsing, N., Gundersen, J., 2014. Seawater and gases. WEB page, <http://www.unisense.com/files/PDF/Diverse/Seawater%20and%20Gases%20table.pdf>, pp. 1–20.
- Rasmussen, H., Jørgensen, B.B., 1992. Microelectrode studies of seasonal oxygen uptake in a coastal sediment: role of molecular diffusion. *Mar. Ecol. Prog. Ser.* 81, 289–303.
- Reed, D.C., Slomp, C.P., Gustafsson, B.G., 2011. Sedimentary phosphorus dynamics and the evolution of bottom-water hypoxia: A coupled benthic-pelagic model of a coastal system. *Limnol. Oceanogr.* 56, 1075–1092.
- Reissmann, J.H., Burchard, H., Feistel, R., Hagen, E., Lass, H.U., Mohrholz, V., Nausch, G., Umlauf, L., Wiczorek, G., 2009. Vertical mixing in the Baltic Sea and consequences for eutrophication – A review. *Prog. Oceanogr.* 82, 47–80.
- Sanders, R., Jickells, T., Malcolm, S., Brown, J., Kirkwood, D., Reeve, A., Taylor, J., Horrobin, T., Ashcroft, C., 1997. Nutrient fluxes through the Humber estuary. *J. Sea Res.* 37, 3–23.
- Savchuk, O., 2013. Large-scale dynamics of hypoxia in the Baltic Sea. In: Yakushev, E.V. (Ed.), Chemical structure of pelagic redox interfaces. Springer Berlin Heidelberg, pp. 137–160.
- Savchuk, O.P., 2002. Nutrient biogeochemical cycles in the Gulf of Riga: scaling up field studies with a mathematical model. *J. Mar. Syst.* 32, 253–280.
- Schneider, B., 2011. PO<sub>4</sub> release at the sediment surface under anoxic conditions: a contribution to the eutrophication of the Baltic Sea? *Oceanologia* 415–429.
- SHARK, 2014. Svenskt HavsARKiv, online database. Swedish Meteorological and Hydrological Institute (<http://www.smhi.se/klimatdata/oceanografi/havsmiljodata>).
- Skogen, M.D., Eilola, K., Hansen, J.L.S., Meier, H.E.M., Molchanov, M.S., Ryabchenko, V.A., 2014. Eutrophication status of the North Sea, Skagerrak, Kattegat and the Baltic Sea in present and future climates: A model study. *J. Mar. Syst.* 132, 174–184.
- Skog, A., Hall, P.O.J., Hulth, S., Paxeus, N., Van Der Loeff, M.R., Westerlund, S., 1996. Early diagenetic production and sediment-water exchange of fluorescent dissolved organic matter in the coastal environment. *Geochim. Cosmochim. Acta* 60, 3619–3629.
- Slomp, C.P., Mort, H.P., Jilbert, T., Reed, D.C., Gustafsson, B.G., Wolthers, M., 2013. Coupled dynamics of iron and phosphorus in sediments of an oligotrophic coastal basin and the impact of anaerobic oxidation of methane. *PLoS ONE* 8, e62386.
- Soetaert, K., Middelburg, J.J., Herman, P.M.J., Buis, K., 2000. On the coupling of benthic and pelagic biogeochemical models. *Earth Sci. Rev.* 51, 173–201.
- Steenbergh, A.K., Bodelier, P.L., Hoogveld, H.L., Slomp, C.P., Laanbroek, H.J., 2011. Phosphatases relieve carbon limitation of microbial activity in Baltic Sea sediments along a redox-gradient. *Limnol. Oceanogr.* 56, 2018–2026.

- Stevens, D.P., 1991. The open boundary condition in the United Kingdom fine-resolution Antarctic model. *J. Phys. Oceanogr.* 21, 1494–1499.
- Stigebrandt, A., 2001. Physical oceanography of the Baltic Sea. In: Wulff, F., Rahm, L., Larsson, P. (Eds.), *A system analysis of the Baltic Sea*. Springer-Verlag, Berlin-Heidelberg, p. 455.
- Stigebrandt, A., Rahm, L., Viktorsson, L., Ödalen, M., Hall, P.O.J., Liljebadh, B., 2014. A New phosphorus paradigm for the Baltic proper. *Ambio* 43, 634–643.
- Sundby, B., Gobeil, C., Silverberg, N., Mucci, A., 1992. The phosphorus cycle in coastal marine sediments. *Limnol. Oceanogr.* 37, 1129–1145.
- Van Beusekom, J., De Jonge, V., 1998. Retention of phosphorus and nitrogen in the Ems estuary. *Estuaries* 21, 527–539.
- Wenzhöfer, F., Greeff, O., Riess, W., 2002. Benthic carbon mineralization in sediments of Gotland Basin, Baltic Sea, measured in situ with benthic landers. In: Taillefert, M., Rozan, T.F. (Eds.), *Environmental electrochemistry*. American Chemical Society, pp. 162–185.
- Viktorsson, L., Almroth-Rosell, E., Tengberg, A., Vankevich, R., Neelov, I., Isaev, A., Kravtsov, V., Hall, P.O.J., 2012. Benthic phosphorus dynamics in the gulf of Finland, Baltic Sea. *Aquat. Geochem.* 18, 543–564.
- Viktorsson, L., Ekeröth, N., Nilsson, M., Kononets, M., Hall, P.O.J., 2013. Phosphorus recycling in sediments of the central Baltic Sea. *Biogeosciences* 10, 3901–3916.
- Väli, G., Meier, H.E.M., Elken, J., 2013. Simulated halocline variability in the Baltic Sea and its impact on hypoxia during 1961–2007. *J. Geophys. Res. Oceans* 118, 1–19.